STUDY AND DYNAMIC MODELING OF A PRESSURE
TRANSDUCER THAT IS BASED ON
THE PRINCIPLE OF
FORCE BALANCE

A Thesis

by

Adalberto José Soares
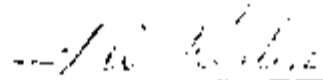
December 1982

Nuclear Engineering Department

THE UNIVERSITY OF TENNESSEE
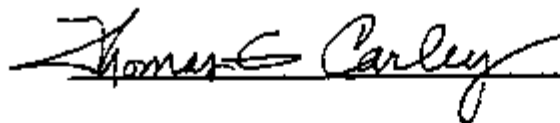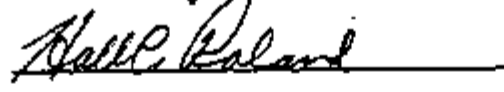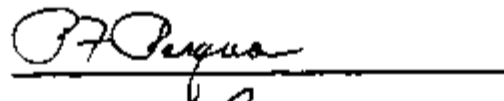Knoxville, Tennessee

To the Graduate Council:

     I am submitting herewith a dissertation written by Adalberto Jose Soares entitled "Study and Dynamic Modeling of a Pressure Transducer that is Based on the Principle of Force Balance." I recommend that it be accepted in partial fulfillment of the requirements for the degree of Doctor of Philosophy, with a major in Nuclear Engineering.

_____
T. W. Kerlin, Major Professor

We have read this dissertation
and recommend its acceptance:

_____

_____

_____

Accepted for the Council:

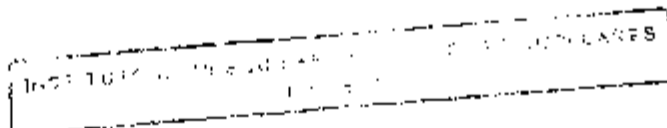_____
Vice Chancellor
Graduate Studies and Research

STUDY AND DYNAMIC MODELING OF A PRESSURE

TRANSDUCER THAT IS BASED ON

THE PRINCIPLE OF

FORCE BALANCE

A Dissertation

Presented for the

Doctor of Philosophy

Degree

The University of Tennessee, Knoxville

Adalberto José Soares

December 1982

To my wife Angela
and my children
Carla Alessandra and
Marco Antonio

ACKNOWLEDGMENTS

The author thanks Dr. T. W. Kerlin, the major professor
and research advisor, for his patience in smoothing the rough
spots during the course of this work. His constant encouragement
and guidance were essential for the successful completion of
this dissertation.

The author wishes to express his gratitude to Dr. P. F.
Pasqua, head of the Nuclear Engineering Department, for making
the completion of the Ph. D. program possible through a graduate
assistantship.

He also thanks Drs. L. F. Miller and Z. Luo for their
help in editing the text, checking equations and help with the
experimental work.

The author thanks Mr. E. L. Machado, Mr. J. March-Leuba
and Dr. W. T. King for their help with the computational programs
and useful discussions.

The use of the facilities of the University of Tennessee
Computer Center and the facilities of the Oak Ridge National
Laboratory - Instrumentation and Controls Division are highly
acknowledged.

ABSTRACT

The work reported here shows the development of an analytical model for one type of pressure transducer that is used in nuclear power plants. It is a Foxboro E13DM force balance transducer with applications for flow, level and low pressure measurements.

The model is based in studying the propagation of mechanical vibrations through the mechanical linkages of the transducer. The electronic circuit of the transducer is responsible for the feedback force that balances the system, and it was considered in the model.

The frequency response as predicted by the model was compared with three sets of experimental data. The results showed good agreement in the region of analysis.

The non-linear behavior of the transducer is explained, and the conditions for linear response are discussed.

Two 'in-situ' tests were developed for the transducer. One can be performed remotely, during normal operation of the plant. The other requires access to the transducer. The tests allow one to obtain the step response of the transducer.

Neither of the tests require access to the pressure line.

TABLE OF CONTENTS

LIST OF FIGURES

FIGURE   PAGE

CHAPTER 1

INTRODUCTION

1.1 General Considerations

The optimum values of all variables of a nuclear power plant, and the limits that they can reach during transient conditions are determined during the design phase of the plant. In order to monitor the variables and to assure that they do not exceed the safety limits, process instrumentation is installed in the plant. Process instrumentation includes the devices that are used to convert the measured process variable into an electrical signal, which is more suitable for manipulation. These devices are called transducers[*], and can be veiwed as physical interfaces between the variable being measured and the information that we receive.

The fact that the response of the transducers is not instantaneous means that the information received from the transducer does not necessarily represent the actual state of the variable associated with it. The time interval between the instant in which the process variable reaches a given value, and the instant in which the transducer indicates that the value was reached is defined as the response time of the transducer. In nuclear power plants the response time is particularly important for transducers that are part of the protective system.

---

[*] In the existing literature these devices are also called a sensor or a transmitter.

Because of the adverse environment in which some transducers
are located, their response time may deteriorate during the lifetime
of the plant and endanger a safety action during transient conditions.
To avoid this the Nuclear Regulatory Commission, in its Regulatory
Guide 1.118 (1), recommends that, "Safety system response time
measurements shall be made periodically to verify the overall response
time (assumed in the safety analysis of the plant) of all portions of
the system from and including the sensor to operation of the
actuator." It also states that, "Where the entire set of equipment
from sensor to activated equipment cannot be tested at once,
verification of system response time may be accomplished by measuring
the response times of discrete portions of the system and showing
that the sum of the response times of all portions is equal to or
less than the overall system requirement."

According to the second statement the required response time
measurement can be divided in two parts: one comprising the portion
of the system from the process to the sensor output, and the other
comprising the portion of the system from the sensor output to the
operation of the actuator.

1.2 Presentation of the Problem

The electrical output of the tranducer is easily simulated,
but practical ways of measuring the response time of the transducer
require new technical developments. Considerable interest exists in
developing practical methods for response time measurements of
transducers, especially methods that allow the measurements during
normal operation of the plant, with the transducer 'in-situ'.

The process instrumentation of a nuclear power plant is
mainly designed to monitor state variables such as flow, level,
pressure and temperature (2). Since the measurement of flow and
level is usually done with differential pressure transducers, the
process instrumentation consists basically of temperature and
pressure transducers.

In addition to monitoring state variables, temperature and
pressure transducers are important tools for surveillance and
diagnostic measurements (3,4,5,6). Because the vibration of
mechanical components create pressure fluctuations, particular
importance is given to pressure transducers. It has been shown that
low-level signals (noise) from pressure transducers contain important
information for reactor vibration monitoring systems (7,8,9,10).
Low-level signals can also be used to monitor the response time of
transducers (11). In order to interpret the information contained
in low-level signals it is desirable to develop mathematical models
for the system and for the transducer that is being used to collect
the information. A mathematical model is important because it gives
guidelines to interpret the measured information.

1.3 Review of the Work Performed

The work reported here shows the development of an analytical
model for one type of pressure transducer that is used in nuclear
power plants. It is a Foxboro E13DM force balance transducer with
applications for flow, level and low pressure measurements. With
minor modifications the analytical model developed here can be

extended to the other models of Foxboro transducers.

In addition two 'in-situ' tests were developed, and are presented here. The first one is remote, and can be performed during normal operation of the plant. It provides the response of the transducer to a increasing step in pressure, and can be used to monitor the dynamic response of the transducer. The second test requires access to the transducer. It allows one to obtain the necessary information to predict the response of the transducer to an increasing and/or decreasing step in pressure. Neither of the tests require access to the pressure sensing line.

1.4 Prior Related Work

Pressure transducers can be divided into two classes, motion balance and force balance. For both classes, a differential pressure across the two sides of the sensing element causes a displacement. The sensing element is the part of the transducer that is in contact with the pressure line. In motion balance transducers, the electronic system generates an electric signal that is proportional to the displacement of the sensing element. In force balance transducers the electronic system generates a force that balances the differential pressure, and cancels the displacement.

Dynamic models have been developed previously for motion balance pressure transducers. In general the sensing element is assumed as a lumped mass with an effective area. The area multiplied by the differential pressure results in a force that causes the mass to be accelerated. For normal conditions of operation the displacement is proportional to the differential pressure, a

situation similar to a spring under the action of a force. This justifies the inclusion of a term proportional to the displacement in the dynamic equation for the element. The 'spring' constant is a function of the elastic properties of the sensing element. Usually the sensing element is filled with some viscous fluid. The function of the fluid is to damp the motion of the element, making it less sensitive to mechanical vibrations. The damping motion requires that a term proportional to the velocity be included in the dynamic equation of the element.

The simplest dynamic model for the sensing element of a motion balance transducer is:

$$I \frac{d^2x(t)}{dt^2} + C \frac{dx(t)}{dt} + Kx(t) = AP(t) \qquad (1-1)$$

where x is the position of the element, I is its inertia, C is the damping coefficient, A is the effective area and P is the differential pressure.

The model described by Equation 1-1 is given in reference 12, and used by Jones (13), Cain (14) and Hunt (15) in studying the dynamic behavior of pressure transducers. No work was found in which the propagation of the mechanical vibrations through the linkages of the transducer were taken into account. Abdullah and Finkelstein (16) used the lumped model described by Equation 1-1 to study the dynamic behavior of different sensing elements. They also explain how to model individual components of an electric and/or magnetic circuit.

In force balance transducers the balancing force is a feedback action generated by the electronic part of the transducer. Therefore, the dynamic response of the transducer is strongly dependent of the electronic circuit. No work was found in which the electronic part of a pressure transducer was analyzed as a system.

Regarding 'in-situ' tests of pressure transducers, low-level measurements have been suggested as a method to monitor the response time (17). Wu and Ouyang have used low level signals to estimate the time constant of one pressure transducer. In a first report (18), an ARMA model was found adequate to characterize the transducer, and the time constant was estimated as 28.6 msec. In a second report (19), a correction was made, and the time constant was estimated as 1.8 msec. The transducer used in the analysis was a Rosemount model 1152GP (a explanation of Rosemount transducers is given in Appendix A). The Rosemount Company specifies that the time constant for the transducer in reference is "continuously adjustable between .2 and 1.67 sec."

Foster et al. (20) have developed one method for 'in-situ' measurements of the response time of pressure transducers. The method requires that a ramp input be applied to the sensing line, and in nuclear plants it can be performed only during shutdown periods. No work was found in which a large signal is used for remote tests of pressure transducers.

CHAPTER 2

DESCRIPTION OF FOXBORO PRESSURE TRANSDUCERS

2.1 Introduction

Pressure transducers can be divided into two classes, motion balance and force balance. Both types provide pressure readings by a two step process. In the first step they transform a differential pressure existing across the transducer into a displacement. In the second step they convert the displacement into an electrical signal.

The characteristic of force balance transducers is that they use the electrical signal to create a force that balances the pressure, cancelling the displacement. In motion balance transducers, the displacement remains while the transducer is under the action of the differential pressure.

The Foxboro pressure transducers used in the nuclear industry are of the force balance type. Table 2-1 gives a list of the different models and their applications.

To explain the operation of the transducer we divide it into two major systems: mechanical and electronic. The function of the mechanical system is to transform the differential pressure into a displacement of a ferrite detector that activates the electrical system. The function of the electrical system is to generate a DC current output signal.

2.2 Mechanical System

The mechanical system may be divided in five subsystems: sensing element, C-flexure, force bar, vector mechanism and lever

Table 2-1. Foxboro pressure transducers

model	application	sensing element
E 11AH	absolute pressure	bellows
E 11AL	absolute	diaphragm
E 11AM	absolute	diaphragm
E11DM	differential	bellows
E 11GH	gauge	Bourdon tube
E 11GM	gauge	bellows
E 13DH	differential	diaphragm
E 13DL	differential	diaphragm
E 13DM	differential	diaphragm

system (these names are the same as used by The Foxboro Company in
its technical specifications).

Figure 2-1 is a schematic diagram for the transducer model
E13DM. It is a differential pressure transducer, with applications
for flow, level and low pressure measurements. It will be used to
explain how the pressure signal is transmitted through the mechanical
linkages to activate the electrical system.

The major difference between model E13DM and the other
Foxboro models is the sensing element. The sensing element for model
E13DM is the diaphragm (D) shown in Figure 2-1. Details of the
diaphragm are given in section 3.2.1. Other sensing elements are
shown in Figure 2-2. The sensing element is subject to a high
pressure on one side (H), and a low pressure on the other side (L).
The product of the difference in pressure and the effective area of
the diaphragm results in a force that is transmitted through a small
bar to a flexural system called the C-flexure.

The function of the C-flexure, shown in detail in Figure
2-3, is to transmit the force to the force bar. The combination of
the sensing element plus the C-flexure form a system called the
capsule.

A diaphragm (A) attached to the structure of the transducer
as shown in Figure 2-1 works as a fulcrum point about which the
force bar rotates to transmit the force to the vector mechanism.
The rotation is clockwise for increasing pressure.

The length of the upper part of the force bar is greater than
the length of the lower part. It therefore acts as a reduction
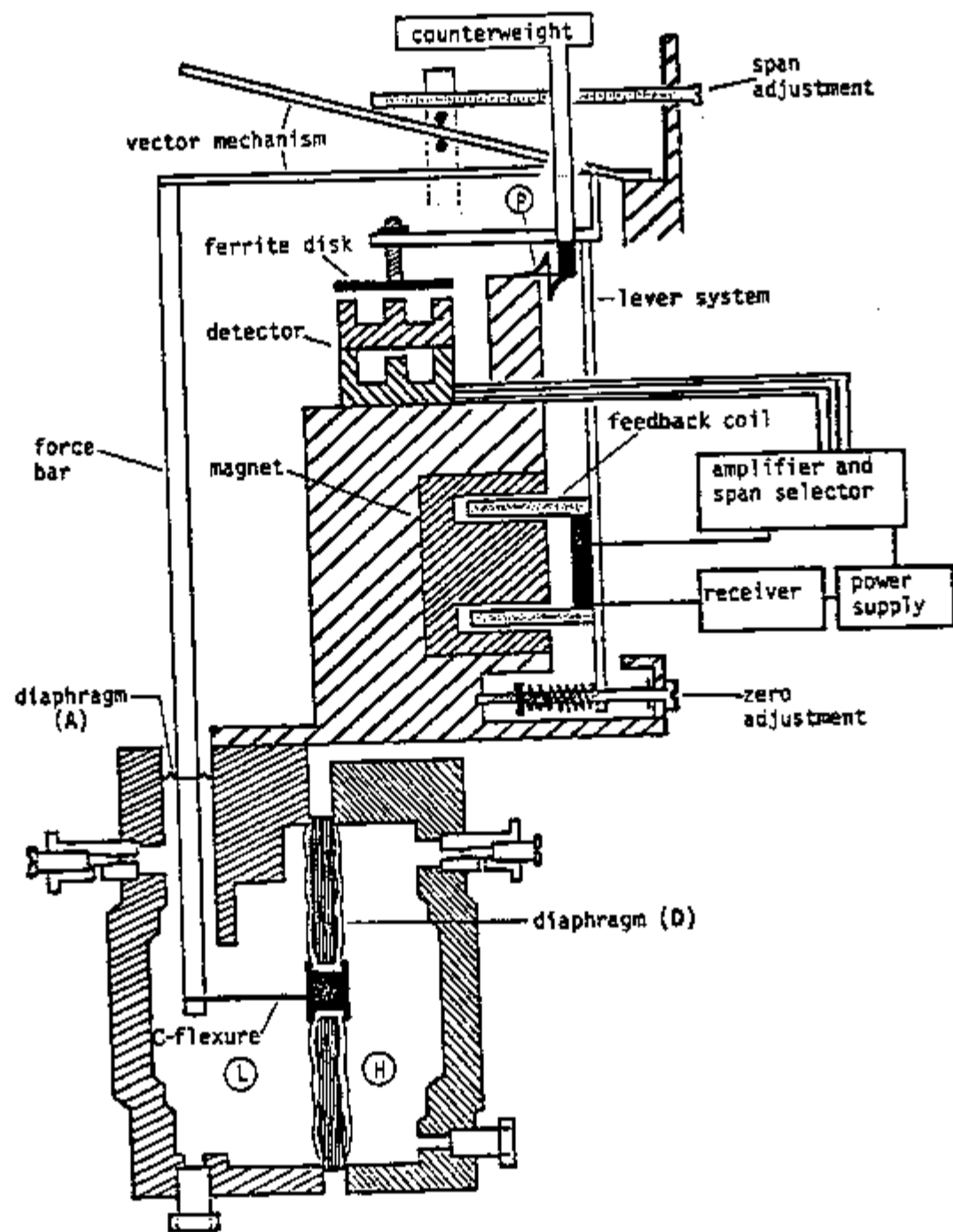
Figure 2-1.   Foxboro pressure transducer model E13DM
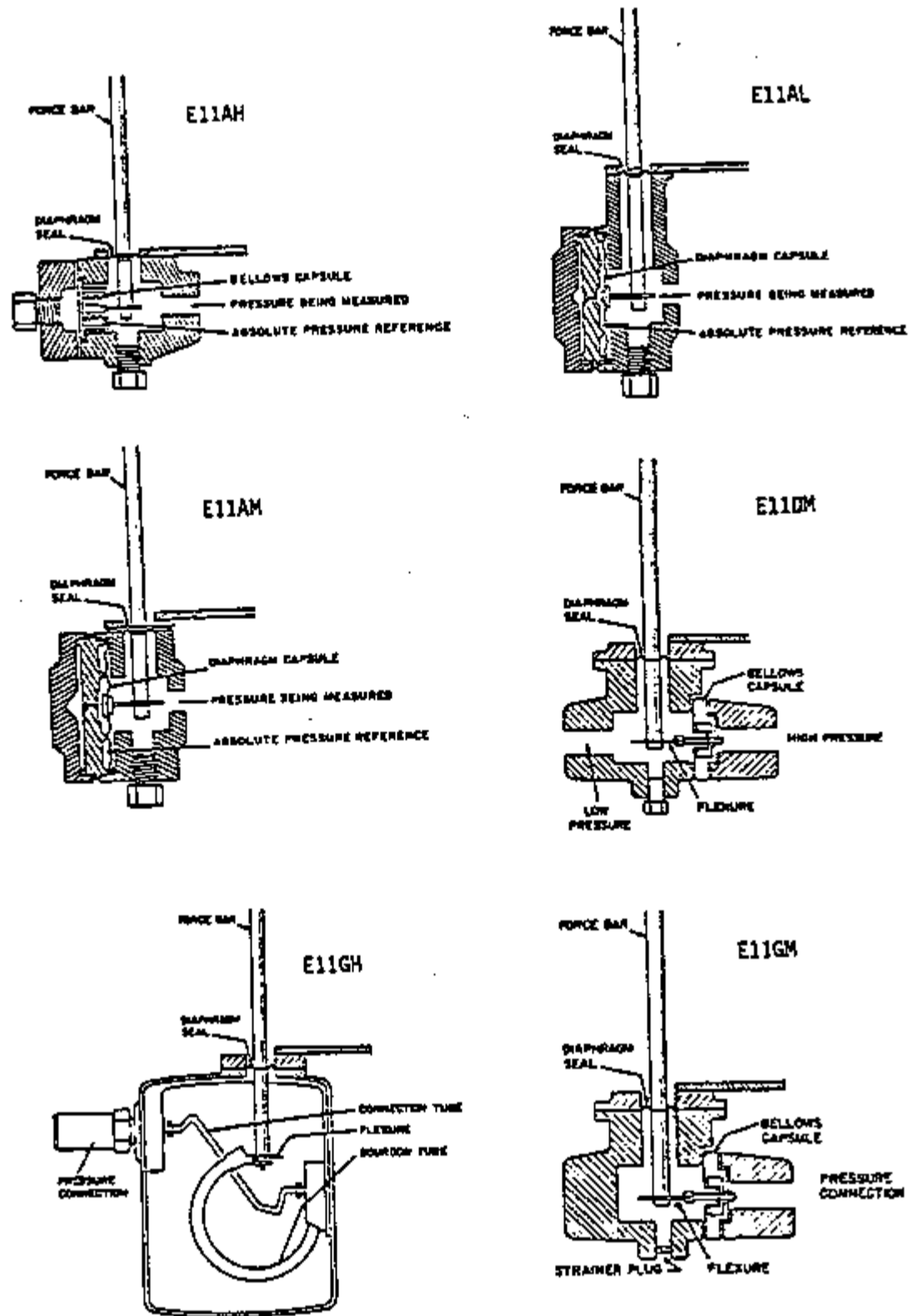
Figure 2-2.   Sensing elements for Foxboro pressure transducers
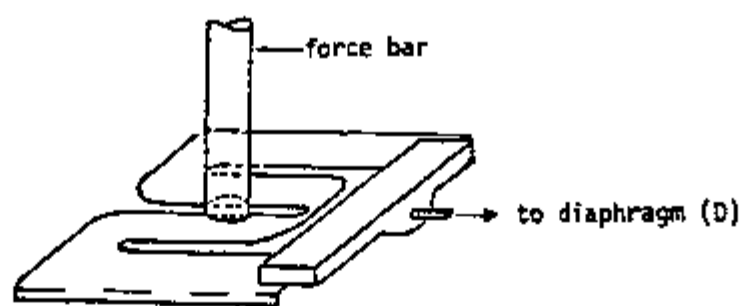
Figure 2-3. Flexural system

system in the sense that the force that is transmitted is only a
fraction of the force that acts on the lower end. The value of the
fraction is given by the ratio of the lower length divided by the
upper length.

The vector mechanism, shown in detail in Figure 2-4, may be
divided into three sections: upper-outer defined by the section
comprising points T, R, V, V' and T'; upper-inner defined by section
ZZ', and lower defined by section SZ. Points T and T' are fixed
points attached to the structure of the transducer. Point R is a
point that is selected at the time of installation of the transducer,
and is responsible for the span of operation. Point R is adjusted by
turning a screw that moves a mechanical system that slides on the
section VT, shown in Figure 2-4a, of the mechanism. Once the
transducer has been calibrated point R remains the same until a new
calibration is performed. Since points T, R and T' are fixed, the
upper-outer section of the vector mechanism remains rigid during
operation of the transducer.

The upper-outer section of the mechanism is connected to the
upper-inner section by a plate welded on top of both sections. This
plate is very thin, and the reason for its thinness is to allow
it to bend, creating a hinging point for the upper-inner section.

As shown in Figure 2-4b there are three forces acting on the
mechanism: a horizontal force F_h applied at point S, a vertical
force F_v applied at point Z, and a force F_r which is transmitted to
the structure of the transducer through the upper-outer section.
During steady state operation the resultant of the three forces is

a)

b)
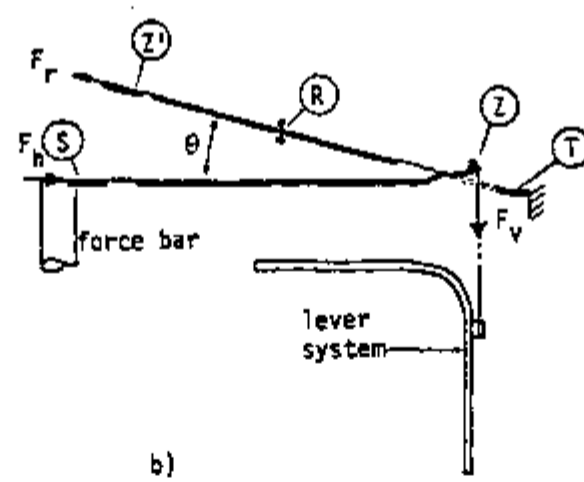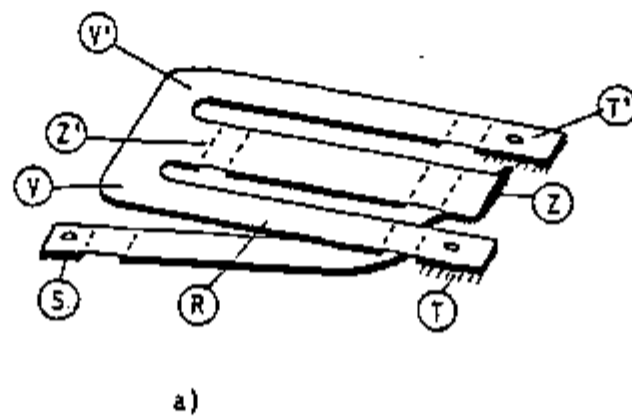
Figure 2-4. Vector mechanism

zero, the mechanism remains in equilibrium, and the forces F_v and F_h are related by: $F_v = F_h \tan\theta$. For small values of θ, $\tan\theta$ may be approximated by θ, and the relation between F_v and F_h becomes linear. Furthermore, since θ determines the variation of F_v for a given variation of F_h, and since its value is adjustable, then it is used as a span adjuster for the transducer.

An increase in pressure rotates the force bar in the clockwise direction causing an increase on the horizontal force F_h. This increasing force unbalances the system and causes the lower section to move to the right. Due to the constraint imposed by the upper-outer section, the upper-inner section is forced to undergo a counterclockwise rotation. This causes an increase on the vertical force F_v that acts on point Z, which is the force that the mechanism transmits to the lever system.

The connection between the vector mechanism and the lever system is made by a thin plate. The plate is thin enough to avoid changes in the vertical force that is transmitted (its bending is negligible).

The lever system is a structure that rotates when under the action of a torque. The ferrite disk and the support of the feedback coil are part of the system. Also included is a counterweight that balances the weight of the lever system to allow the installation of the transducer in the horizontal position. As can be seen in Figure 2-1, point P is the pivoting point for the lever system. During steady state operation the lever system is under the action of several forces, in such way that the resultant moment is zero. The

forces acting on the lever system are: a force due to a spring attached at the end of the system which is used for zero adjustment of the transducer, a magnetic force that is generated by a current that passes through a coil placed in a magnetic field (feedback coil in Figure 2-1), and the force that is transmitted from the vector mechanism.

In addition, there is a moment that is generated when the system leaves its equilibrium position. This moment is due to the physical arrangement of the pivot point P, that is formed by thin plates in a cruciform configuration, as shown in Figure 2-5.

When the force transmitted from the vector mechanism increases, the resultant moment acting on the lever system is no longer zero, and the system undergoes a counterclockwise rotation about point P. As the lever system undergoes the counterclockwise rotation, the ferrite disk approaches the detector, decreasing the air gap that separates them. Since the detector and the ferrite disk compose a differential transformer (as explained in section 2.3), the displacement of the ferrite disk is an action that actuates the electrical system of the transducer. The action of the electrical system is to increase the current that flows through the feedback coil. The increase in current causes the magnetic force to increase. The moment due to the magnetic force is negative and causes the ferrite disk to return to its equilibrium position.

As seen in Figure 2-1, the motion of the lever system is restricted in both ways. It is restricted in the counterclockwise direction by a stop located underneath the force motor, and in the
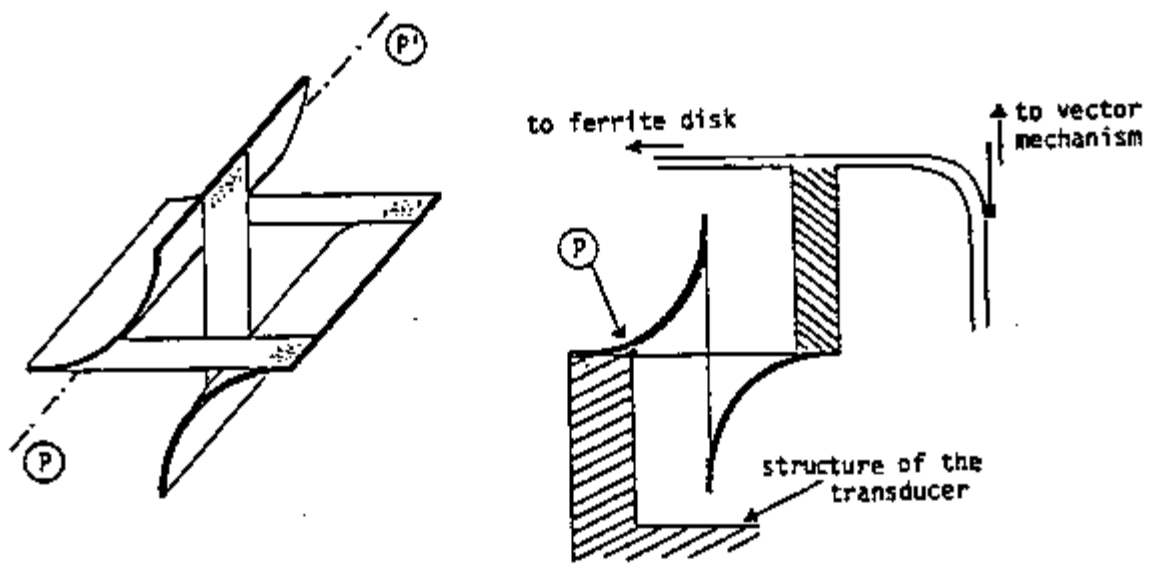
Figure 2-5. Pivoting point formation

clockwise direction by the physical presence of the structure of the transducer. This means that the displacement of the ferrite disk, and consequently the air gap between the disk and the detector are bounded. Furthermore considering the air gap that exists when the ferrite disk is at the equilibrium position as reference, the difference between the reference gap and the minimum gap allowed is not necessarelly the same as the difference between the reference and the maximum gap allowed.

A change in the air gap triggers the electrical system in such a way that a decrease in the gap size increases the output signal of the transducer. Consequently the minimum gap is associated with the highest positive gradient of the output signal, and, conversely, the maximum gap is associated with the highest negative gradient. (This observation will be important in the discussion of the remote test procedure for the transducer. See chapter 6).

2.3 Electrical System

Foxboro pressure transducers are available with two different electrical systems, one to generate a DC current signal between 4 and 20 mA, and the other to generate a DC current signal between 10 and 50 mA. Both systems are used in nuclear power plants. Since the transducer available for experimental work has an output current signal between 10 and 50 mA, this is the system analyzed here Figure 2-6 shows a diagram of the system that operates between 10 and 50 mA. It is divided into seven subsystems: power supply, receiver load, detector, oscillator, rectifier, amplifier and force motor. For purpose of illustrating the circuit designed to operate between 4

Figure 2-6. Electronic circuit for transducer with output current between 10 and 50 mA
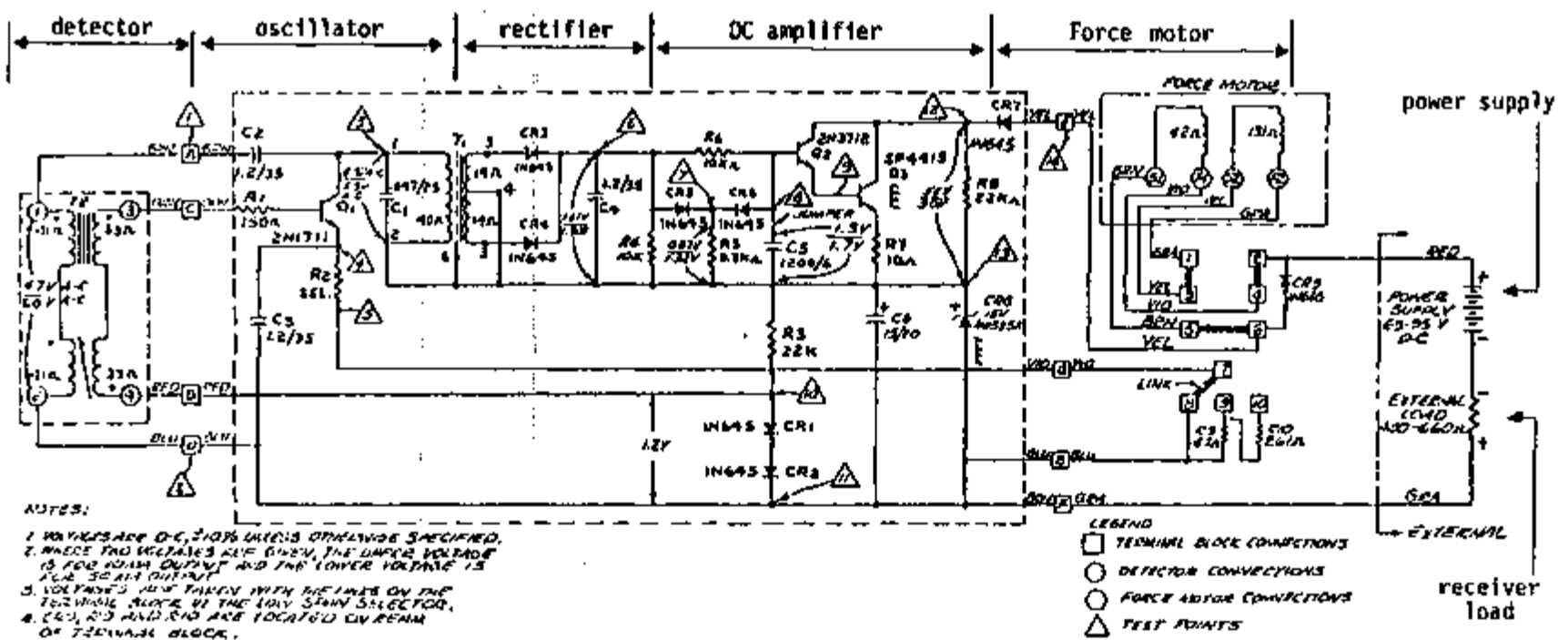
SPAN SELECTION	LINK ARRANGEMENT (on terminal block)				FORCE MOTOR RESISTANCE Ohms
HIGH	1-2	3-4	5-6	7-10	173
MEDIUM	1-2	3-5	4-6	7-9	173
LOW	1-3	2-4	5-6	7-8	42

and 20 mA is shown in Figure 2-7.

The power supply works as a current generator, in the sense
that its function is to generate the current that the system
requires.

The receiver load is a resistance which is used to transform
the current that circulates through the system into a voltage signal.
The total resistance of the load must be about 600 ohms, and can be
composed of one or more resistor elements.

The detector consists of two ferrite cores, one ferrite disk
and two coils arranged as shown in Figure 2-8. The two ferrite cores
and the ferrite disk, combined with the existing air gaps, form two
magnetic circuits that together form a differential transformer. A
change in pressure causes a displacement of the ferrite disk.
Therefore the air gap and the inductive coupling of the upper circuit
are variable. The air gap and the inductive coupling of the lower
circuit are constant.

The primary coil of the transformer is the coil between
points A and B in Figure 2-6, and the secondary coil is the one
between points C and D. The secondary coil is wrapped on the ferrite
cores in such a way that the portion on the upper core has a polarity
opposite to the polarity existing in the lower core. With this
configuration, equal effective air gaps in both magnetic circuits
result in zero net current induced on the secondary coil. Any change
in the upper air gap generates an error signal that is used to induce
current in the secondary coil. The induced current determines the
amplitude of the AC voltage in the oscillator system.
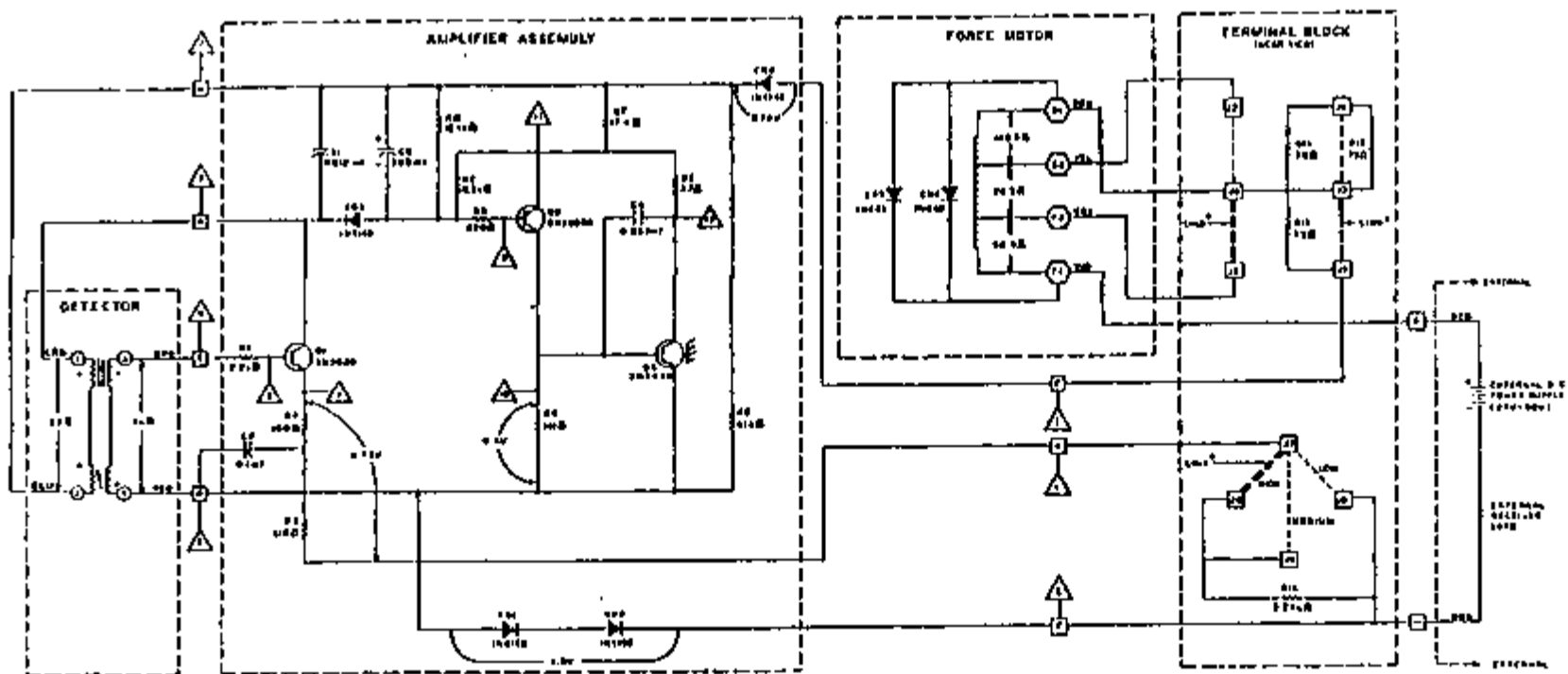
LEGEND:
☐ TERMINAL CONNECTIONS
◯ DETECTOR CONNECTIONS
◯ FORCE MOTOR CONNECTIONS
△ TEST POINTS

SPAN SELECTION	LINK ARRANGEMENT (on terminal block)		
	Link 1	Link 2	Link 3
LOW	Open	J4-J6	J7-J8
MEDIUM	J1-J3	J2-J4	J7-J9
HIGH	J3-J5	Open	J7-J10

Figure 2-7. Electronic circuit for transducer with output current between 4 and 20 mA

21

ferrite
disk

air gap

top
core

air gap

bottom
core

primary
coil

secondary
coil
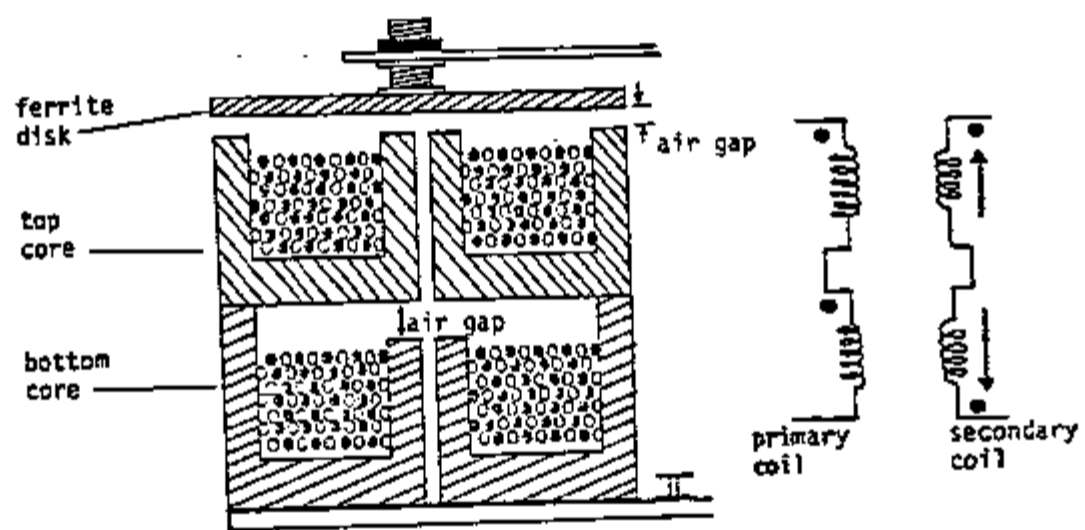
Figure 2-8. Differential transformer

The oscillator is composed of an amplifier, a feedback system and a selector system which is responsible for the frequency of oscillation. The amplifier is the transistor Q1. The feedback system is the differential transformer that composes the detector. The selector system is the capacitor C2 and the primary coil of the detector, that together form a circuit LC. The AC current induced in the secondary coil enters the base of the transistor, is amplified and fed back through the differential transformer. The AC current creates an AC voltage at the collector of the transistor Q1. The AC voltage is the input for the rectifier system. The frequency of oscillation, according to Foxboro, is not critical, and is approximately 4 Khz.

The rectifier is composed of a transformer, two diodes and one capacitor. The transformer and the two diodes form a full wave rectifier, with the capacitor acting as a filter to smooth the output. The output of the rectifier system is fed into a DC amplifier, which results in the 10 to 50 mA DC signal that is the output of the transducer.

The DC amplifier is basically a Darlington amplifier (21), composed of transistors Q2 and Q3. The diode-resistance network, at the base of Q2, provides, according to Foxboro, an equal response time upscale and downscale.

The force motor is the feedback coil shown in Figure 2-1. It consists of two coils connected in series with the output of the DC amplifier. The coils have different lengths, and are placed in a magnetic field in such way that the DC current passing through the

coils generates a magnetic force. This is the force that balances the system and returns ferrite disk to its original position.

The length of each coil, and the force that it generates, can be assumed proportional to its resistance. One coil has a resistance of 131 ohms, and the other 42 ohms.

As shown in the Table present on Figure 2-6, the coils can be arranged in 3 different ways, according to the range of operation of the transducer. For the operation identified as 'high' the 2 coils are connected to give a force equivalent to the force of a coil with resistance 173 ohms. For the operation identified as 'medium' the equivalent resistance is 89 ohms. For operation 'low' the resultant force is equivalent to the force of one coil with resistance 42 ohms. (This information will be important for discussing the remote testing of the transducer. See chapter 6).

The transducer used for experimental work had the following jumper positions: 1-2, 3-4, 5-6 and 7-10 (see Figure 2-6). These positions correspond to a force motor with an effective coil of 173 ohms.

CHAPTER 3

DEVELOPMENT OF THE MATHEMATICAL MODEL

3.1 Introduction

The development of a mathematical model is an essential part
of the dynamic analysis of a system. In low-level measurements the
model gives guidelines for a proper interpretation of the results. In
large signal analysis it allows a prediction of the response of the
system to any anticipated input.

The mathematical model developed in this chapter is based on
the assumption that the transducer is a linear system. As will be
explained in chapter 5, the response of the transducer to a large
signal perturbation is different from the response to a small
perturbation, but a linear model and an adequate division of the
transducer into subsystems will allow prediction of the response for
both small and large signals.

To know the dynamic behavior of a linear system, it is
sufficient to obtain its transfer function. The transfer function of
the transducer can be assumed to be a combination of the transfer
functions of several subsystems, each one with its own dynamic
characteristics. Figure 3-1 shows the adopted division of the
transducer and the input and output signals for each one of the
subsystems.

In order to determine the transfer function for each
mechanical subsystem, an analysis is performed to determine its
vibrational behavior when under the action of a system of forces.
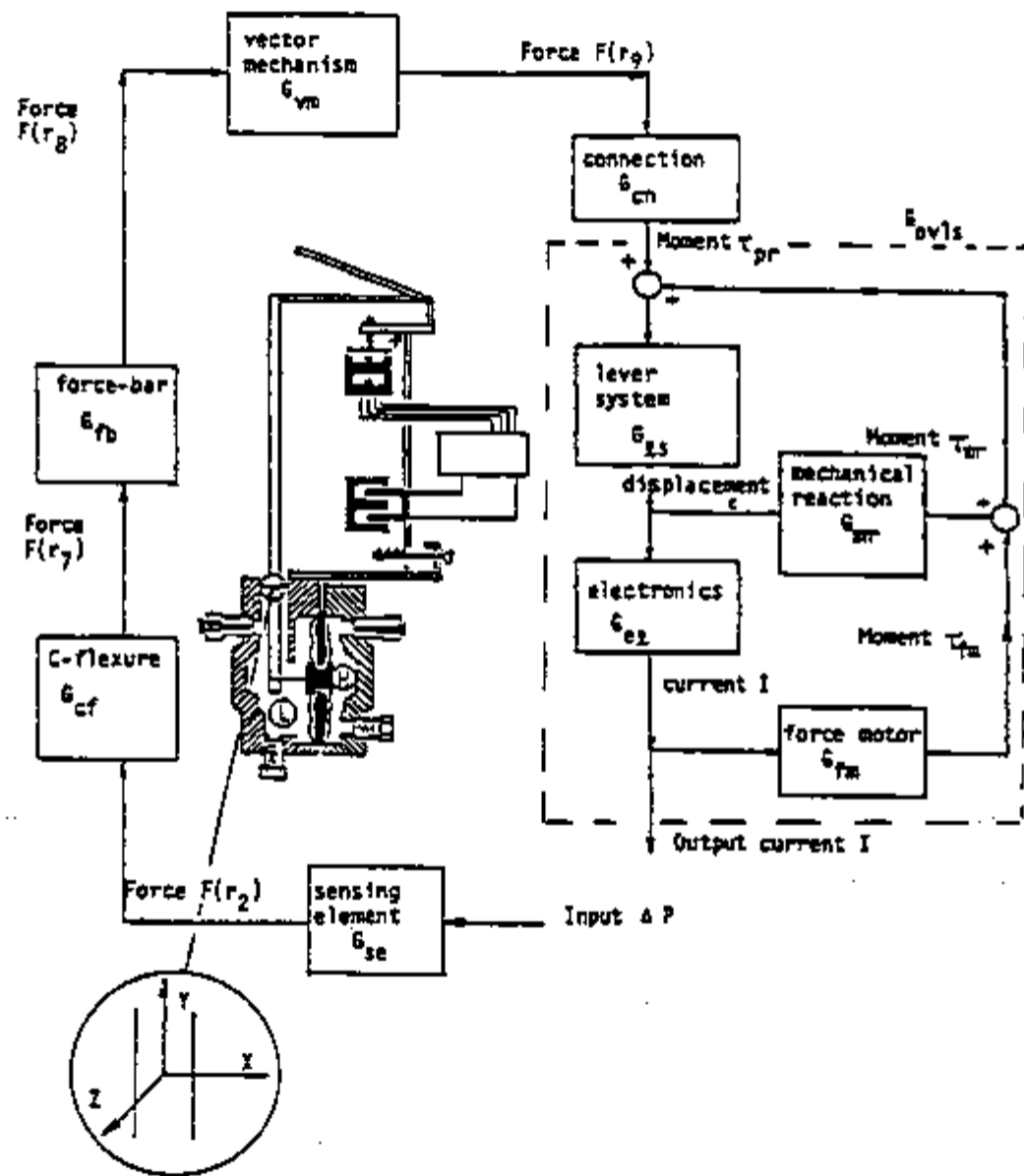
Figure 3-1. Subsystems of the transducer

The basic equations used for the analysis are derived in detail in Appendix B.

In this chapter the variable $\delta u(x,y,z)$ represents the displaced position of a point that was originally at position (x,y,z). The origin of the adopted coordinate system is shown in Figure 3-1. The symbol δ is used to indicate that the analysis is performed considering variations from equilibrium positions. In order to obtain the final equations in a comprehensible form, the coordinates of the points used in the development of the model are as follows. If the point will be present in the final equations then it is given a sequential number, for example (x_2, y_2, z_2). However, if the point is used only for development of the final equations, then it is given a letter, for example (x_a, y_a, z_a). If at a given equation δu is not a function of one of the coordinates, then that coordinate will be omitted. Also, the following nomenclature is adopted in this chapter:

A = cross sectional area

E = elasticity modulus

ρ = density

L = length

I = inertia moment of area or inertia moment of mass (whichever applies to the equation)

c = constant used to simplify the presentation of the equations

d, $a(i,j)$, $b(i,j)$ = simplified representation for known parameters and coefficients that are functions of the Laplace variable s.

$B_i(s)$ = unknown coefficients or functions of s that need to be
determined

Due to the complex geometry of some parts of the mechanical
system, some assumptions are made. In this chapter the assumptions
are mentioned, but not discussed. The effects of the assumptions made
are discussed in Chapter 4.

Unless otherwise specified, all the examples and relations
derived in this chapter will be based on an assumed increase in the
pressure at the high pressure chamber of the transducer (identified by
H on Figure 3-1).

Due to the complexity of the electronic part of the transducer,
it is not analyzed theoretically. Rather, an experimental analysis is
presented to provide an empirical model.

3.2 Mathematical Study of the Mechanical Subsystems

3.2.1 Sensing element

The sensing element for the model E13DM is a diaphragm system.
As shown in Figure 3-2, it is composed of two external corrugated
diaphragms welded at the boundary to a backup plate. The backup plate
is very thick and can be assumed as rigid and static. The two
diaphragms are connected in the center by a spool. In order to
protect the diaphragms from overranging, the backup plate is machined
to have a surface that adjusts to the diaphragm corrugations. During
normal operation there is a small distance separating the diaphragms
and the backup plate. The internal space of the element is filled
with a viscous silicone fluid which is transferred from one side of
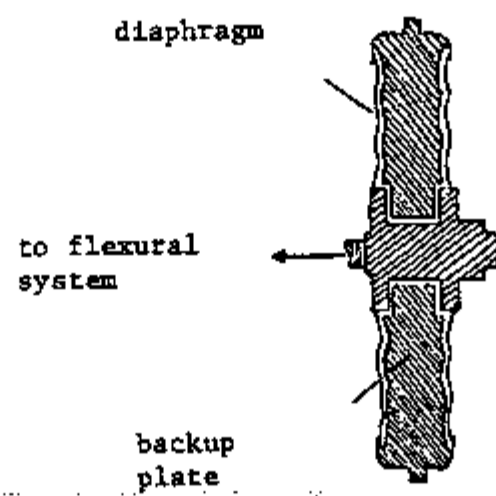
Figure 3-2. Sensing element (diaphragm)

the backup plate to the other through the space between the spool and the plate. The viscosity of the fluid and the dimensions of the space available for transference of fluid are chosen to result in a proper damping of the response. According to the information received from The Foxboro Company (see Appendix C) the spool has a diameter equal to 13.6 mm. An annular ring .7 mm wide separates the spool from the backup plate. The internal space filled with the viscous fluid has a volume between 5 and 6 cm^3. In the standard diaphragm the kinematic viscosity of the fluid is $5*10^{-4}m^2$/sec. The diaphragm is optionally available with a fluid with viscosity equal to $22*10^{-4}m^2$/sec.

For reasons that will be explained in section 4.4 the effect of the natural frequencies of the corrugated diaphragm can be neglected. With this assumption, the sensing element may be assumed to be a rigid system with a set of springs and dash pots (for damping of the motion) connecting it to the backup plate. This model is illustrated in Figure 3-3. For this model we define the following effective coefficients: K_{se} is the value of the overall spring constant, C_{se} is the value of the overall damping coefficient, I_{se} is the value of the total inertia of the system, and A_{se} is the effective area of the diaphragm. The dynamic equation describing the motion of the central portion of the element is:

$$I_{se} \frac{d^2 \delta u_1(t)}{dt^2} + C_{se} \frac{d \delta u_1(t)}{dt} + K_{se} \delta u_1(t) = -A_{se} \delta P(t) + \delta F_1(t) \quad (3-1)$$

where δu_1 is the displaced position of the element in the x direction,
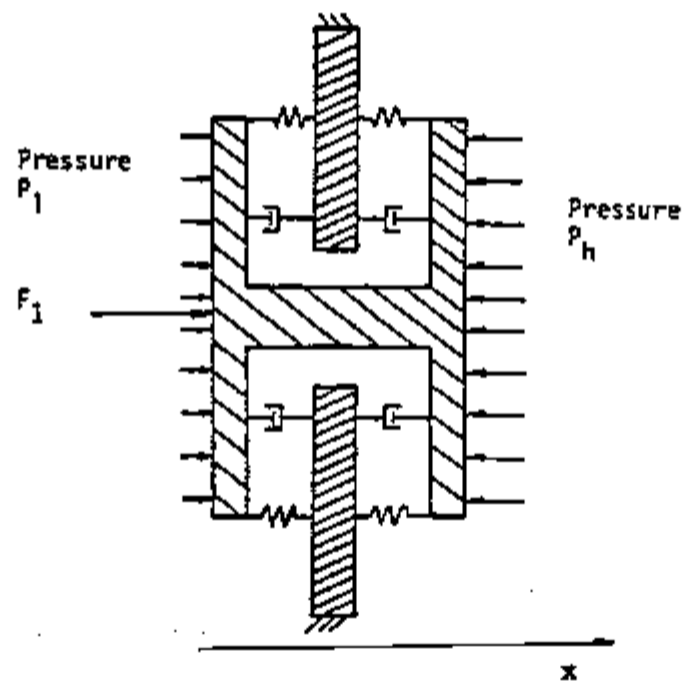
Figure 3-3. Model for the sensing element

δP is the variation in the differential pressure $P_h - P_l$ and δF_1 is the variation in the reaction force being applied by the feedback system of the transducer. The subindex 1 identifies the sensing element as the first element of the mechanical system.

It has been shown that when a pressure is applied to a corrugated diaphragm the displacement of the central portion of the diaphragm is linearly proportional to the applied pressure if the ratio (displacement/diameter of diaphragm) is lower than .02 (22). This behavior is analogous to the behavior of a spring, in which the displacement is proportional to the force and is the reason for the term $K_{se}\delta u_1$ in equation 3-1.

In order to obtain an empirical value for K_{se} an experiment was performed in which pressure was applied on one side of the diaphragm to measure the displacement of its central portion. The result of the experiment is shown in Figure 3-4. Since the design of the transducer is such that the displacement of the central part of the diaphragm never exceeds .05 mm (The reason for this will be explained in section 5.2), we can use the linear portion of the result shown in Figure 3-4 to determine the value of K_{se}. A least squares fit of a straight line for the points with displacement lower than .5 mm resulted in a value of K_{se} equal to $2.33 \ast 10^7 \ast A_{se}$ N/m, when A_{se} is expressed in m^2.

The value of A_{se} was obtained from an experiment where a force was applied at a point on one side of the diaphragm and a pressure was applied on the other side. The pressure was adjusted until the central point of the element returned to the position occupied before
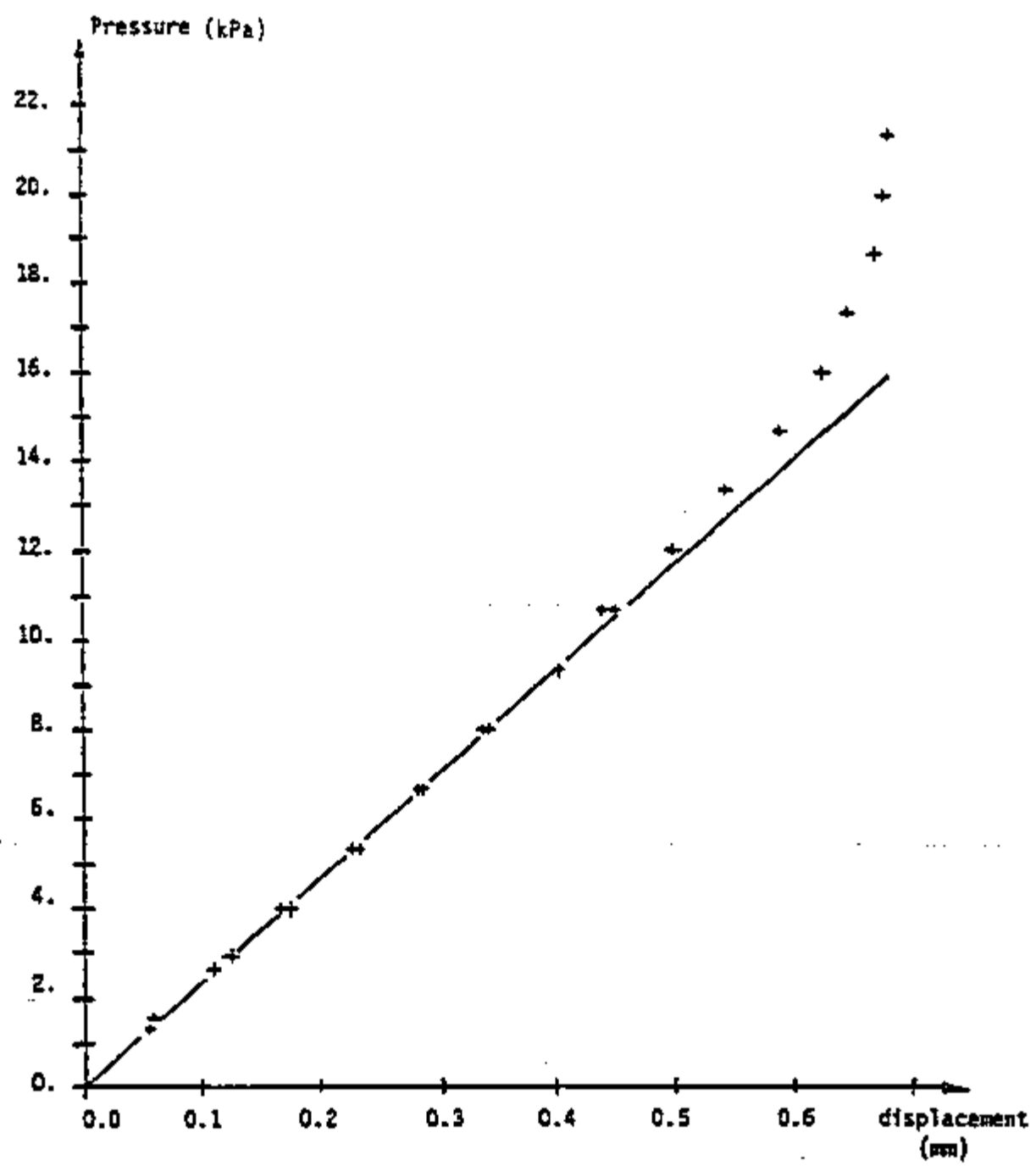
Figure 3-4. Determination of the spring constant for the sensing element

the application of any force. The result of the experiment is shown in Figure 3-5, and resulted in a value of $2.5*10^{-3}m^2$ for A_{se}. With this value for A_{se} the value for K_{se} is $5.66*10^4$ N/m.

The damping coefficient in the model described by Equation 3-1 is due to the viscous fluid that fills the internal space of the element, and slows down its motion. Besides damping the motion of the element the viscous fluid also contributes to the effective inertia of the element. When the element is accelerated a new velocity profile is developed within the space available for transfer of fluid. In order to develop this new profile, a force is necessary to overcome the shear forces existing between the fluid and the wall of the hole where the fluid flows. The other contribution for the inertia of the element is the mass of the spool that is accelerated during a transient.

Laplace transforming Equation 3-1, the equation describing the motion of the element, gives:

$$\delta u_1(s) = b(1,1)\delta P(s) + b(1,2)\delta F_1(s) \tag{3-2}$$

where $b(1,1) = -A_{se}/(I_{se}s^2 + C_{se}s + K_{se})$

and $b(1,2) = 1/(I_{se}s^2 + C_{se}s + K_{se})$

Since a theoretical determination of the damping coefficient is impractical, an experiment was performed to determine its value, and the value of I_{se}. The experiment consisted of displacing the diaphragm from its equilibrium position with subsequent release. It was performed with the diaphragm removed from the transducer and
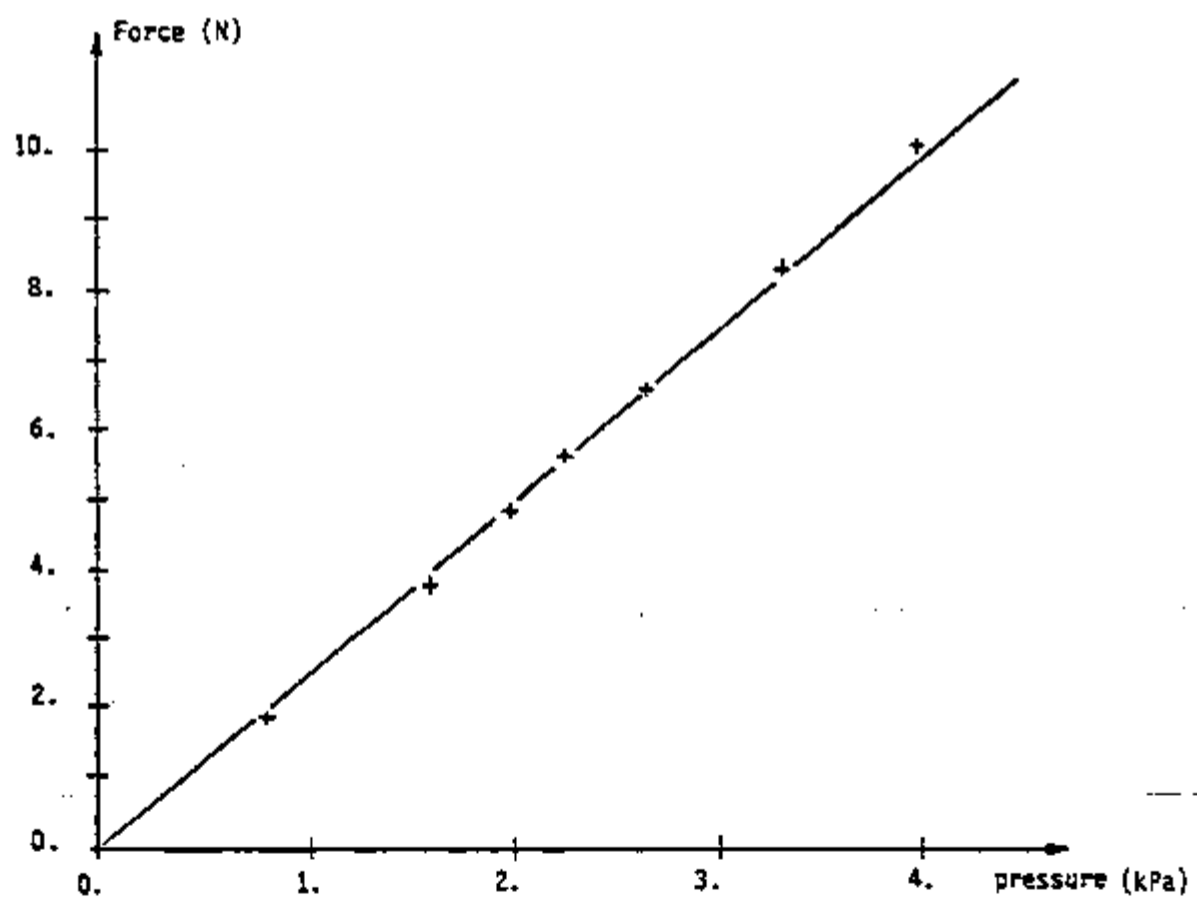
Figure 3-5. Determination of effective area for the sensing element

installed in a system made of plexiglas that simulated the two

pressure chambers of the transducer. The section simulating the low

pressure chamber was open to the atmosphere. The system was

pressurized with helium to create the displacement, and suddenly

depressurized. The result of the experiment is shown in Figure 3-6.

We note that according to Figure 3-6 the motion of the sensing

element is very slow when compared with the motion of a single

corrugated plate. The reason for the slow response is that there is a

viscous fluid that fills the internal space of the element. The

purpose of the viscous fluid is to damp the motion of the element, but

it also increases the inertia of the system.

The perturbation applied to the element is a negative step.

For this negative step in pressure and no reaction force ($\delta F_1 = 0$),

Equation 3-2 gives:

$$\delta u_1(t) = C_1 \left[1 - \frac{s_2 e^{s_1 t} - s_1 e^{s_2 t}}{(s_2 - s_1)} \right] \tag{3-3}$$

where C_1 is a constant and s_1 and s_2 are the roots of

$$I_{se} s^2 + C_{se} s + K_{se} = 0.$$

A least squares fit of Equation 3-3 to the result shown in

Figure 3-6 resulted in C_{se} equal to $3.78*10^4$ Nsec/m and I_{se} equal to

$5.68*10^2$ Nsec^2/m.

The initial sudden decrease present in Figure 3-6 was

attributed to the elastic properties of the plexiglas ring used to

hold the diaphragm. The effect decreased considerably when less

pressure was applied to the system.

relative
position of
central portion of
sensing element

• • fitted points

0.   1.   2.   3.   4.   5.   time
(sec)
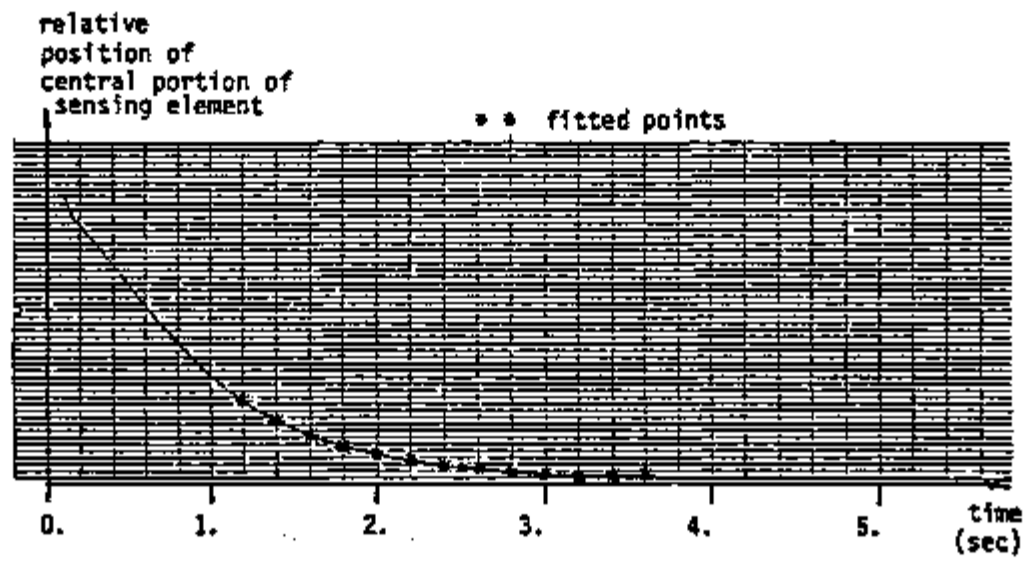
Figure 3-6.   Response of the sensing element to a step
perturbation

The experimental work was performed with the diaphragm removed from the transducer, and repeated with another diaphragm recently bought from The Foxboro Company. The new diaphragm was of the same type as the one installed in the transducer. The result obtained with the new diaphragm was very similar to the result obtained with the original one.

3.2.2 Flexural system (C-flexure)

The flexural system is composed of 6 beams arranged in a symmetrical geometry. For purposes of analysis the flexural system is divided into elements, with each beam as an element. The division is shown in Figure 3-7, where the encircled number is used to identify each element. Since the number 1 was used to identify the sensing element (diaphragm), the first element of the flexural system is defined as element number 2. Figure 3-7 also shows the coordinates of the extremes of each element. According to the adopted coordinate system (see Figure 3-1), the flexural system is located on the plane of constant Y, equal to y_7. Figure 3-8 shows the forces that act on each element. The parameters for the flexural system are given on Table 3-1.

Element number 2 is the beam that connects the flexural system to the spool of the sensing element. It is very small, and during transients it can undergo longitudinal vibrations.

Using Equation B-12 from appendix B the motion of a cross section plane originally at x, in Laplace domain, is given by:
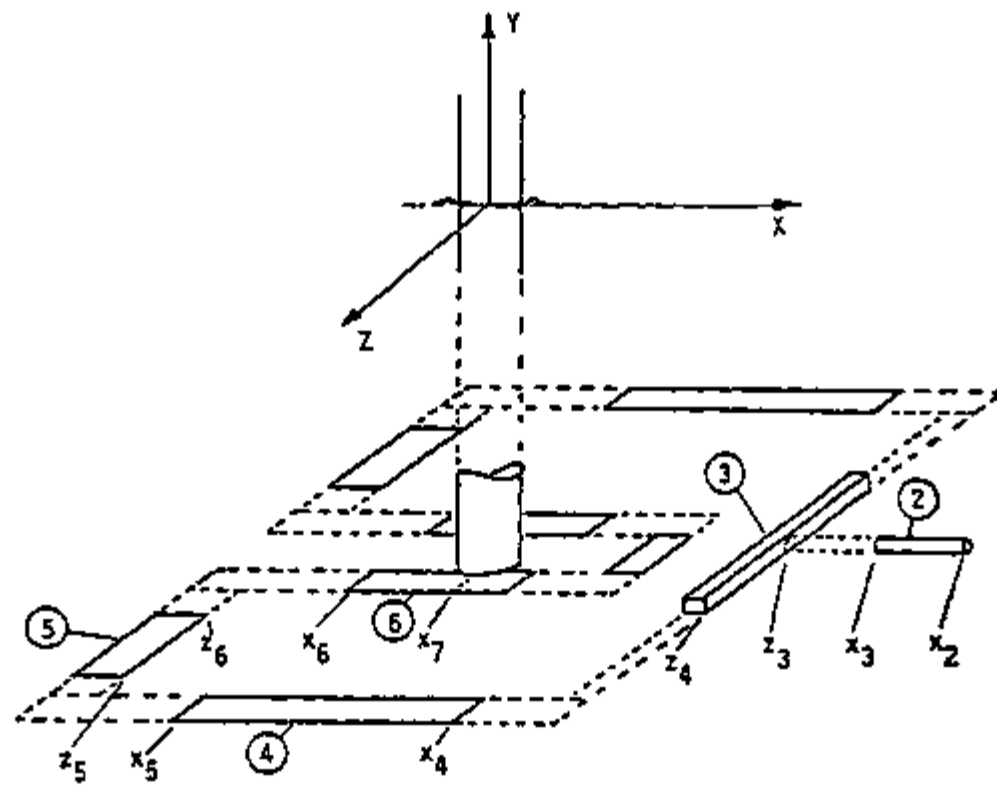
Figure 3-7. Division of flexural system into elements
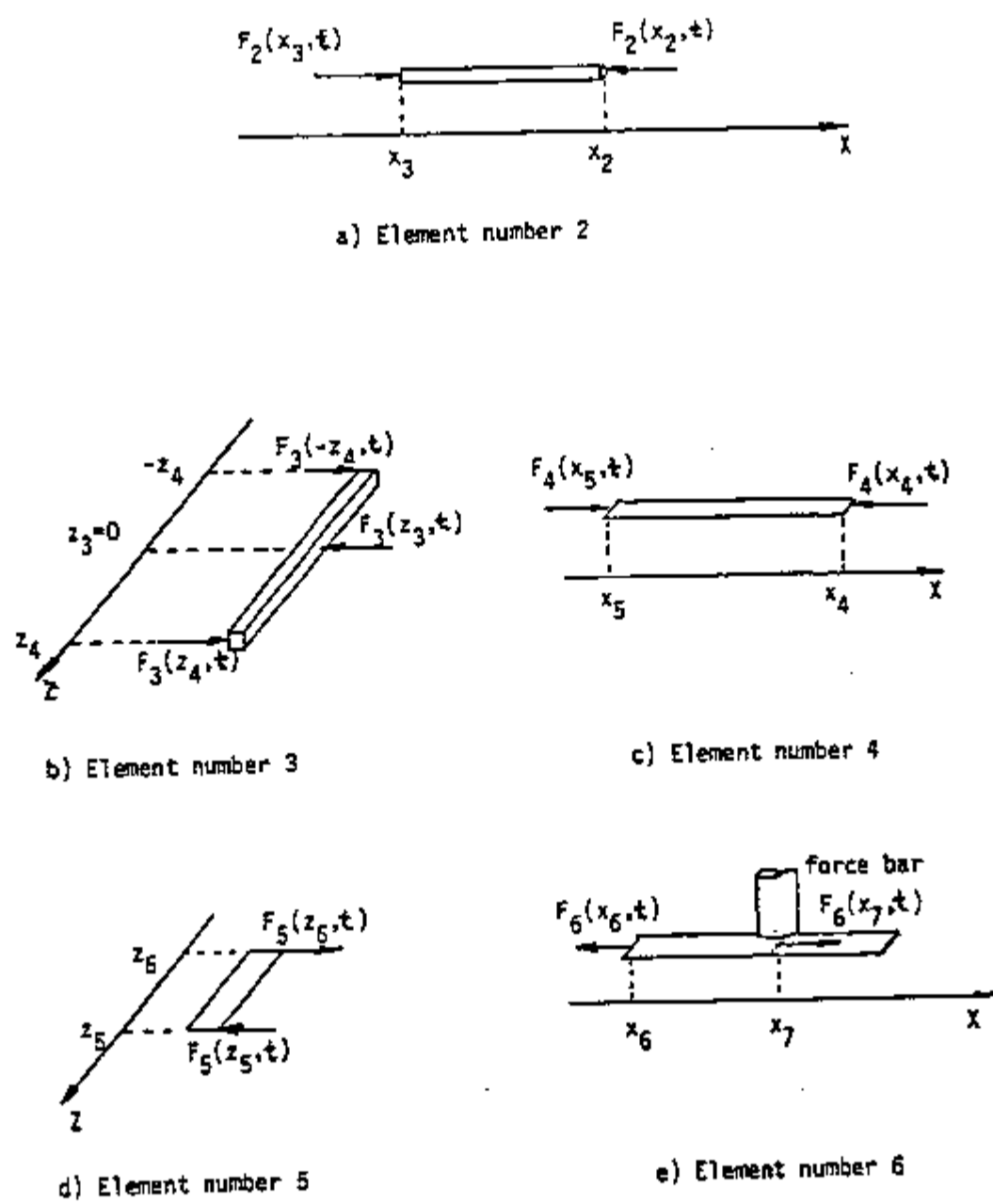
Figure 3-8. Forces acting on the elements of the flexural system

Table 3-1. Parameters for flexural system

General: Material. . . . . 316 Stainless Steel

Elasticity Modulus[*](E). . . . . . $1.93*10^{11}$ N/m^2

Density[*](ρ) . . . . $6.*10^3$ Kg/m^3

Thickness . . . . .36 mm

Element number 2

Length (L_2) . . . . 2.3 mm

Cross sectional area (A_2) . . . . . . 22.8 mm^2

Element number 3

Length (L_3) . . . . 30.2 mm

Cross sectional area (A_3) . . . . . . 7.4 mm^2

Inertia moment of area (I_3) . . . . . 2.7 mm^4

Element number 4

Length (L_4) . . . . 17.5 mm

Cross sectional area (A_4) . . . . . . 1.7 mm^2

Element number 5

Length (L_5) . . . . 11.4 mm

Cross sectional area (A_5) . . . . . . 1.8 mm^2

Inertia moment of area (I_5) . . . . . 3.6 mm^4

Shear Modulus (G) . . . . $7.5*10^{10}$ N/m^2

Geometric Factor[**](K) 5/6

Element number 6

Length (L_6) . . . . 6.3 mm

Cross sectional area (A_6) . . . . . . 1.8 mm^2

* from ref. 23
** from ref. 24

$$\delta u_2(x,s) = \frac{c_2}{sA_2E_2} \frac{\{\delta F_2(x_3,s)\cosh[(x-x_2)\frac{s}{c_2}] - \delta F_2(x_2,s)\cosh[(x-x_3)\frac{s}{c_2}]\}}{\sinh \ (\frac{sL_2}{c_2})}$$

(3-4)

where $c_2 = \sqrt{\frac{E_2}{\rho_2}}$

the forces $\delta F_2(x_2,s)$ and $\delta F_2(x_3,s)$ are as shown in Figure 3-8a, and the subindex 2 is to indicate that the parameters are for element number 2.

For the points of interest (x_2,y_2,z_2) and (x_3,y_3,z_3) Equation 3-4 may be simplified as follows:

$$\delta u_2(x_2,s) = a(2,2)\delta F_2(x_2,s) + a(2,3)\delta F_2(x_3,s)$$

(3-5)

$$\delta u_2(x_3,s) = b(2,2)\delta F_2(x_2,s) + b(2,3)\delta F_2(x_3,s)$$

(3-6)

where

$$a(2,2) = -b(2,3) = -\frac{c_2 \cosh \ (\frac{sL_2}{c_2})}{sA_2E_2\sinh \ (\frac{sL_2}{c_2})}$$

(3-7)

and

$$a(2,3) = -b(2,2) = \frac{c_2}{sA_2E_2\sinh \ (\frac{sL_2}{c_2})}$$

(3-8)

Element number 3 is symmetric with respect to the plane $z=0$, and the forces acting on it are assumed to be applied as shown in

Figure 3-8b. During transients it can undergo transversal vibrations.

Since the cross sectional dimensions are smaller than the length of the element, the Euler-Bernoulli formulation (25) is applicable. Equation B-31 from Appendix B is the general solution for the vibration of the beam in the region where there is no force being applied:

$$\delta u_3(z,s) = B_1(s)e^{\sqrt{jsc_3}\,z} + B_2(s)e^{-\sqrt{jsc_3}\,z} + B_3(s)e^{j\sqrt{jsc_3}\,z} + B_4(s)e^{-j\sqrt{jsc_3}\,z}$$

$$(3-9)$$

where $c_3 = \sqrt{\dfrac{\rho_3 A_3}{E_3 I_3}}$

and $j = \sqrt{-1}$.

For point $z=0$ Equation B-32 from Appendix B and the symmetry condition are used to obtain:

$$2E_3 I_3 \left. \frac{\partial^3 \delta u_3(z,s)}{\partial z^3} \right|_{z=0} = -\delta F_3(0,s) \qquad (3-10)$$

where the negative sign is used because the force is being applied in the direction opposite to δu.

For point $z=z_4$ the technique of images is used. A symmetric element is assumed to be connected to element number 3 and a force equal to two times the original is assumed. Then the application of Equation B-32 gives:

$$-E_3 I_3 \left. \frac{\partial^3 \delta u_3(z,s)}{\partial z^3} \right|_{z \,=\, z_4} = \delta F_3(z_4,s) \tag{3-11}$$

Using the condition of continuity for $\delta u_3(z,s)$ Equations 3-10 and 3-11 become two of the four boundary conditions needed to solve Equation 3-9. Due to the restraint imposed by element number 4 that is connected to element number 3, we can assume a relative clamped edge situation, in the sense that element number 3 is clamped by the element number 4. This gives the third boundary condition. The fourth boundary condition is obtained by assuming symmetry and continuity of the first derivative of $\delta u_3(z,s)$ about point $z = 0$. The two last conditions are mathematically expressed as:

$$\left. \frac{\partial \delta u_3(z,s)}{\partial z} \right|_{z \,=\, z_4} = 0 \tag{3-12}$$

and

$$\left. \frac{\partial \delta u_3(z,s)}{\partial z} \right|_{z \,=\, 0} = 0 \tag{3-13}$$

Using Equations 3-10 through 3-13 as boundary conditions for Equation 3-9 we obtain:

$$\delta u_3(z,s) = \{ [\delta F_3(z_4,s)\sin\nu_3 z\sinh\nu_3 z - \frac{\delta F_3(z_3,s)}{2} \sin\nu_3(z-z_4)\sinh\nu_3(z-z_4)]*$$

$$*[\sin\nu_3 z_4 \cosh\nu_3 z_4 - \cos\nu_3 z_4 \sinh\nu_3 z_4] +$$

$$[\delta F_3(z_4,s)\cos\nu_3 z\cosh\nu_3 z - \frac{\delta F_3(z_3,s)}{2} \cos\nu_3(z-z_4)\cosh\nu_3(z-z_4)]*$$

$$\frac{*[\sin\nu_3 z_4 \cosh\nu_3 z_4 + \cos\nu_3 z_4 \sinh\nu_3 z_4]\}}{E_3 I_3 (\sqrt{sc_3})^3 \sqrt{2} \ [\sin^2\nu_3 z_4 + \sinh^2\nu_3 z_4]} \tag{3-14}$$

where $\nu_3 = \sqrt{\dfrac{sc_3}{2}}$

As it was done for element number 2 the equation above is developed for the points of interest (x_3, y_3, z_3) and (x_4, y_4, z_4) in a simplified way:

$$\delta u_3(z_3,s) = a(3,3)\delta F_3(z_3,s) + a(3,4)\delta F_3(z_4,s) \tag{3-15}$$

$$\delta u_3(z_4,s) = b(3,3)\delta F_3(z_3,s) + b(3,4)\delta F_3(z_4,s) \tag{3-16}$$

where $a(3,3)$, $a(3,4)$, $b(3,3)$ and $b(3,4)$ are functions of s obtained from Equation 3-14.

As can be seen in Figures 3-8a and 3-8c, the situation for element number 4 is the same as for element number 2. It undergoes longitudinal vibrations. By analogy with element number 2 the motion of element number 4 is given by:

$$\delta u_4(x,s) = \frac{c_4}{sA_4E_4} \frac{\{\delta F_4(x_5,s)\cosh[(x-x_4)\frac{s}{c_4}] - \delta F_4(x_4,s)\cosh[(x-x_5)\frac{s}{c_4}]\}}{\sinh(\frac{sL_4}{c_4})}$$

$$(3-17)$$

where $c_4 = \sqrt{\dfrac{E_4}{\rho_4}}$

For the points of interest, (x_4, y_4, z_4) and (x_5, y_5, z_5), we have:

$$\delta u_4(x_4,s) = a(4,4)\delta F_4(x_4,s) + a(4,5)\delta F_4(x_5,s) \qquad (3-18)$$

$$\delta u_4(x_5,s) = b(4,4)\delta F_4(x_4,s) + b(4,5)\delta F_4(x_5,s) \qquad (3-19)$$

where

$$a(4,4) = -b(4,5) = -\frac{c_4 \cosh(\frac{sL_4}{c_4})}{sA_4E_4 \sinh(\frac{sL_4}{c_4})} \qquad (3-20)$$

and

$$a(4,5) = -b(4,4) = \frac{c_4}{sA_4E_4 \sinh(\frac{sL_4}{c_4})} \qquad (3-21)$$

Element number 5 undergoes transversal vibrations. Due to the fact that the cross sectional dimensions of the element are comparable to the length, the Euler-Bernoulli formulation is not suitable. Instead, Timoshenko's formulation is appropriate (26). The dynamic equations for this formulation are explained in Appendix B, and repeated here:

$$E_5 I_5 \frac{\partial^2 \delta\psi(z,s)}{\partial z^2} + KGA_5 \frac{\partial \delta u_5(z,s)}{\partial z} - [KGA_5 + Js^2]\delta\psi(z,s) = 0 \qquad (3\text{-}22)$$

$$\rho_5 A_5 s^2 \delta u_5(z,s) - KGA_5 \frac{\partial^2 \delta u_5(z,s)}{\partial z^2} + KGA_5 \frac{\partial \delta\psi(z,s)}{\partial z} = \delta F_5(z,s) \quad (3\text{-}23)$$

The parameters K, G, J and the variable ψ are defined in Appendix B.

We assume that the forces applied on element number 5 are as shown in Figure 3-8d. For the region between points z_5 and z_6, where there is no force being applied, Equations 3-22 and 3-23 are solved using the following procedure:

1- differentiate Equation 3-23 with respect to z, and obtain

$\frac{\partial^2 \delta\psi(z,s)}{\partial z^2}$ as a function of $\frac{\partial \delta u_5(z,s)}{\partial z}$ and $\frac{\partial^3 \delta u_5(z,s)}{\partial z^3}$

2- substitute $\frac{\partial^2 \delta\psi(z,s)}{\partial z^2}$ obtained in step 1 into Equation 3-22 to obtain:

$$\frac{\partial^3 \delta u_5(z,s)}{\partial z^3} + [\frac{KGA_5}{E_5 I_5} - \frac{\rho_5 s^2}{KG}]\frac{\partial \delta u_5(z,s)}{\partial z} - [\frac{KGA_5 + Js^2}{E_5 I_5}]\delta\psi(z,s) = 0 \quad (3\text{-}24)$$

3- differentiate Equation 3-24 with respect to z and substitute $\frac{\partial \delta\psi(z,s)}{\partial z}$ from Equation 3-23 into the result to obtain:

$$\frac{\partial^4 \delta u_5(z,s)}{\partial z^4} - [\frac{\rho_5 s^2}{KG} + \frac{Js^2}{E_5 I_5}] \frac{\partial^2 \delta u_5(z,s)}{\partial z^2} + \frac{\rho_5 s^2[KGA_5 + Js^2]}{KGE_5 I_5} \delta u_5(z,s) = 0$$

$$(3-25)$$

The general solution of Equation 3-25 is:

$$\delta u_5(z,s) = B_1(s)e^{d_1 z} + B_2(s)e^{-d_1 z} + B_3(s)e^{d_2 z} + B_4(s)e^{-d_2 z} \qquad (3-26)$$

where

$$d_n = \frac{\{(\frac{\rho_5 s^2}{KG} + \frac{Js^2}{E_5 I_5}) + (-1)^n [(\frac{\rho_5 s^2}{KG} - \frac{Js^2}{E_5 I_5})^2 - \frac{4\rho_5 A_5 s^2}{E_5 I_5}]^{1/2}\}^{1/2}}{\sqrt{2}}$$

$$\text{for } n = 1,2$$

To determine the constants B_i ($i=1,2,3,4$), we need four boundary conditions. The first one is obtained by analysing point $z=z_5$. For point $z=z_5$, we use the same technique used in element number 3. Assume a symmetric beam connected to element number 5 at point z_5 and a force with twice the value of $\delta F_5(z_5,s)$. With this configuration we integrate Equation 3-25 in the interval Δz about z_5 and take the limit as Δz goes to zero, to obtain:

$$\lim_{\Delta z \to 0} \{-KGA_5 [\frac{\partial \delta u_5(z,s)}{\partial z} - \delta\psi(z,s)]\} \Big|_{z_5 - \Delta z}^{z_5 + \Delta z} = -2\delta F_5(z_5,s) \qquad (3-27)$$

Assuming conditions of symmetry and continuity for functions

$\delta u_5(z,s)$ and $\delta\psi(z,s)$ at point $z=z_5$, and using $\delta\psi(z,s)$ from Equation 3-24 the following boundary condition is obtained for $\delta u_5(z,s)$ at $z=z_5$:

$$[-\frac{\partial^3 \delta u_5(z,s)}{\partial z^3} + (\frac{Js^2}{E_5 I_5} + \frac{\rho_5 s^2}{KG}) \frac{\partial \delta u_5(z,s)}{\partial z}]_{z=z_5} = -\frac{(KA_5 G + Js^2)}{E_5 I_5 A_5 KG} \delta F_5(z_5,s)$$

(3-28)

Similarly for point $z=z_6$ we obtain:

$$[\frac{\partial^3 \delta u_5(z,s)}{\partial z^3} - (\frac{Js^2}{E_5 I_5} + \frac{\rho_5 s^2}{KG}) \frac{\partial \delta u_5(z,5)}{\partial z}]_{z=z_6} = \frac{(KA_5 G + Js^2)}{E_5 I_5 A_5 KG} \delta F_5(z,s)$$

(3-29)

Equation 3-29 is the second boundary condition that must be satisfied by $\delta u_5(z,s)$. To obtain the two other boundary conditions we assume a relative clamped end situation (as it was done with element number 3). This condition is mathematically expressed as:

$$\frac{\partial \delta u_5(z,s)}{\partial z} \Big|_{z = z_5} = 0$$

(3-30)

$$\frac{\partial \delta u_5(z,s)}{\partial z} \Big|_{z = z_6} = 0$$

(3-31)

Using the four boundary conditions described by Equations 3-28 through 3-31 the solution for $\delta u_5(z,s)$ is:

$$\delta u_5(z,s) = \frac{d_1 d_2}{(d_2^2 - d_1^2)\rho_5 A_5 s^2} \left\{ \left[\frac{d_1 \cosh[d_2(z-z_6)]}{\sinh(d_2 L_5)} - \frac{d_2 \cosh[d_1(z-z_6)]}{\sinh(d_1 L_5)} \right] \delta F_5(z_5, s) \right.$$

$$\left. - \left[\frac{d_1 \cosh[d_2(z-z_5)]}{\sinh(d_2 L_5)} - \frac{d_2 \cosh[d_1(z-z_5)]}{\sinh(d_1 L_5)} \right] \delta F_5(z_6, s) \right\}$$

$$(3\text{-}32)$$

For the points of interest (x_5, y_5, z_5) and (x_6, y_6, z_6) we have:

$$\delta u_5(z_5, s) = a(5,5)\delta F_5(z_5, s) + a(5,6)\delta F_5(z_6, s) \qquad (3\text{-}33)$$

$$\delta u_5(z_6, s) = b(5,5)\delta F_5(z_5, s) + b(5,6)\delta F_5(z_6, s) \qquad (3\text{-}34)$$

where the coefficients are obtained by comparison with Equation 3-32 when solved for the respective points.

Element number 6 must now be modelled for the flexural system. Except for the orientation of the forces element number 6 is similar to elements 2 and 4, and by analogy we have:

$$\delta u_6(x,s) = \frac{c_6}{s A_6 E_6} \frac{\left\{ \delta F_6(x_7, s)\cosh[(x-x_6)\frac{s}{c_6}] - \delta F_6(X_6, s)\cosh[(x-x_7)\frac{s}{c_6}] \right\}}{\sinh(\frac{s L_6}{c_6})}$$

$$(3\text{-}35)$$

where $c_6 = \sqrt{\dfrac{E_6}{\rho_6}}$

For the points of interest (x_6, y_6, z_6) and (x_7, y_7, z_7) we have:

$$\delta u_6(x_6,s) = a(6,6)\delta F_6(x_6,s) + a(6,7)\delta F_6(x_7,s) \qquad (3-36)$$

$$\delta u_6(x_7,s) = b(6,6)\delta F_6(x_6,s) + b(6,7)\delta F_6(x_7,s) \qquad (3-37)$$

where

$$a(6,6) = -b(6,7) = -\frac{c_6 \cosh\left(\frac{sL_6}{c_6}\right)}{sA_6E_6 \sinh\left(\frac{sL_6}{c_6}\right)} \qquad (3-38)$$

and

$$a(6,7) = -b(6,6) = \frac{c_6}{sA_6E_6 \sinh\left(\frac{sL_6}{c_6}\right)} \qquad (3-39)$$

3.2.3 Force bar

The force bar is the beam system that transfers the force from the flexural system to a vector mechanism. It is supported at point $y=0$ by diaphragm (A), as shown in Figure 3-9, that works as a fulcrum point. The parameters for the force bar are given on Table 3-2.

The force bar is subject to three forces that act perpendicularly to the beam, and under transients it undergoes transversal vibrations. According to Equation B-31 from appendix B the general solution for the vibration of the bar is:
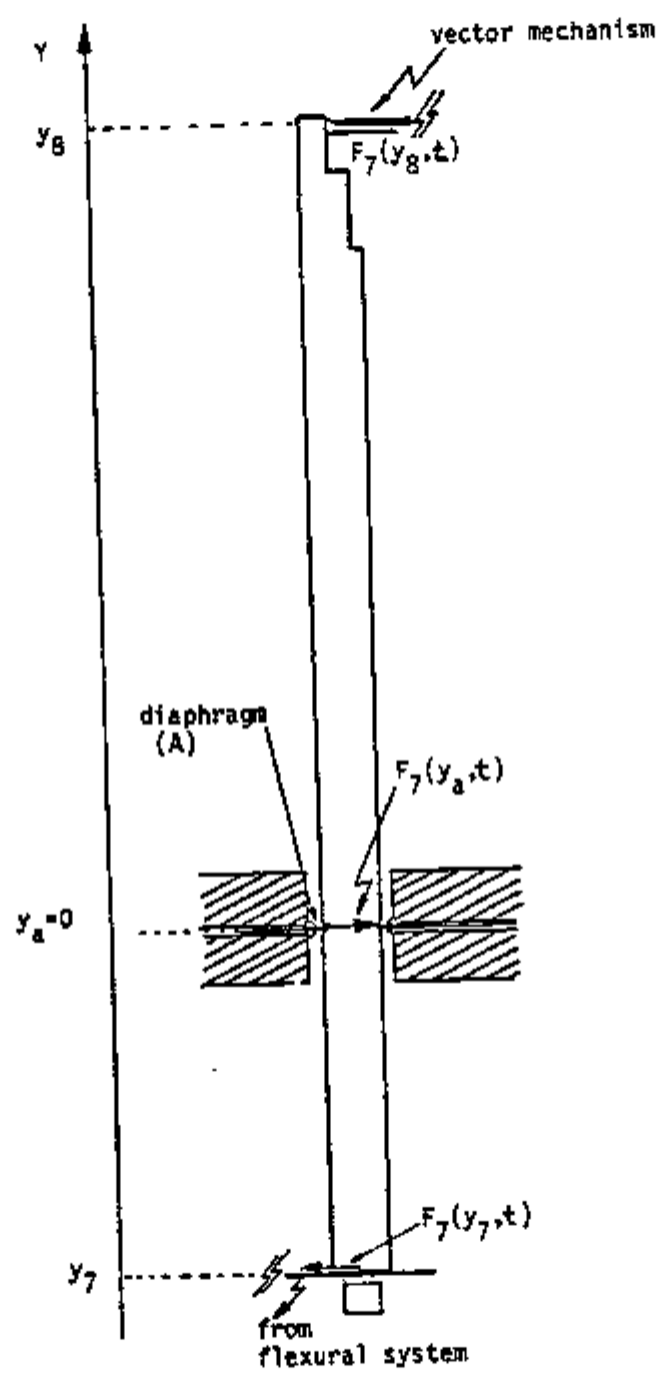
Figure 3-9. Forces acting on the force bar

Table 3-2. Parameters for force bar

Material.	Stainless Steel
Elasticity Modulus*(E).	$1.93*10^{11}$ N/m^2
Density*(ρ)	$8.*10^3$ Kg/m^3
Length $y_7 y_a$	72.2 mm
Length $y_a y_8$	119.8 mm
Cross Sectional area (A_7)	164.5 mm^2
Inertia Moment of area (I_7)	$2.2*10^3$ mm^4

* from ref. 23

$$\delta u_7(y,s) = B_1(s)e^{\sqrt{jsc_7}\ y} + B_2(s)e^{-\sqrt{jsc_7}\ y} + B_3(s)e^{j\sqrt{jsc_7}\ y} + B_4(s)e^{-j\sqrt{jsc_7}\ y}$$

$$\text{for } y_7 < y < y_a \qquad\qquad (3\text{-}40)$$

and

$$\delta u_7(y,s) = B_5(s)e^{\sqrt{jsc_7}\ y} + B_6(s)e^{-\sqrt{jsc_7}\ y} + B_7(s)e^{j\sqrt{jsc_7}\ y} + B_8(s)e^{-j\sqrt{jsc_7}\ y}$$

$$\text{for } y_a < y < y_8 \qquad\qquad (3\text{-}41)$$

where $c_7 = \sqrt{\dfrac{\rho_7 A_7}{E_7 I_7}}$ and $j = \sqrt{-1}$.

For the end points of the beam, that are under the action of forces, we use the condition of continuity for $\delta u_7(y,s)$ and make use of Equation B-32 from Appendix B to obtain the following boundary conditions:

$$E_7 I_7 \left.\frac{\partial^3 \delta u_7(y,s)}{\partial y^3}\right|_{y=y_7} = -\delta F_7(y_7,s) \qquad\qquad (3\text{-}42)$$

$$-E_7 I_7 \left.\frac{\partial^3 \delta u_7(y,s)}{\partial y^3}\right|_{y=y_8} = -\delta F_7(y_8,s) \qquad\qquad (3\text{-}43)$$

The remaining boundary conditions, necessary to obtain the functions $B_i(s)$ $(i=1,2,\ldots,8)$, are obtained by assuming:

    1- there is no bending moment being applied at the extremes of the bar.

2- zero displacement at $y=y_a$.

3- continuity of moment at $y=y_a$.

4- continuity of slope at $y=y_a$.

These conditions are mathematically expressed as:

$$\frac{\partial^2 \delta u_7(y,s)}{\partial y^2}\bigg|_{y=y_7} = 0 \tag{3-44}$$

$$\frac{\partial^2 \delta u_7(y,s)}{\partial y^2}\bigg|_{y=y_8} = 0 \tag{3-45}$$

$$\lim_{\Delta y \to 0} \delta u_7(y,s)\bigg|_{y_a-\Delta y} = 0 \tag{3-46}$$

$$\lim_{\Delta y \to 0} \delta u_7(y,s)\bigg|_{y_a+\Delta y} = 0 \tag{3-47}$$

$$\lim_{\Delta y \to 0} \frac{\partial^2 \delta u_7(y,s)}{\partial y^2}\bigg|_{y_a+\Delta y} = \lim_{\Delta y \to 0} \frac{\partial^2 \delta u_7(y,s)}{\partial y^2}\bigg|_{y_a-\Delta y} \tag{3-48}$$

$$\lim_{\Delta y \to 0} \frac{\partial \delta u_7(y,s)}{\partial y}\bigg|_{y_a+\Delta y} = \lim_{\Delta y \to 0} \frac{\partial \delta u_7(y,s)}{\partial y}\bigg|_{y_a-\Delta y} \tag{3-49}$$

With these conditions, the final results for Equations 3-40 and 3-41 are:

$$\delta u_7(y,s) = \frac{\delta F_7(y_8 s)}{\Gamma} (\cosh p \sin p + \cos p \sinh p)*$$

$$*[\sinh\phi\cos q\cos(q-\phi) + \sin\phi\cosh q\cosh(q-\phi)]$$

$$+ \frac{\delta F_7(y_7,s)}{\Gamma} \{(\cosh^2 p + \cos^2 p)(\sinh q\cos q\sinh\phi\cos\phi + \cosh q\sin q\sin\phi\cosh\phi)$$

$$- (\cosh p\sinh p - \sin p\cos p)[\sinh\phi\cosh q\cos(q-\phi) - \sin\phi\cos q\cosh(q-\phi)]\}$$

$$\text{for } y_7 < y < y_a \qquad (3\text{-}50)$$

and

$$\delta u_7(y,s) = \frac{\delta F_7(y_7,s)}{\Gamma}(\cosh q\sin q + \cos q\sinh q)*$$

$$*[\sinh\phi\cos p\cos(p-\phi) + \sin\phi\cosh p\cosh(p-\phi)]$$

$$+ \frac{\delta F_7(y_8,s)}{\Gamma} \{(\cosh^2 q + \cos^2 q)(\sinh p\cos p\sinh\phi\cos\phi + \cosh p\sin p\sin\phi\cosh\phi)$$

$$- (\cosh q\sinh q - \sin q\cos q)[\sinh\phi\cosh p\cos(p-\phi) - \sin\phi\cos p\cosh(p-\phi)]\}$$

$$\text{for } y_a < y < y_8 \qquad (3\text{-}51)$$

where

$$\Gamma = 2E_7 I_7 (\frac{c_7 s}{2})^{3/2} [(\sin p\cos p - \sinh p\cosh p)(\cos^2 q + \cosh^2 q)$$
$$+ (\sinh q\cosh q - \cos q\sin q)(\cosh^2 p + \cos^2 p)]$$

$$q = \sqrt{\frac{c_7 s}{2}} \; y_7; \qquad p = \sqrt{\frac{c_7 s}{2}} \; y_8 \qquad \text{and} \qquad \phi = \sqrt{\frac{c_7 s}{2}} \; y$$

For the points of interest (x_7, y_7, z_7) and (x_8, y_8, z_8) we obtain:

$$\delta u_7(y_7,s) = a(7,7)\delta F_7(y_7,s) + a(7,8)\delta F_7(y_8,s) \qquad (3-52)$$

$$\delta u_7(y_8,s) = b(7,7)\delta F_7(y_7,s) + b(7,8)\delta F_7(y_8,s) \qquad (3-53)$$

where $a(7,7)$ and $a(7,8)$ are functions of s obtained from Equation 3-50, and $b(7,7)$ and $b(7,8)$ are obtained from Equation 3-51.

3.2.4 Vector mechanism

Figure 3-10 shows a distorted schematic of the vector mechanism. It shows only the lower and inner-upper parts (the definition of these parts is given in section 2.2), which are the parts that determine the dynamic behavior of the mechanism.

In Figure 3-10, points (x_g,y_g) and (x_b,y_b) are connected by a thin plate with the purpose of allowing bending to occur. The same is valid for points (x_d,y_d) and (x_e,y_e); and points (x_f,y_f), and (x_h,y_h). The other elements of the mechanism can be assumed to be rigid parts. The parameters for the vector mechanism are given on Table 3-3.

From a dynamic point of view, the part that needs to be analyzed is the element limited by points (x_g,y_g), (x_d,y_d) and (x_9,y_9). This element will be referred to as transferring element.

The forces acting on the transferring element are $F_8(x_8,t)$, $F_8(y_9,t)$, $F_8(x_d,y_d,t)$, $F_a(t)$ and $F_b(t)$. $F_8(x_8,t)$ is the force transmitted from the force-bar to the vector mechanism, $F_8(y_9,t)$ is the reaction to the force that the mechanism transfers to the next subsystem, and $F_8(x_d,y_d,t)$ is the force that is transmitted to the upper part of the mechanism.
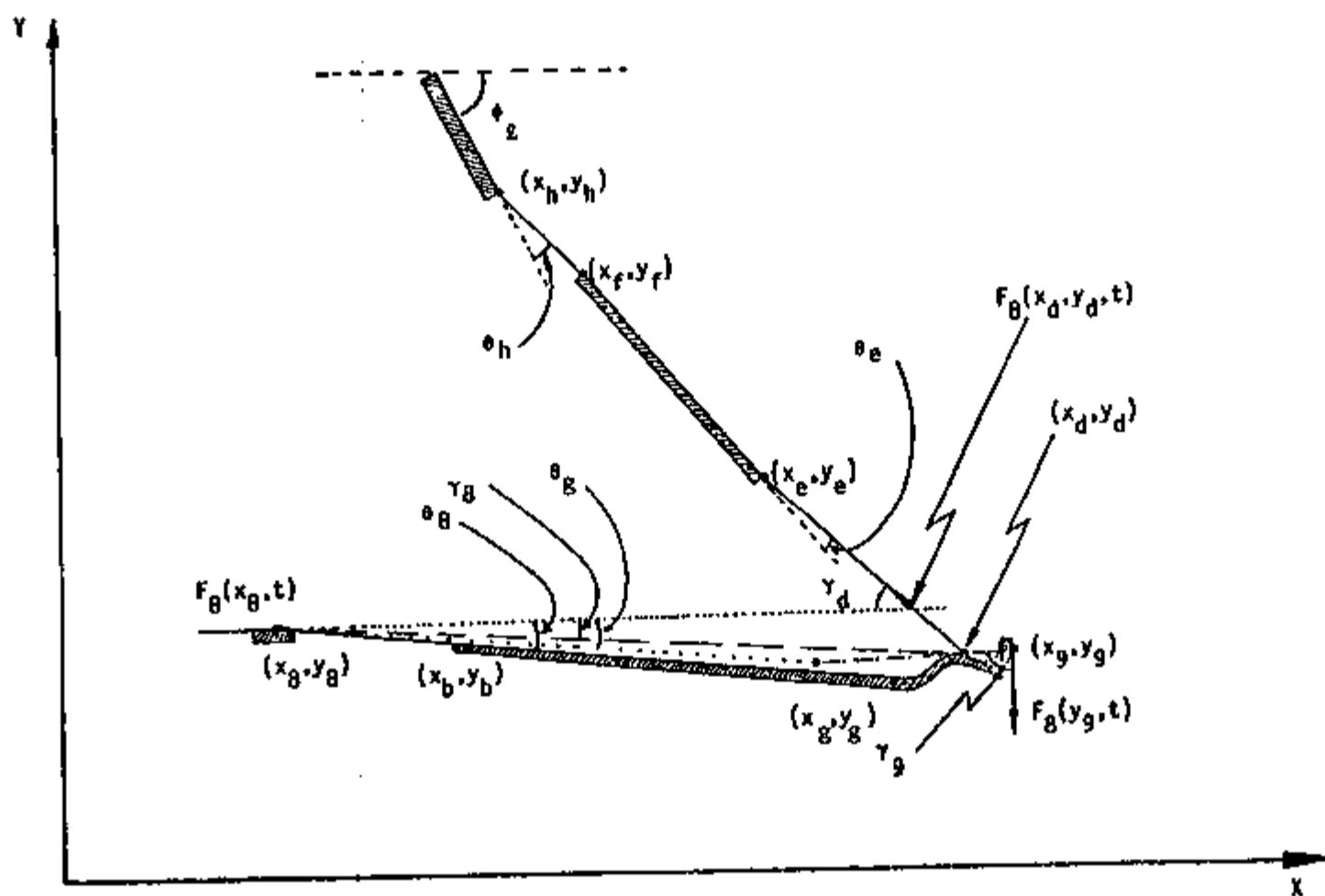
Figure 3-10. Vector Mechanism

Table 3-3. Parameters for vector mechanism

General :	Material.	Ni-Span C
	Elasticity Modulus*(E). . .	$2.07*10^{11}$ N/m^2
	Density*.	$8.3*10^3$ Kg/m^3
Section I	Thickness	.13mm
	Length.	4.8 mm
	Cross sectional area. . . .	1.6 mm^2
	Inertia moment of area. . .	$2.1*10^{-3}$ mm^4
Section I	Thickness	1.6mm
	Length.	43.2 mm
	Cross sectional area. . . .	20. mm^2
	Inertia moment of area. . .	4.1 mm^4
Section III	Thickness	.13 mm
	Length.	4.8 mm
	Cross sectional area. . . .	1.6 mm^2
	Inertia moment of area. . .	$2.1*10^{-3}$ mm^4
Section IV	Thickness	.26 mm
	Length.	2.8 mm
	Cross sectional area. . . .	3.2 mm^2
	Inertia moment of area. . .	$1.7*10^{-2}$ mm^4
Section V	Thickness	1.6mm
	Length.	76.0 mm
	Cross sectional area. . . .	22.0 mm^2
	Inertia moment of area. . .	5.0 mm^4

Table 3-3. (Continued)

Distances	$P_8 P_g$	44.0 mm
	$P_9 P_g$	35.0 mm
Angles	$\gamma_8(0)$	.025 rad
	ϕ_1	.184
	$\theta_h(0)$	0.
	$\theta_e(0)$	0.
	$\theta_g(0)$	.045
	$\gamma_d(0)$	.140
	$\theta_8(0)$	.055
	$\gamma_9(0)$	$\frac{\pi}{2} - .035$
Calculated Parameters		
	C_1	-1.07
	C_2	1.37
	C_3	- .011 m
	C_4	- .013 m
	C_5	- .044 m
	D_0	.44 N^{-1}
	D_1	8.45 $(Nm)^{-1}$
	D_2	.013 m^2
	D_3	- .068 m/N
	K_a	2.59 Nm/rad
	K_b	2.04 Nm/rad

* from ref. 23

To understand the nature of F_a and F_b, we divide the mechanism into two elements: a transferring element, already defined, and a supporting one, composed by the upper part of the mechanism. Both elements are shown in Figure 3-11. Figure 3-11 shows two new axis, w and μ. These axis indicate the direction of the supporting and transferring elements, respectively, during steady state condition.

To deflect the supporting element from its equilibrium position, a force is applied at point (x_d, y_d), as shown in Figure 3-11a. We recall that point (x_h, y_h) is a fixed point, and the sections $\overline{(x_f, y_f)(x_h, y_h)}$ and $\overline{(x_d, y_d)(x_e, y_e)}$ are thin plates that undergo bending action. The displacements involved are very small (fractions of millimeters), therefore the supporting element can be assumed to be a torsional spring, with the bending moment expressed as:

$$M = F_b w_d = K_b \theta_h \qquad (3-54)$$

where K_b = torsional constant of the spring

θ_h = angle of torsion

F_b = force applied at end of element and required to obtain the angle of torsion θ_h.

w_d = length of element.

The nature of F_a is the same, except that it is applied to the transferring element, and the pivoting point is now (x_g, y_g), as shown in Figure 3-11b.

With this explanation we can view F_b as a force being applied by the transferring element on the supporting element, and F_a as a force applied by the supporting element on the transferring element.
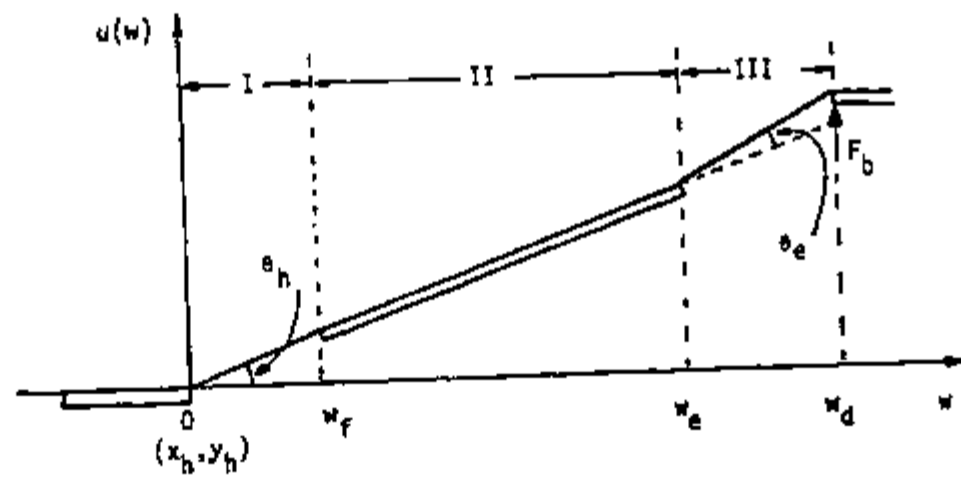
a) supporting element
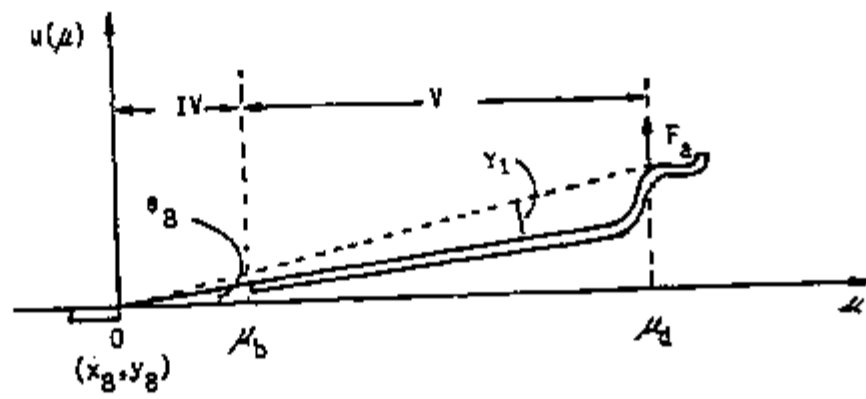
b) transferring element

Figure 3-11. Division of vector mechanism

K_b is a function of the structural properties and geometry of the supporting element. Once we have obtained K_b we use Equation 3-54 to obtain F_b as a function of θ_h. In order to determine K_b we assume that it is constant for both situations: static and dynamic. For steady state conditions Equation B-27 from Appendix B may be written as:

$$EI \frac{\partial^4 u(w)}{\partial w^4} = F(w) \tag{3-55}$$

At any point different from w_d $F(w)$ is equal to 0 and the solution of Equation 3-55 is:

$$u_I(w) = B_0 + B_1 w + B_2 w^2 + B_3 w^3 \quad \text{for } 0 < w < w_f \tag{3-56}$$

$$u_{II}(w) = B_4 + B_5 w + B_6 w^2 + B_7 w^3 \quad \text{for } w_f < w < w_e \tag{3-57}$$

$$u_{III}(w) = B_8 + B_9 w + B_{10} w^2 + B_{11} w^3 \quad \text{for } w_e < w < w_d \tag{3-58}$$

The subindexes I, II and III are used to identify the sections shown in Figure 3-11a.

To obtain the constants present in equations 3-56 through 3-58 we have the following boundary conditions:

1- clamped end at $w = 0$.

2- continuity of displacement at $w = w_f$ and w_e.

3- continuity of slope at $w = w_f$ and w_e.

4- continuity of bending moment at $w = w_f$ and w_e.

5- continuity of shear at $w = w_f$ and w_e.

6- relative clamped end at $w = w_d$.

These conditions are mathematically expressed as:

$$u_I(w=0) = 0 \qquad\qquad (3-59)$$

$$\left. \frac{\partial u_I(w)}{\partial w} \right|_{w = 0} = 0 \qquad\qquad (3-60)$$

$$u_I(w_f) = u_{II}(w_f) \qquad\qquad (3-61)$$

$$u_{II}(w_e) = u_{III}(w_e) \qquad\qquad (3-62)$$

$$\left. \frac{\partial u_I(w)}{\partial w} \right|_{w = w_f} = \left. \frac{\partial u_{II}(w)}{\partial w} \right|_{w = w_f} \qquad\qquad (3-63)$$

$$\left. \frac{\partial u_{II}(w)}{\partial w} \right|_{w = w_e} = \left. \frac{\partial u_{III}(w)}{\partial w} \right|_{w = w_e} \qquad\qquad (3-64)$$

$$E_I I_I \left. \frac{\partial^2 u_I(w)}{\partial w^2} \right|_{w = w_f} = E_{II} I_{II} \left. \frac{\partial^2 u_{II}(w)}{\partial w^2} \right|_{w = w_f} \qquad\qquad (3-65)$$

$$E_{II} I_{II} \left. \frac{\partial^2 u_{II}(w)}{\partial w^2} \right|_{w = w_e} = E_{III} I_{III} \left. \frac{\partial^2 u_{III}(w)}{\partial w^2} \right|_{w = w_e} \qquad\qquad (3-66)$$

$$E_I I_I \left. \frac{\partial^3 u_I(w)}{\partial w^3} \right|_{w = w_f} = E_{II} I_{II} \left. \frac{\partial^3 u_{II}(w)}{\partial w^3} \right|_{w = w_f} \qquad\qquad (3-67)$$

$$E_{II}I_{II} \left. \frac{\partial^3 u_{II}(w)}{\partial w^3} \right|_{w = w_e} = E_{III}I_{III} \left. \frac{\partial^3 u_{III}(w)}{\partial w^3} \right|_{w = w_e} \qquad (3\text{-}68)$$

$$\left. \frac{\partial u_{III}(w)}{\partial w} \right|_{w = w_d} = 0 \qquad (3\text{-}69)$$

To obtain the last boundary condition needed we use the technique of images to integrate Equation 3-55 about point w_d. Assume a symmetric element and a force with twice the value of F_b to obtain:

$$-E_{III}I_{III} \left. \frac{\partial^3 u_{III}(w)}{\partial w^3} \right|_{w = w_d} = F_b \qquad (3\text{-}70)$$

With conditions described by Equations 3-59 through 3-70 we obtain the constants B_i ($i=0,1,2,...11$) that substituted in Equations 3-56 through 3-58 give the following displacements for the points w_f, w_e and w_d:

$$u(w_f) = \frac{F_b w_f^2}{12(E_I I_I)} \left\{ 3 \frac{D_0}{D_1} - 2w_f \right\} \qquad (3\text{-}71)$$

$$u(w_e) = \frac{F_b w_e^2}{12(E_{II}I_{II})} \left\{ \frac{3D_0}{D_1} - 2w_e \right\} + \frac{F_b w_f}{12} \left\{ \frac{1}{(E_I I_I)} - \frac{1}{(E_{II}I_{II})} \right\} D_2 \qquad (3\text{-}72)$$

$$u(w_d) = \frac{F_b w_d^2}{12(E_{III}I_{III})} \left\{ \frac{3D_0}{D_1} - 2w_d \right\} + \frac{F_b}{12} D_3 \qquad (3\text{-}73)$$

where

$$D_0 = \frac{(w_d{}^2 - w_e{}^2)}{(E_{III}I_{III})} + \frac{(w_e{}^2 - w_f{}^2)}{(E_{II}I_{II})} + \frac{w_f{}^2}{(E_I I_I)}$$

$$D_1 = \frac{(w_d - w_e)}{(E_{III}I_{III})} + \frac{(w_e - w_f)}{(E_{II}I_{II})} + \frac{w_f}{(E_I I_I)}$$

$$D_2 = 4w_f{}^2 - 6w_f w_e + (6w_e - 3w_f)\frac{D_0}{D_1}$$

$$D_3 = w_f D_2 \left\{\frac{1}{(E_I I_I)} - \frac{1}{(E_{II}I_{II})}\right\} + w_e{}^2 \left\{\frac{3D_0}{D_1} - 2w_e\right\} \left\{\frac{1}{(E_{II}I_{II})} - \frac{1}{(E_{III}I_{III})}\right\}$$

$$+ \frac{6w_d}{E_{III}I_{III}} \left\{w_d - \frac{D_0}{D_1}\right\} \left\{w_d - w_e\right\}$$

Since the displacement $u(w_f)$ is very small (see Figure 3-11a), we can assume that:

$$\theta_h = \frac{u(w_f)}{w_f} \tag{3-74}$$

and Equation 3-54 can be rewritten as:

$$M_b = K_b \theta_h = F_b w_d = K_b \frac{u(w_f)}{w_f} \tag{3-75}$$

Using Equations 3-71 and 3-75 we obtain (Equations 3-72 and 3-73 will be used later):

$$(3-76)$$

$$K_b = \frac{12(E_I I_I)\ w_d\left[\dfrac{w_d - w_e}{(E_{III}I_{III})} + \dfrac{w_e - w_f}{(E_{II}I_{II})} + \dfrac{w_f}{(E_I I_I)}\right]}{w_f\left[\dfrac{3w_d^2 - 3w_e^2 - 2w_f w_d + 2w_f w_e}{(E_{III}I_{III})} + \dfrac{3w_e^2 - w_f^2 - 2w_e w_f}{(E_{II}I_{II})} + \dfrac{w_f^2}{(E_I I_I)}\right]}$$

As is was done for F_b, F_a can also be expressed in terms of a torsional spring constant K_a. To obtain K_a we use the same procedure as the one followed to obtain K_b. The situation for the transferring element is shown in Figure 3-11b, and the boundary conditions are:

1- clamped end at $\mu = 0$.

2- continuity of displacement at $\mu = \mu_b$.

3- continuity of slope at $\mu = \mu_b$.

4- continuity of bending moment at $\mu = \mu_b$.

5- continuity of shear at $\mu = \mu_b$.

6- shear equal to F_a at $\mu = \mu_d$.

The mathematical expressions for these boundary conditions are analogous to Equations 3-59 through 3-70, and the final result for the deflection of points μ_b and μ_d of the transferring element is:

$$u(\mu_b) = \frac{F_a \mu_b^2}{6}\left\{\frac{3\mu_d}{(E_{IV}I_{IV})} - \frac{\mu_b}{(E_V I_V)}\right\} \tag{3-77}$$

$$u(\mu_d) = \frac{F_a \mu_b}{6}\left\{\frac{1}{(E_{IV}I_{IV})} - \frac{1}{E_V I_V}\right\}\left\{2\mu_b^2 - 6\mu_b \mu_d + 6\mu_d^2\right\} + \frac{F_a \mu_d^3}{3(E_V I_V)} \tag{3-78}$$

The subindexes IV and V identify the sections shown in Figure 3-11b.

We define the torsional angle for the transferring element as being θ_g. Therefore, for the transferring element the bending moment can be expressed as $M = K_a\theta_g = F_a\mu_d$. Using the fact that the displacement $u(w_b)$ is very small we use for θ_g the same approach as used for θ_h in Equation 3-74, to obtain:

$$K_a = \frac{F_a\mu_d}{\theta_g} = \frac{F_a\mu_d}{u(\mu_b)/\mu_b} = \frac{6\mu_d/\mu_b}{[\frac{3\mu_d}{(E_{IV}I_{IV})} - \frac{\mu_b}{(E_VI_V)}]} \qquad (3-79)$$

The dynamics of the vector mechanism are now considered. Since F_a and F_b are forces that are applied perpendicularly to the transferring and supporting elements, respectively, the dynamic equations for the transferring element are:

$$M_t \frac{\partial^2 x_g(t)}{\partial t^2} = F_g(x_g,t) - F_g(x_d,y_d,t)\cos\gamma_d(t) -$$

$$\frac{K_a}{\mu_d}[\theta_g(p)-\theta_g(t)]\sin\gamma_g(t) - \frac{K_b}{w_d}[\theta_h(t)-\theta_h(p)]\sin\gamma_d(t) \qquad (3-80)$$

and

$$M_t \frac{\partial^2 y_g(t)}{\partial t^2} = - F_g(y_g,t) + F_g(x_d,y_d,t)\sin\gamma_d(t) -$$

$$\frac{K_a}{\mu_d}[\theta_g(p)-\theta_g(t)]\cos\gamma_g(t) - \frac{K_b}{w_d}[\theta_h(t)-\theta_h(p)]\cos\gamma_d(t) \qquad (3-81)$$

where M_t is the mass of the transferring element, x_g and y_g are the coordinates of its center of mass and $\theta(p)$ are the angles under which there is no bending moment being applied to the elements.

In order to obtain the transfer function of the mechanism, we have to combine Equations 3-80 and 3-81 to obtain only one equation relating $F_g(x_g,t)$, $F_g(y_g,t)$ and another variable that is needed to describe the position of the element. This variable was selected as θ_g, the angle between the horizontal axis and the line that connects point (x_g,y_g) with the center of mass of the transferring element (point (x_g,y_g) in Figure 3-10).

With this choice we start by deriving a relation between the geometric quantities present on Equations 3-80 and 3-81 and the angle θ_g. To obtain an equation in terms of deviation from equilibrium we assume that all quantities can be regarded as made up of an equilibrium portion plus a transient portion. For example, all angles can be assumed as

$$\theta(t) = \theta(0) + \delta\theta(t) \tag{3-82}$$

and since the values of $\delta\theta(t)$ are very small, the following geometric relations are accepted:

$$\cos[\theta(0) + \delta\theta(t)] = \cos\theta(0) - \sin\theta(0)\delta\theta(t) \tag{3-83}$$

$$\sin[\theta(0) + \delta\theta(t)] = \sin\theta(0) + \cos\theta(0)\delta\theta(t) \tag{3-84}$$

Using Equations 3-83, 3-84 and Figure 3-10 we obtain the following geometric expressions for the vector mechanism:

$$\overline{P_hP_e}\,\sin[\phi_\ell - \theta_h(0)]\,\delta\theta_h(t) + \overline{P_eP_d}\,\sin[\phi_\ell - \theta_h(0) - \theta_e(0)]*$$

$$[\delta\theta_h(t) + \delta\theta_e(t)] = \delta x_g(t) - \overline{P_gP_d}\,\sin\gamma_g(0)\delta\gamma_g(t) \tag{3-85}$$

$$\overline{P_h P_e} \cos[\phi_\ell - \theta_h(0)] \, \delta\theta_h(t) + \overline{P_e P_d} \cos[\phi_\ell - \theta_h(0) - \theta_e(0)]*$$

$$[\delta\theta_h(t) + \delta\theta_e(t)] = -\overline{P_g P_d} \cos\gamma_g(0)\delta\gamma_g(t) \tag{3-86}$$

Where $\overline{P_k P_1}$ represents the distance between points (x_k, y_k) and (x_1, y_1).

As explained in section 2.2 the upper-outer section of the vector mechanism is held fixed, therefore, the angle ϕ_ℓ is constant. Since the displacements involved are small we can approximate θ_e by

$$\theta_e = \frac{u(w_d) - u(w_e)}{w_d - w_e} - \frac{du(w)}{dw}\bigg|_{w=w_e}$$

The angle θ_h can also be approximated:

$$\theta_h = \frac{u(w_f)}{w_f}$$

Using expressions above for θ_e and θ_h and Equations 3-71 through 3-73, 3-83 and 3-84 we can relate the variation in θ_h as a function of the variation in θ_e:

$$\delta\theta_h(t) = C_1 \delta\theta_e(t) \tag{3-87}$$

where

$$C_1 = \frac{\dfrac{u(w_f)}{w_f}}{\dfrac{u(w_d) - u(w_e)}{(w_d - w_e)} - \dfrac{du(w)}{dw}\bigg|_{w = w_e}}$$

$$\frac{du(w)}{dw} = \frac{F_b w_e}{2(E_{II} I_{II})} \left[\frac{D_0}{D_1} - w_e\right] - \frac{F_b w_f}{2} \left[\frac{1}{(E_I I_I)} - \frac{1}{(E_{II} I_{II})}\right] \left[w_f - \frac{D_0}{D_1}\right]$$

and parameters D_0 and D_1 are defined in Equations 3-71 through 3-73.

Since $\delta\theta_g(t)$, $\delta\theta_g(t)$ and $\delta\gamma_g(t)$ are the same, we combine Equations 3-86 and 3-87 to obtain the variation in θ_e as a function of the variation in θ_g:

$$\delta\theta_e(t) = C_2 \delta\theta_g(t) \tag{3-88}$$

where

$$C_2 = \frac{-\overline{P_g P_d} \cos \gamma_g(0)}{C_1 \overline{P_h P_e} \cos[\phi_\ell - \theta_h(0)] + (C_1 + 1) \overline{P_e P_d} \cos[\phi_\ell - \theta_h(0) - \theta_e(0)]}$$

Once we have obtained $\delta\theta_e$ as a function of $\delta\theta_g$, we use Equations 3-87 and 3-88 to express $\delta\theta_h$ as a function of $\delta\theta_g$.

Before we relate the variation in x_g with the variation in θ_g we need to relate the variation in x_g with the variation in θ_g. Combining Equations 3-85, 3-87 and 3-88 we obtain:

$$\delta x_g(t) = C_3 \delta\theta_g(t) \tag{3-89}$$

where

$$C_3 = \overline{P_g P_d} \sin\gamma_g(0) + C_1 C_2 \overline{P_h P_e} \sin[\phi_\ell - \theta_h(0)]$$

$$+ (C_1 + 1) C_2 \overline{P_e P_d} \sin[\phi_\ell - \theta_h(0) - \theta_e(0)]$$

Now we relate the variations in x_g and y_g with the variation in θ_g. From a geometric analysis of Figure 3-10 combined with Equations 3-83, 3-84 and 3-89, we obtain:

$$\delta x_g(t) = C_4 \delta\theta_g(t) \qquad (3\text{-}90)$$

and

$$\delta y_g(t) = C_5 \delta\theta_g(t) \qquad (3\text{-}91)$$

where

$$C_4 = C_3 - \overline{P_8 P_g} \sin\theta_g(0)$$

and

$$C_5 = - \overline{P_8 P_g} \cos\theta_g(0)$$

With these relations we return our attention to Equations 3-80 and 3-81. To obtain the desired equation relating $F_8(x_8,s)$, $F_8(y_9,s)$ and $\theta_g(s)$ we start by substituting Equations 3-90 and 3-91 for the values of x_g and y_g in Equations 3-80 and 3-81. Then we perform the following steps:

1- multiply Equation 3-80 by $\cos\gamma_d(t)$ and subtract, from the result Equation 3-81 multiplied by $\sin\gamma_d(t)$.

2- use the perturbation formulation for all parameters present in the result of step 1 that are not constant.

3- use geometric approximations given by Equations 3-83 and 3-84 in result from step 2 to obtain:

$$M_t \left\{ [C_4 \cos\gamma_d(0) - C_5 \sin\gamma_d(0)] - [C_4 \sin\gamma_d(0) + C_5 \cos\gamma_d(0)] \delta\gamma_d(t) \right\} \frac{\partial^2 \delta\theta_g(t)}{\partial_t^2}$$

$$= -F_g(x_g,0)\sin\gamma_d(0)\delta\gamma_d(t) + \cos\gamma_d(0)\delta F_g(x_g,t) - \sin\gamma_d(0)\delta F_g(x_g,t)\delta\gamma_d(t)$$

$$+ F_g(y_g,0)\cos\gamma_d(0)\delta\gamma_d(t) + \sin\gamma_d(0)\delta F_g(y_g,t) + \cos\gamma_d(0)\delta F_g(y_g,t)\delta\gamma_d(t)$$

$$- \delta F_g(x_d,y_d,t) + \frac{K_a}{\mu_d}[\theta_g(p) - \theta_g(0)]\cos[\gamma_d(0) - \gamma_g(0)][\delta\gamma_d(t) - \delta\gamma_g(t)]$$

$$- \frac{K_a}{\mu_d}\sin[\gamma_d(0) - \gamma_g(0)]\delta\theta_g(t) - \frac{K_a}{\mu_d}\cos[\gamma_d(0) - \gamma_g(0)]\delta\theta_g(t)[\delta\gamma_d(t) - \delta\gamma_g(t)]$$

$$(3-92)$$

4- use the perturbation formulation in Equation 3-80.

5- use the geometric approximations biven by Equations 3-83 and 3-84 in the result of step 4 and multiply the result by $\cos\gamma_d(0)$.

6- use the perturbation formulation in Equation 3-81.

7- use the geometric approximation on the result of step 6 and multiply the result by $\sin\gamma_d(0)$.

8- subtract the result of step 7 from the result of step 5 to obtain:

$$M_t\{C_4\cos\gamma_d(0)-C_5\sin\gamma_d(0)\}\frac{\partial^2\delta\theta_g(t)}{\partial_t^2} =$$

$$\cos\gamma_d(0)\delta F_g(x_g,t) + \sin\gamma_d(0)\delta F_g(y_g,t) - \delta F_g(x_d,y_d,t)$$

$$- \frac{K_a}{u_d}[\theta_g(p)-\theta_g(0)]\cos[\gamma_d(0)-\gamma_g(0)]\delta\gamma_g(t)$$

$$- \frac{K_a}{u_d}\sin[\gamma_d(0)-\gamma_g(0)]\delta\theta_g(t) + \frac{K_a}{u_d}\cos[\gamma_d(0)-\gamma_g(0)]\delta\theta_g(t)\delta\gamma_g(t)$$

$$- \frac{K_b}{w_d}[\theta_h(0)-\theta_h(p)]\delta\gamma_d(t) - \frac{K_b}{w_d}\delta\gamma_d(t)\delta\theta_h(t) \qquad (3\text{-}93)$$

9- subtract Equation 3-93 from Equation 3-92.

10- Substitute $\delta\theta_h$ using Equations 3-87 and 3-88 into the result of step 9 and recall that $\delta\theta_g$, and $\delta\gamma_g$ are equal to $\delta\theta_g$.

11- Apply steady state condition (the variation of any variable at time $t=0$ is zero).

12- Laplace transform the result of step 11 to obtain:

$$-M_t\{C_4\sin\gamma_d(0) + C_5\cos\gamma_d(0)\}s^2\delta\theta_g(s) =$$

$$- \sin\gamma_d(0)\delta F_g(x_g,s) + \cos\gamma_d(0)\delta F_g(y_g,s)$$

$$+ \{\frac{K_b}{w_d}C_1C_2 - \frac{K_a}{u_d}\cos[\gamma_g(0) - \gamma_d(0)]\}\delta\theta_g(s) \qquad (3\text{-}94)$$

Using Equations 3-89, 3-94, and a geometric relation between $\delta y_g(t)$ and $\delta\theta g(t)$ the following equations are obtained:

$$\delta u_8(X_8,s) = \delta x_8(s) = a(8,8)\delta F_8(x_8,s) + a(8,9)\delta F_8(y_9,s) \qquad (3\text{-}95)$$

$$\delta u_8(y_9,s) = \delta y_9(s) = b(8,8)\delta F_8(x_8,s) + b(8,9)\delta F_8(y_9,s) \qquad (3\text{-}96)$$

where

$$a(8,8) = \frac{C_3 \sin\gamma_d(0)}{C_6}$$

$$a(8,9) = \frac{-C_3 \cos\gamma_d(0)}{C_6}$$

$$b(8,8) = -[\overline{P_8 P_g}\,\cos\theta_g(0) + \overline{P_9 P_g}\,\sin\gamma_9(0)]\,\frac{\sin\gamma_d(0)}{C_6}$$

$$b(8,9) = [\overline{P_8 P_g}\,\cos\theta_g(0) + \overline{P_9 P_g}\,\sin\gamma_9(0)]\,\frac{\cos\gamma_d(0)}{C_6}$$

and

$$C_6 = M_t[C_4 \sin\gamma_d(0) + C_5\cos\gamma_d(0)]s^2 + \frac{K_b}{w_d}C_1 C_2 - \frac{K_a}{u_d}\cos[\gamma_8(0) - \gamma_d(0)]$$

3.2.5 Connection

The connection element is a thin plate that connects the vector mechanism to the lever system. It converts the force transmitted from the vector mechanism into a moment on the lever system. The situation for the element is shown in Figure 3-12, and by analogy with element number 6 of the flexural system we obtain the following equation for its vibrational motion:
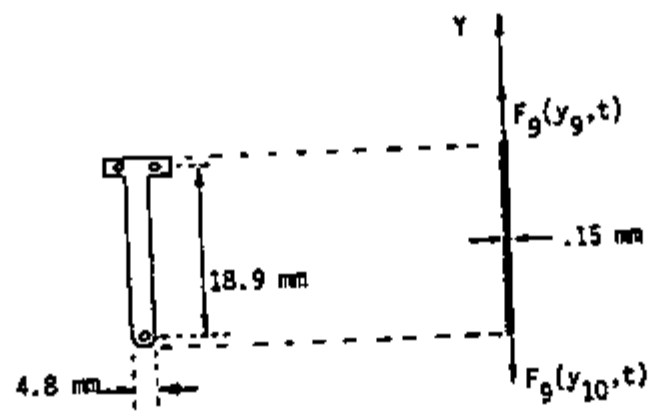
Figure 3-12. Connection

$$\delta u_9(y,s) = \frac{c_9}{sA_9E_9} \frac{\{\delta F_9(y_9,s)\cosh[(y-y_{10})\frac{s}{c_9}] - \delta F_9(y_{10},s)\cosh[(y-y_9)\frac{s}{c_9}]\}}{\sinh(\frac{sL_9}{c_9})}$$

(3-97)

where $c_9 = \sqrt{\frac{E_9}{\rho_9}}$

For the point of interest, (x_9,y_9,z_9) and (x_{10},y_{10},z_{10}), we have:

$$\delta u_9(y_9,s) = a(9,9)\delta F_9(y_9,s) + a(9,10)\delta F_9(y_{10},s)$$

(3-98)

$$\delta u_9(y_{10},s) = b(9,9)\delta F_9(y_9,s) + b(9,10)\delta F_9(y_{10},s)$$

(3-99)

where

$$a(9,9) = -b(9,10) = \frac{c_9 \cosh (\frac{sL_9}{c_9})}{sA_9E_9\sinh(\frac{sL_9}{c_9})}$$

(3-100)

$$a(9,10) = -b(9,9) = -\frac{c_9}{sA_9E_9\sinh(\frac{sL_9}{c_9})}$$

(3-101)

The material of the connection element was assumed to be Ni-Span C (the same as the bending parts of the vector mechanism). The parameters for the connection are shown in Figure 3-12.

3.2.6 - Lever system

The lever system is the last element of the mechanical system. Figure 3-13 shows the geometry and dimensions for the system. It is composed of a structure that rotates when under the action of a moment. This moment is the result of the application of three forces and a bendig moment. As explained in section 2.2 the three forces are: the force transmitted from the vector mechanism through the connection; the force due to the spring used for zero adjustments; and a magnetic force that is responsible for the balancing of the forces acting on the system. The bending moment is generated when the system leaves its equilibrium position, and is due to the configuraion of the pivoting point P shown in Figure 3-14.

Due to the dimensions of the system we can assume it to be a rigid body system whose dynamics are described by:

$$I_{\ell s} \frac{d^2 \psi(t)}{dt^2} + C_{\ell s} \frac{d\psi(t)}{dt} + M(t) = \tau(t) \tag{3-102}$$

where $I_{\ell s}$ is the inertia moment of mass for the system, $\psi(t)$ is its counterclockwise rotation angle, $C_{\ell s}$ is a damping coefficient, $M(t)$ is the bending reaction of the mechanism that composes the pivoting point P, and $\tau(t)$ is the resultant moment applied to the system. Figure 3-13 show the geometry and dimensions for the system.

Since the displacements involved are very small we can assume the pivoting point mechanism as a torsional spring, with the bending moment given by $M = K_{pv}\psi$, where K_{pv} is the constant of the torsional spring.
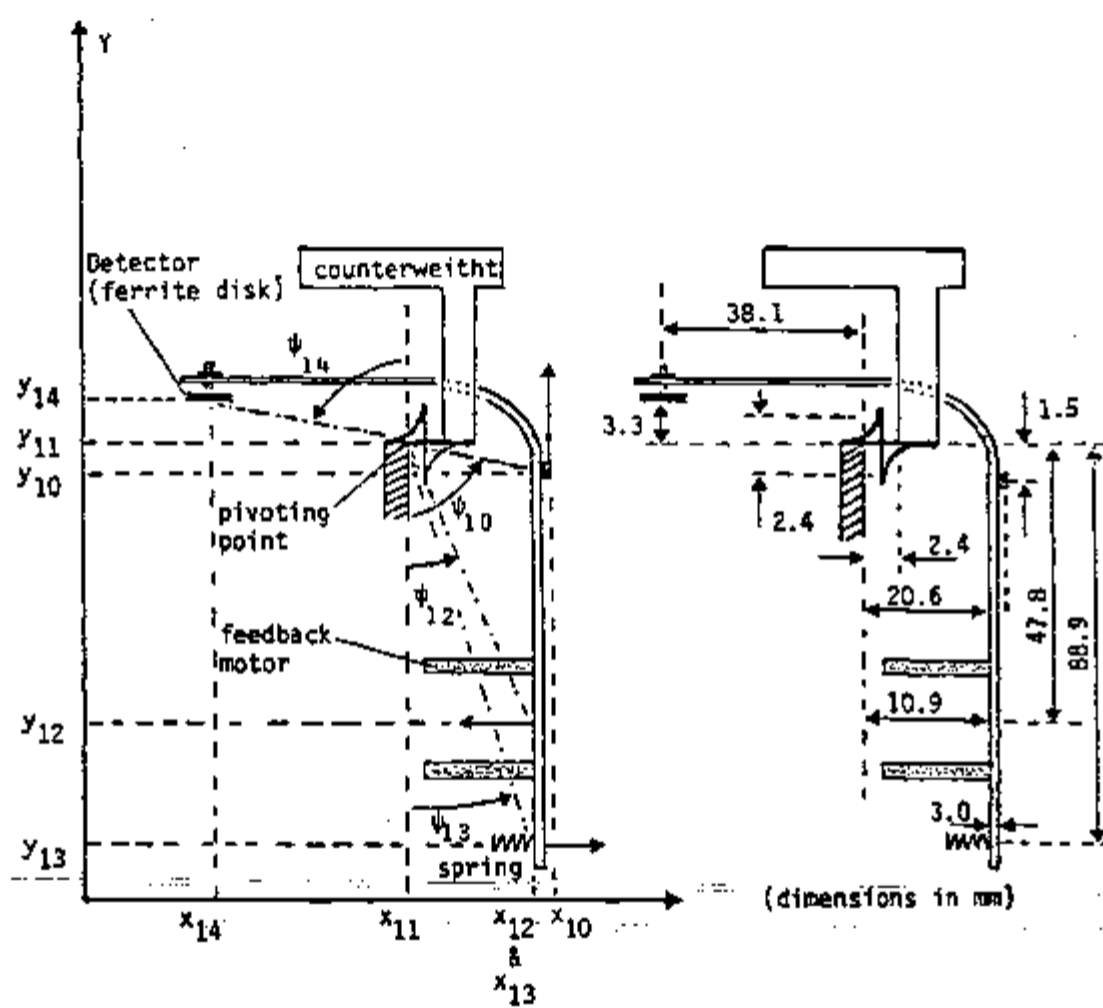
Figure 3-13. Lever system

The dimensions of the pivoting mechanism are shown in Figure 3-14. Its material is Ni-Span C.

Using the perturbation formulation, we can rewrite Equation 3-102 as:

$$I_{\ell s} \frac{d^2 \delta\psi(t)}{dt^2} + C_{\ell s} \frac{d\delta\psi(t)}{dt} + K_{pv} \delta\psi(t) = \delta\tau(t) \qquad (3\text{-}103)$$

Since the lever system is assumed to be a rigid body system, to which the ferrite disk is attached, we can relate the displacement $\epsilon(t)$ of the disk with the rotation $\psi(t)$. Using the approximation given by Equation 3-83 we obtain:

$$\delta\psi(t) = \frac{\delta\epsilon(t)}{\overline{P_{11}P_{14}} \, \sin\psi_{14}(0)} \qquad (3\text{-}104)$$

Where $\overline{P_{11}P_{14}}$ is the distance between points (x_{11}, y_{11}) and (x_{14}, y_{14}). For reasons that will be explained in section 3.3-3, $\delta\epsilon(t)$ is assumed positive if the ferrite disk approaches the detector (downward motion).

Substituting Equation 3-104 into Equation 3-103 and Laplace transforming the result we obtain:

$$\delta\epsilon(s) = \frac{\overline{P_{11}P_{14}} \, \sin\psi_{14}(0)}{[s^2 I_{\ell s} + K_{pv} + C_{\ell s} s]} \, \delta\tau(s) \qquad (3\text{-}105)$$

To obtain the value of K_{pv} we follow the same procedure as the one used in dealing with the thin plates of the vector mechanism: use
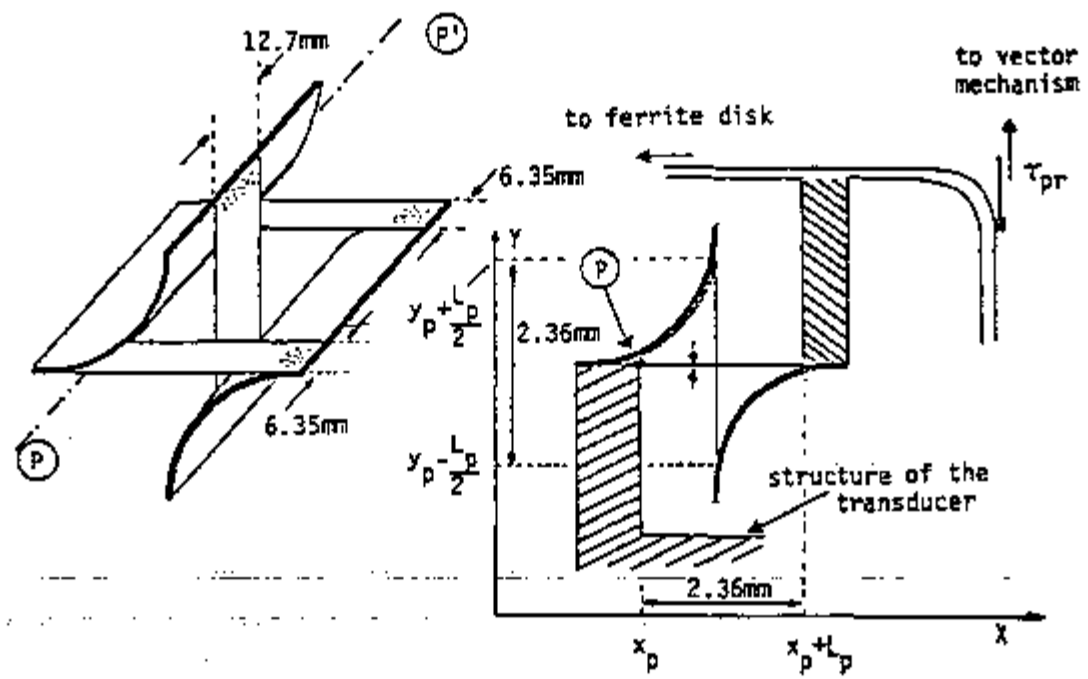
Figure 3-14.   Dimensions of pivoting point formation

static condition to determine how much each plate bends when under the action of a static force, then assume that the bending is the same for a dynamic force. For each plate $\underline{m}$ we determine the contribution $K_{pv}(m)$ of the plate to the total constant K_{pv}. Using Equation B-28 from Appendix B and the following boundary conditions (see Figure 3-14):

1- clamped end at $x = x_p$ and at $y = y_p + \dfrac{L_p}{2}$

2- free end at $x = x_p + L_p$ and at $y = y_p - \dfrac{L_p}{2}$

we obtain:

$$K_{pv}(m) = \frac{3E_m I_m}{L_m} \tag{3-106}$$

where E is the elasticity modulus and I is the inertia moment of area.

Associating all three plates gives:

$$K_{pv} = K_{pv}(1) + K_{pv}(2) + K_{pv}(3) \tag{3-107}$$

The obtained value for K_{pv} is 1.14 Nm.

The main source of damping for the lever system is the geometry of the force motor. As seen in Figure 2-1 (see page 10), the feedback coil combined with the magnet form a 'dash pot', with the internal space filled with air. Since the air gap separating the ferrite disk and the detector is very small, the motion of the disk also contributes to the damping of the motion.

To determine the effective damping coefficient $C_{\ell\theta}$, and the inertia moment of the system $I_{\ell\theta}$, an experiment was performed where the lever system was displaced from its equilibrium position and then

released. This perturbation is a step in the moment applied to the system. For a step perturbation in the moment Equation 3-103 gives the following solution for $\delta\psi(t)$:

$$\delta\psi(t) = A_1 \left\{ 1 - \frac{s_1 e^{s_2 t} - s_2 e^{s_1 t}}{(s_1 - s_2)} \right\} \qquad (3\text{-}108)$$

where A_1 is a constant and s_1 and s_2 are the roots of:

$$I_{\ell s} s^2 + C_{\ell s} s + K_{pv} +$$

$$K_{sp} \left\{ [\overline{P_{11}P_{13}} \cos\psi_{13}(0)]^2 - [\overline{P_{11}P_{13}} \sin\psi_{13}(0)]^2 \right\} = 0 \qquad (3\text{-}109)$$

The term in Equation 3-109 that contains K_{sp} represents the contribution to the moment due to the spring used for zero adjustment. Since a spring has a damping coefficient, it was found necessary to include it in the experiment performed to determine $C_{\ell s}$. Using the information present in section 3.3.1 and on Figure 3-13 the value of the term containing K_{sp} is obtained as .90 Nm.

If $\delta\psi(t)$ has an underdamped motion, the roots of Equation 3-109 are complex, and can be written as:

$$s_n = -a + (-1)^n jb \qquad \text{for } n=1,2$$

where $a = \dfrac{C_{\ell s}}{2I_{\ell s}}$

$$b = \sqrt{\frac{K_{pv} + K_{sp}\left\{[\overline{P_{11}P_{13}}\cos\psi_{13}(0)]^2 - [\overline{P_{11}P_{13}}\sin\psi_{13}(0)]^2\right\}}{I_{\ell s}} - \left(\frac{C_{\ell s}}{2I_{\ell s}}\right)^2}$$

and $j = \sqrt{-1}$.

Furthermore, if the motion is toward the equilibrium position, the final condition is $\lim_{t \to \infty} \delta\psi(t) = 0$. Using this condition $\delta\psi(t)$ can be written as:

$$\delta\psi(t) = A_2 e^{-at}[\frac{a}{b} \sin(bt) + \cos(bt)] \qquad (3\text{-}110)$$

where A2 is a constant.

The experiment to determine $C_{\ell s}$ and $I_{\ell s}$ was performed using positive and negative steps for the moment. The positive step was generated by moving the lever system toward the structure of the transducer and releasing it. The negative step was generated by moving the system toward the stopping point with subsequent release. The result of the experiment is shown in Figure 3-15. A least squares fit of Equation 3-110 to the data resulted in a=17.4 sec^{-1} and b=62.3 sec^{-1}. From these values we obtain:

$$I_{\ell s} = 4.9*10^{-4} \text{ Nmsec}^2$$

and $\quad C_{\ell s} = 1.7*10^{-2} \text{ Nmsec}^2.$

3.3 Transfer Functions of the Subsystems

The transfer functions shown in Figure 3-1 are now developed to complete the model. The procedure used to obtain the transfer functions is discussed in more details in section 4.3.

The transfer function is by definition a complex quantity. One way of presenting a transfer function is to show its magnitude as a function of the complex variable $s = a + jb$, where a and b are real and j is $\sqrt{-1}$. A computer program was written to calculate the real and imaginary parts for the transfer functions shown in Figure 3-1 at discrete values of s. A list of the program is given in Appendix D.
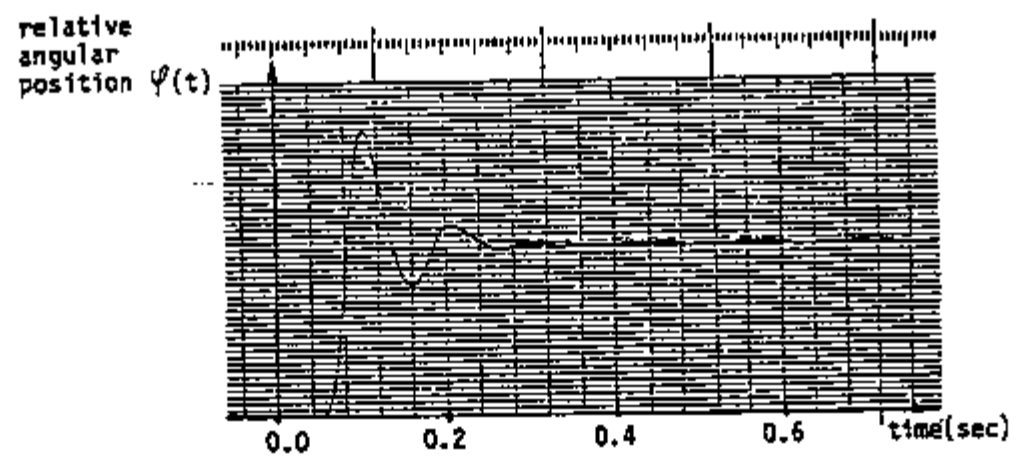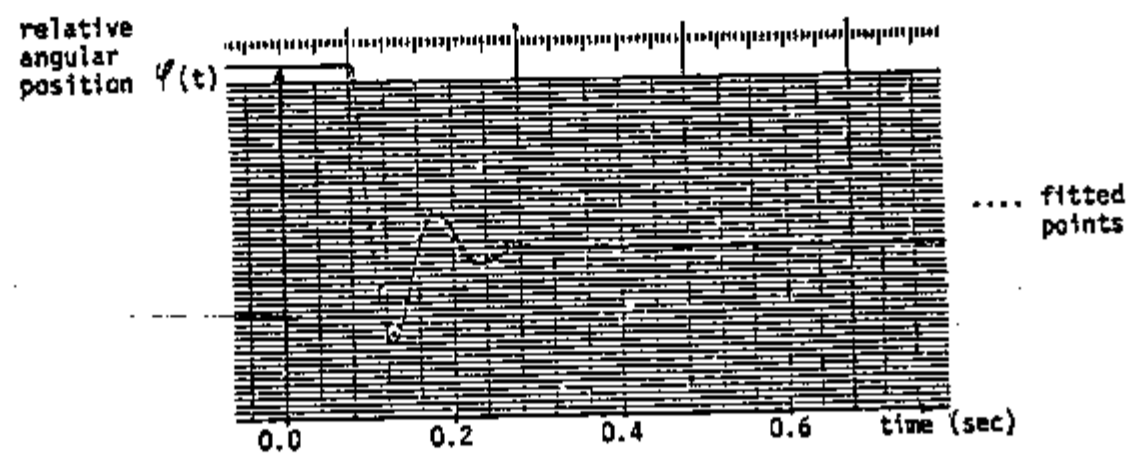
Figure 3-15. Response of the lever system to a step perturbation

Since the frequency response is the transfer function calculated at points $s=jw$ the same program was used to calculate the frequency response.

In transfer function calculations the output of the program is a list containing the magnitude of the transfer function for several values of a and b. The increment in the values of a is selected by the user. The same increment is used for b. For frequency response calculations the output is selected by the user. It can be magnitude of phase. The output of the program is stored in a datafile for subsequent processing. An output of the datafile for frequency response calculations is shown at the end of Appendix D.

A plotting subroutine developed at the Instrumentation and Controls Division of the Oak Ridge National Laboratory (27) was used to read the datafile and construct the plots shown in this section and in section 3.5. For results of transfer function the plots show the magnitude as a function of the real and imaginary parts of s. For results of frequency response (section 3.5) the plots show magnitude and phase as function of frequency.

3.3.1 Mechanical reaction

The mechanical reaction considered here is the moment generated by the reaction of the spring used for zero adjustment. The transfer function for the mechanical reaction, $G_{mr}(s)$, relates the moment created by the spring and the displacement of the ferrite disk. The spring is stretched when the lever system undergoes counterclockwise rotation and compressed under clockwise rotation. The magnitude of the moment is given by the magnitude of the vector product between,

the distance from the pivoting point to the point of application of the force, and the force applied by the spring. Since the force of the spring can be expressed as a constant times its displacement, the moment due to the mechanical reaction can be written as:

$$\tau_{mr}(t) = -K_{sp} \ [x_{13}(t) - x_{13}(0)] \ \overline{P_{11}P_{13}} \ \cos\psi_{13}(t) \tag{3-111}$$

The value of K_{sp}, the constant of the spring, was obtained by extending the spring with several suspended masses, and measuring its elongation. The results for such experiment, from which K_{sp} is determined as 115.6 N/m, are shown in Figure 3-16 (the manufacturer specifies Ksp as 122.6 N/m).

Using the fact that the variation in ψ_{13} is the same as the variation in ψ_{14} (see Figure 3-13 on page 79), we can relate the displacement of the ferrite disk with the displacement of the spring. Using Equations 3-83, 3-104, 3-111, perturbation formulation and Laplace transform we obtain:

$$G_{mr}(s) = \frac{\delta\tau_{mr}(s)}{\delta\varepsilon(s)} = -K_{sp} \ \frac{\{ \ [\overline{P_{11}P_{13}} \ \cos\psi_{13}(0)]^2 - [\overline{P_{11}P_{13}} \ \sin\psi_{13}(0)]^2 \}}{\overline{P_{11}P_{14}} \ \sin\psi_{14}(0)}$$

$$\tag{3-112}$$

Using the information present in Figure 3-13, the value for G_{mr} is -23.6 Nm/m.

3.3.2 Force motor

The transfer function for the force motor, G_{fm}, relates the moment generated by the DC current that flows through the transducer and the current. The current flows through a coil placed in a magne-
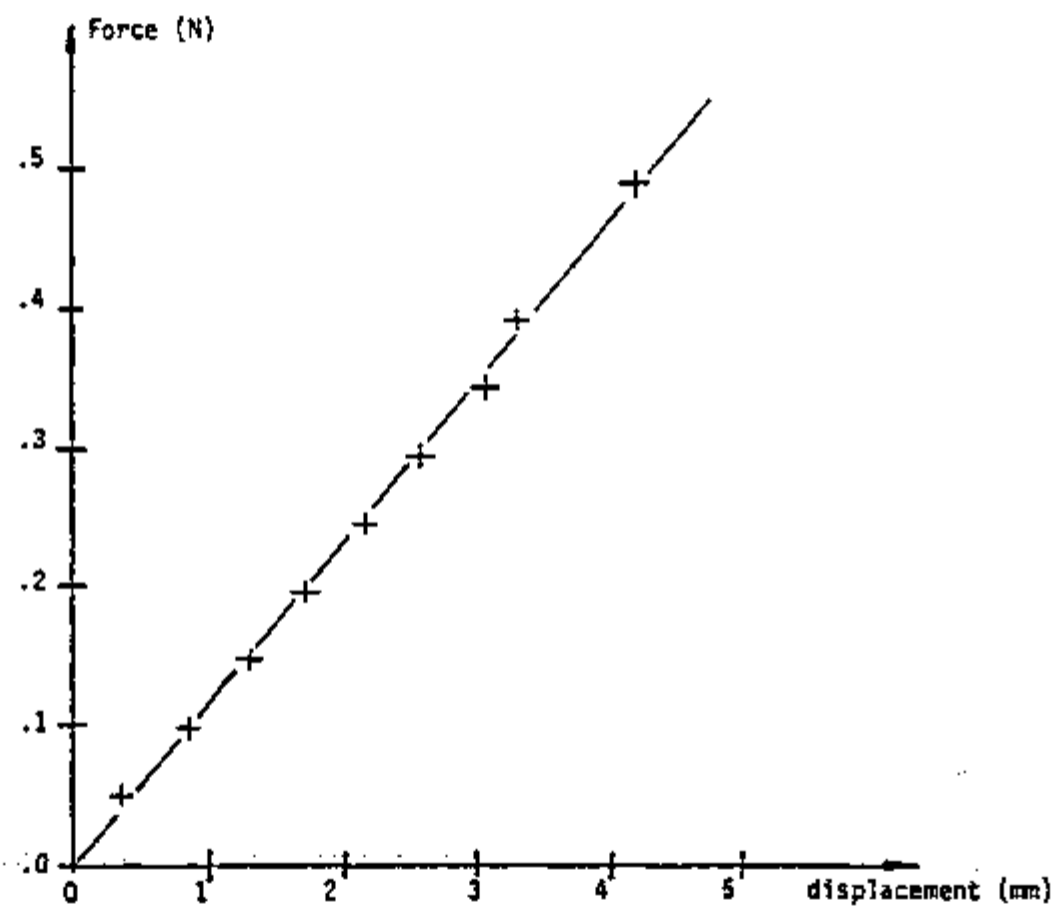
Figure 3-16. Determination of the constant for the
spring used for zero adjustment

tic field, generating a magnetic force. Any change in the current
causes the magnetic force to change, changing the moment that is
applied to the lever system. The moment due to the force motor is
given by:

$$\tau_{fm}(t) = -K_{fm}I_{dc}(t) \qquad (3-113)$$

where K_{fm} is a constant that depends on the number of turns in the coil
and the magnitude of the magnetic field in the region occupied by the
coil and $I_{dc}(t)$ is the DC current. The negative sign is used because
an increase in I_{dc} generates a negative moment (in the clockwise
direction). The effect of the current in the magnetic field during
transients is neglected.

Using the perturbation formulation and Laplace transforming
Equation 3-113 we obtain:

$$G_{fm}(s) = \frac{\delta\tau_{fm}(s)}{\delta I_{dc}(s)} = -K_{fm} \qquad (3-114)$$

The value of K_{fm} was obtained by applying a moment to the
lever system and measuring the current needed to balance the applied
moment. The moment was applied by compressing the spring used for zero
adjustment. The result for the experiment, from which K_{fm} was deter-
mined as $3.53*10^{-3}$ Nm/mA, is shown in Figure 3-17.

3.3.3 Electronics

Included on the electronic part of the transducer there are
diodes, transistors and magnetic cores. As seen in the literature
(21,28) a theoretical analysis of such components is very difficult.
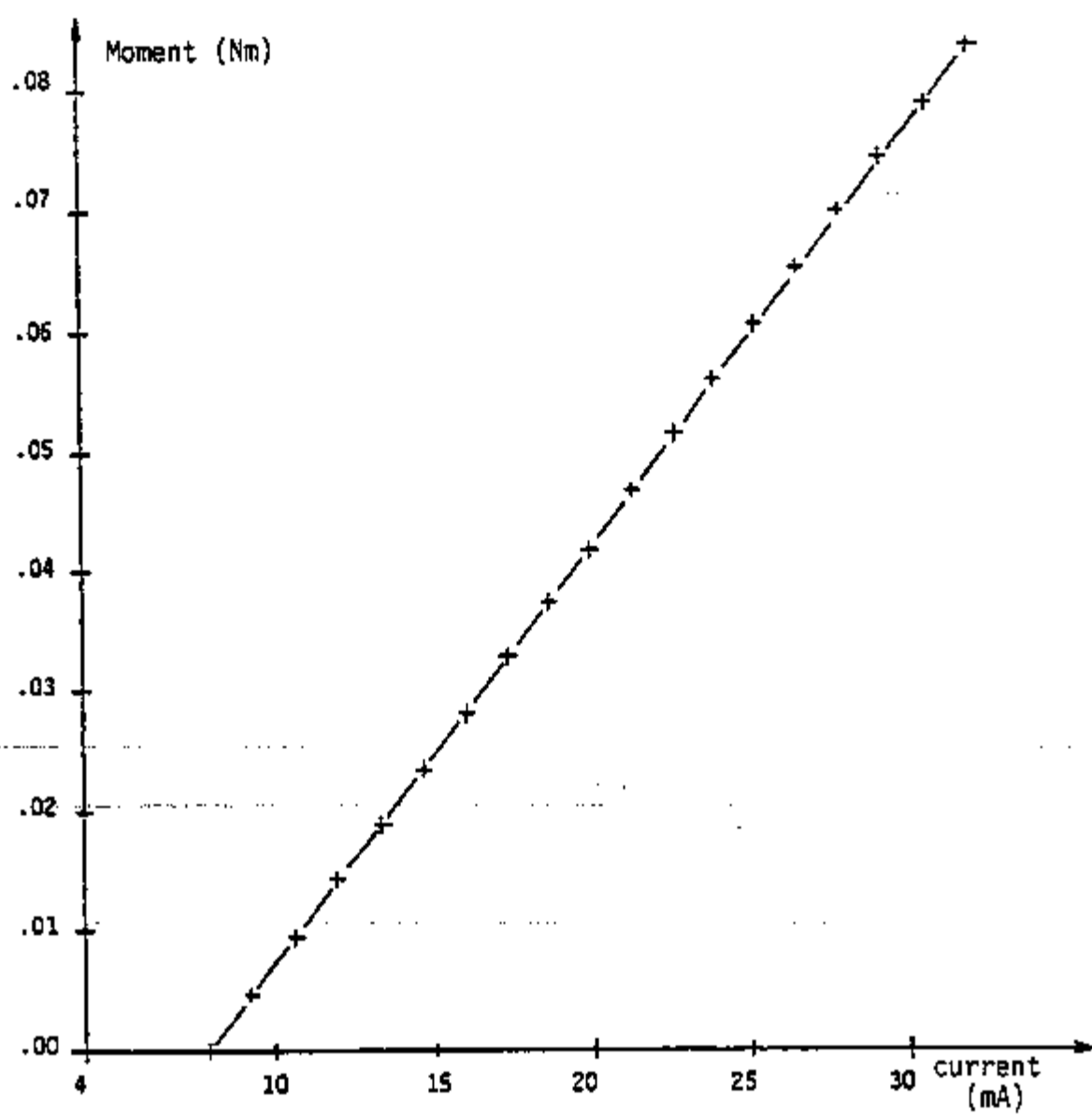
Figure 3-17. Determination of the constant for the force motor

In view of this it was found more practical to perform an experimental analysis to determine an empirical transfer function for the electronic system $(G_{e\ell})$. $G_{e\ell}$ relates the variation in the output DC current with the variation in the position of the ferrite disk.

A first estimate of $G_{e\ell}$ was obtained when it was observed that a step in the position of the ferrite disk (in the downward direction) generated an increasing output signal that for a small time interval was a linear function of the time. With this result it was assumed that $G_{e\ell}$ is inversely proportional to s:

$$G_{e\ell}(s) = \frac{\delta I_{dc}(s)}{\delta \epsilon(s)} = \frac{C_{e\ell}}{s} \tag{3-115}$$

where $C_{e\ell}$ is a positive constant.

Since the frequency response of a stable system is the transfer function calculated at points $s = 0 + jw$, an experiment was performed to determine the empirical transfer function for the electronic system based on its frequency response. The purpose of the experiment was to determine whether the assumption was right or not and to determine the value of $C_{e\ell}$.

The frequency response of a system can be obtained when the input and output signals are analyzed in the frequency domain. The conversion of the signal from the time domain to the frequency domain is usually performed with the Fast Fourier Transform algorithm (29), a standard feature of digital computers available for Fourier analysis.

A experimental arrangement was devised to generate a perturbation on the position of the ferrite disk. The perturbation consisted of rotating an eccentric cylinder seated on the upper part

of the disk support. In order to avoid the feedback effect of the lever system, the support where the disk was mounted was disconnected from the remainder of the lever system.

A proximitor probe was used to monitor the motion of the ferrite disk. It was a Bently Nevada model 3106-2800-190. It has a frequency range from DC up to 10 kHz, and its signal was assumed to be a correct indication of the position of the ferrite disk.

Since the probe had to be mounted above the disk support and since the output signal of the probe is directly proportional to the air gap separating the probe and the disk support, the measurement of $\frac{\partial \varepsilon(t)}{\partial t}$ is positive if the motion of the disk is in the downward direction. Therefore, $\delta \varepsilon(t)$ was adopted to be positive when the disk was below the equilibrium position.

The eccentric cylinder was rotated with the frequency being continuously changed. A record of the output from the transducer and from the proximitor probe was made and Fourier analized using a Hewlett-Packard Fourier Analyzer model 5420A. The result of the analysis is shown in Figures 3-18 through 3-20.

Part a) of Figures 3-18 through 3-20 show the Auto Power Spectral Density (APSD) of the signal from the proximitor probe (input signal). The APSD gives the power density as a function of frequency. It is an indication of how each component contributes to the total power of the signal.

Part b) of the Figures show the APSD of the DC output current from the electronic system of the transducer.
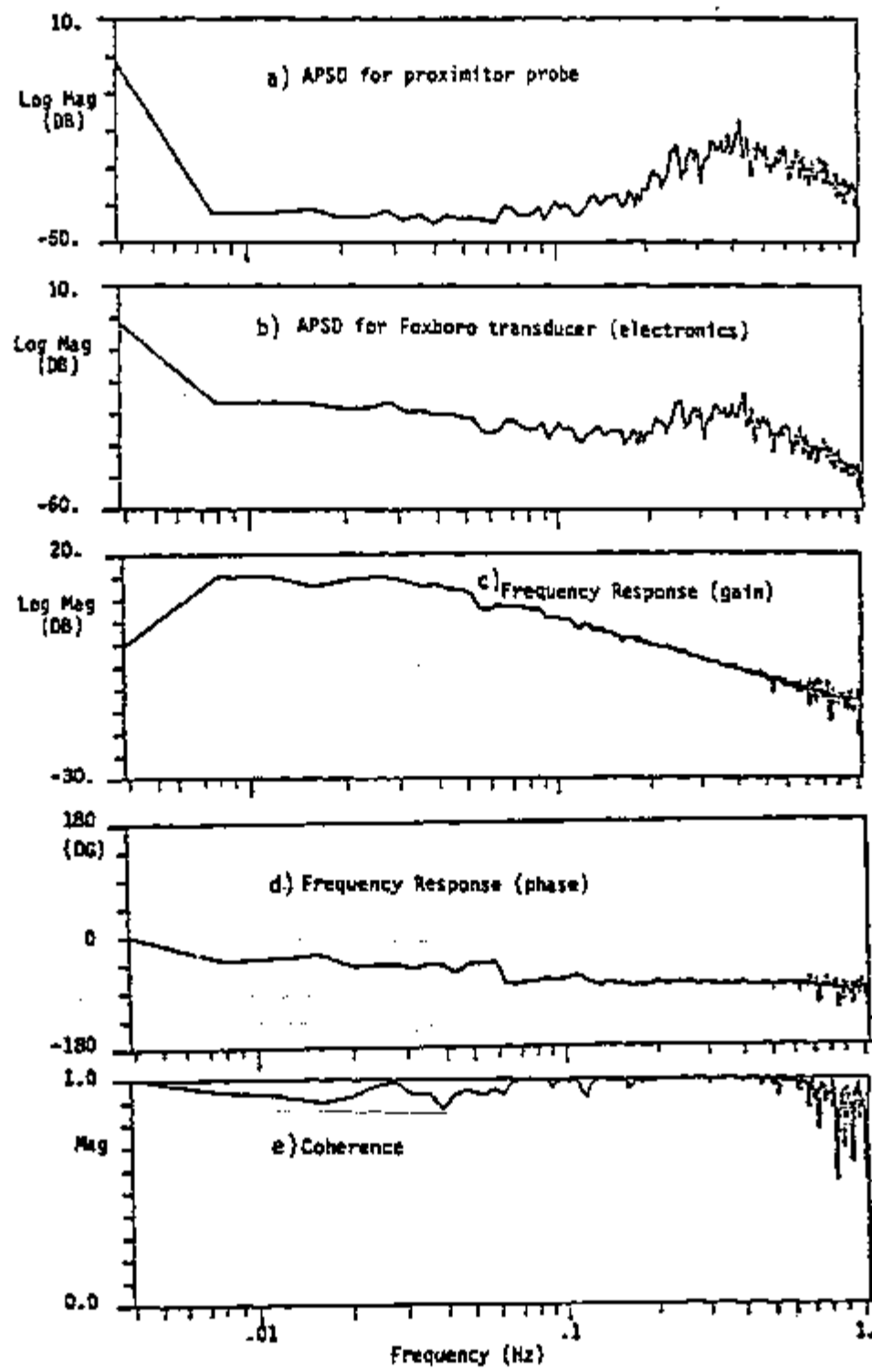
Figure 3-18. Frequency response of electronic system in the interval .004 to 1. Hz
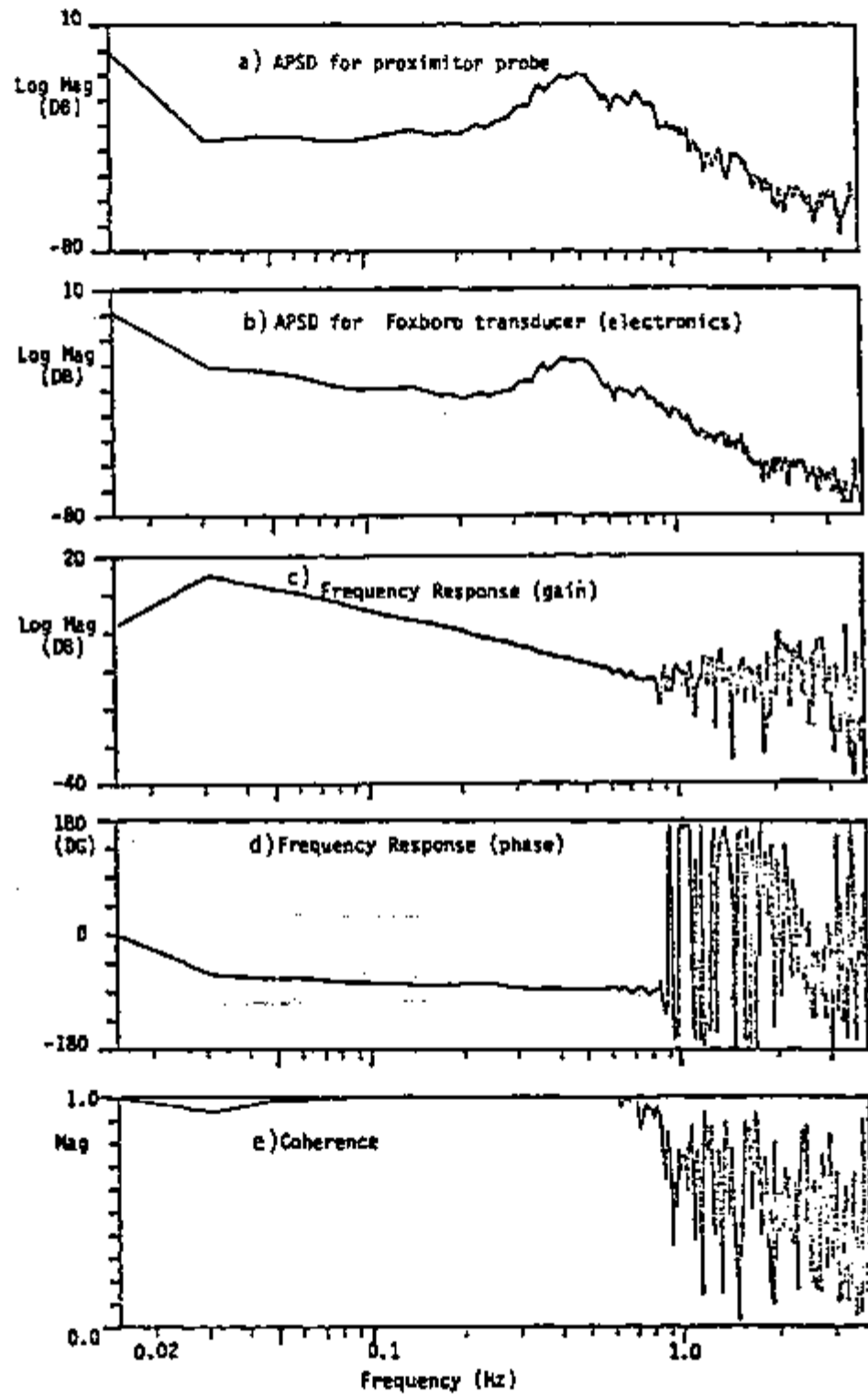
Figure 3-19. Frequency response of electronic system in the interval .02 to 3. Hz
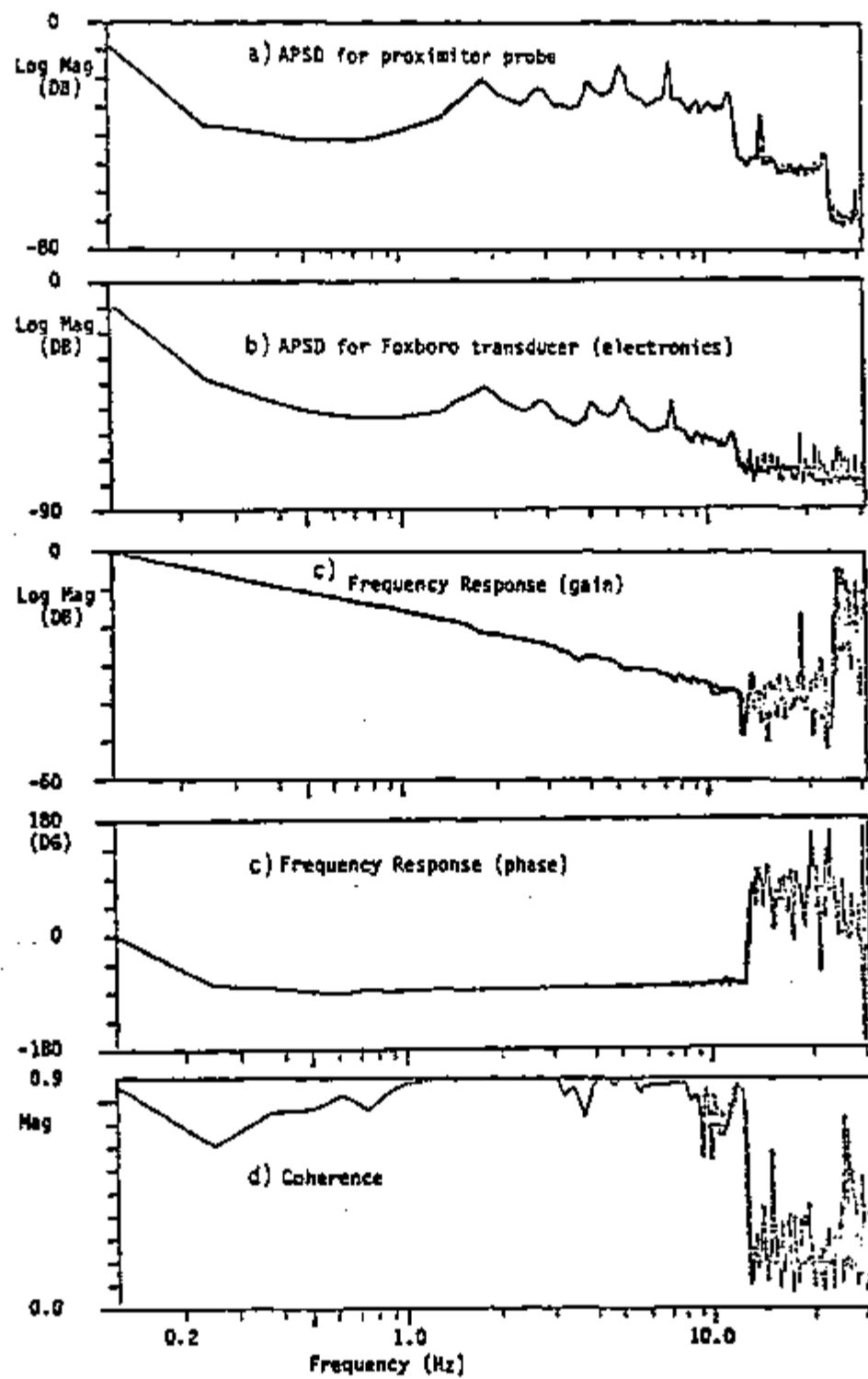
Figure 3-20. Frequency response of electronic system
in the interval .2 to 30. Hz

The frequency response is shown in parts c) and d) of the Figures. According to the technical specifications of the signal analyzer used, the frequency response is calculated using the ratio between the averaged Cross Power Spectral Density (CPSD) and the averaged APSD of the input signal (see references 29 and 30 for more information about the method).

Due to the fact that electronic equipment can introduce noise in the signals, the coherence function is useful to determine how much of the output signal is due to the input signal. The coherence function is shown in part e) of Figures 3-18 through 3-20.

Figure 3-18 indicates that the magnitude of the frequency response is constant for frequencies up to about .036 Hz, after which it starts to decrease with a ratio of 20 decibels per decade of frequency. Also, the phase starts at zero and goes to a value close to -90 degrees. The result is typical of a first order system with a pole at $p = -2\pi*.036 = -.225 \ sec^{-1}$, therefore, a better representation for the transfer function $G_{e\ell}$ is:

$$G_{e\ell}(s) = \frac{C_{e\ell}}{s + .225}$$
(3-116)

The value of $C_{e\ell}$ was obtained using the calibration curve of the proximitor and the magnitude of the frequency response. $C_{e\ell}$ was determined as $1.04*10^5 \ mA/(sec m)$.

3.3.4 Lever system

The transfer function of the lever system, $G_{\ell s}$, relates the displacement of the ferrite disk and the moment applied to the lever system. It is obtained from Equation 3-105 that gives:

$$G_{\ell s}(s) = \frac{\delta \epsilon(s)}{\delta \tau(s)} = \frac{\overline{P_{11}P_{14}} \sin \psi_{14}(0)}{(s^2 I_{\ell s} + s C_{\ell s} + K_{pv})} \qquad (3\text{-}117)$$

Here we note that $G_{\ell s}$ does not take in account the feedback effect generated by the force motor. It only relates the displacement of the ferrite disk with the moment applied to the system.

A plot for $G_{\ell s}(s)$ is given in Figure 3-21.

3.3.5 Closed loop transfer function for the lever system

The closed loop transfer function for the lever system, identified by G_{ovls} in Figure 3-1, includes several transfer functions (lever system, the mechanical reaction, the electronics and the force motor). Combining the transfer functions for all these subsystems we obtain the overall transfer function G_{ovls}. It relates the variation in the output current I_{dc} with the variation in the moment τ_{pr} that is transmitted to the system when there is a change in the differential pressure being applied to the transducer:

$$G_{ovls}(s) = \frac{\delta I_{dc}(s)}{\delta \tau_{pr}(s)} = \frac{G_{e\ell}(s)G_{\ell s}(s)}{1. - G_{mr}(s)G_{\ell s}(s) - G_{fm}(s)G_{e\ell}(s)G_{\ell s}(s)} \qquad (3\text{-}118)$$

A plot for $G_{ovls}(s)$ is given in Figure 3-22.

According to Equations 3-112, 3-114, 3-116 and 3-117, Equation

Magnitude
|m|/(N.m))

Im(s)

Re(s)

Figure 3-21. Transfer function for the lever system

99
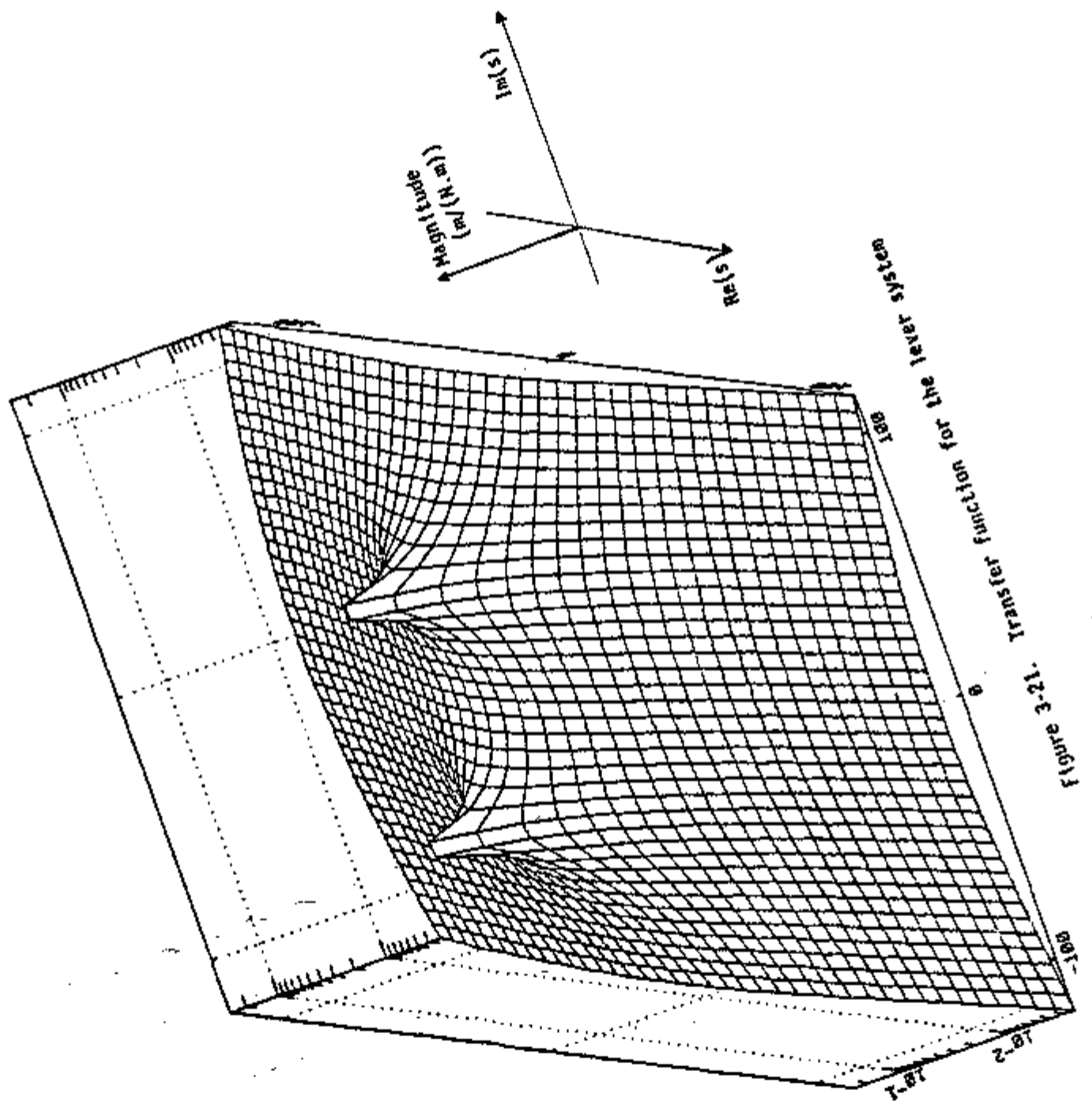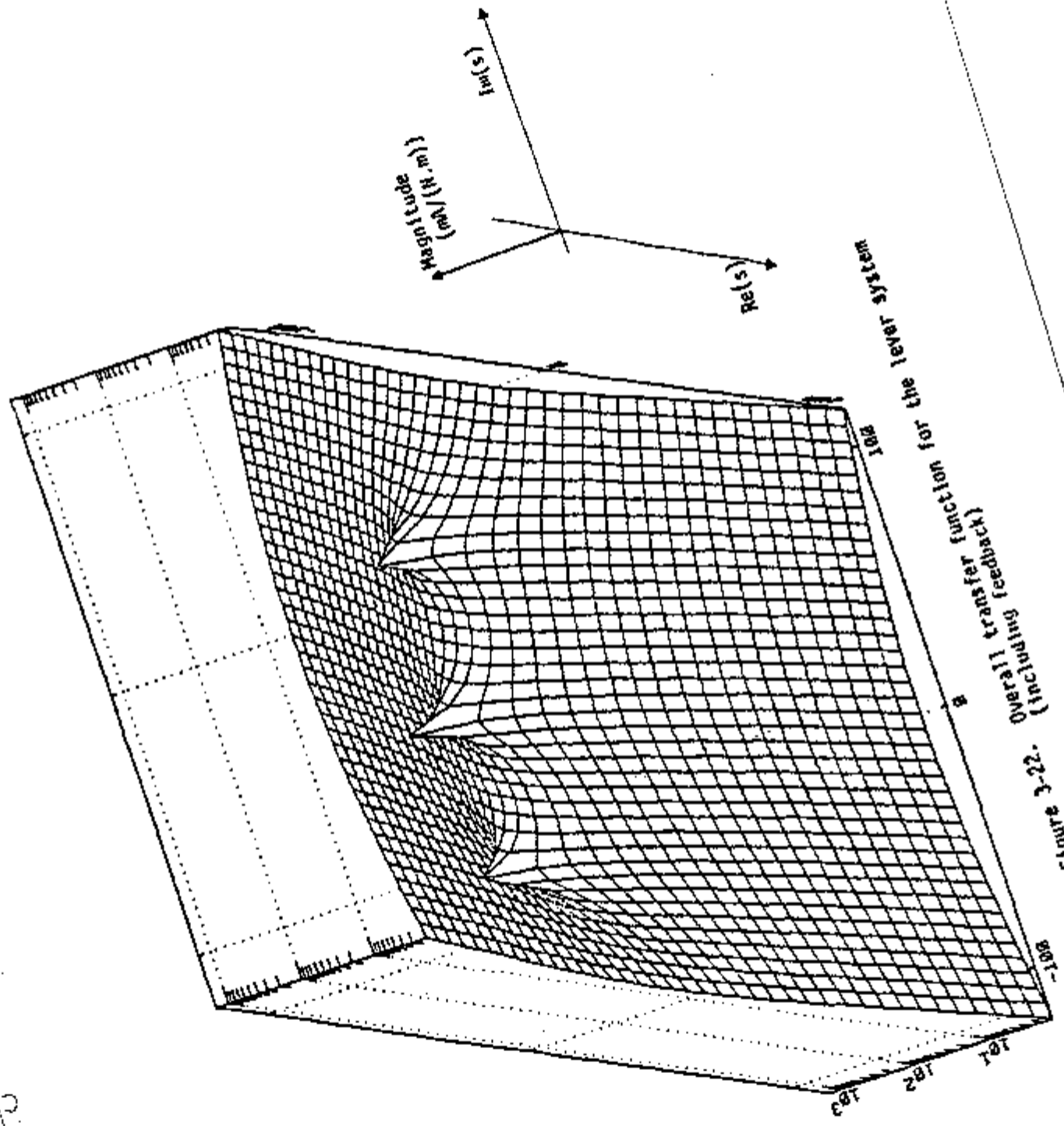
Figure 3-22. Overall transfer function for the lever system (including feedback)

3-118 can be written as:

$$G_{ovls} = \frac{C_{e\ell}\overline{P_{11}P_{14}}\sin\psi_{14}(0)}{\{s^3 I_{\ell s} + s^2[C_{\ell s}+p I_{\ell s}] + s[pC_{\ell s}+K_{pv}-G_{mr}\overline{P_{11}P_{14}}\sin\psi_{14}(0)] + p[K_{pv} -G_{mr}\overline{P_{11}P_{14}}\sin\psi_{14}(0)] - G_{fm}C_{e\ell}\overline{P_{11}P_{14}}\sin\psi_{14}(0)\}} \tag{3-119}$$

where p is the pole of the transfer function for the electronic system.

Substituting the parameters present in Equation 3-119 by their respective values we obtain:

$$G_{ovls} = \frac{C_{e\ell}\overline{P_{11}P_{14}}\sin\psi_{14}(0)}{4.3*10^{-4}s^3 + 1.5*10^{-2}s^2 + 1.8s + 14.} \tag{3-120}$$

From Equation 3-120 we see that G_{ovls} has three poles. Furthermore, for small values of s the contribution of the first two terms in the denominator is negligible and a first approximation for the first pole of G_{ovls} is $s_1 = -14./1.8 = -7.83 \text{ sec}^{-1}$. The correct poles of G_{ovls} are:

$$s_1 = -8.3 \text{ sec}^{-1}$$

$$s_2 = -13.33 + 61.47j \text{ sec}^{-1}$$

$$s3 = -13.33 - 61.47j \text{ sec}^{-1} \qquad \text{where } j = \sqrt{-1}.$$

3.3.6 Connection

The transfer function of the connection, G_{cn}, relates the variation in the moment that is applied on the lever system with the variation in the force $\delta F_9(y_9,s)$, transmitted from the vector mechanism. To obtain the equation that gives G_{cn}, we start by combining Equations 3-115 and 3-118 to obtain:

$$\frac{\delta\varepsilon(s)}{\delta\tau_{pr}(s)} = \frac{G_{ovls}(s)}{G_{e\ell}(s)} \tag{3-121}$$

Since the lever system is assumed to be a rigid body system, we can relate $\delta\varepsilon(s)$ with $\delta y_{10}(s)$ by:

$$\delta\varepsilon(s) = \frac{\overline{P_{11}P_{14}}\ \sin\psi_{14}(0)}{\overline{P_{11}P_{10}}\ \sin\psi_{10}(0)}\ \delta y_{10}(s) \tag{3-122}$$

We can also relate $\delta\tau_{pr}(s)$ with $\delta F_{10}(y_{10},s)$:

$$\delta\tau_{pr}(s) = \overline{P_{10}P_{11}}\ \sin\psi_{10}(0)\delta F_{10}(y_{10},s) \tag{3-123}$$

Substituting Equations 3-122 and 3-123 into Equation 3-121 and rearranging the result we obtain:

$$\delta y_{10}(s) = \frac{G_{ovls}(s)[\overline{P_{11}P_{10}}\ \sin\psi_{10}(0)]^2}{G_{e\ell}(s)[\overline{P_{11}P_{14}}\ \sin\psi_{14}(0)]}\ \delta F_{10}(y_{10},s) \tag{3-124}$$

Since $\delta u_9(y_{10},s)$ is the same as $\delta y_{10}(s)$, and $\delta F_{10}(y_{10},s)$ is equal to $\delta F_9(y_{10},s)$ (one is the reaction of the other), we combine Equations 3-99 and 3-124 to obtain:

$$G_{cn}(s) = \frac{\delta\tau_{pr}(s)}{\delta F_9(y_9,s)} = \frac{b(9,9)\ \overline{P_{11}P_{10}}\ \sin\psi_{10}(0)}{\dfrac{G_{ovls}(s)[\overline{P_{11}P_{10}}\ \sin\psi_{10}(0)]^2}{G_{e\ell}(s)[\overline{P_{11}P_{14}}\ \sin\psi_{14}(0)]} - b(9,10)} \tag{3-125}$$

A plot for G_{cn} is given in Figure 3-23.
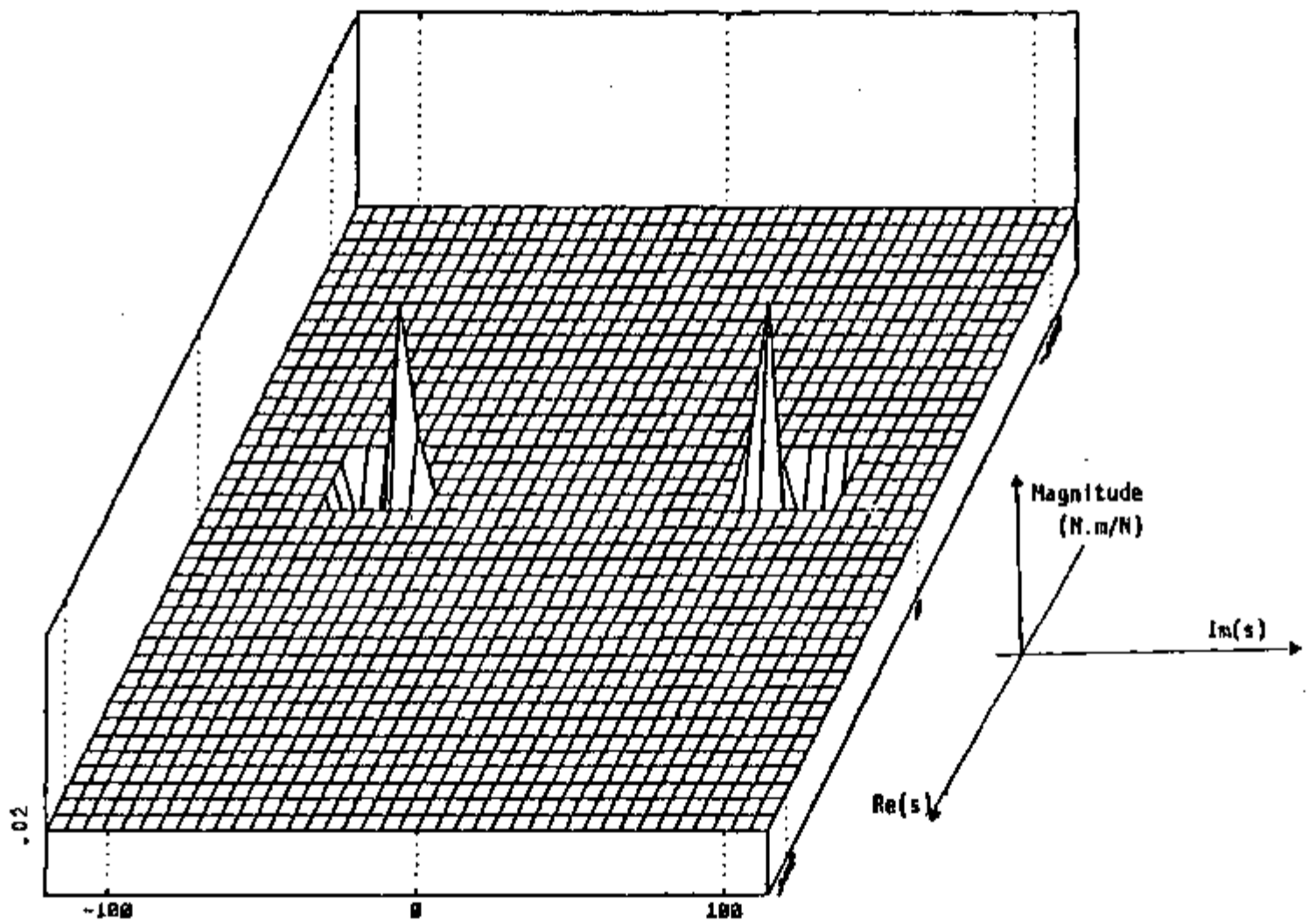
Figure 3-23.   Transfer function for connection

To make a qualitative analysis of G_{cn} we have that for values of s lower than 100 (in magnitude), coefficients b(9,9) and b(9,10), developed in section 3.2.5, can be approximated by $1/(M_c s^2)$ and $-1/(M_c s^2)$, respectively, where M_c is the mass of the connection element. Expressing the denominator of equation 3-120 as $p_3 s^3 + p_2 s^2 + p_1 s + p_0$ and using the approximations for coefficients b(9,9) and b(9,10), Equation 3-125 becomes:

$$G_{cn}(s) = \frac{\overline{P_{10}P_{11}}\sin\psi_{10}(0)[p_3 s^3 + p_2 s^2 + p_1 s + p_0]}{[\overline{P_{10}P_{11}}\sin\psi_{10}(0)]^2(s+p)M_c s^2 + (p_3 s^3 + p_2 s^2 + p_1 s + p_0)}$$

$$(3\text{-}126)$$

Here we note that the poles of G_{ovls} are now the zeros of G_{cn}. Also, since the product $[\overline{P_{10}P_{11}}\sin\psi_{10}(0)]^2 M_c$ is about $7*10^{-5}$ the contribution of the first term in the denominator is very small, and the poles of G_{cn} are very close to the zeros.

A more detailed analysis showed that the increment used in the calculations was much larger than the distance between the location of the first pole and the location of the first zero. This is the reason why they are not seen in Figure 3-23.

3.3.7 Vector mechanism

The transfer function of the vector mechanism, G_{vm}, gives the fraction of force that is transmitted from the force bar to the connection element. To determine G_{vm} we once again analyze points that have the same motion and forces that make a pair action-reaction. Since $\delta u_9(y_9,s)$ is the same as $\delta u_8(y_9,s)$ and $\delta F_9(y_9,s)$ is the reaction to $\delta F_8(y_9,s)$, we use Equations 3-96, 3-98 and 3-125 to obtain:

$$G_{vm}(s) = \frac{\delta F(y_9,s)}{\delta F(x_8,s)} = \frac{b(8,8)}{a(9,9) + \dfrac{a(9,10)\, G_{cn}(s)}{\overline{P_{11}P_{10}}\, \sin\psi_{10}(0)} - b(8,9)} \qquad (3\text{-}127)$$

A plot for Gvm is given in Figure 3-24.

For values of s lower than 100 (in magnitude) coefficients $a(9,9)$ and $a(9,10)$ can be approximated by $1/(M_c s^2)$ and $-1/(M_c s^2)$, respectively, where M_c is the mass of the connection element. Using this approach and equation 3-126 we rewrite Equation 3-127 as:

$$G_{vm}(s) = \frac{b(8,8)}{\dfrac{[\overline{P_{10}P_{11}}\sin\psi_{10}(0)]^2(s+p)}{\{[\overline{P_{10}P_{11}}\sin\psi_{10}(0)]^2(s+p)M_c s^2 + (p_3 s^3 + p_2 s^2 + p_1 s + p_0)\}} - b(8,9)}$$

$$\qquad (3\text{-}128)$$

Since coefficients $b(8,8)$ and $b(8,9)$ are constants divided by a same polynomial of order 2 (see Equation 3-96), we conclude that G_{vm} is a ratio of two polynomials of order three each.

Comparing Equations 3-126 and 3-128 we note that the poles of G_{cn} are now the zeros of G_{vm}.

3.3.8 Force bar

The transfer function for the force bar, G_{fb}, relates the variation in the force transmitted to the vector mechanism with the variation in the force transmitted from the flexural system. To obtain G_{fb} we follow the same procedure as the one used in the determination of G_{vm} and G_{cn}. Consider the equations that give the same
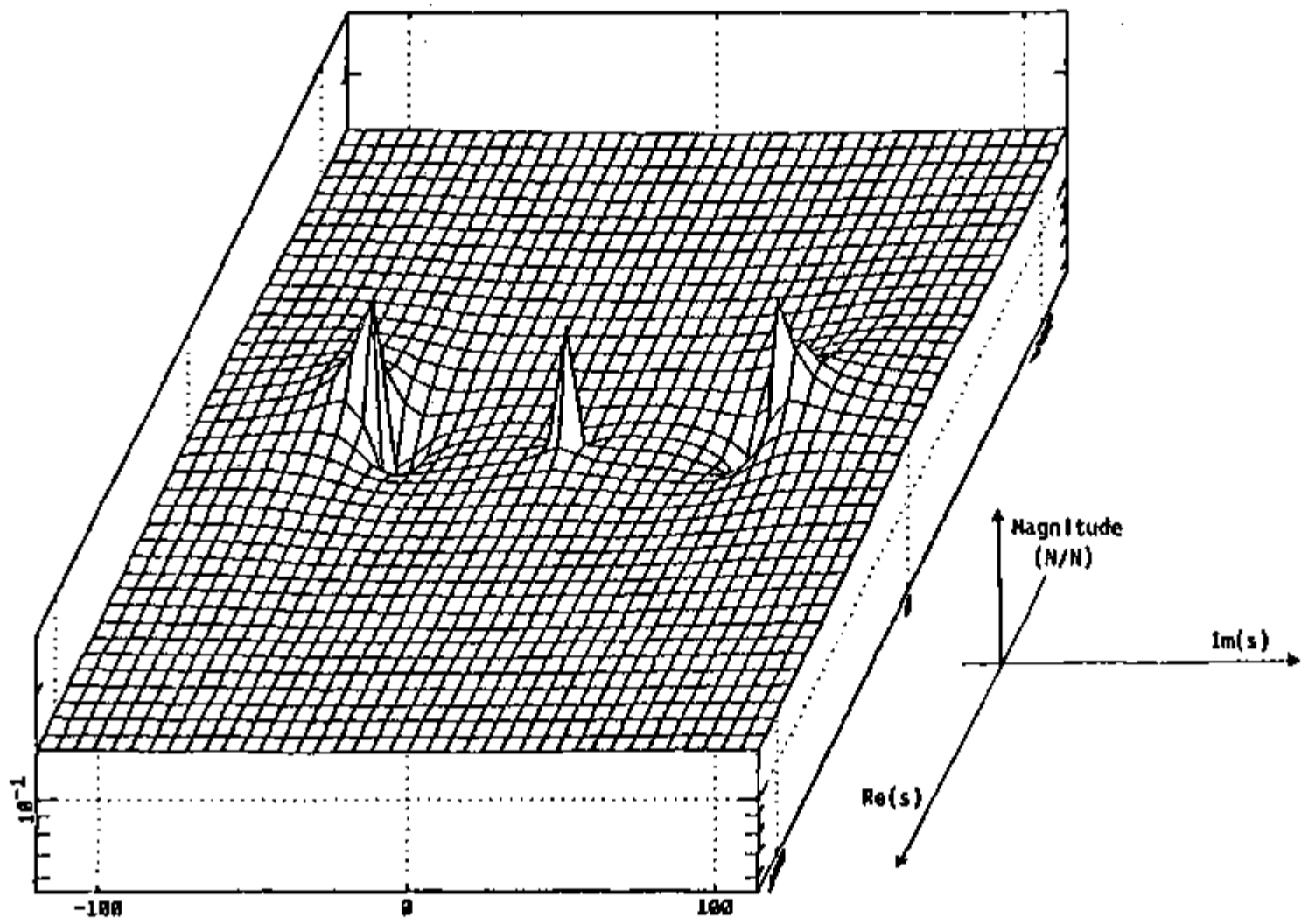
Figure 3-24. Transfer function for vector mechanism

displacement; $\delta u_8(x_8,s)$ and $\delta u_7(y_8,s)$; and the pair of forces where one is the reaction of the other: $\delta F_7(y_8,s)$ and $\delta F_8(x_8,s)$. Using Equations 3-53, 3-95 and 3-127 we obtain:

$$G_{fb}(s) = \frac{\delta F(y_8,s)}{\delta F(y_7,s)} = \frac{b(7,7)}{[a(8,8) + a(8,9)\, G_{vm} - b(7,8)]} \qquad (3\text{-}129)$$

A plot for G_{fb} is given in Figure 3-25.

The analysis of G_{fb} is similar to the analysis of G_{vm}. In the region shown in Figure 3-25, G_{fb} is a ratio of two polynomials of order three each, and the poles of G_{vm} are now the zeros of G_{fb}.

3.3.9 Flexural system (C-flexure)

The transfer function of the flexural system relates the variation in the force that is transmitted to the force bar with the variation in the force transmitted from the sensing element. It is the combination of the transfer functions of each beam that make up the system. In order to determine the transfer function G_{cfi} for each beam $\underline{i}$ we follow the same procedure as in previous cases. Consider the two equations that describe the motion of the same point, and make use of the transfer function that relates two of the forces present in the equations. Using Equations 3-37, 3-52 and 3-129 we obtain:

$$G_{cf5} = \frac{\delta F(x_7,s)}{\delta F(x_6,s)} = \frac{b(6,6)}{a(7,7) + a(7,8)G_{fb} - b(6,7)} \qquad (3\text{-}130)$$

Using Equations 3-34, 3-36 and 3-130 we obtain:
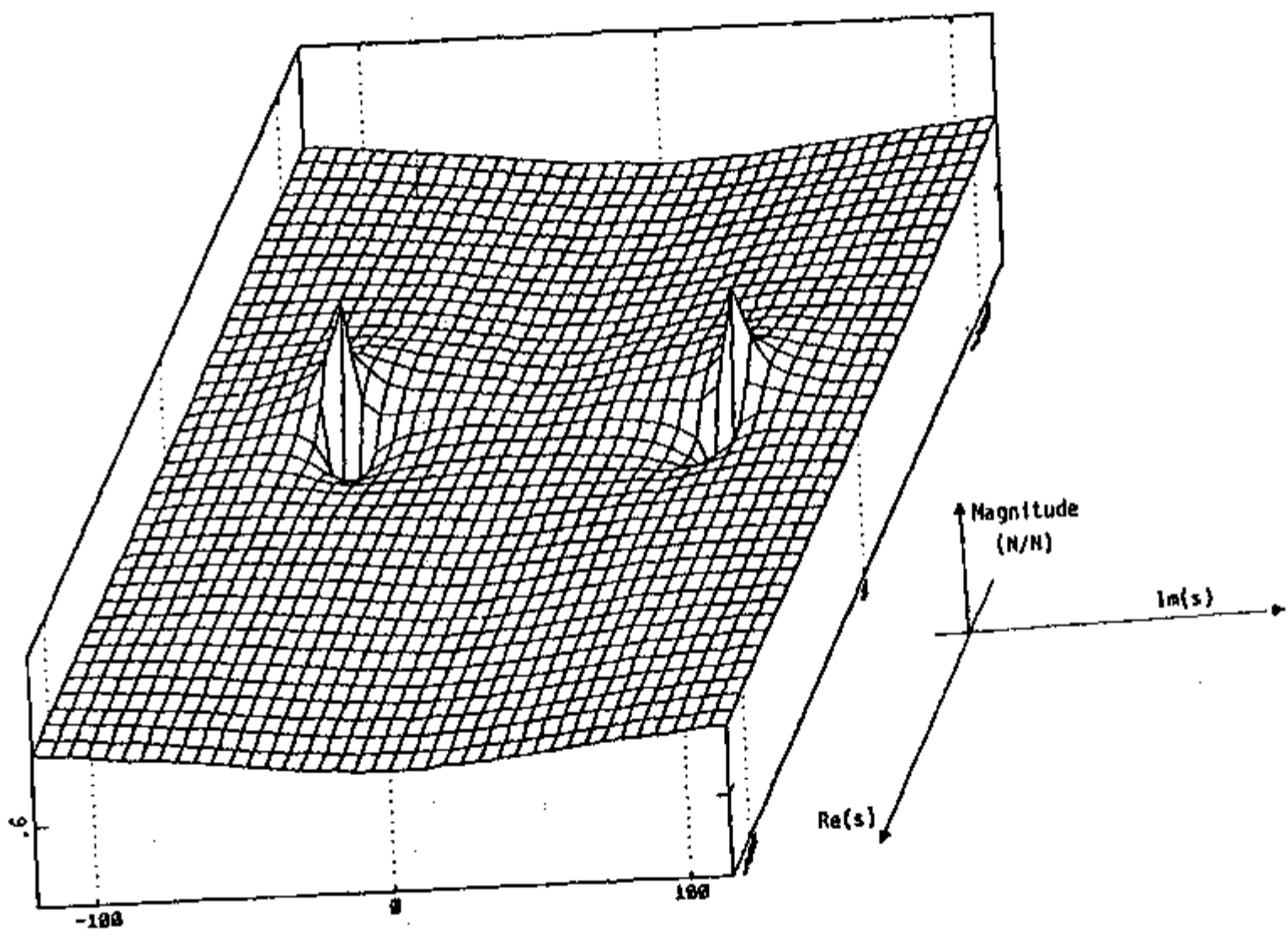
Figure 3-25. Transfer function for force bar

$$G_{cf4} = \frac{\delta F(z_6,s)}{\delta F(z_5,s)} = \frac{b(5,5)}{a(6,6) + a(6,7)G_{cf5} - b(5,6)} \qquad (3\text{-}131)$$

Using Equations 3-19, 3-33 and 3-131 we obtain:

$$G_{cf3} = \frac{\delta F(x_5,s)}{\delta F(x_4,s)} = \frac{b(4,4)}{a(5,5) + a(5,6)G_{cf4} - b(4,5)} \qquad (3\text{-}132)$$

Using Equations 3-16, 3-18 and 3-132 we obtain:

$$G_{cf2} = \frac{\delta F(z_4,s)}{\delta F(z_3,s)} = \frac{b(3,3)}{a(4,4) + a(4,5)G_{cf3} - b(3,4)} \qquad (3\text{-}133)$$

Using Equations 3-6, 3-15 and 3-133 we obtain:

$$G_{cf1} = \frac{\delta F(x_3,s)}{\delta F(x_2,s)} = \frac{b(2,2)}{a(3,3) + a(3,4)G_{cf2} - b(2,3)} \qquad (3\text{-}134)$$

Combining Equations 3-130 through 3-134 we obtain

$$G_{cf} = \frac{\delta F(x_7,s)}{\delta F(x_2,s)} = G_{cf1}G_{cf2}G_{cf3}G_{cf4}G_{cf5} \qquad (3\text{-}135)$$

A plot for G_{cf} is given in Figure 3-26.

The analysis of the several components of G_{cf} is similar to the analysis of G_{vm} (see section 3.3.7). In the region of interest G_{cfi} is a ratio of two polynomials of order three each, and the poles of G_{cfi-1} are the zeros of G_{cfi},
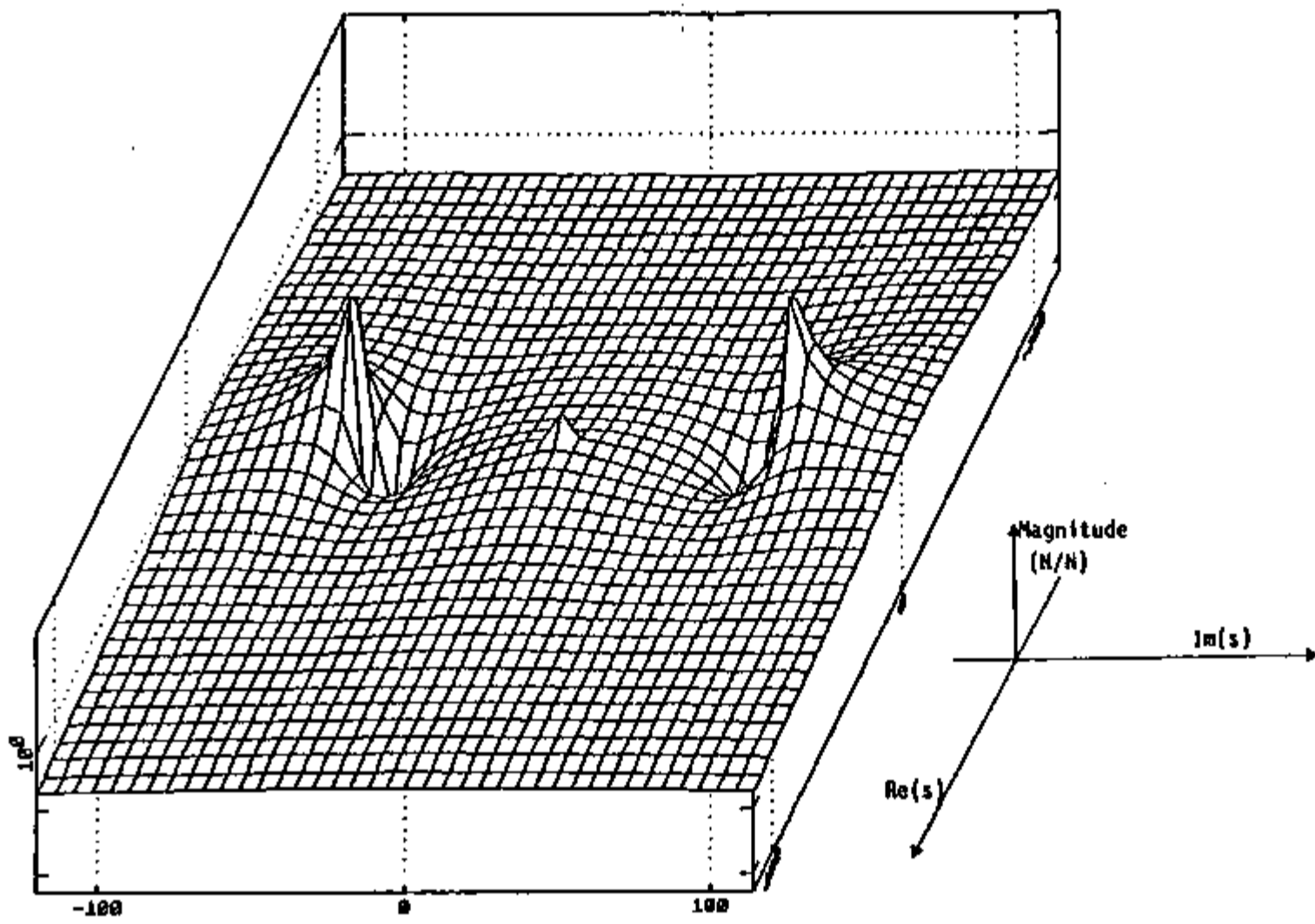
Figure 3-26. Transfer function for flexural system

3.3.10 Sensing element (diaphragm)

The transfer function G_{se} of the diaphragm gives the relation between the differential pressure being applied to it and the force that is transmitted to the flexural system. It is obtained by combining Equations 3-2, 3-5 and 3-134. The result is:

$$G_{se} = \frac{\delta F_1(x_2,s)}{\delta P(s)} = \frac{b(1,1)}{a(2,2) + a(2,3)\ G_{cfl} - b(1,2)} \tag{3-136}$$

The plot of G_{se} is given in Figure 3-27.

For values of s lower than 100, in magnitude, coefficients $a(2,2)$ and $a(2,3)$ can be written as:

$$a(2,2) = -\frac{1 + \frac{s^2}{2}}{M_2 s^2}$$

$$a(2,3) = \frac{1}{M_2 s^2}$$

where M_2 is the mass of element number 2 described in section 3.2.2.

With this approach the transfer function for the diaphragm can be written as:

$$G_{se} = \frac{b(1,1)}{\frac{1}{M_2 s^2}(G_{cfl} - 1 - \frac{s^2}{2}) - b(1,2)} \tag{3-137}$$

From the previous analysis we have that G_{cfl} can be approximated by a ratio of two polynomials of order three. If z_i (i=0,1,2,3) are the coefficients of the polynomial in the numerator, and q_i (i=0,1,2,3) are the coefficients of the polynomial in the denomina-
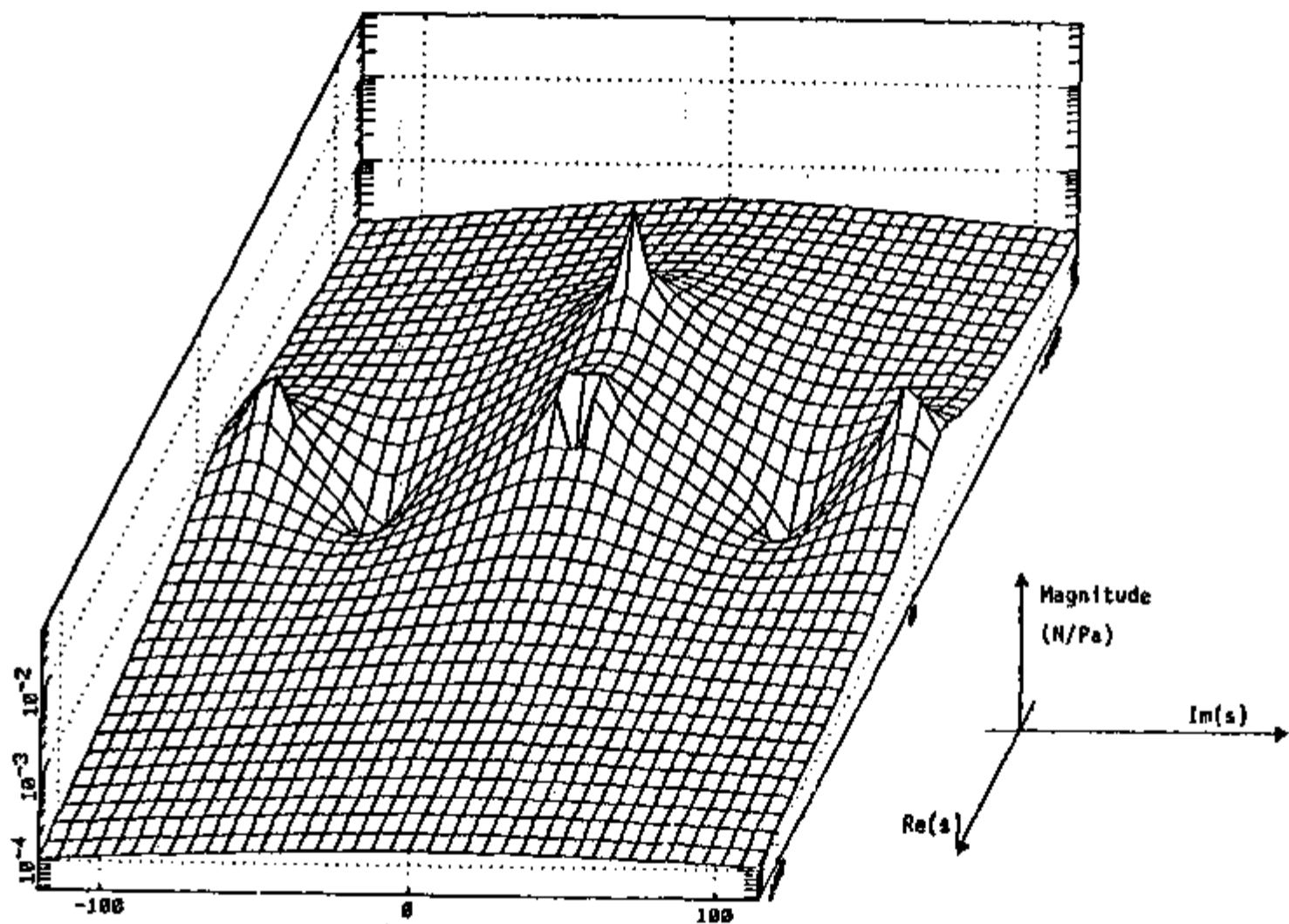
Figure 3-27. Transfer function for diaphragm

tor, $G_{cfl}-1$ can be expressed as:

$$G_{cfl}-1 = \frac{(z_3-q_3)s^3 + (z_2-q_2)s^2 + (z_1-q_1)s + (z_0-q_0)}{q_3s^3 + q_2s^2 + q_1s + q_0}$$

A more detailed analysis showed that the terms (z_1-q_1) and (z_0-q_0) are negligible. Therefore, the transfer function G_{se} can be written as

$$G_{se}(s) = \frac{b(1,1)}{\dfrac{-q_3s^3-q_2s^2+(2z_3-2q_3-q_1)s+(2z_2-2q_2-q_0)}{2M_2(q_3s^3 + q_2s^2 + q_1s + q_0)}} - b(1,2)$$

$$(3-139)$$

Since coefficients $b(1,1)$ and $b(1,2)$ are constants divided by a same polynomial of order two, the result of G_{se} is a polynomial of order three divided by a polynomial of order five. Figure 3-27 indicates that G_{se} has 3 zeros and 5 poles.

We note here that if the coefficients of the denominator of $b(1,1)$ and $b(1,2)$ were small, the contribution of the terms in s^5 and s^4, to the denominator of G_{se} would be negligible, and G_{se} would be a ratio of two polynomials of order three each.

3.4 Overall Transfer Function for the Transducer

The overall transfer function, $G_{overall}$, for the transducer is the combination of the transfer functions of each subsystem:

$$G_{overall} = G_{se}G_{cf}G_{fb}G_{vm}G_{cn}G_{ovls} \qquad (3-140)$$

A plot for $G_{overall}$ is given in Figure 3-28.
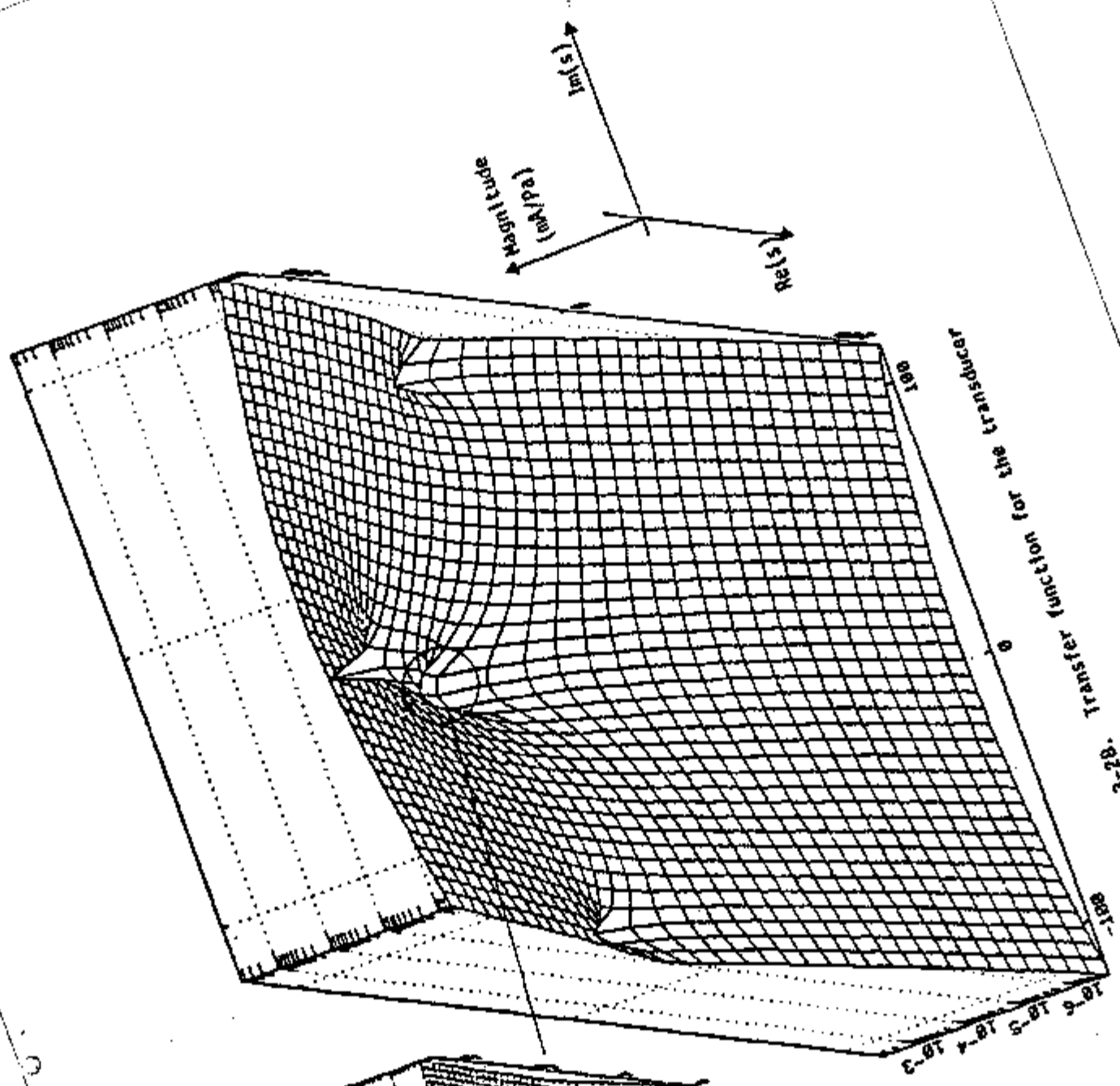
Figure 3-28. Transfer function for the transducer
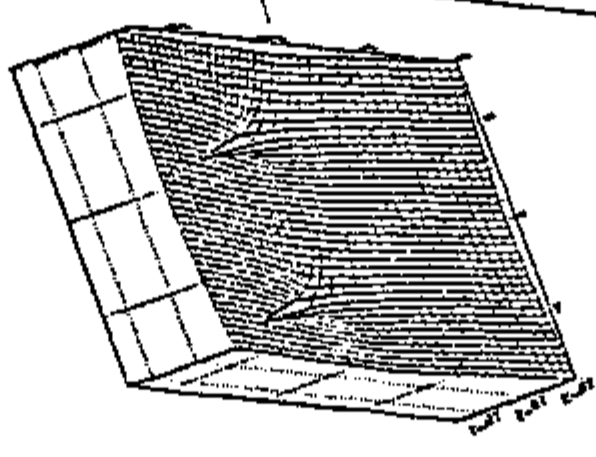
3.5 Frequency Response

Since the results present in Figures 3-21 through 3-28 do not show peaks in the region where Real(s) > 0, the transducer and each one of the subsystems are stable systems. Therefore, their frequency response curves are obtained simply by substituting jw for s in the calculations. The result of such calculations, the frequency response of each subsystem, is shown in Figures 3-29 through 3-36.

115
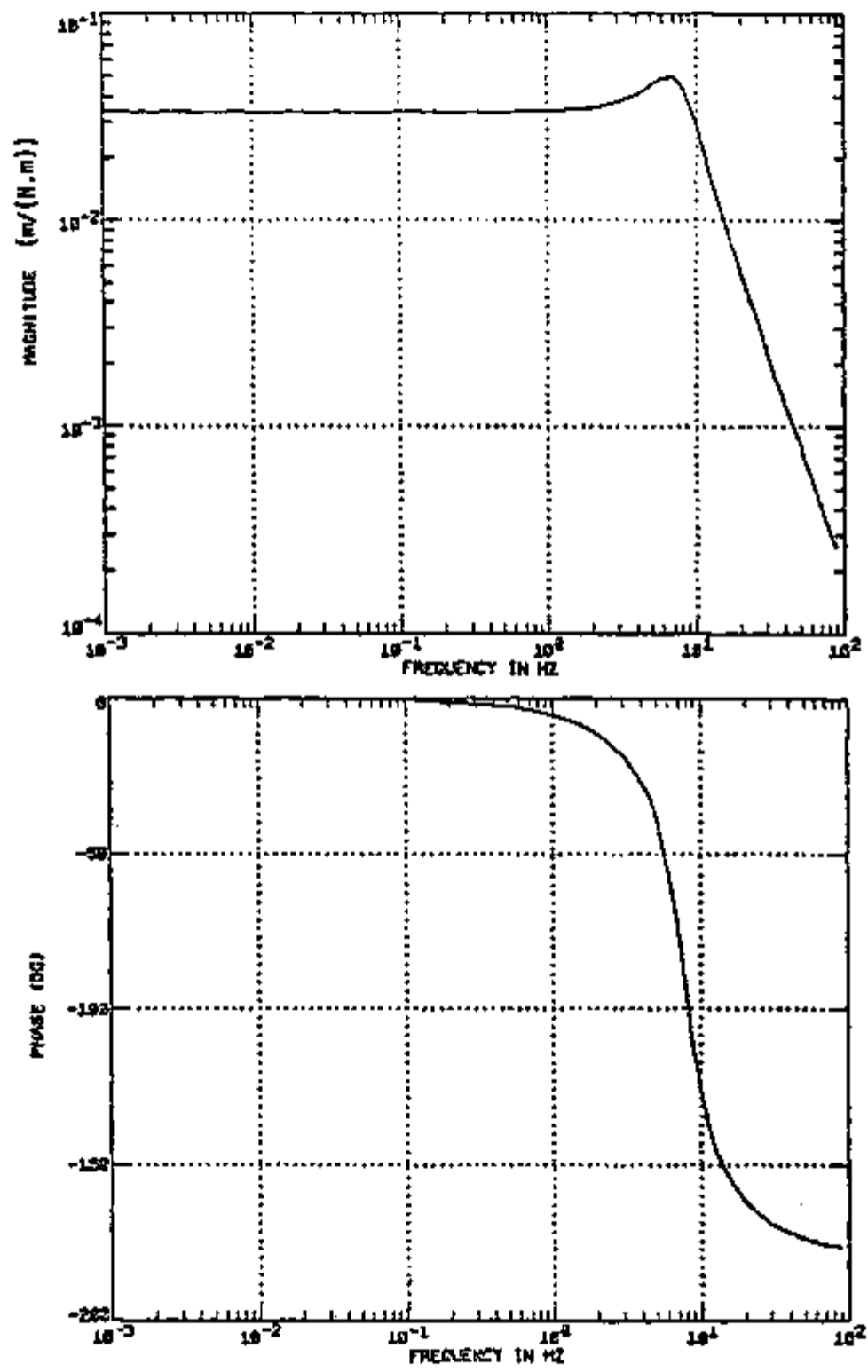
Figure 3-29. Frequency response for lever system
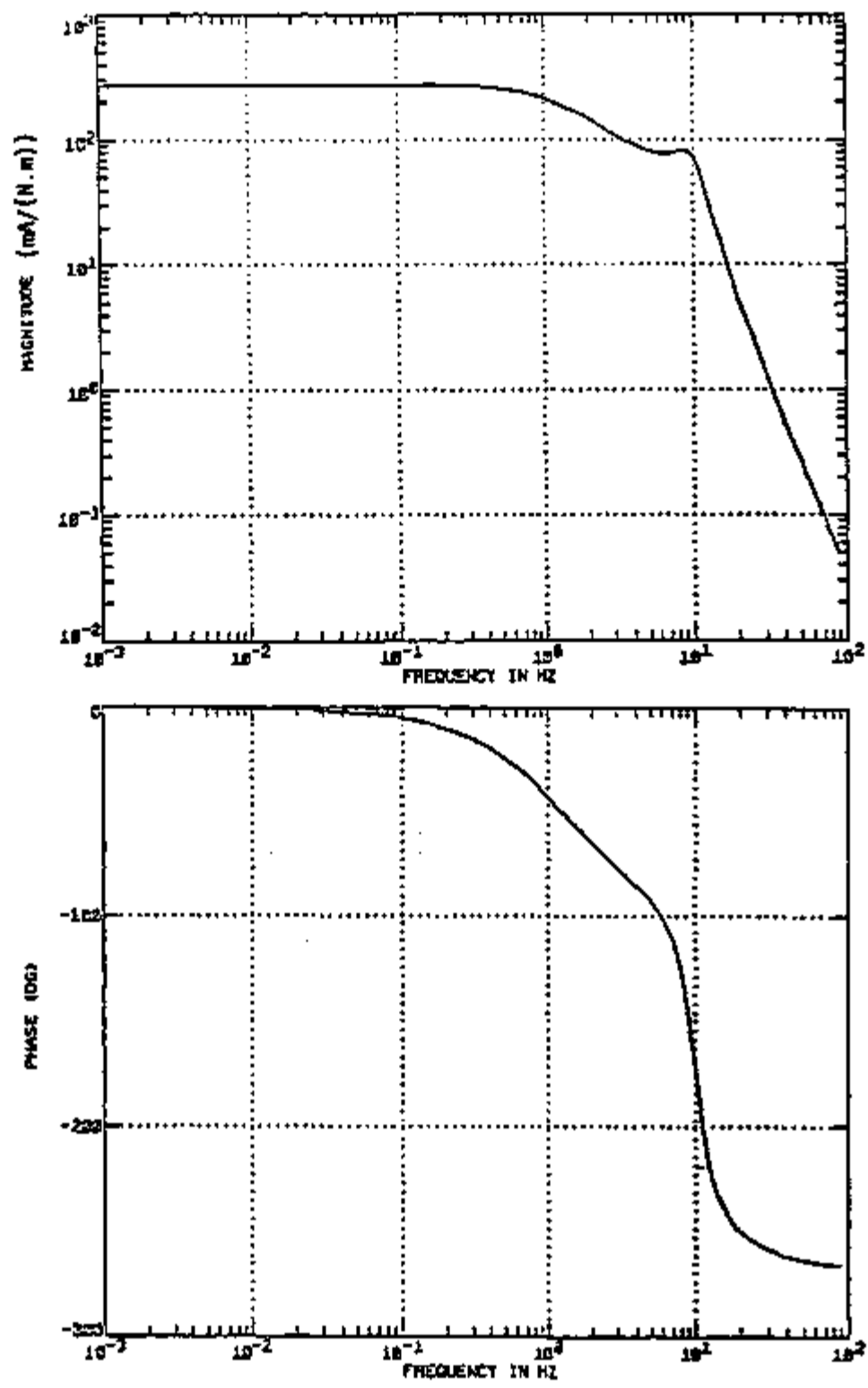
Figure 3-30. Frequency response for lever system
considering feedback
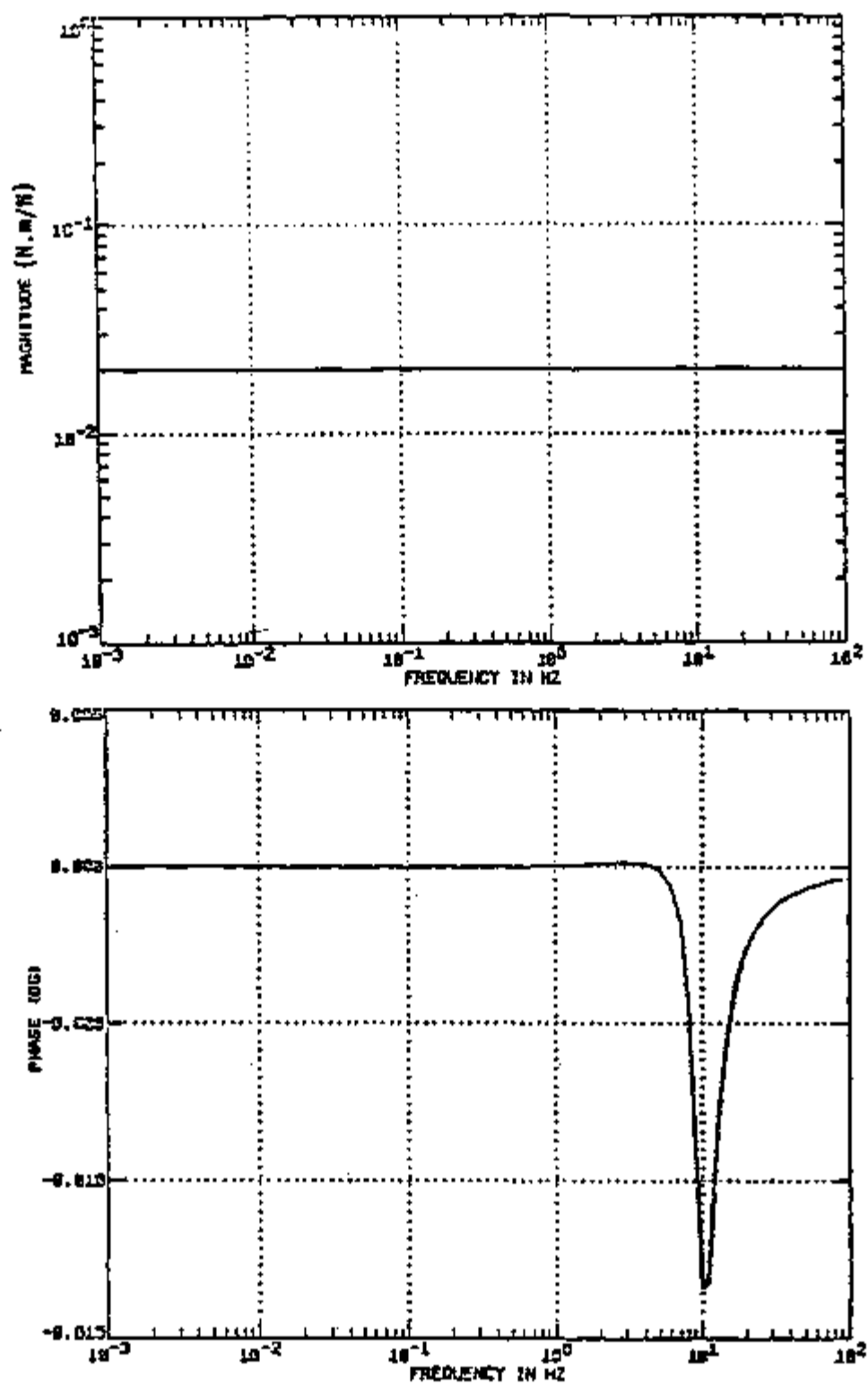
Figure 3-31. Frequency response for connection
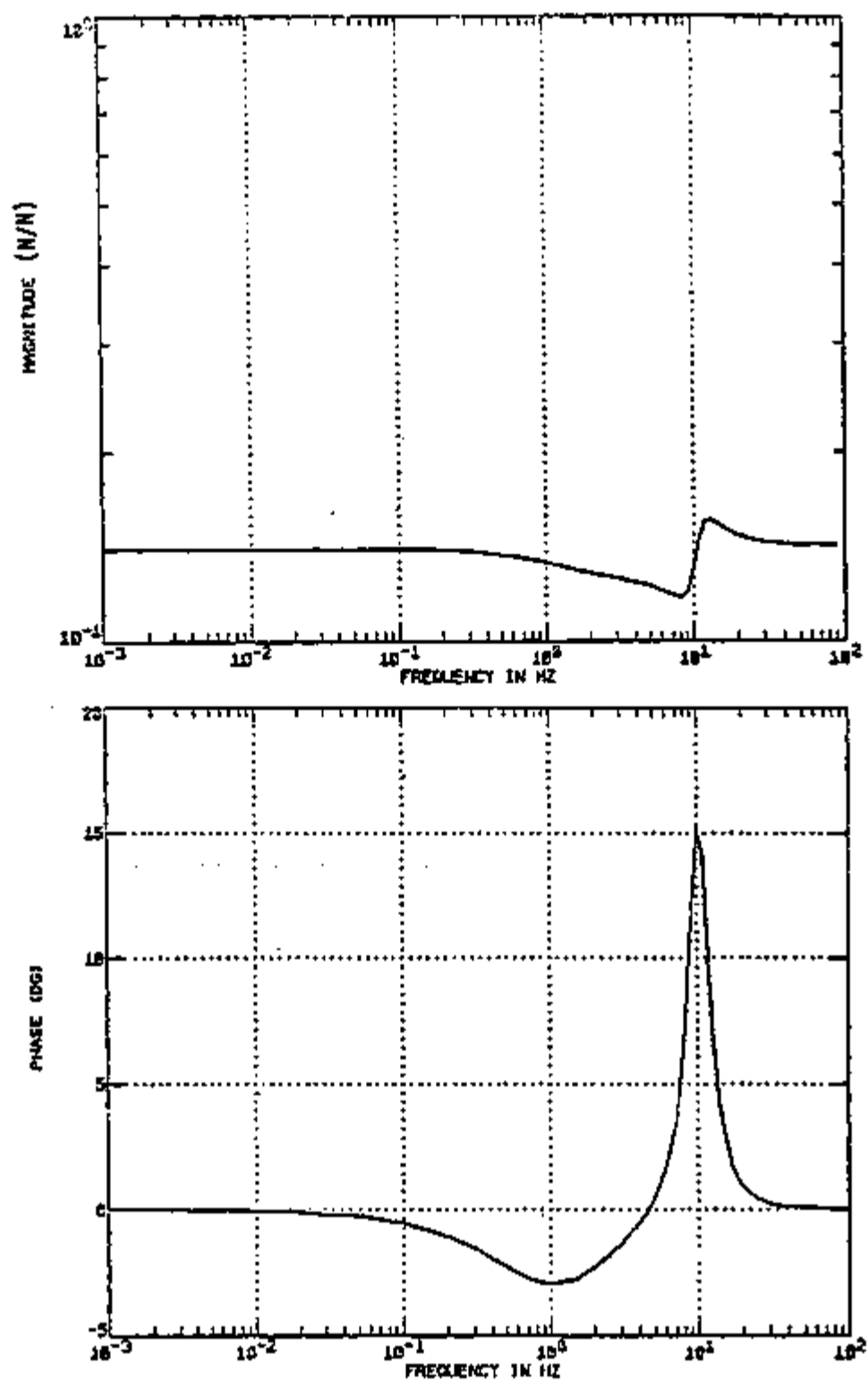
Figure 3-32. Frequency response for vector mechanism
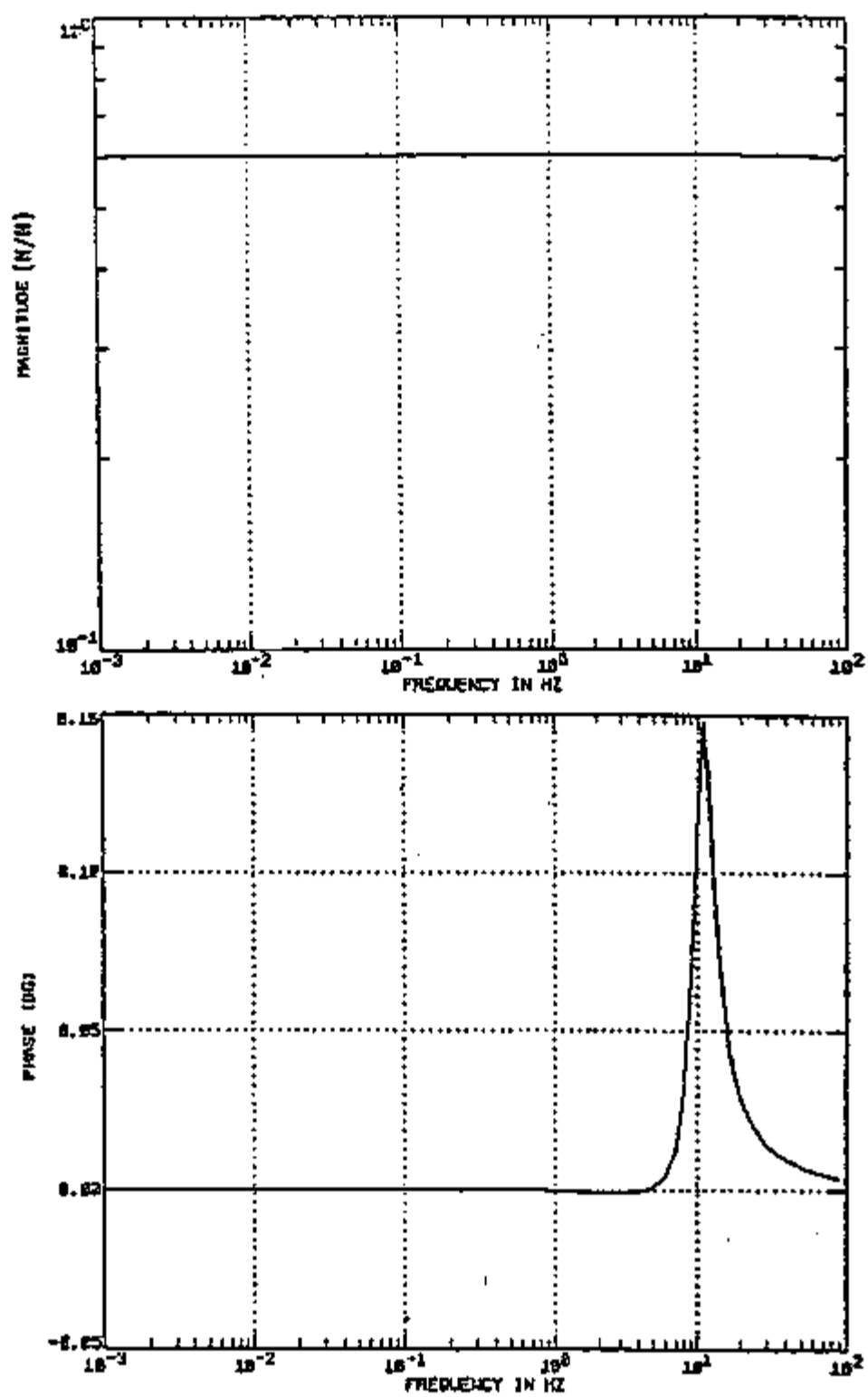
Figure 3-33. Frequency response for force bar
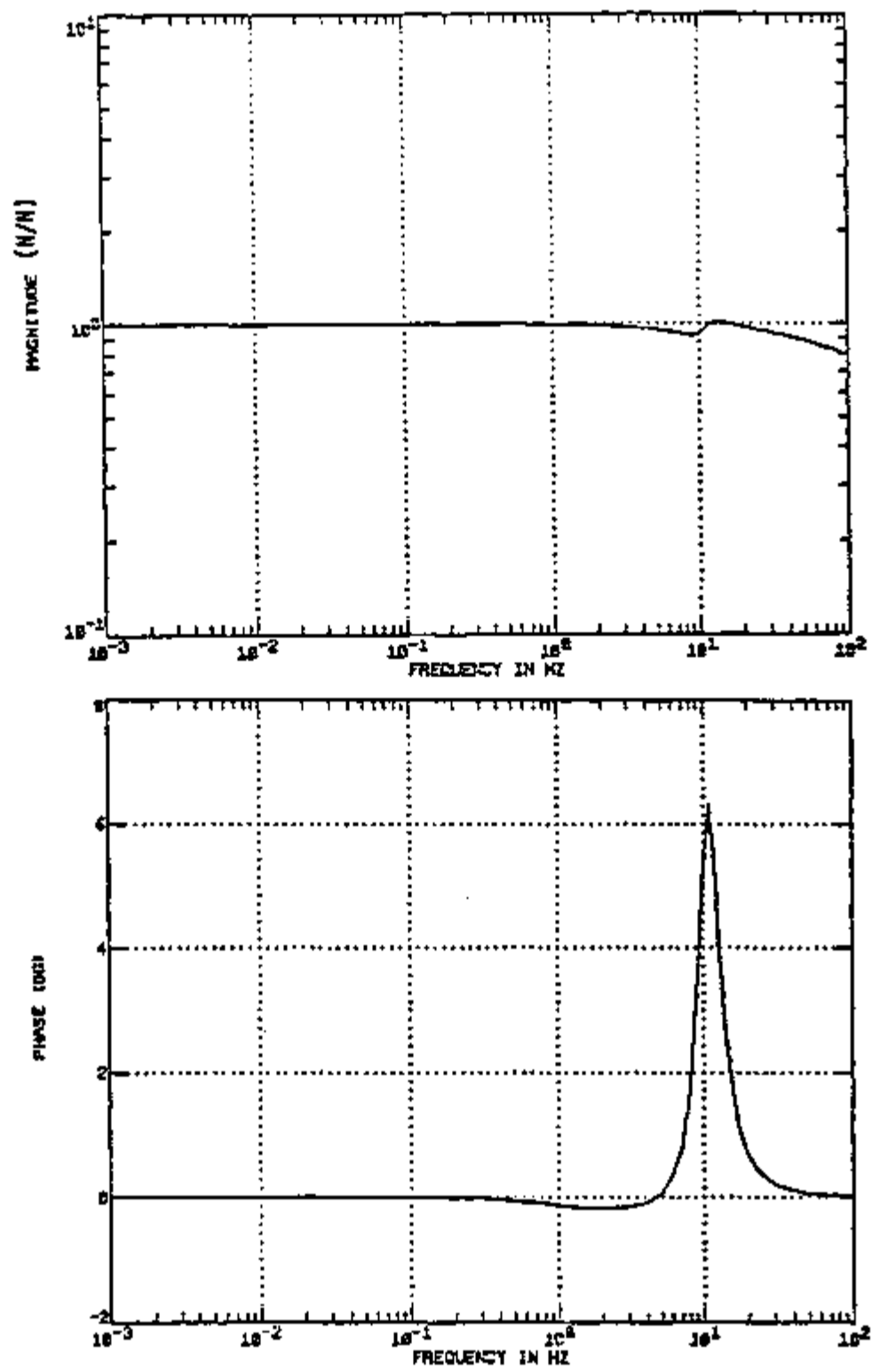
Figure 3-34.   Frequency response for flexural system
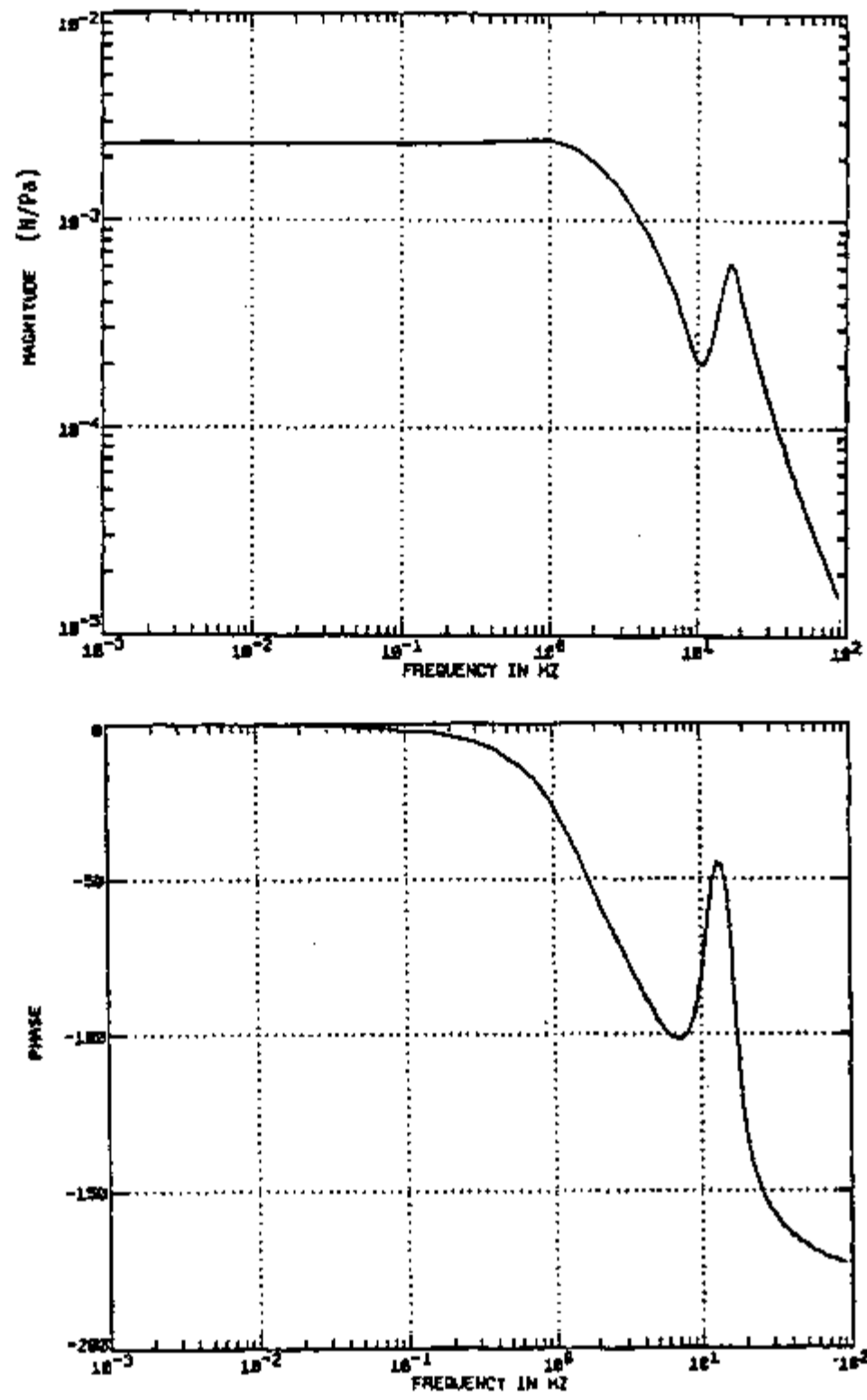
Figure 3-35. Frequency response for diaphragm
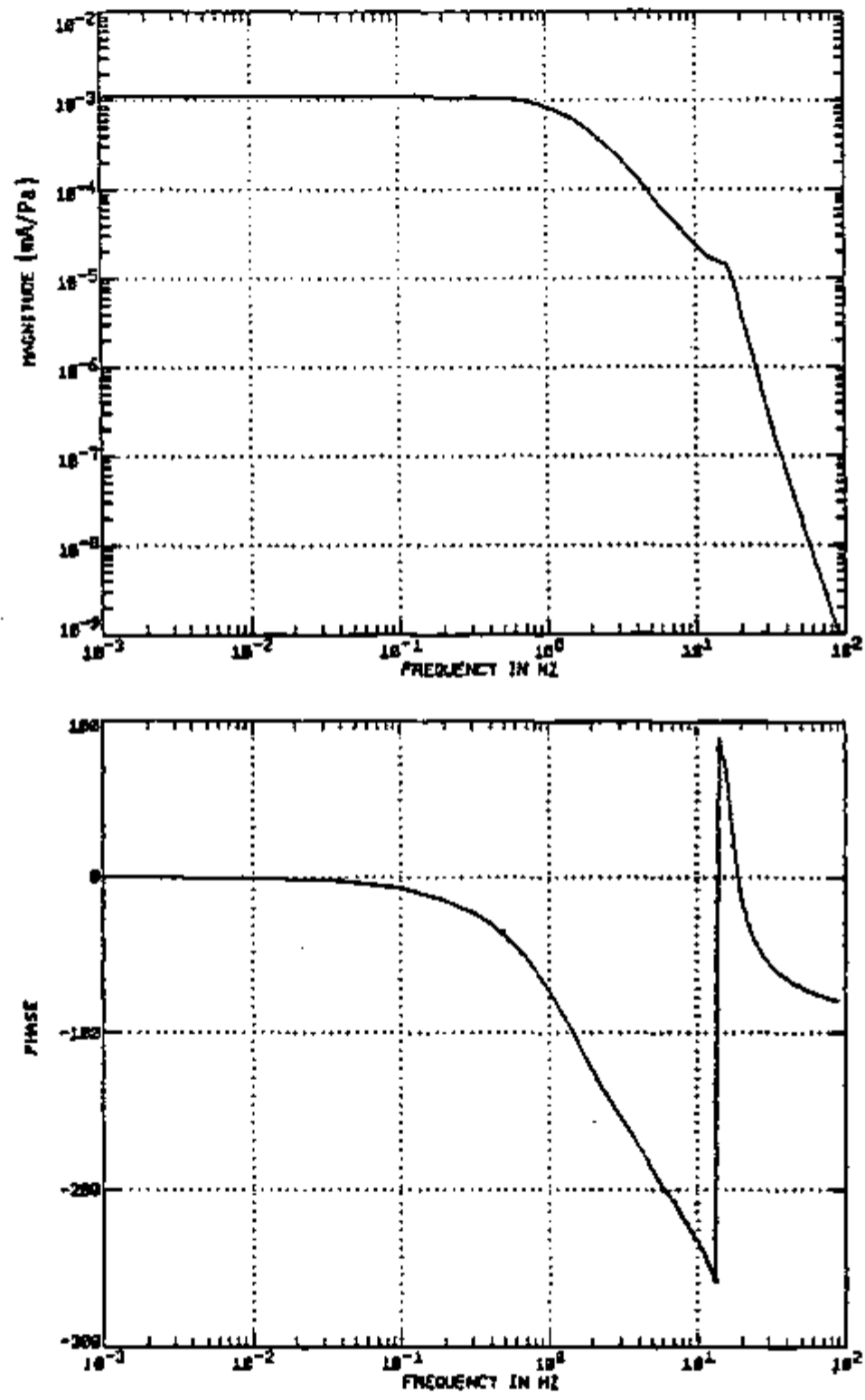
Figure 3-36. Frequency response for the transducer

CHAPTER 4

MODEL VALIDATION

4.1 Introduction

Once we have obtained the equations that describe the dynamic
behavior of the transducer, the next step is to validate the model
described by such equations. Due to the fact that the response of
the transducer to large perturbations is different from the response
to small perturbations it is a non-linear system. However (as will
be discussed in chapter 5), for a step input of magnitude as large as
15% of the adjusted span and ramp inputs with ramp rates lower than
30% of the span per second its behavior is linear. Therefore a
linear model is very useful. In this chapter we discuss the model
developed in chapter 3, and compare the frequency response of the
model with experimental results.

4.2 Model Validation

In order to validate the model developed in chapter 3 a
comparison is made with three sets of experimental data that are
available for the transducer being analyzed. The first two sets are
the frequency responses obtained for two different transducers of the
same model as the one used as the reference in this work. These
results were provided by The Foxboro Company. The first set of data
was taken with a transducer (serial number 2060606) calibrated to
operate in the interval 0 to 100 inches of water. The second set was
taken with a transducer (serial number 2032612) calibrated to operate
between 0 and 150 inches of water. These sensors have a sensing

element identified as 'medium range capsule' by The Foxboro Company. This is the same type of sensing element as the one in the reference transducer used in this study. In the Foxboro frequency response, the transducers were submitted to a pressure of 50% of the adjusted span, with a superimposed sinusoidal perturbation of 5%. The sinusoidal perturbation was generated using a current to air pressure converter, and a faster transducer was used as reference. A copy of the information given by The Foxboro Company is given in appendix C.

The third set of data was taken in The University of Tennessee laboratory, and gives the frequency response of the transducer when correlated with the response of a faster transducer (a Validyne pressure transducer model DP15TL). The experimental equipment used to obtain the correlation is shown in Figure 4-1. With the 'pressure source valve' slightly open, the 'bleed valve' was used to control the amount of air in the accumulator, and consequently the pressure. The pressure was continuously measured using both transducers. The signals from the transducers were recorded using a four channel Lockheed tape recorder in the direct mode for subsequent analysis. The analysis was performed using the Hewlett-Packard Fourier Analyzer model 5420A mentioned in section 3.3.3.

The experimental frequency responses were compared with the frequency response obtained using the model described in chapter 3. A Bode plot of all four cases is shown in Figure 4-2. There is good agreement between the information given by The Foxboro Company and the results obtained with the model. However, the data obtained at

bleed

output
signal
(Foxboro)

pressure
source

Accumulator

Validyne
transducer

drain
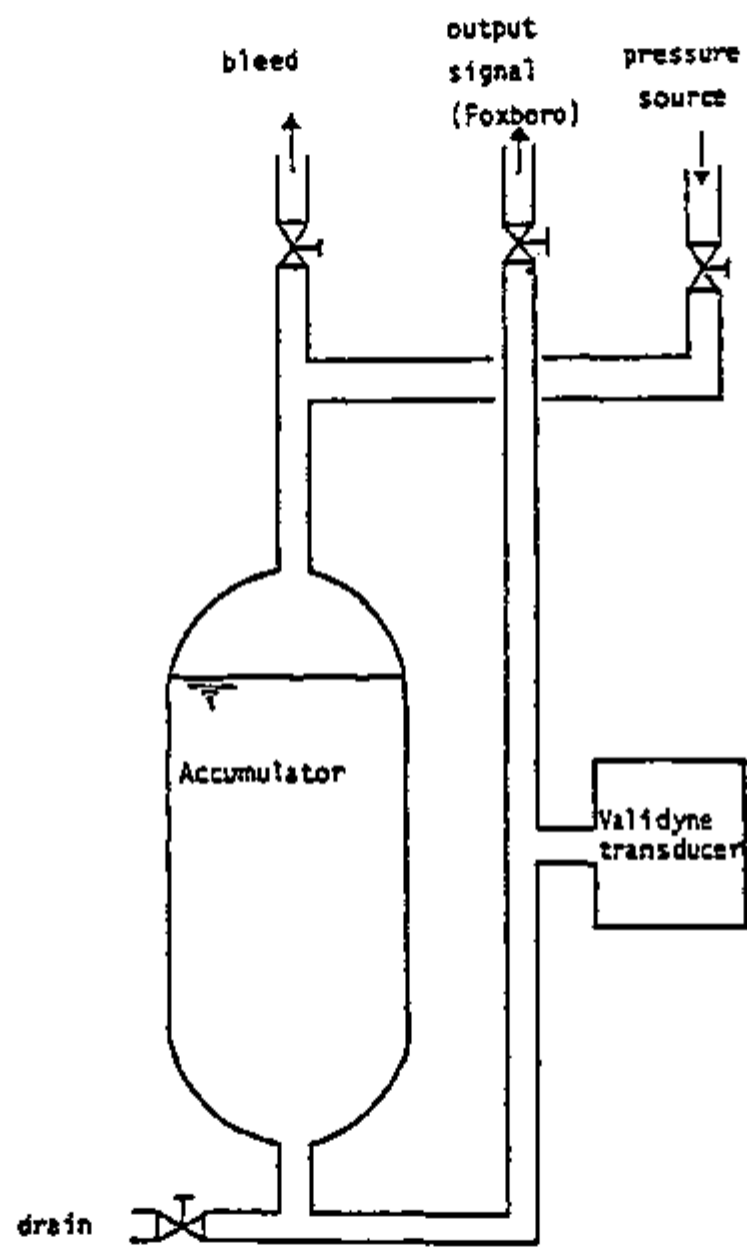
Figure 4-1. Experimental equipment for analysis of frequency
response
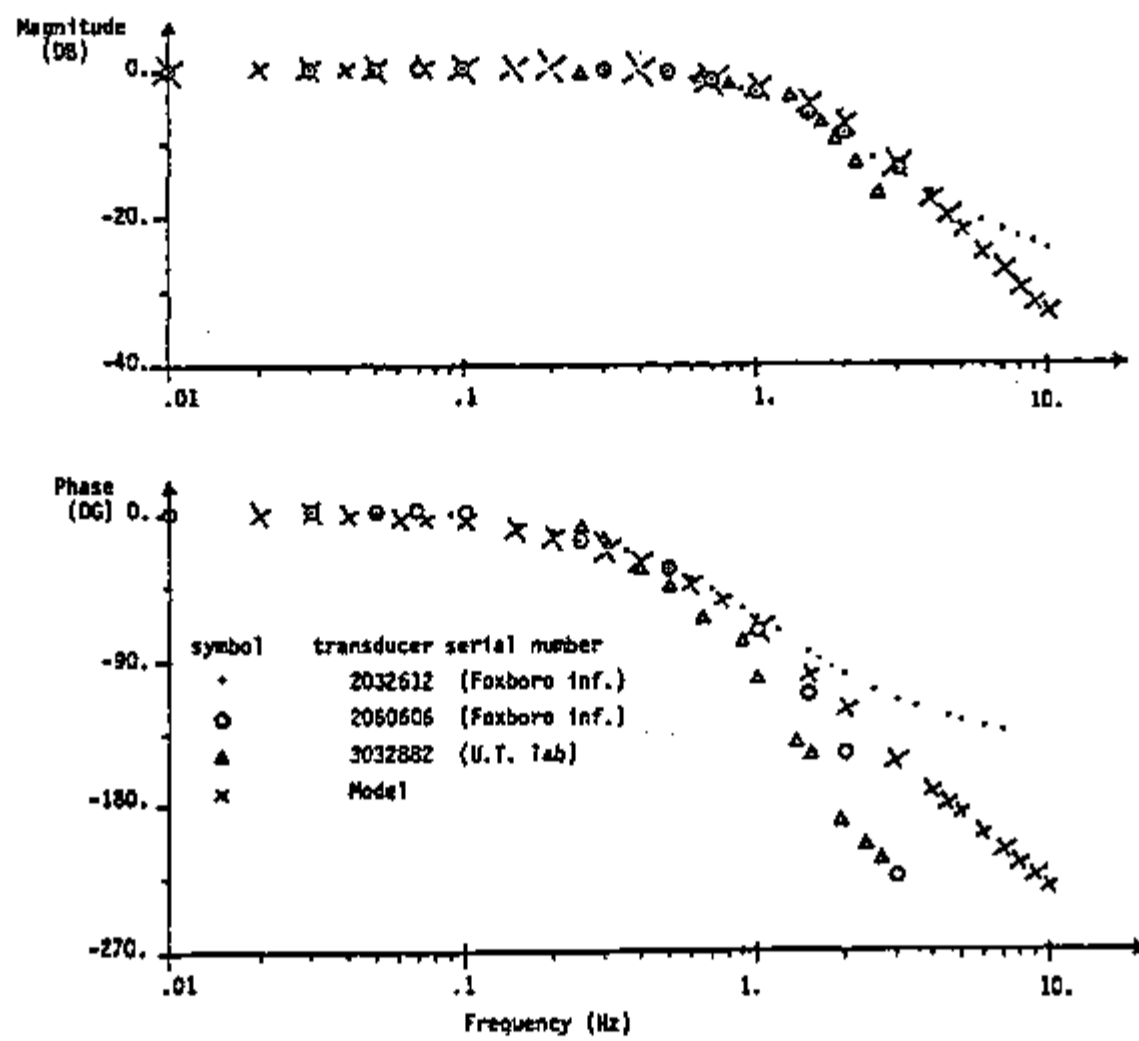
Figure 4-2. Frequency response for transducer model E130M

the University of Tennessee laboratory agree with the other three
only up to about 2 Hz, after which it starts to diverge.

The reasons for the divergence of the third set of data are
attributed to two sources: the Validyne transducer that was used as
reference, and the pressure lines. The result of the analysis
performed with the data taken in The University of Tennessee
laboratory is shown in detail in Figure 4-3. It shows that there is
a sudden decrease in the power spectral density of the signal from
the Validyne transducer in the region close to 3 Hz. Since the
signal from the Foxboro transducer does not show the same behavior, it
is believed that the sudden decrease is a characteristic of the
Validyne transducer (or a characteristic of the place where it was
installed). Therefore, it was concluded that the transfer function
for the signal from the Validyne transducer in the frequency range of
the analysis is not constant. The pressure lines are suspected as an
additional cause for the divergence of the result because they were
long (about 3 meters), with many curves, and they were flexible.

4.3 Discussion of the Calculational Procedure

The model developed in chapter 3 considers the transducer as
a system composed of several mechanical elements. With the exception
of the diaphragm and the lever system, all other elements are
connected to two adjacent elements. The diaphragm and the lever
system are connected to only one element each. For each element
there is a dynamic equation that describes the motion of any point in
the element as a function of the forces acting on the element. For
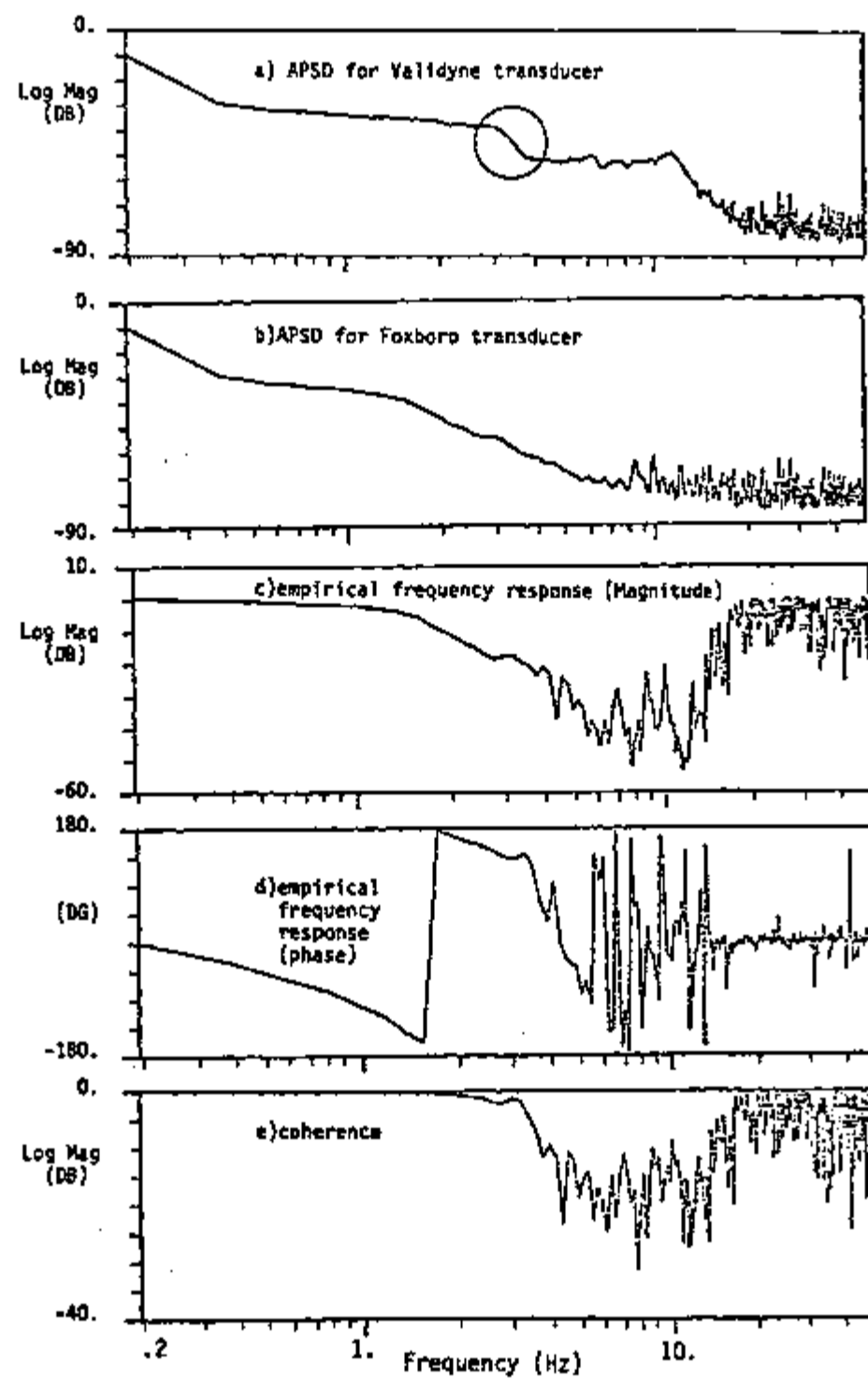
figure 4-3. Experimental frequency response

each connecting point there are two different equations describing its motion. For example, consider elements number 4 and 5 show in Figure 3-7 (page 39). According to Equations 3-19 and 3-33, the motion of point (x_5, y_5, z_5) can be described as:

$$\delta u(r_5, s) = b(4,4)\delta F_4(r_4, s) + b(4,5)\delta F_4(r_5, s) \qquad (4-1)$$

or

$$\delta u(r_5, s) = a(5,5)\delta F_5(r_5, s) + a(5,6)\delta F_5(r_6, s) \qquad (4-2)$$

where r_1 indicates the coordinates of point (x_1, y_1, z_1). Since point (x_5, y_5, z_5) is unique, Equations 4-1 and 4-2 must be equal. Furthermore, considering that the force $\delta F_4(r_5, s)$ is the reaction to the force $\delta F_5(r_5, s)$, the absolute values of these two forces are the same.

For the first and last elements of the mechanical system there is only one force present in the equation of motion. The first element is the diaphragm. It is subject to a differential pressure P existing accross the transducer and one force $F_1(r_2, s)$ that is generated by the feedback reaction of the transducer. Equation 3-2 describes the motion of the diaphragm:

$$\delta u(r_2, s) = b(1,1)\delta P(s) + b(1,2)\delta F_1(r_2, s) \qquad (4-3)$$

For the lever system (the last element), Equation 3-124 may be rewritten as:

$$\delta u(r_{10}, s) = a(10,10)\delta F_{10}(r_{10}, s) \qquad (4-4)$$

Combining Equations 4-1 through 4-4 and all other equations
developed in chapter 3, the motion of the connecting points can be
expressed as:

$$\underline{u} = \underline{\underline{A}} \cdot \underline{f}$$

or

$$\underline{u} = \underline{\underline{B}} \cdot \underline{f} + \underline{g} \delta P$$

where vectors $\underline{u}$, $\underline{f}$, $\underline{g}$, and matrices $\underline{\underline{A}}$ and $\underline{\underline{B}}$ are defined in the next
page.

Defining matrix $\underline{\underline{C}}$ as $\underline{\underline{A}} - \underline{\underline{B}}$, the vector $\underline{f}$ can be determined
as

$$\underline{f} = \underline{\underline{C}}^{-1} \underline{g} \delta P$$

It was found that the coefficients of the matrices $\underline{\underline{A}}$ and $\underline{\underline{B}}$
are such that the direct inversion of matrix $\underline{\underline{C}}$ has numerical problems
(overflow). Since matrices $\underline{\underline{A}}$ and $\underline{\underline{B}}$ are composed of only two
diagonals, it was found to be more practical to obtain the component
$\delta F(r_n, s)$ as a function of the component $\delta F(r_{n-1}, s)$. Due to the fact
that only the first element of the vector $\underline{g}$ is non zero, the
calculation is easily accomplished when we start with the last line
of matrices $\underline{\underline{A}}$ and $\underline{\underline{B}}$ and move toward the first line. This was the
procedure used in developing the transfer functions between forces
described in section 3.3.

The combination of the transfer functions between forces and
Equation 3-118 provide the overall transfer function for the
transducer, as given by Equation 3-140.

The numerical values obtained with the model were used as

$$
\underline{u} = \begin{bmatrix} u(r_2,s) \\ u(r_3,s) \\ u(r_4,s) \\ u(r_5,s) \\ u(r_6,s) \\ u(r_7,s) \\ u(r_8,s) \\ u(r_9,s) \\ u(r_{10},s) \end{bmatrix}
\qquad
\underline{f} = \begin{bmatrix} F(r_2,s) \\ F(r_3,s) \\ F(r_4,s) \\ F(r_5,s) \\ F(r_6,s) \\ F(r_7,s) \\ F(r_8,s) \\ F(r_9,s) \\ F(r_{10},s) \end{bmatrix}
\qquad
\underline{g} = \begin{bmatrix} b(1,1) \\ 0 \\ 0 \\ 0 \\ 0 \\ 0 \\ 0 \\ 0 \\ 0 \end{bmatrix}
$$

$$
\underline{A} = \begin{bmatrix}
a(2,2) & a(2,3) & 0 & 0 & 0 & 0 & 0 & 0 & 0 \\
0 & a(3,3) & a(3,4) & 0 & 0 & 0 & 0 & 0 & 0 \\
0 & 0 & a(4,4) & a(4,5) & 0 & 0 & 0 & 0 & 0 \\
0 & 0 & 0 & a(5,5) & a(5,6) & 0 & 0 & 0 & 0 \\
0 & 0 & 0 & 0 & a(6,6) & a(6,7) & 0 & 0 & 0 \\
0 & 0 & 0 & 0 & 0 & a(7,7) & a(7,8) & 0 & 0 \\
0 & 0 & 0 & 0 & 0 & 0 & a(8,8) & a(8,9) & 0 \\
0 & 0 & 0 & 0 & 0 & 0 & 0 & a(9,9) & a(9,10) \\
0 & 0 & 0 & 0 & 0 & 0 & 0 & 0 & a(10,10)
\end{bmatrix}
$$

$$
\underline{B} = \begin{bmatrix}
b(1,2) & 0 & 0 & 0 & 0 & 0 & 0 & 0 & 0 \\
b(2,2) & b(2,3) & 0 & 0 & 0 & 0 & 0 & 0 & 0 \\
0 & b(3,3) & b(3,4) & 0 & 0 & 0 & 0 & 0 & 0 \\
0 & 0 & b(4,4) & b(4,5) & 0 & 0 & 0 & 0 & 0 \\
0 & 0 & 0 & b(5,5) & b(5,6) & 0 & 0 & 0 & 0 \\
0 & 0 & 0 & 0 & b(6,6) & b(6,7) & 0 & 0 & 0 \\
0 & 0 & 0 & 0 & 0 & b(7,7) & b(7,8) & 0 & 0 \\
0 & 0 & 0 & 0 & 0 & 0 & b(8,8) & b(8,9) & 0 \\
0 & 0 & 0 & 0 & 0 & 0 & 0 & b(9,9) & b(9,10)
\end{bmatrix}
$$

input data to a program developed at the Instrumentation and Controls Division of the Oak Ridge National Laboratory to fit a transfer function (31). The result of the fit was a transfer function with five poles and no zeros. The difference between the numerical values obtained with the model developed in chapter 3 and the fitted frequency response are lower than 1% for frequencies up to 17 Hz. The fitted poles are given in Table 4-1. The result of the fit is shown in Figure 4-4.

Table 4-1. Fitted poles for the model

$$s_1 = -52.1 \text{ sec}^{-1}$$
$$s_2 = -18.2 - 104.7j \text{ sec}^{-1}$$
$$s_3 = -18.2 + 104.7j \text{ sec}^{-1}$$
$$s_4 = -8.5 - 4.3j \text{ sec}^{-1}$$
$$s_5 = -8.5 + 4.3j \text{ sec}^{-1}$$

4.4 Sensitivity Analysis

The sensitivity analysis was performed to determine which parameters have more influence in the dynamic response of the transducer. The procedure used in the analysis was to determine the percent of variation in the frequency response per percent of variation in the parameter. To perform the calculations the following expression was used:
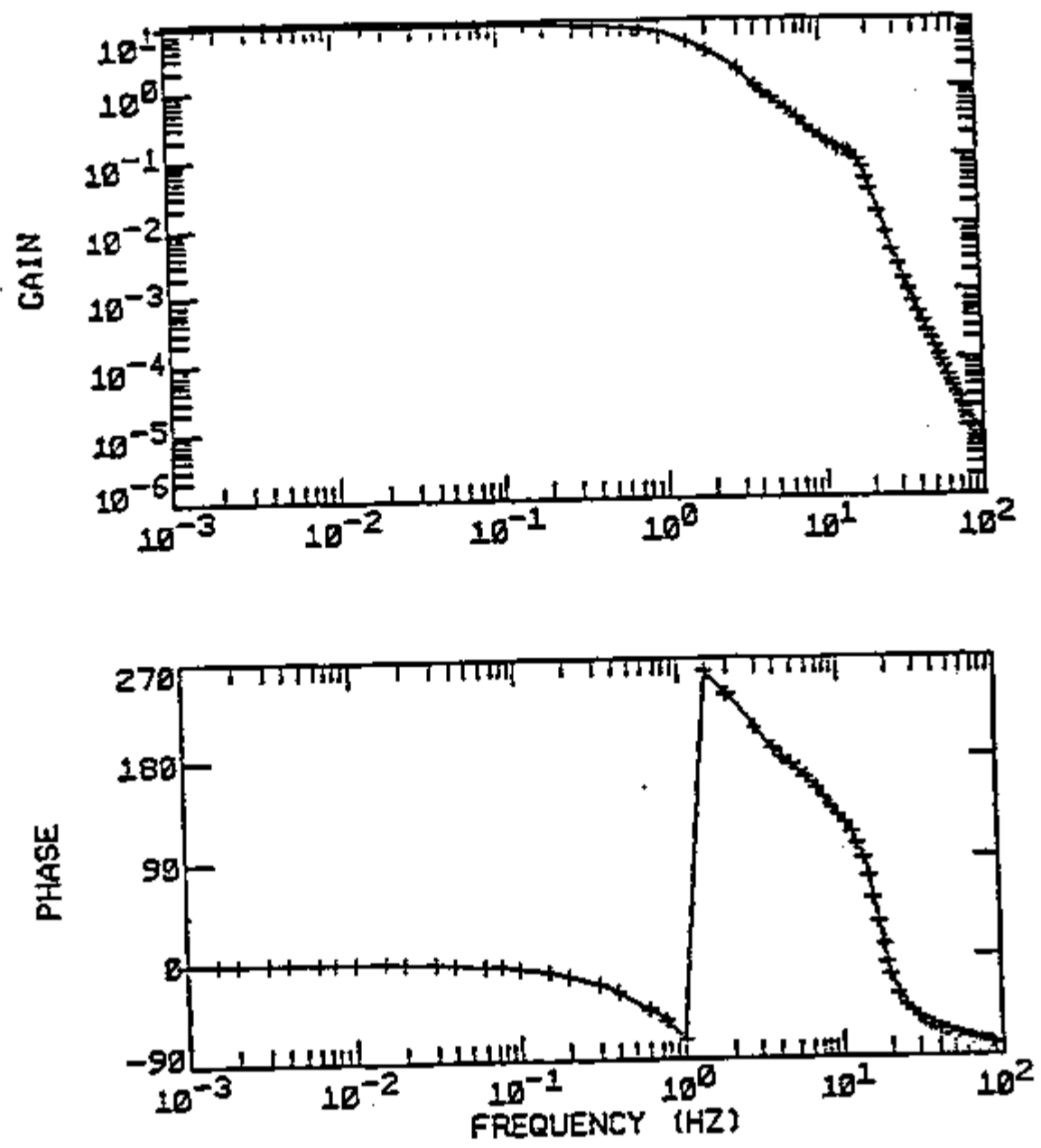
Figure 4-4. Fitted frequency response using output data of the model

$$\text{sensitivity to parameter 'par'} = \frac{G(jw,p+.1p) - G(jw,p)}{10} * 100$$

where p represents the original value of the parameter 'par'.

Before discussing the results of the sensitivity analysis it is necessary to explain the assumption made about the natural vibration of the diaphragm. According to reference (26) the first natural frequency of a circular plate with clamped edge is given by:

$$f = \frac{10.2}{2\pi a^2} \sqrt{\frac{D}{\rho h}}$$

where a = radius of diaphragm

D = flexural rigidity

h = thickness

ρ = density

From reference (32) the deflection of the central portion of a circular plate uniformly loaded is given by

$$\delta = \frac{qa^4}{64D}$$

where q is the load per unit area (pressure). Using the information present in Figure 3-4 (see page 33), we obtain that the value of $a^4/64D$ is $4.3*10^{-8} N/m^3$. Since the radius of the diaphragm is .038 m, we obtain an effective value of D equal to .77 Nm. Assuming that the diaphragm can be represented by one circular plate with an effective D of .77 Nm, the first natural frequency of the plate will be 1.0 KHz. This is well above the frequency range of interest. Because of

the assumption made the sensitivity of the frequency response with respect to the area of the diaphragm is constant.

The results of the sensitivity analysis can be classified according to three distinct regions of frequency. The first region is for frequencies up to 1 Hz, the second for frequencies between 1 and 20 Hz, and the third for frequencies above 20Hz. Table 4-2 is a summary of the most important parameters in the sensitivity analysis. It also shows the frequency range where they affect the results most strongly. The results are shown in Figures 4-5 through 4-23. Additional results are given in Appendix E.

During steady state, the relation between the output DC current I and the differential pressure P applied to the transducer is:

$$I(P) = 10 + \frac{A_{se}(y_a-y_7)\tan\gamma_d(0)\overline{P_{10}P_{11}}\sin\psi_{10}(0)}{(y_8-y_a)K_{fm}} P \qquad (4-5)$$

As shown in Table 4-2 with exception of the parameter $\psi_{10}(0)$ the parameters present in Equation 4-5 are the ones that strongly affect the response of the transducer in the region of low frequency. The value of $\psi_{10}(0)$ is very close to $\pi/2$. For values close to $\pi/2$ the function sin does not change significantly. This is why the frequency response is not strongly affected by $\psi_{10}(0)$.

We also note that for frequencies above 20 Hz a high sensitivity in magnitude does not mean that the parameter affects the results strongly. For these frequencies the magnitude of the frequency response is very small.

Table 4-2. Sensitivity Results

Parameter	Region of importance			See Figure
	1 up to 1 Hz	2 1 to 20 Hz	3 above 20 Hz	
Elasticity Modulus(E)			x	4-5
Diaphragm				
Inertia(I_{ae})			x	4-6
Damping coef.(C_{ae})		x		4-7
Area (A_{ae})	x	x	x	4-8
Flexural system				
Length (L_3)			x	4-9
Force bar				
Lower length (y_6-y_7)	x	x	x	4-10
Upper length (y_5-y_6)	x		x	4-11
Inertia moment(I_7)			x	4-12
Vector mechanism				
Length P_8P_g		x		4-13
Length P_9P_g		x		4-14
Constant C_3		x		4-15
Angle y_4(0)	x		x	4-16
Lever system				
Torsional constant K_{pv}			x	4-17
Inertia $I_{\ell v}$			x	4-18
Damping coeff. $C_{\ell v}$		x		4-19
Distance $P_{10}P_{11}$	x		x	4-20
Distance $P_{11}P_{14}$		x	x	4-21
Electronics				
Gain $C_{e\ell}$		x	x	4-22
Force motor F_{fm}	x			4-23

Figure 4-5. Sensitivity with respect to parameter E

Figure 4-6. Sensitivity with respect to parameter I_{se}

Figure 4-7. Sensitivity with respect to parameter C_{se}

Figure 4-8. Sensitivity with respect to parameter A_{se}

Figure 4-9. Sensitivity with respect to parameter L_3
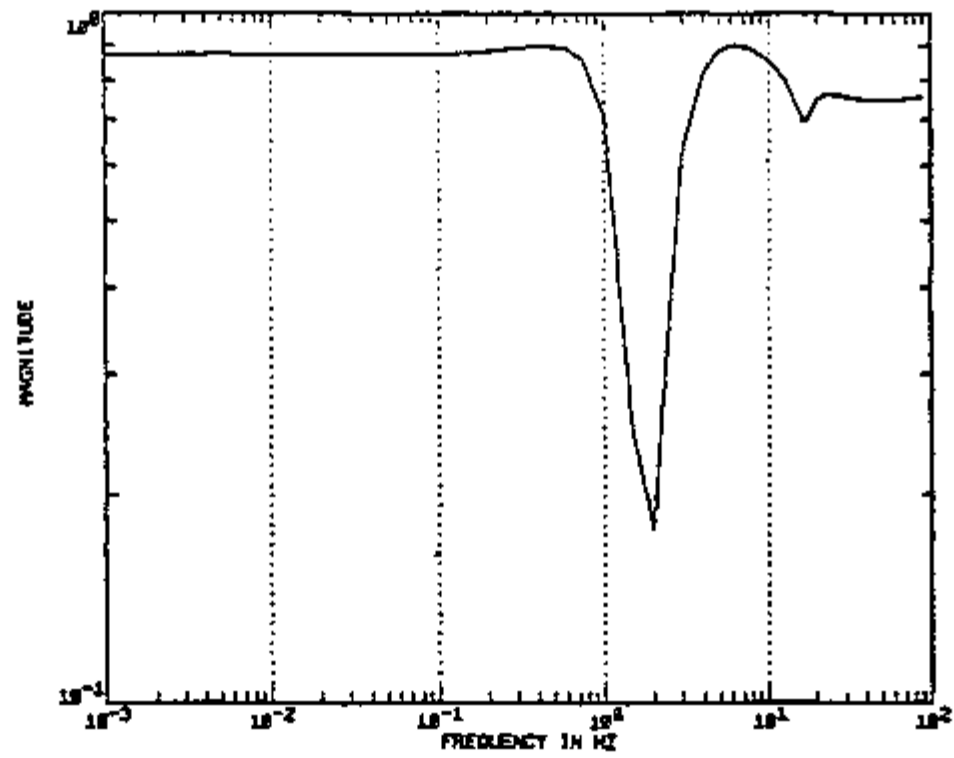
Figure 4-10. Sensitivity with respect to parameter Y_8-Y_7

Figure 4-11. Sensitivity with respect to parameter Y_8-Y_4

Figure 4-12. Sensitivity with respect to parameter I_7
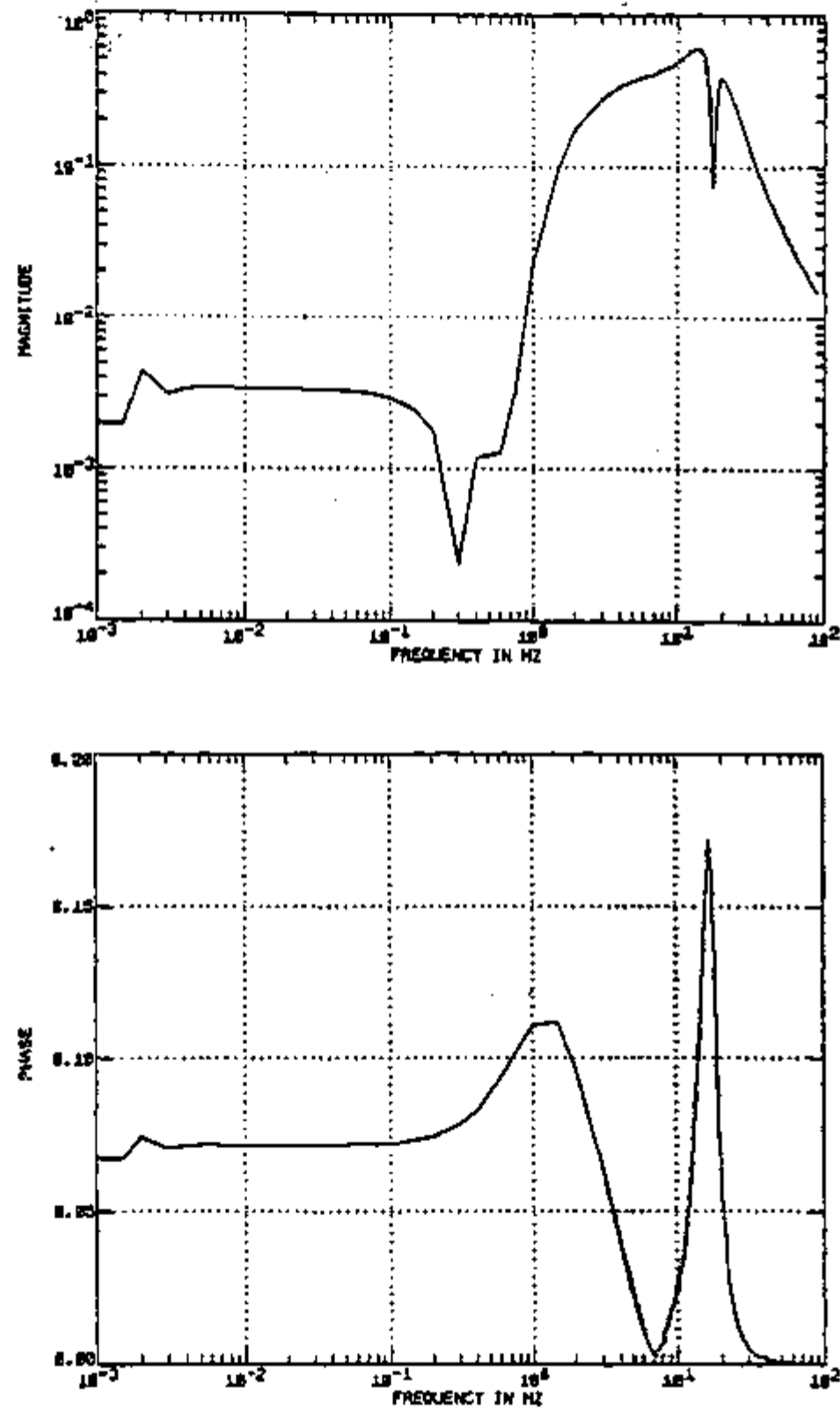
Figure 4-13. Sensitivity with respect to parameter $P_8 P_9$
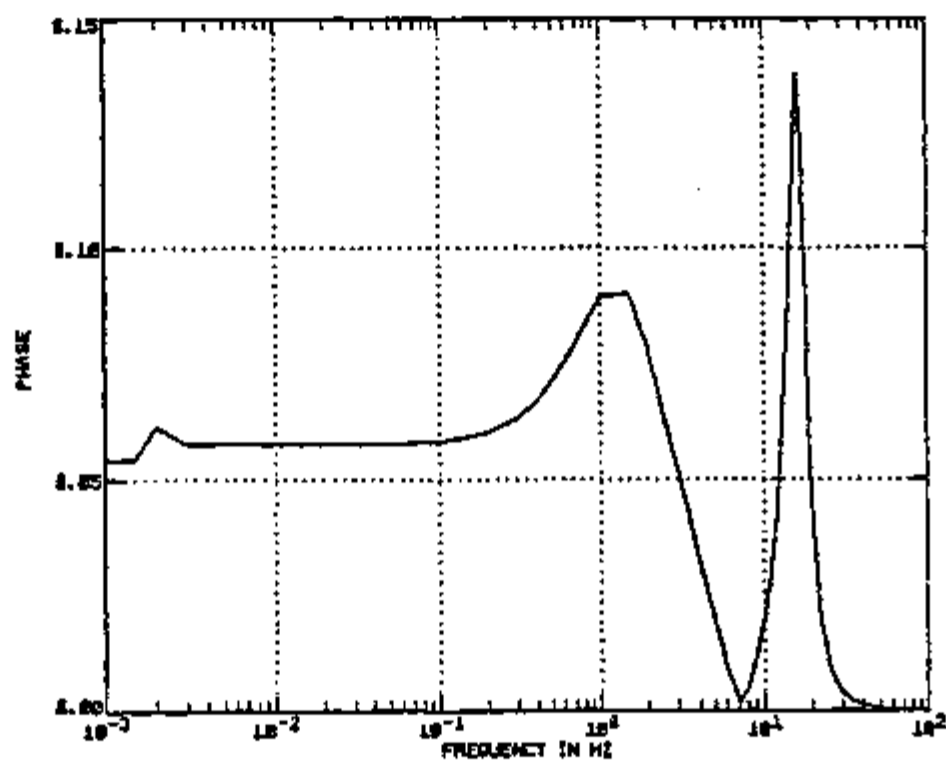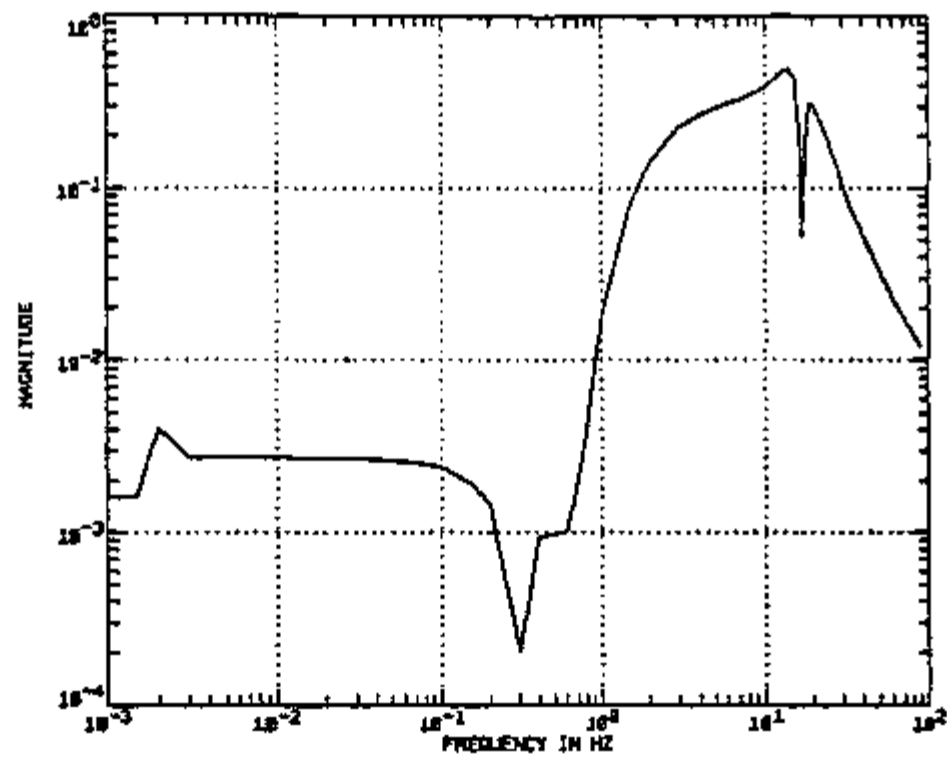
Figure 4-14. Sensitivity with respect to parameter $P_g P_g$
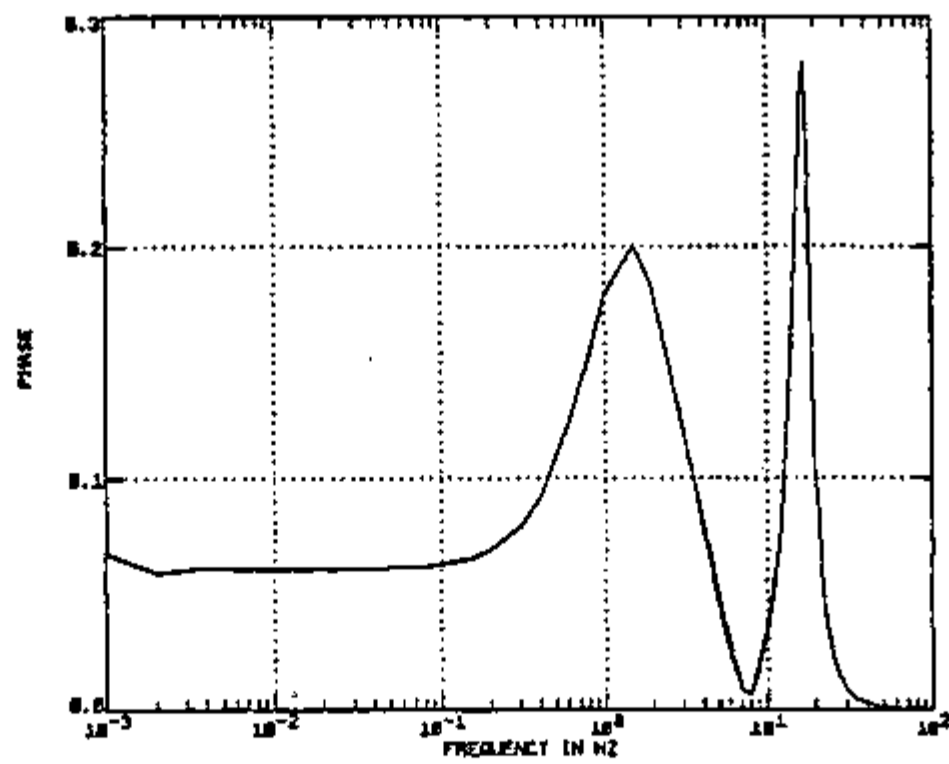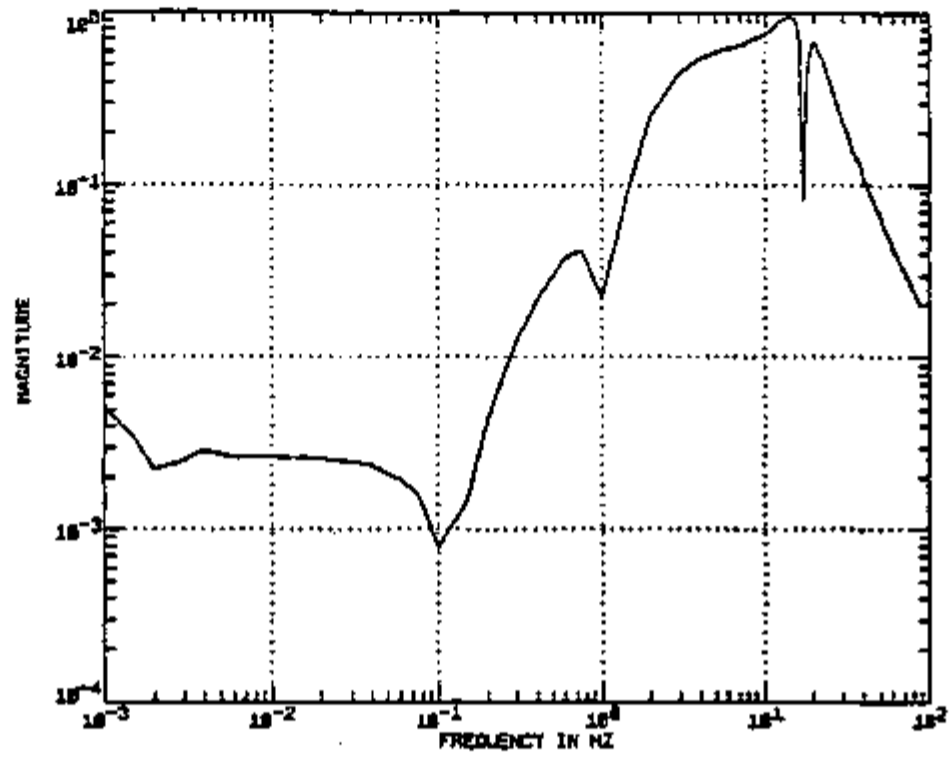
Figure 4-15. Sensitivity with respect to parameter C_3
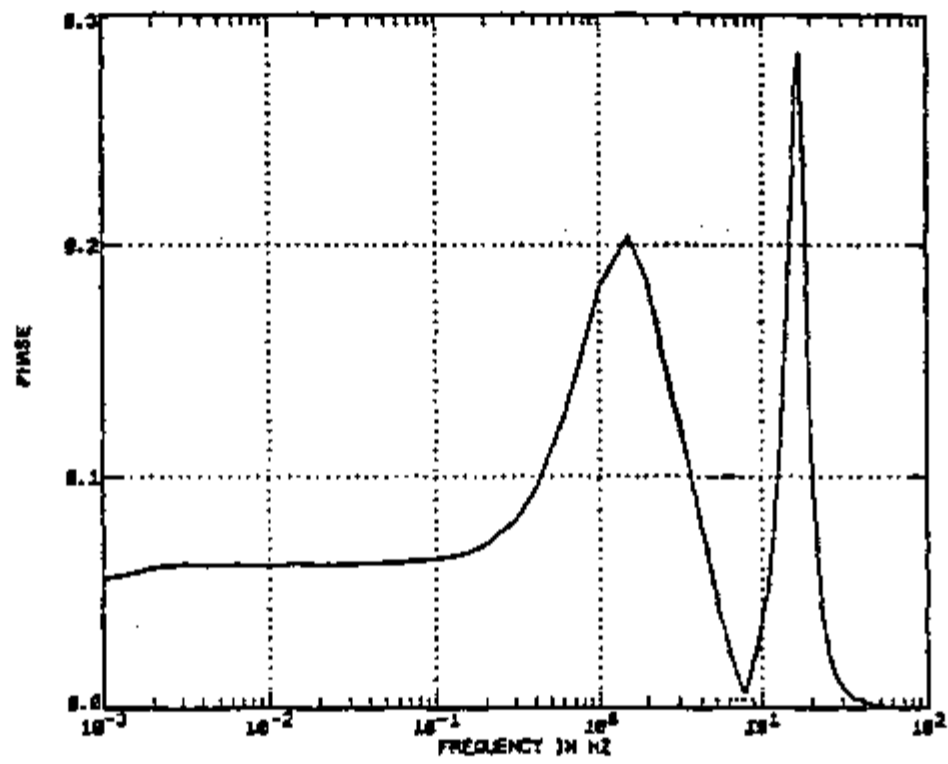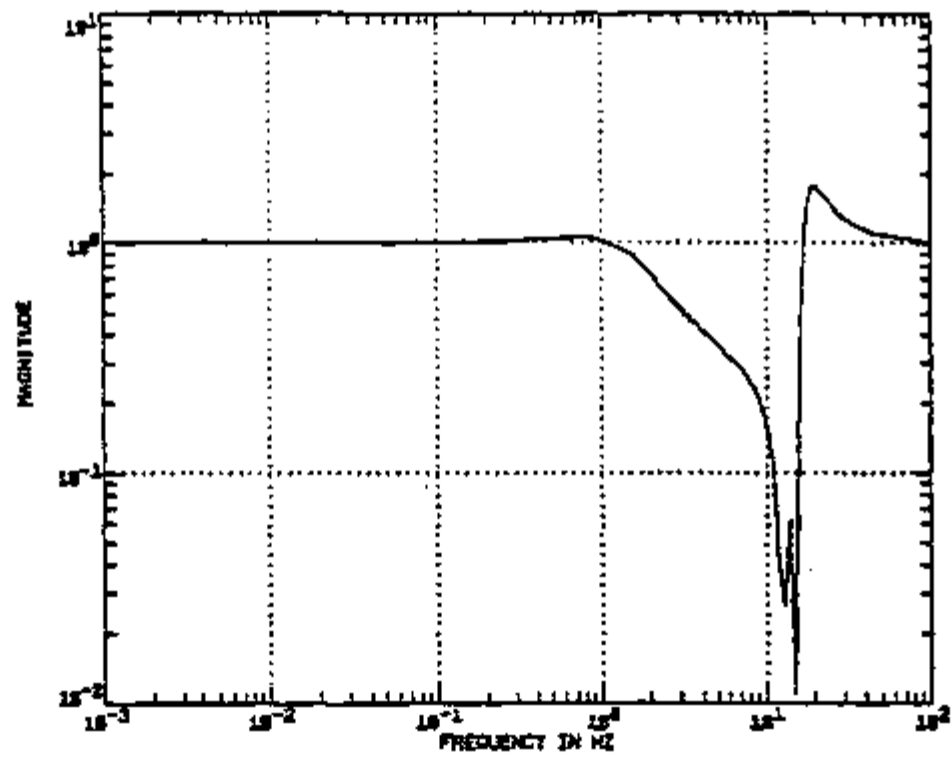
Figure 4-16. Sensitivity with respect to parameter $\gamma_d(0)$
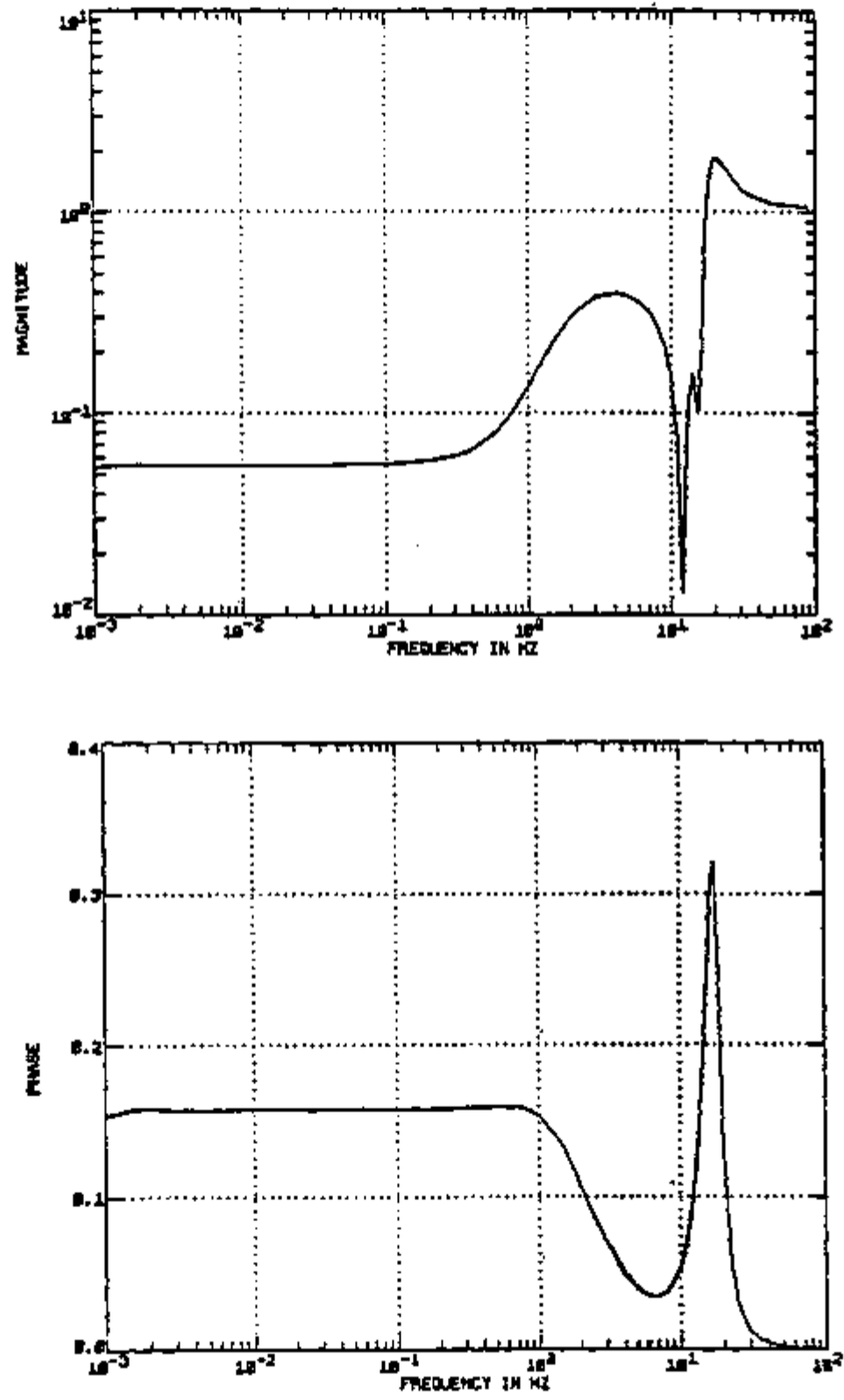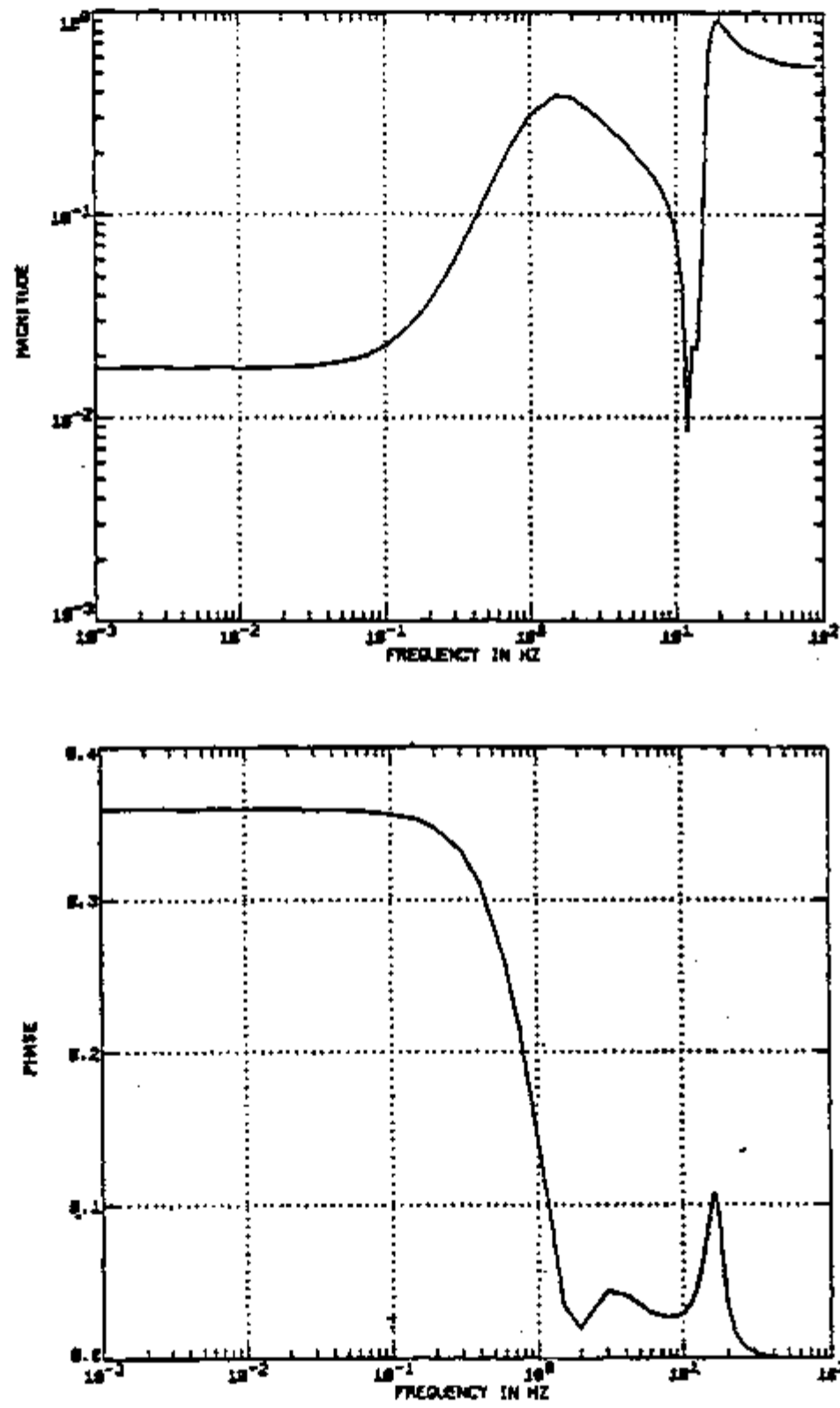
Figure 4-17. Sensitivity with respect to parameter K_{pv}
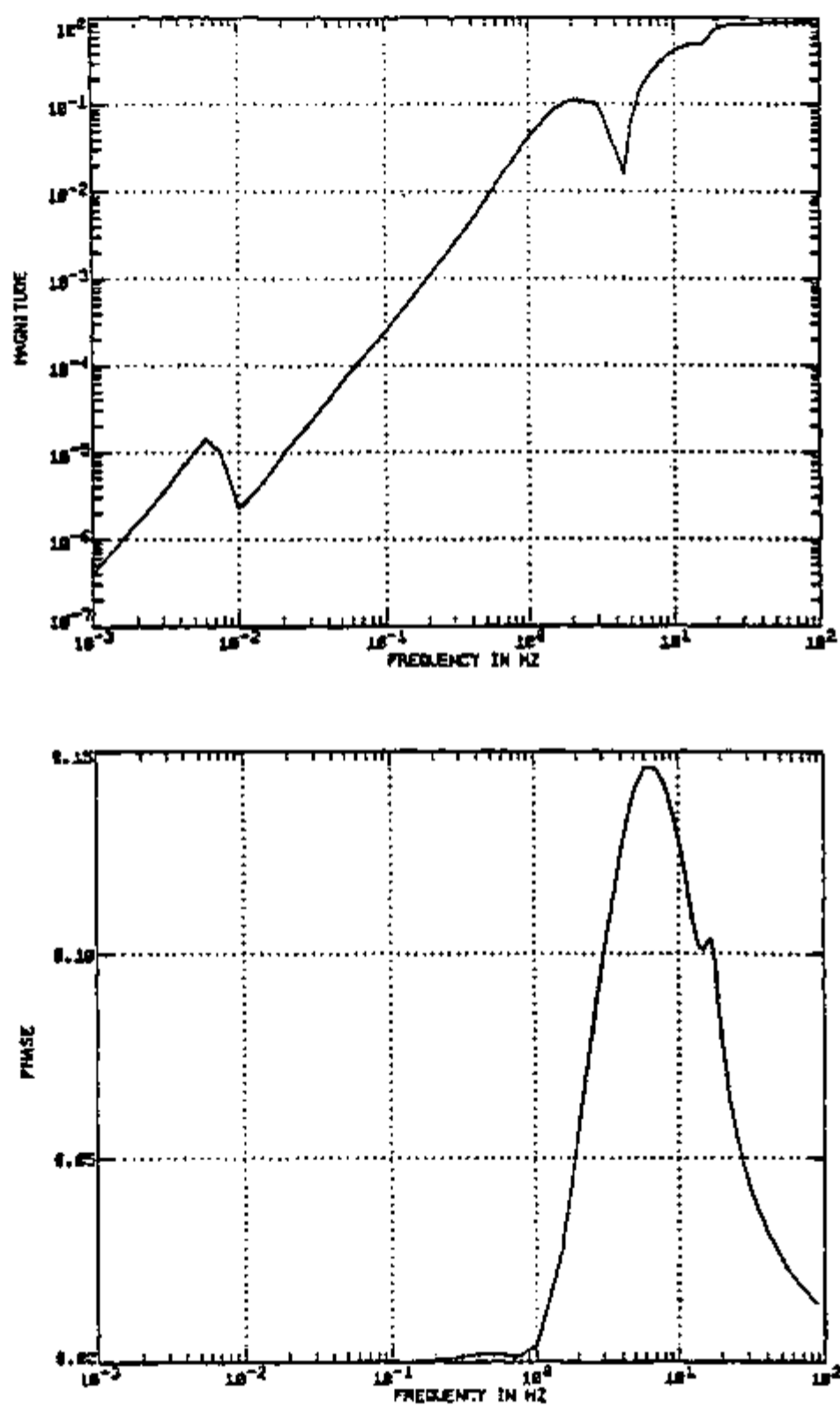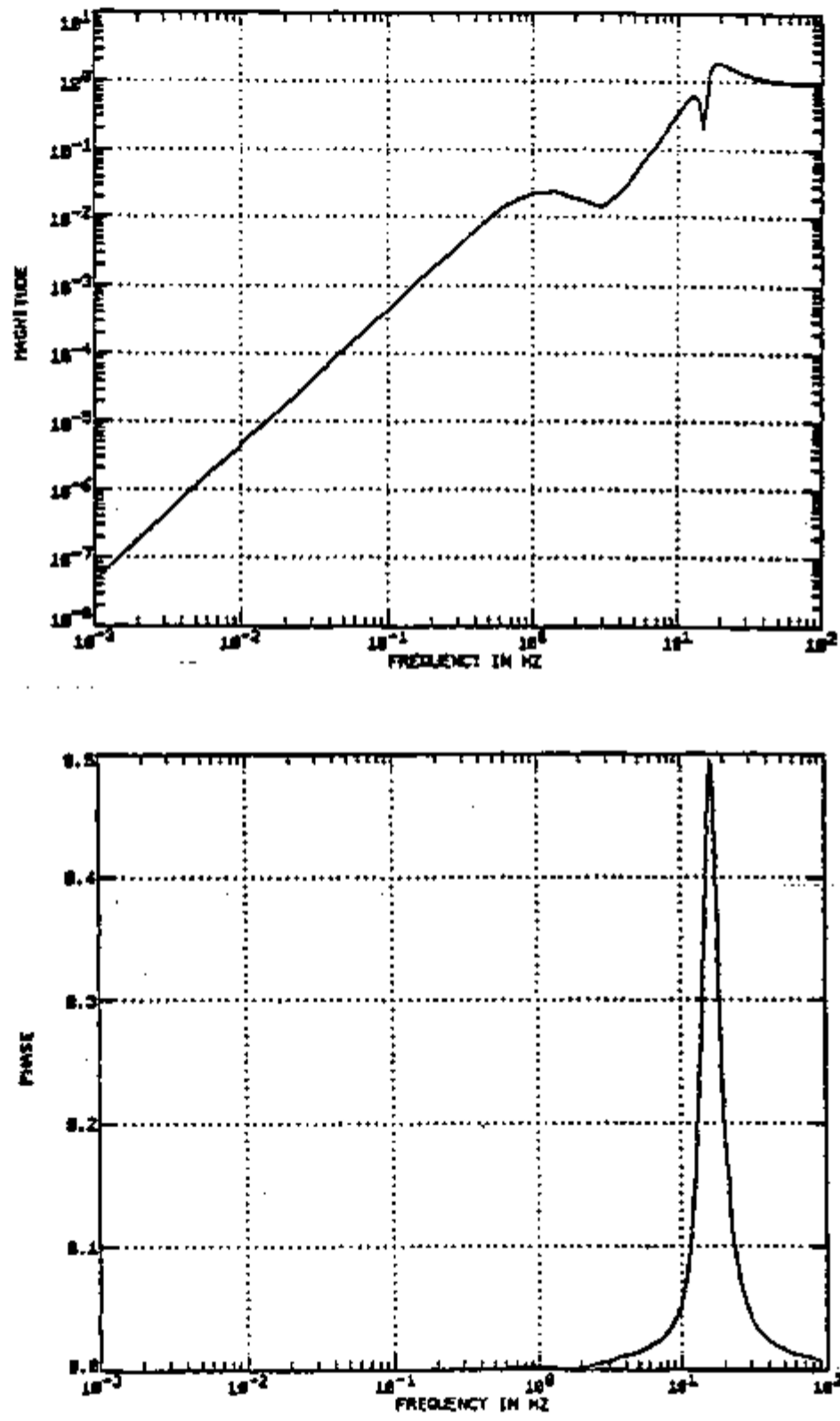
Figure 4-18. Sensitivity with respect to parameter $I_{\ell s}$
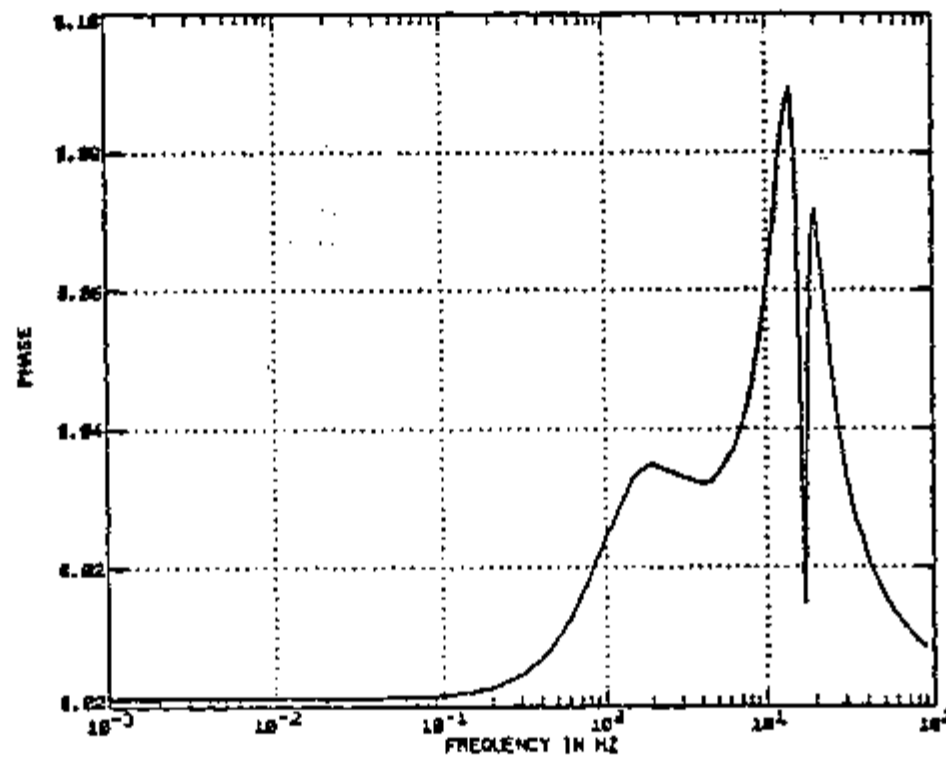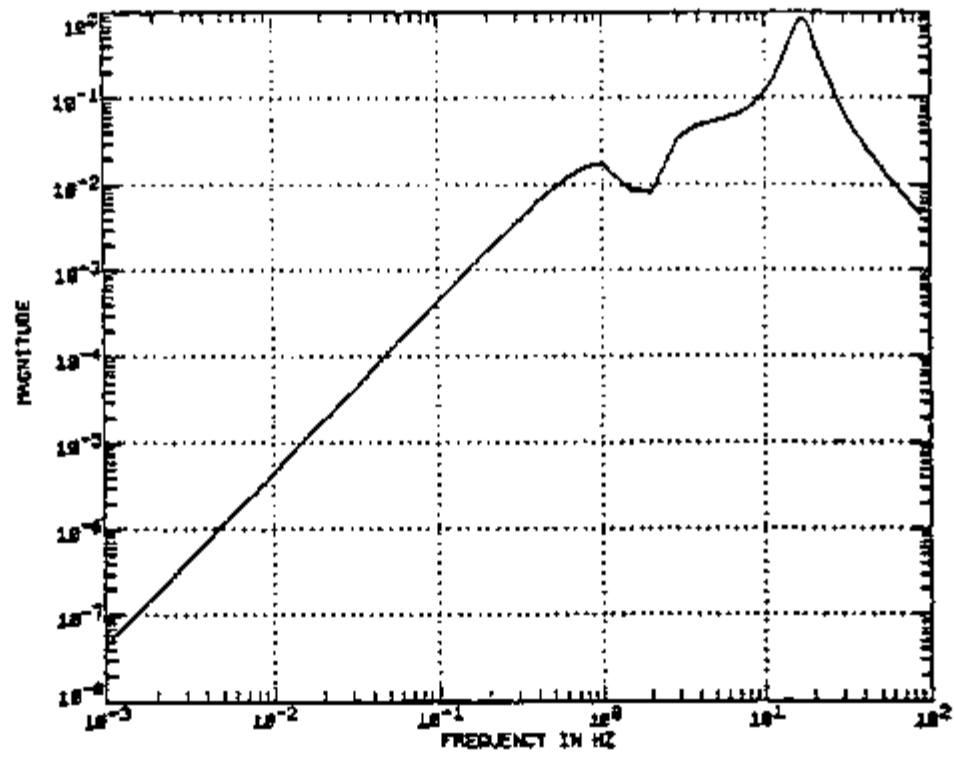
Figure 4-19. Sensitivity with respect to parameter C_{ℓ_S}
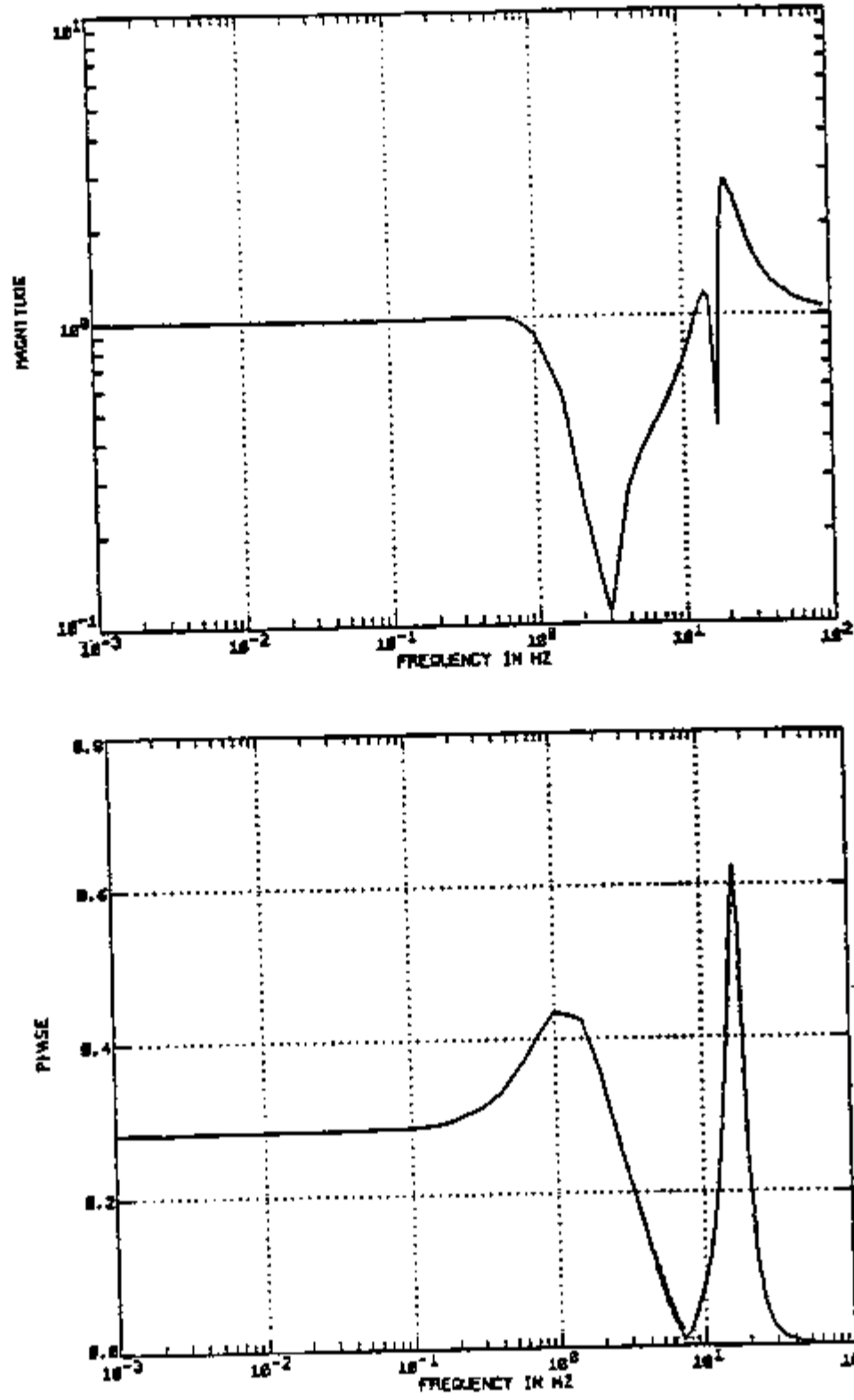
Figure 4-20. Sensitivity with respect to parameter $P_{10}P_{11}$
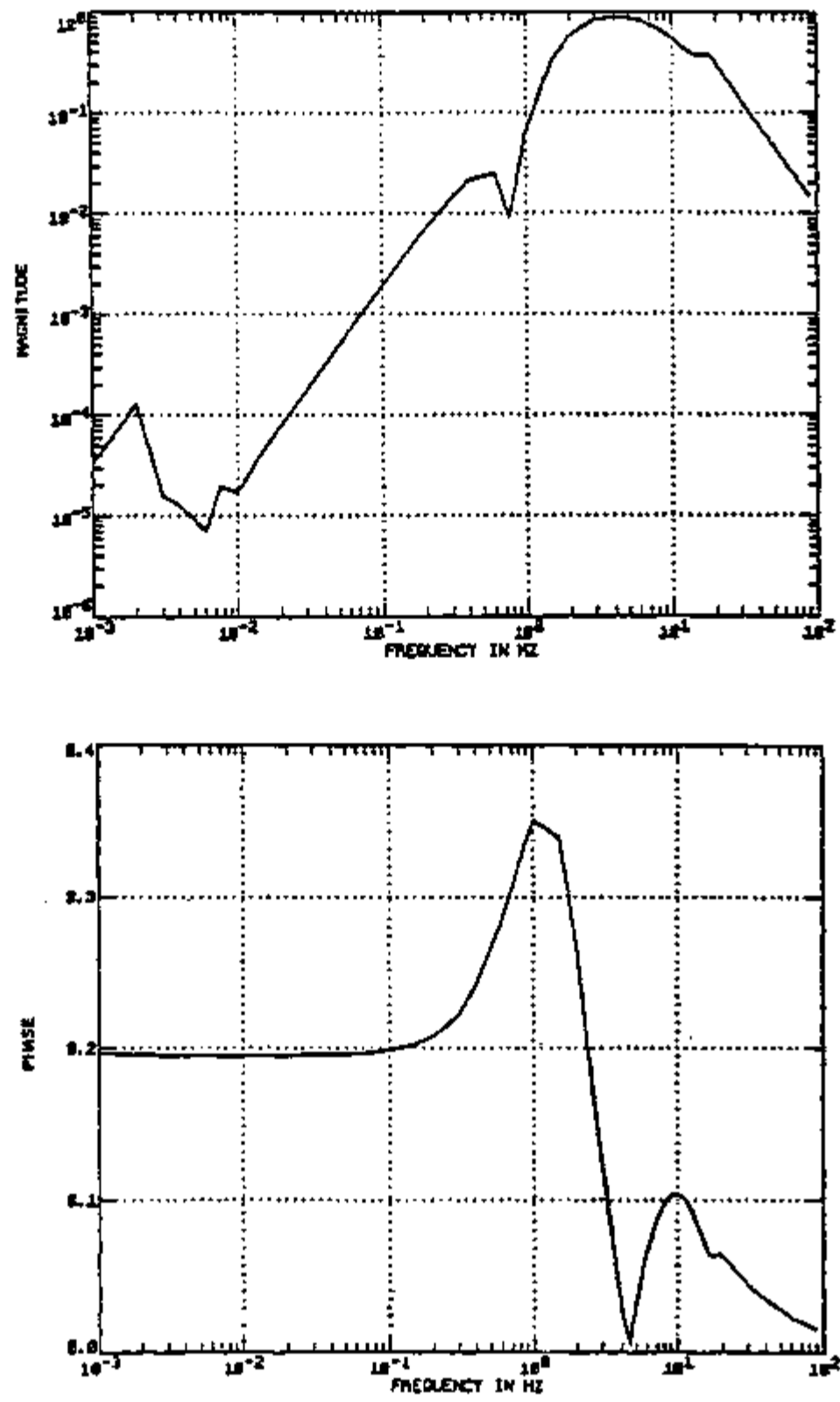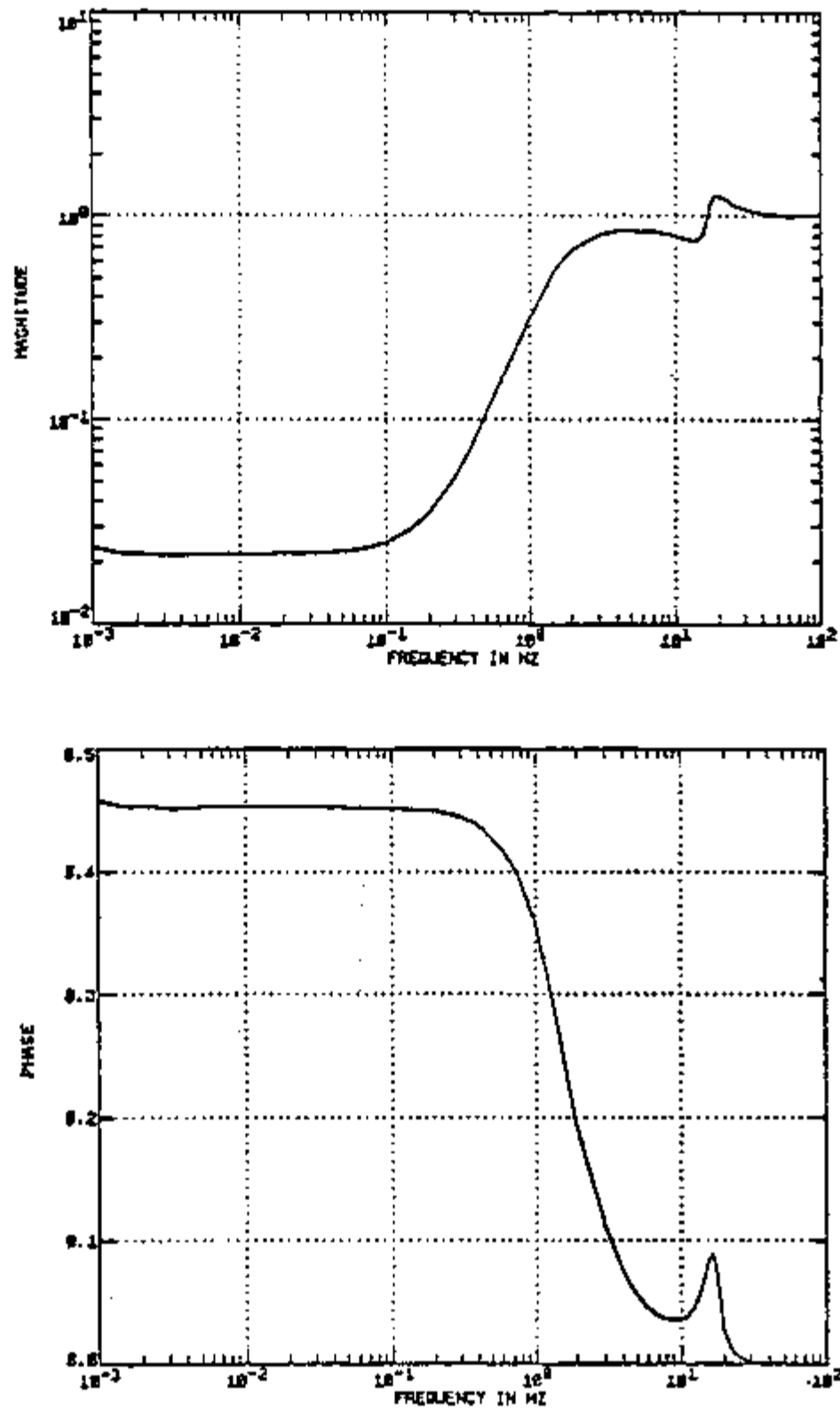
Figure 4-21. Sensitivity with respect to parameter $P_{11}P_{14}$
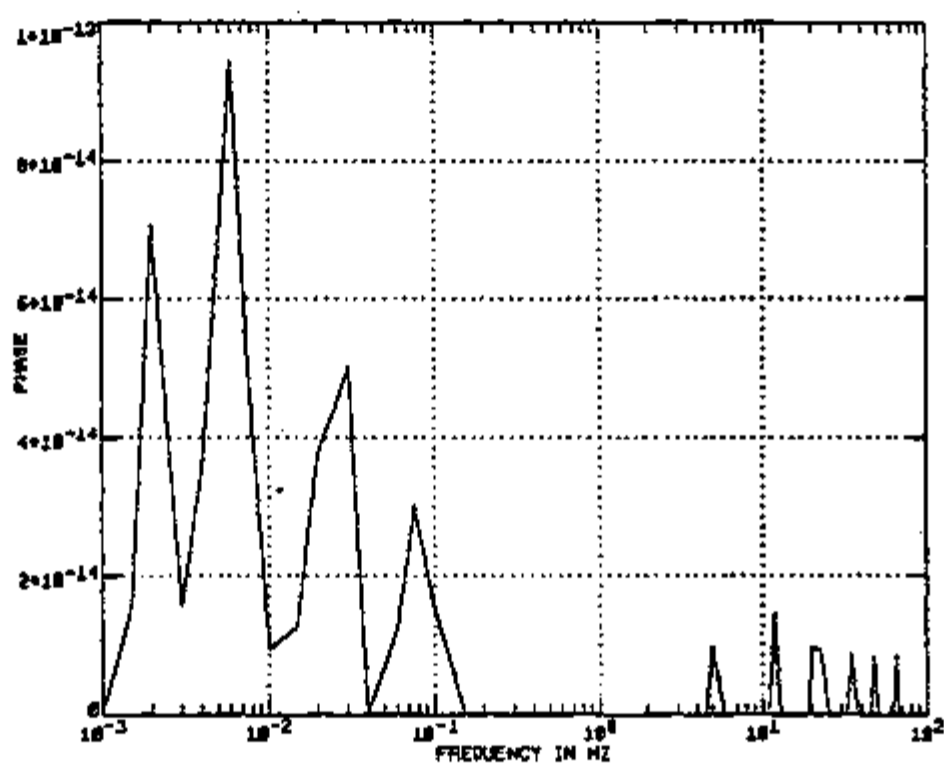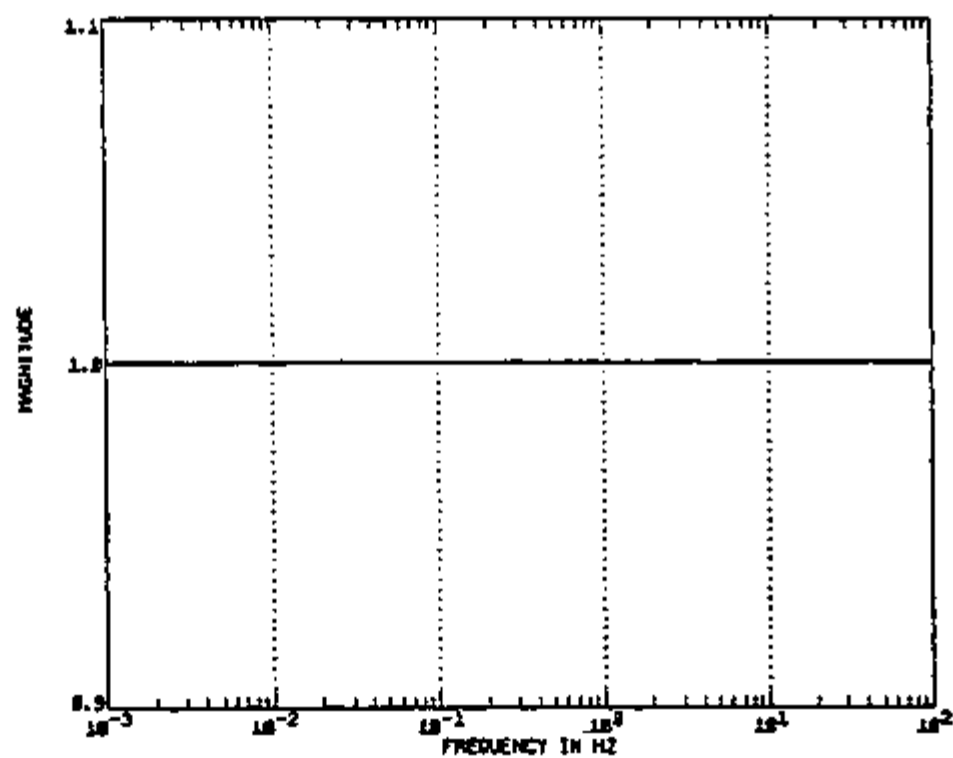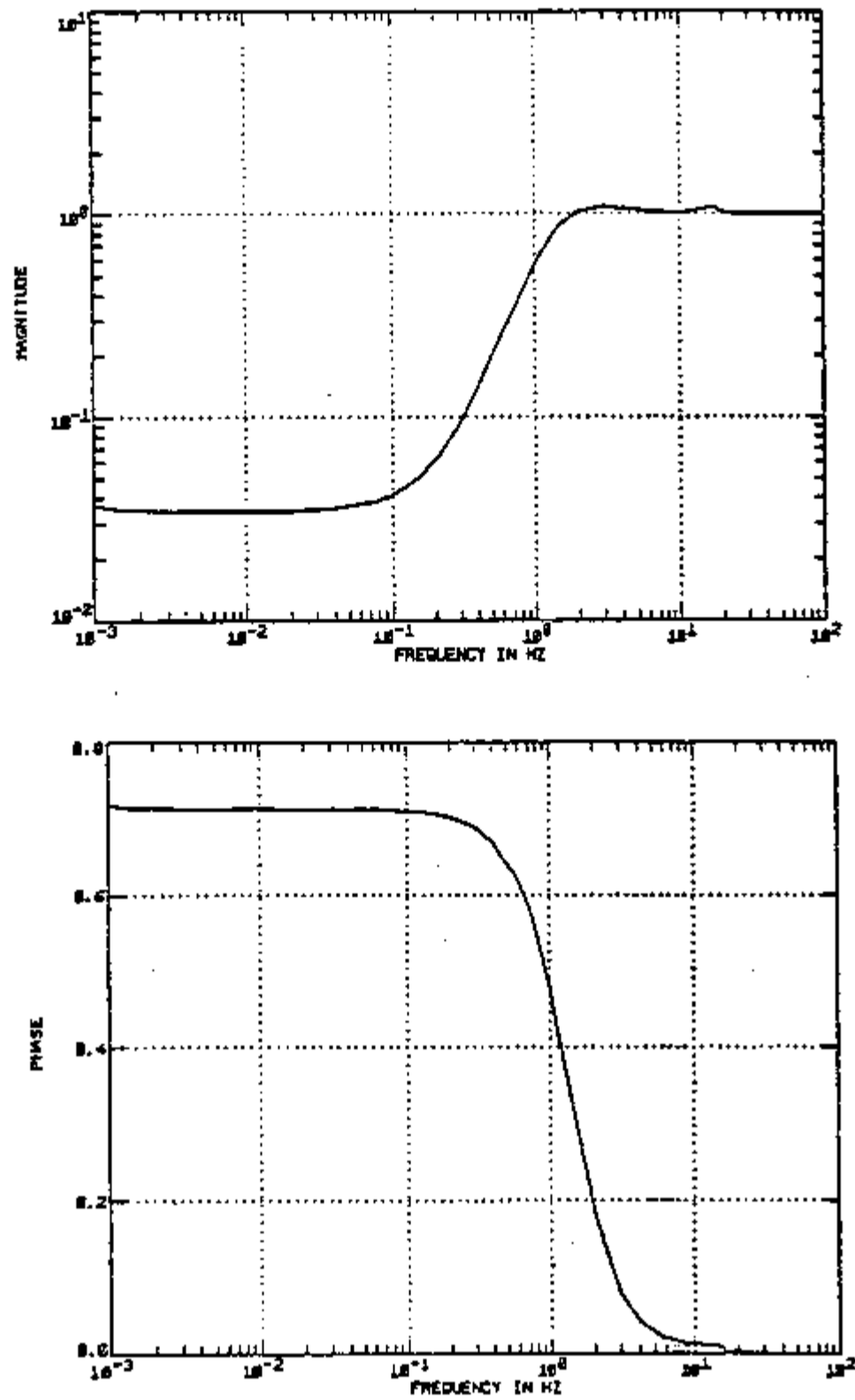
Figure 4-22. Sensitivity with respect to parameter $C_{e\ell}$
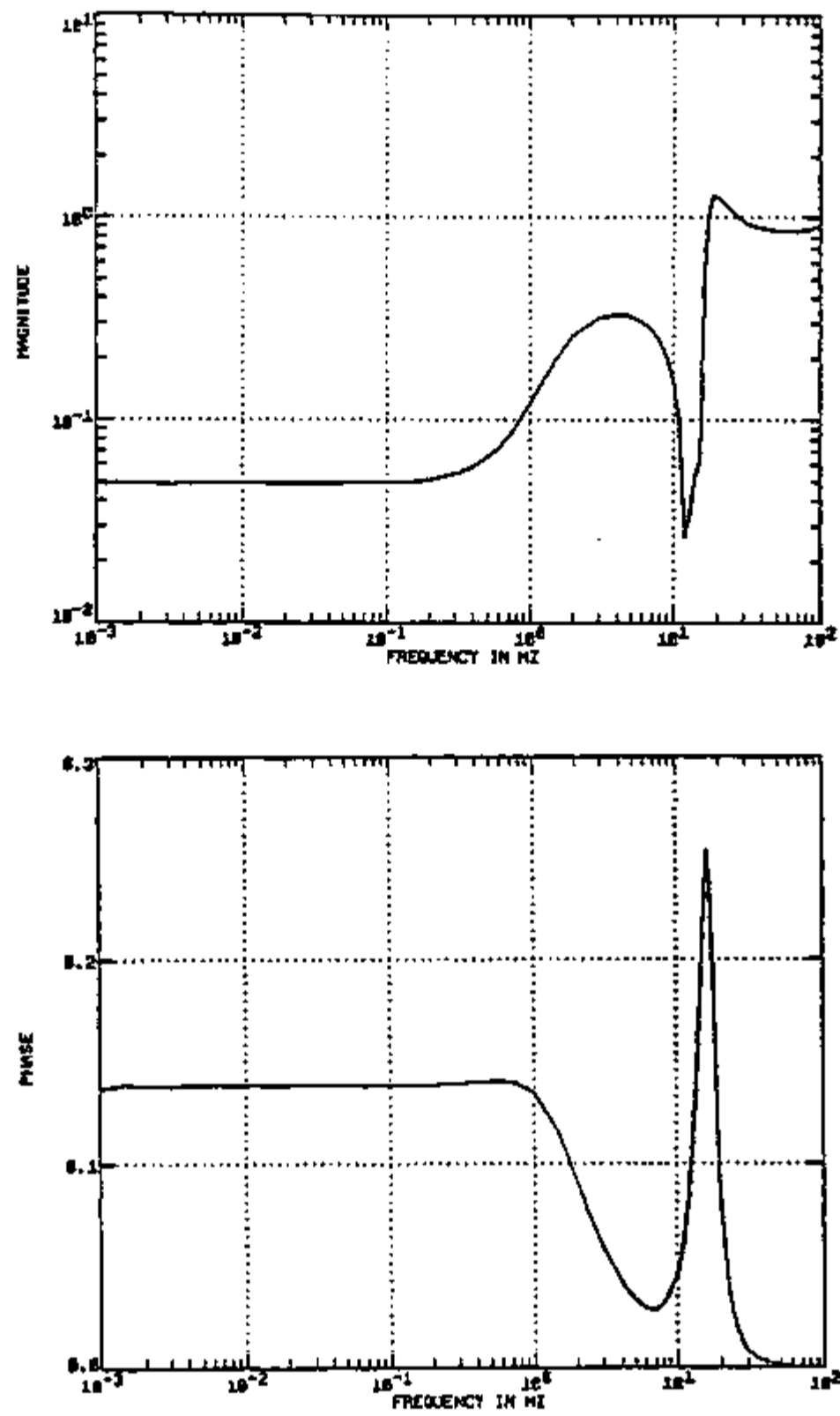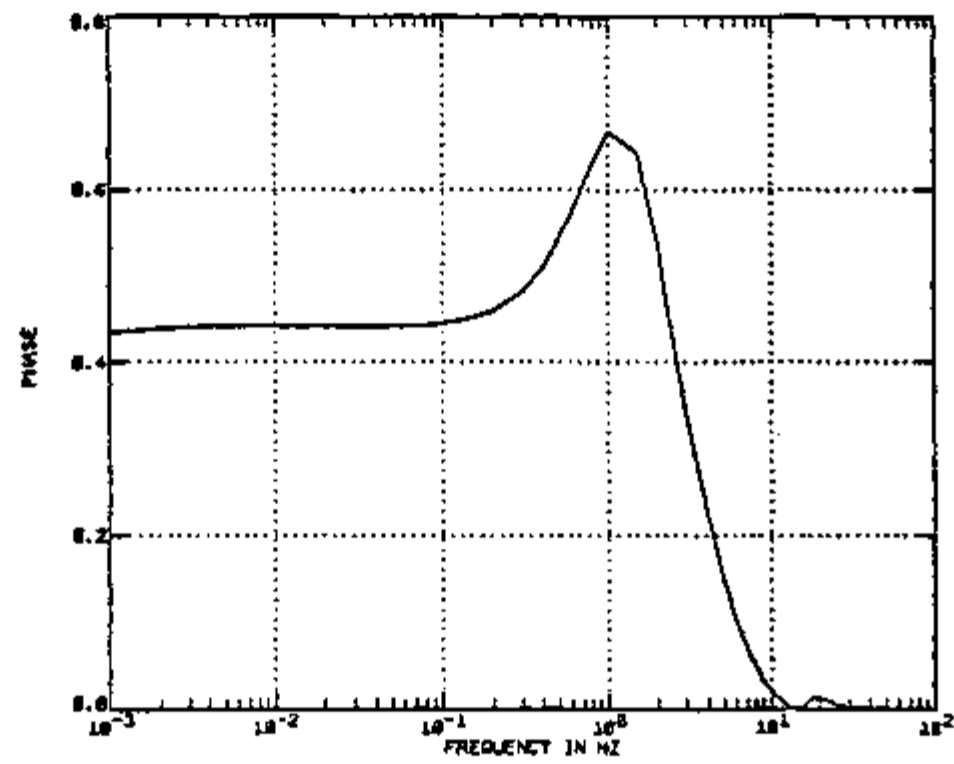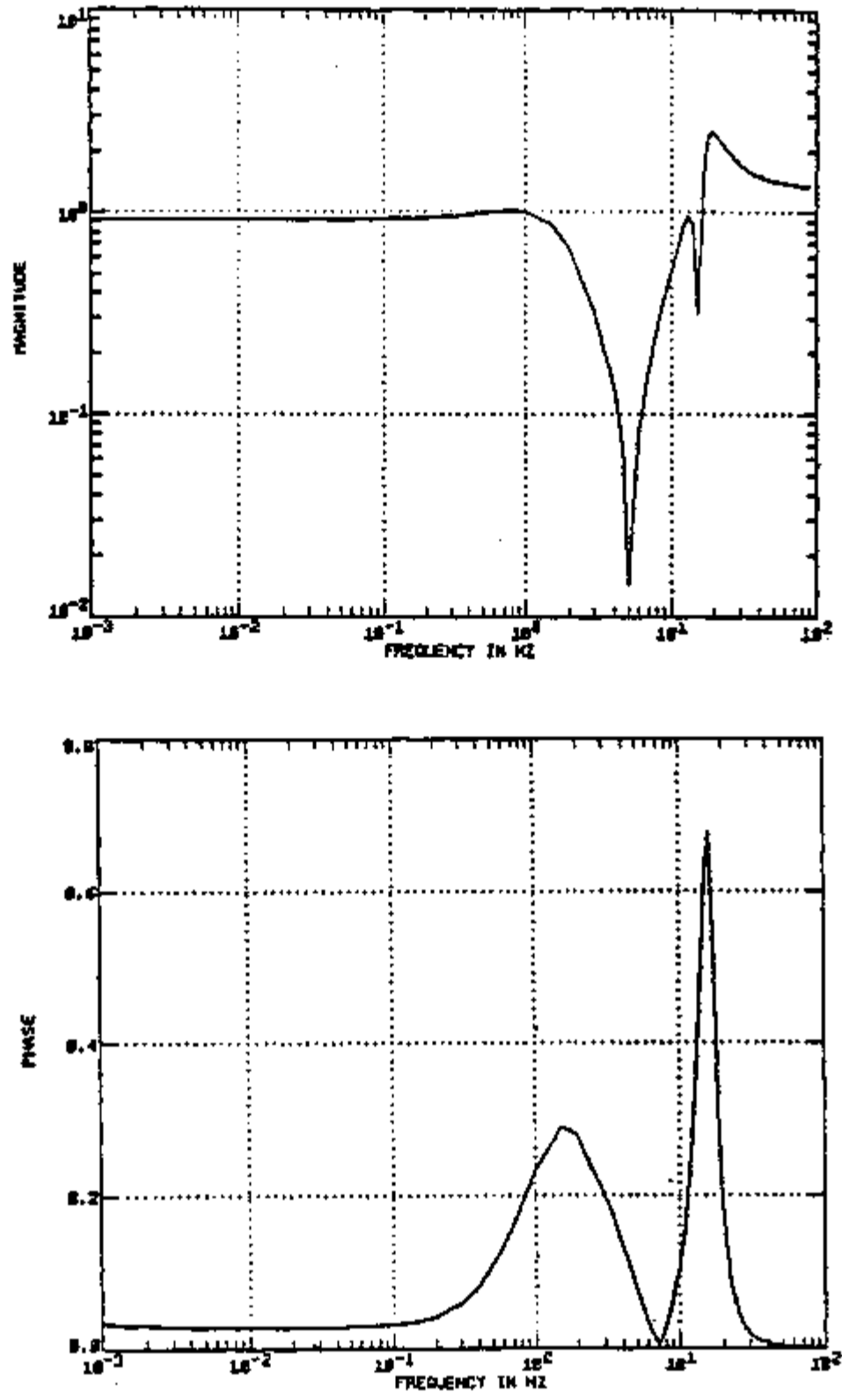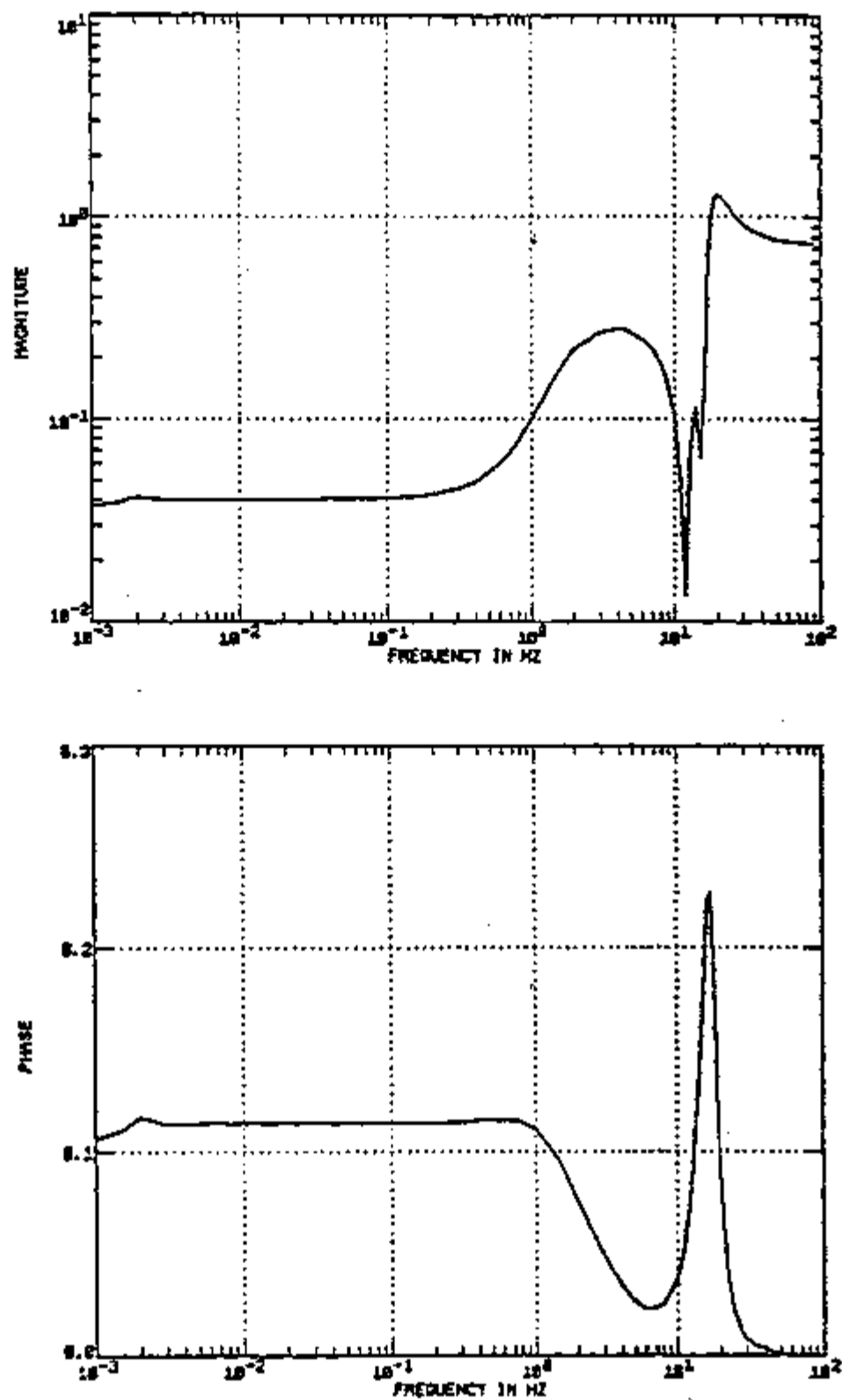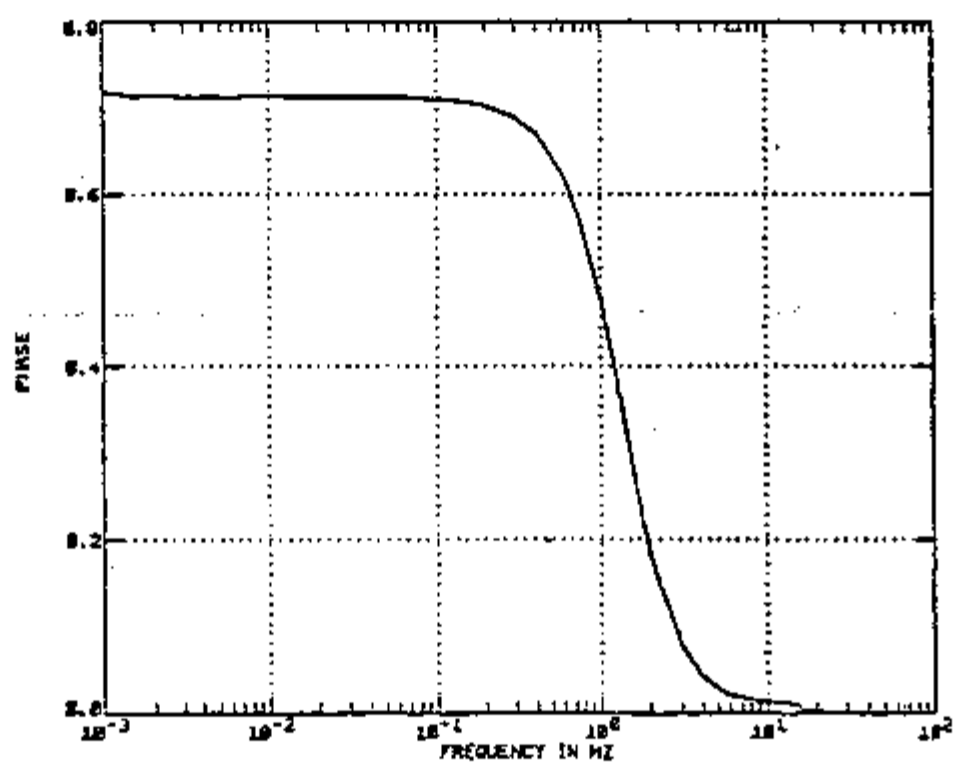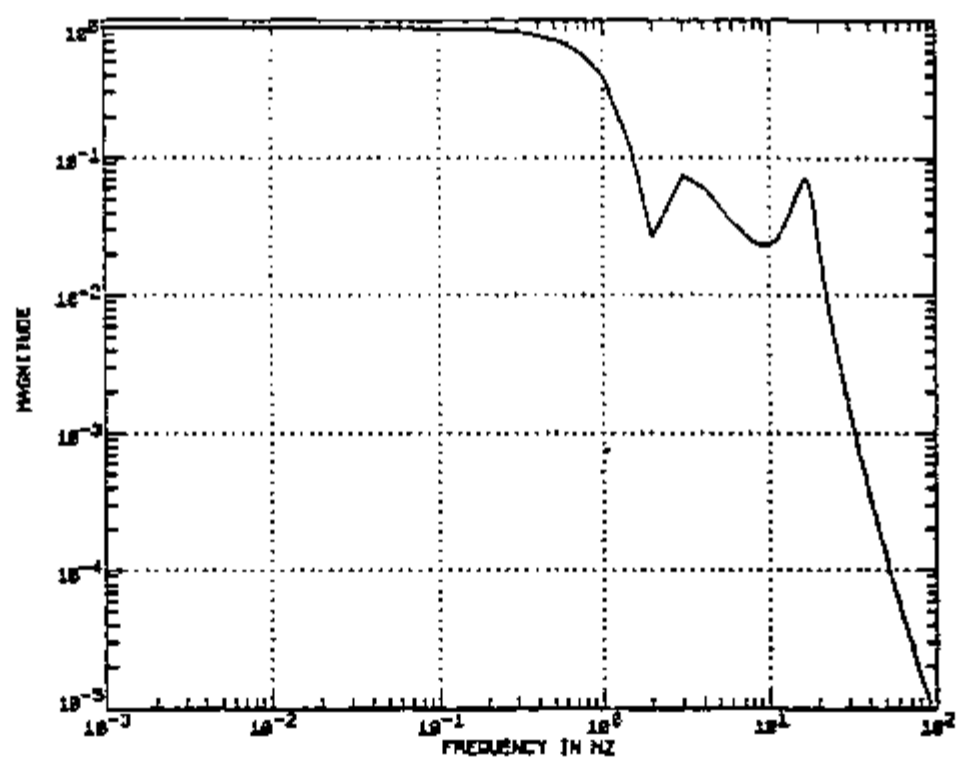
Figure 4-23. Sensitivity with respect to parameter K_{fm}

With reference to the division adopted for the flexural system (see section 3.2.2), it was found that the most significative result was the sensitivity with respect to the length of the element number 3. The sensitivity for this parameter is lower than 1% for the magnitude, and lower than .25% for the phase. The sensitivity with respect to the other parameters of the flexural system is about 10 times lower.

In order to illustrate the usefulness of the sensitivity analysis we analyse the results shown in Figures 4-19 and 4-22. Figure 4-19 shows the sensitivity of the frequency response of the transducer with respect to parameter $C_{\ell s}$ (see page 151). $C_{\ell s}$ is the damping coefficient for the lever system. As explained in section 3.2.6 the value of $C_{\ell s}$ is very small (.017 Nmsec^2). As a result of the small value of $C_{\ell s}$ the motion of the lever system is underdamped, as seen in Figure 3-15 on page 85. Mathematically the underdamped motion is characterised by a pair of complex poles in the transfer function of the system (see Figure 3-21 on page 98). The influence of the complex poles in the overall frequency response of the transducer is represented by a small peak present in Figure 3-36, in the region close to 18 Hz (see page 122).

It may be concluded that an increase in $C_{\ell s}$ causes the small peak shown in Figure 3-36 to decrease, making the transducer a more stable system. Converselly, a decrease in $C_{\ell s}$ causes the peak to increase, making the transducer a less stable system.

In addition to the analysis described we note that one characteristic of the Foxboro pressure transducer is that a small

displacement of the sensing element implies a large displacement of the end portion of the lever system (the end portion of the lever system is defined as the region close to the position of the spring used for zero adjustment). Therefore, it is concluded that a damping device installed at the end of the lever system is more efficient than the same device installed at the position of the sensing element.

Now we analyze the sensitivity of the frequency response of the transducer with respect to the parameter $C_{e\ell}$ (see Figure 4-22 on page 154). $C_{e\ell}$ is a parameter that is proportional to the gain of the transfer function for the electronic system. Since the electronic system generates the feedback force, it is understood that one way of improving the response of the transducer is to increase the gain of the transfer function for the electronic system (which means to increase $C_{e\ell}$).

To analyse the influence of $C_{e\ell}$ in the low frequency region, we make use of Equation 3-119 (see page 100). It was found that for small values of s (in magnitude), the main contribution for the denominator of Equation 3-119 is from the last term $(G_{fm} C_{e\ell} \overline{P_{11} P_{14}} \sin\psi_{14}(0))$. This means that for low frequencies the overall transfer function for the lever system (G_{ovls}) may be approximated by $1/G_{fm}$, which is a constant. According to this analysis the change in $C_{e\ell}$ affects mainly the frequency response of the transducer in the region of high frequencies (the region above the first break frequency of G_{ovls}, or about 1 Hz). As seen in Figure 4-22 (see page 154) this analysis agrees with the result of the sensitivity analysis.

4.5 Extension of the Model to Other Foxboro Transducers

The model developed in chapter 3 showed that the dynamic behavior of the transducer used as the reference in this work depends mainly of three subsystems: lever system, electronics, and sensing element. The geometry of the lever system is the same for all models of Foxboro transducers. Therefore the effect of the lever system in the response of the transducer is expected to be the same for all models. The effect of the electronic circuit depends of the circuit used. As explained in chapter 2 there are two electronic circuits available for Foxboro pressure transducers. One to give an output DC current signal between 4 and 20 mA. The other to give an output DC current between 10 and 50 mA. The effect of the electronic circuit also depends of the calibration of the transducer. As explained in section 2.3 there is a jumper selection that is adjusted according to the span of operation. The sensing element depends of the model of the transducer and can be a diaphragm, a bellows or a Bourdon tube. Each sensing element can affect the response of the sensor in a different way.

The sensitivity analysis developed in section 4.4 showed that the effect of the electronic system in the response of the transducer is mainly due to the force motor. The feedback coil is the main component of the force motor and, as explained in section 2.3, can be arranged in three different configurations. The effective resistance on the coil can be 173, 89 or 42 ohms, depending on the jumper configuration selected. As explained in section 3.3.2 the transfer function for the force motor is a constant (K_{fm}). The value of K_{fm}

is given by a constant multiplied by the effective resistance of the feedback coil. The model developed in chapter 3 predicts that when the effective resistance of the feedback coil decreases the response of the transducer becomes slower. Figure 4-24 shows the frequency response as predicted by the model for the three effective resistances of the feedback coil. This behavior, (slower response for lower effective resistance in the feedback coil), was noticed in experimental work with transducers that operate between 4 and 20 mA (33). Since the gain of the transfer function is a function of R_{fm} (see Equation 4-5), the magnitudes shown in Figure 4-24 are normalized to 1 for comparison. We note here that the results shown in Figure 4-24 do not take into account the change in the parameter C_{el} present in equation 3-116.

It is understood that the transfer function for the different configurations of the electronic system and the dynamic equations for the different sensing elements used in Foxboro transducers can be obtained empirically (as described in sections 3.2.1 and 3.2.10). Once these equations have been obtained the result can be easily implemented in the model developed in chapter 3 to predict the frequency response of the transducer.

Comparison between the results shown in Figure 4-2 and results obtained with other models of Foxboro transducers showed that the frequency response does not change very much. The main differences observed were:

1- the break frequency changed between 1 and 3 Hz.
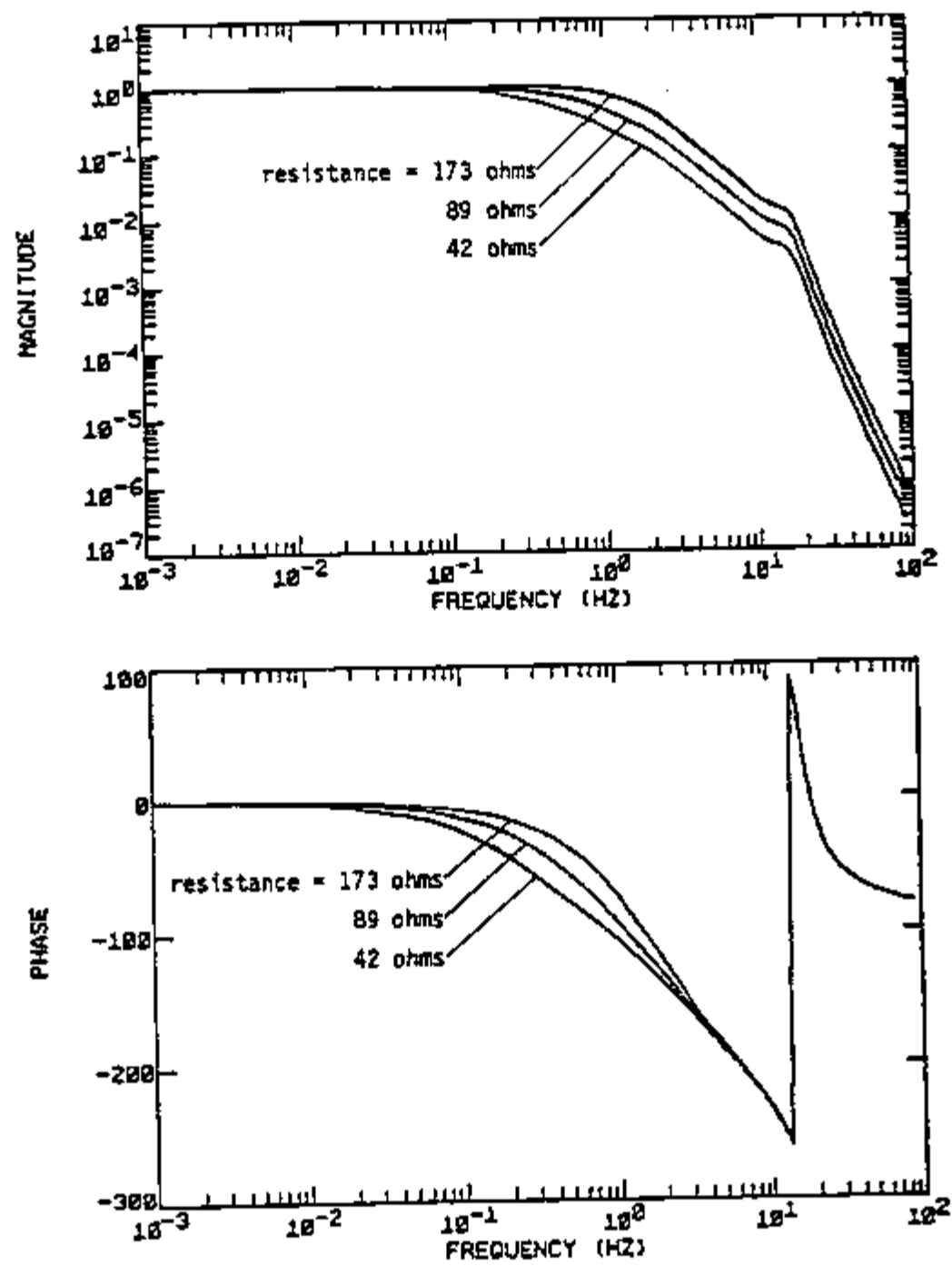
Figure 4-24. Predicted frequency response for different effective resistances of the force motor

161

2- the shape of the frequency response, immediately after the break frequency, indicated a second order system (magnitude decreasing at 2 decades per decade of frequency and phase going to -180 degrees), or a first order system (magnitude decreasing with 1 decade by decade and phase going to -90 degrees), depending of the model (33).

CHAPTER 5

STUDY OF NON-LINEARITIES

5.1 Introduction

It has been observed that the response of the Foxboro
transducer to large signal perturbations is different from the
response to small signal perturbations. Therefore the transducer is
a non-linear system. In this chapter we analyze the causes of the
non-linear behavior, and the conditions under which it can be assumed
to be a linear system.

The transducer used in the experimental work had an output
signal between 10 and 50 mA. Once the transducer has been calibrated
there is a linear relation between the pressure being measured and
the output signal of the transducer. Also, for any span adjustment,
the maximum difference in the output signal of the transducer is
40 mA, and it corresponds to 100% of the adjusted span. Therefore,
once we have the calibration curve for the transducer, we can express
the pressure reading as pressure, output current, or percent of the
adjusted span. In this work the pressure readings are given in terms
of the adjusted span. The adjusted span for the transducer used was
37.2 kPa.

5.2 Non-linear Behavior

There are two causes for the non-linear behavior of the
transducer. One is mechanical, and the other electrical. First we
analyze the mechanical cause.

As explained in section 2.2, the function of the mechanical

system is to transform the differential pressure existing across the diaphragm into a displacement of the ferrite disk. This displacement is generated by rotating the lever system, and works as an error signal that triggers the electronic system of the transducer. The rotation of the lever system is restricted in both directions, in the clockwise direction by the structure of the transducer, and in the counterclockwise direction by a stopping point that is installed to protect the transducer from overranging. Since the rotation of the lever system is restricted, the motion of the ferrite disk is also restricted. This means that the magnitude of the error signal that triggers the electronic system is also limited. Therefore, if we define large signal perturbations as any perturbation that causes the lever system to reach a stopping position, then the response of the transducer to a large signal perturbation is limited. If the stopping position is reached the response of the transducer will be the same regardless of the magnitude of the perturbation.

To illustrate the limit in the output of the transducer, an experiment was performed in which the transducer was submitted to five different ramp inputs. The results of the experiment are shown in Figures 5-1 and 5-2. From these Figures we conclude that the transducer is able to follow only ramp inputs with ramp rates up to about 30% of the adjusted span per second.

To explain the electronic cause for the non-linear behavior of the transducer, we use the diagram shown in Figure 2-6 (see page 19). As discussed in section 2.3 the detector consists of a differential transformer that, together with the oscillator, form a
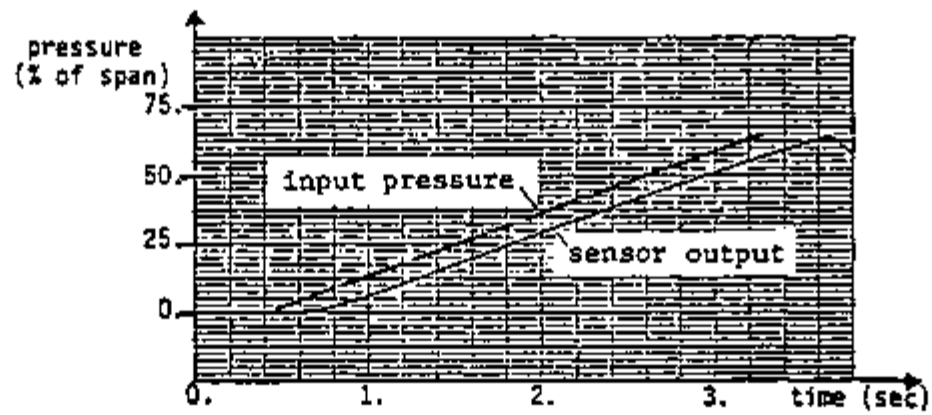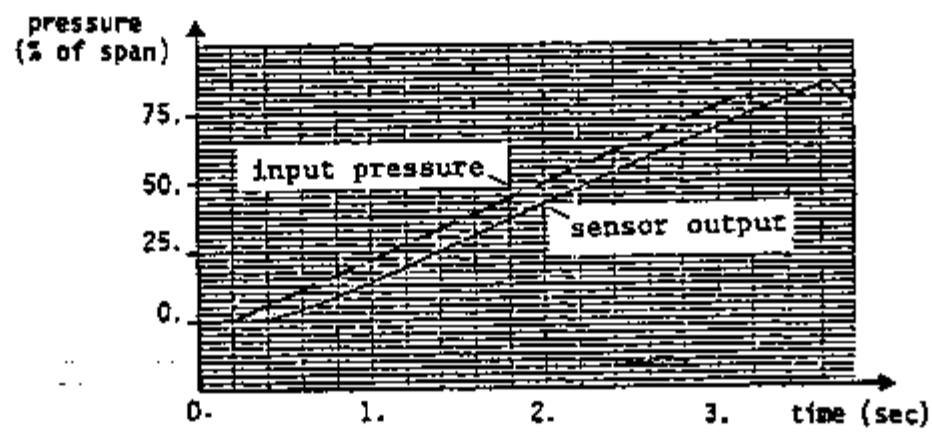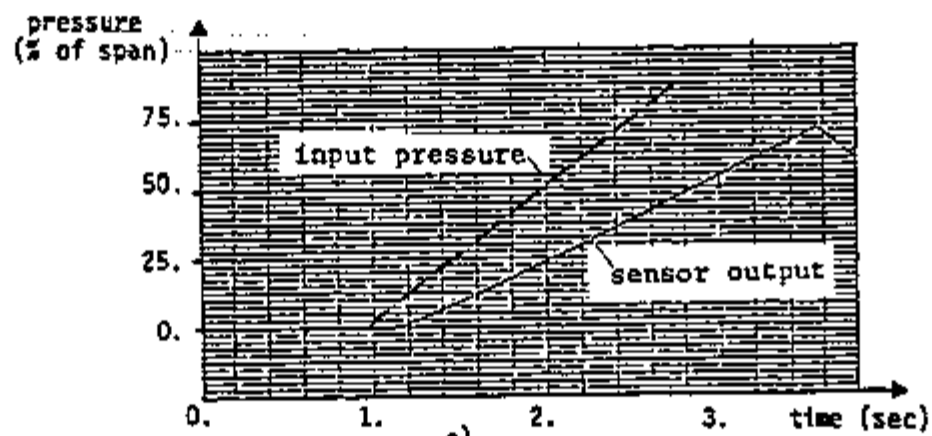
Figure 5-1. Response of the transducer to ramp inputs with ramp rates equal to: a) 23, b) 29, c) 49% of the adjusted span per second
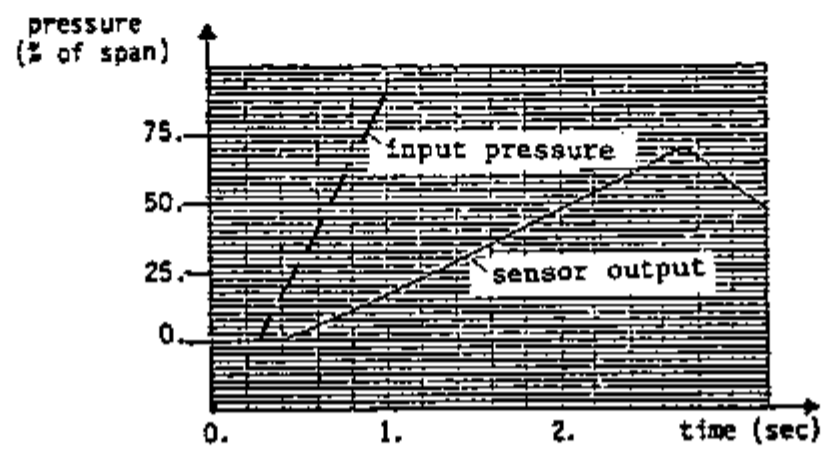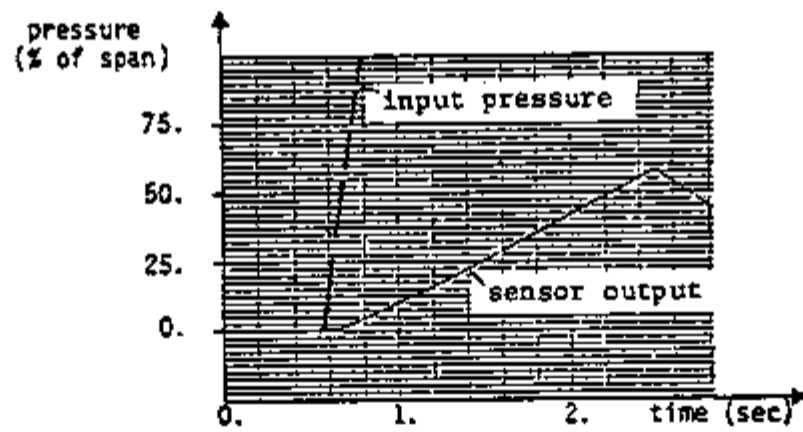
Figure 5-2. Response of the transducer to ramp inputs with ramp rates equal to: a) 125, b) 468% of the adjusted span per second

system that has an intrinsic feedback. The ferrite disk is part of the differential transformer and is mounted on a screw that connects it to a supporting plate. The rotation of the screw permits increasing (or decreasing) the minimum air gap that can exist between the disk and the top core of the detector (see Figure 2-8 on page 22).

The primary coil of the transformer is the coil between points A and B in Figure 2-6 (see page 19), and the secondary coil is the one between points C and D. During steady state conditions the amplitudes of the AC voltages in the coils are constant, and represent a saturated condition for the oscillator. The saturated condition and the amplitude of the AC voltages are functions of the position of the ferrite disk. When the air gap between the ferrite disk and the detector decreases more current is induced in the secondary coil. Increasing the current in the secondary coil causes the amplitude of the AC voltage in the primary coil to increase (because of the amplifying effect of the transistor Q1), and more current is induced in the secondary coil. The final state is achieved when the system reaches a new saturation condition.

Because of the physical characteristics of the components used in the electronic circuit, there is a maximum value for the current that can be induced in the secondary coil. Therefore, there is an upper limit for the amplitude of the AC voltages.

Experimental work performed with the electronic system showed that as the ferrite disk goes closer to the detector the higher is the amplitude of the AC voltages, and the higher is the gradient of the output DC current of the transducer. It also showed that the

maximum gradient for the DC current was obtained when the ferrite
disk was allowed to reach the plastic coating that protects the top
of the detector.

The experiment consisted of applying a step pressure to the
transducer after rotating the screw of the ferrite disk as shown in
Figure 5-3. The continuous line in Figure 5-3 is the step response
of one transducer whose ferrite disk was not moved from its original
position.

From the analysis of Figure 5-3 it was concluded that when
the transducer is submitted to a positive perturbation the non-linear
behavior is due to the mechanical cause.

For negative perturbations the amplitude of the AC voltages
in the primary and secondary coils of the detector decreases, and its
lower limit is zero. It was observed that once the AC voltages go to
zero the output DC current of the transducer decreases according to
the following relation:

$$I(t) = (I(0) + 20.)e^{-.36t} - 20. \tag{5-1}$$

The response of the transducer for several negative
steps is given in Figure 5-4.

During the experimental work it was noticed that the
adjustments made by The Foxboro Company are such that the allowed
rotation of the lever system for a negative perturbation (for the
lever system to hit the structure of the transducer) is about 10
times the allowed rotation for a positive perturbation (to hit the
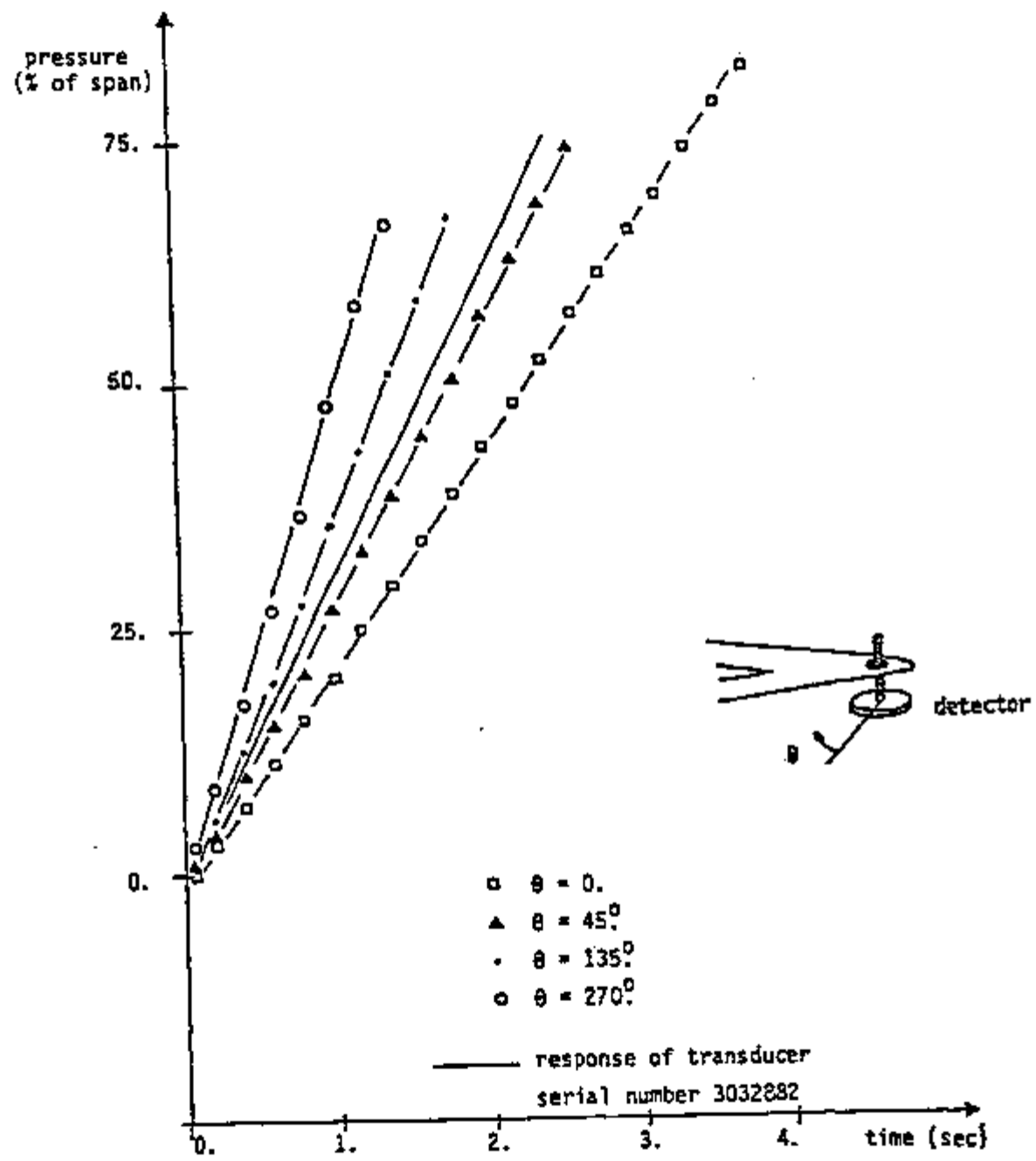
Figure 5-3. Step response as a function of the ferrite position
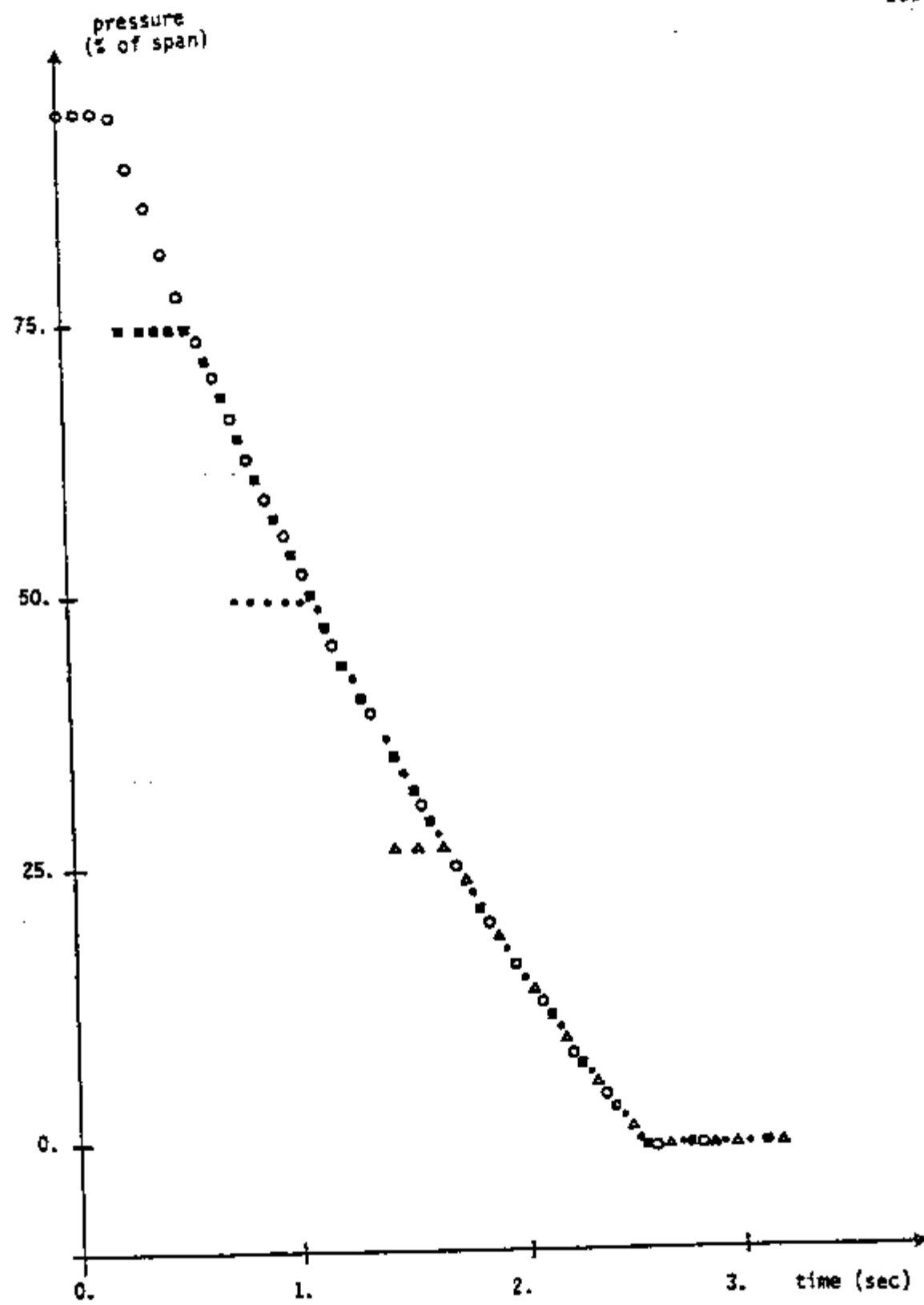
Figure 5-4. Response of the transducer to several negative step inputs

stopping point). Therefore it was concluded that for negative perturbations the non-linear behavior of the transducer is due to the electronic part of the system.

We note here that the mechanical system of Foxboro transducers is such that a small displacement in the diaphragm is amplified to create a large displacement at the end of the lever system. The maximum displacement at the end of the lever system (distance between the structure of the transducer and the stopping point) is about 3 mm. This corresponds to a displacement of about .1 mm at the position of the diaphragm.

During the experiment to determine the empirical transfer function of the electronic system (as described in section 3.3.3), another non-linearity associated with the electronic system was found. An attempt was made to move the ferrite disk sinusoidally. The signal from the proximitor probe used to monitor the motion of the disk and the output signal of the system were recorded for subsequent analysis. The analysis was performed using the same Hewlett-Packard signal analyzer mentioned in section 3.3.3. The result of the analysis is shown in Figures 5-5 and 5-6. Figure 5-5 reveals that the perturbation consisted mainly of two harmonics, while the output consisted of about 10 harmonics. A more detailed analysis showed that:

1- When a sinusoidal perturbation is applied to the electronic system of the transducer, the output signal is composed of several components, harmonics of the input signal. The first and second harmonics have about 98.0 and 1.8% of the
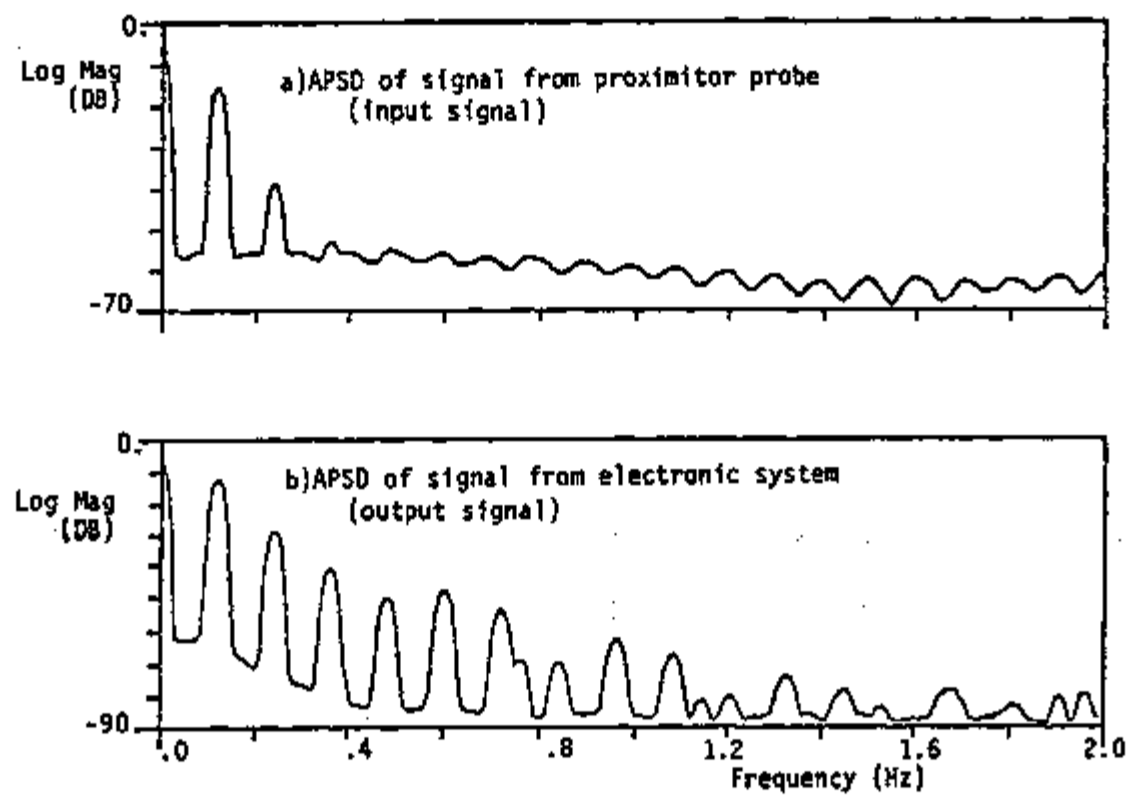
Figure 5-5. Response of electronic system to a sinusoidal
perturbation with frequency equal to .11 Hz
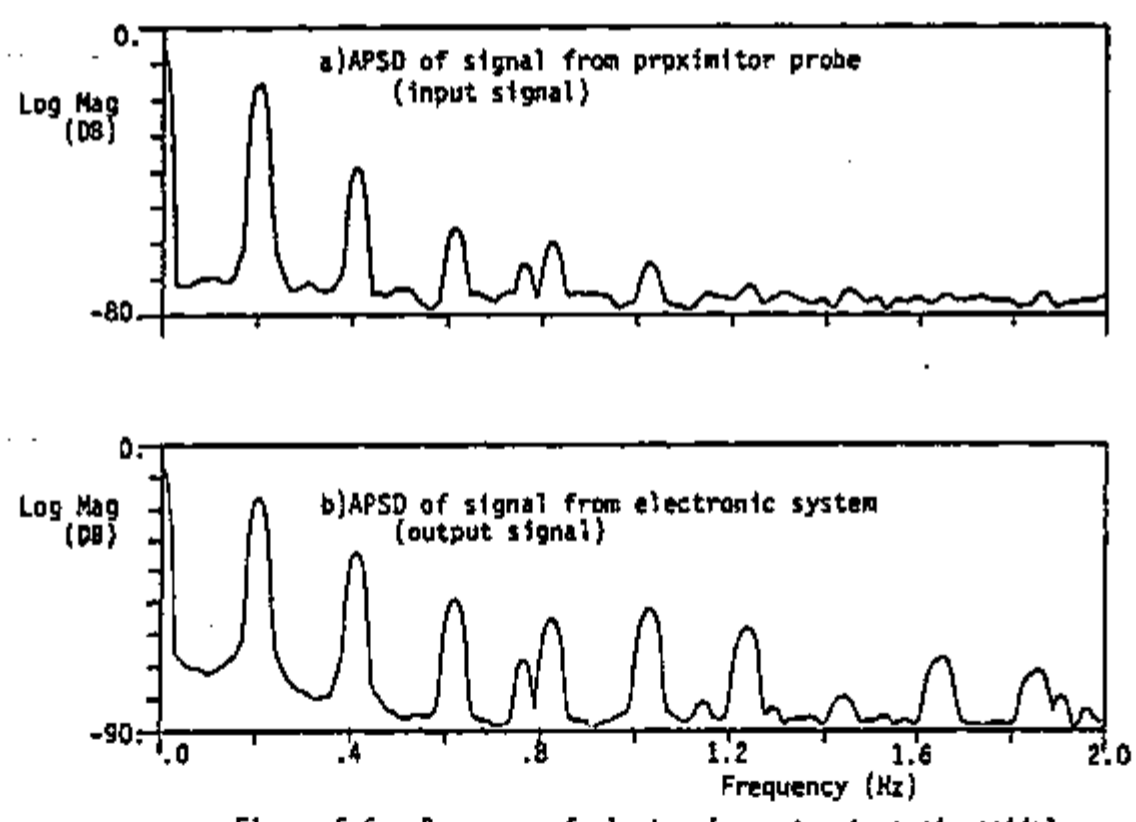
Figure 5-6.   Response of electronic system to a sinusoidal
perturbation with frequency equal to .2 Hz

total output power, respectively.

2- If two sinusoidal perturbations, one with frequency f and the other with frequency 2f, are applied simultaneouslly to the electronic system, the power of the output component with frequency 2f has about 97% of contribution from the input perturbation with frequency 2f, and 3% from the input perturbation with frequency f.

As seen in section 4.4 the model developed in chapter 3 is not very sensitive to the parameters of the electronic system, and this non-linearity can be neglected when:

1- the input perturbation has a power spectral density close to a constant. In this case the contribution of energy from the first harmonic to the second harmonic is constant for all frequencies.

2- the input perturbation has a power spectral density that increases with the frequency. In this case the contribution from the first to the second harmonic decreases.

It is important to mention that in this study the electronic system was submitted to perturbations that caused its output to oscillate with amplitudes of up to 15 mA. This value corresponds to 37.5% of the span of operation of the transducer.

5.3 Conditions for Linearity

It is concluded in this chapter that there are two causes for the non-linear behavior of Foxboro pressure transducers. One is the limitation imposed by the mechanical system of the transducer. The other is the limitation imposed by the electronic system. The

mechanical limitation is explained by the existence of a stop that
is installed to protect the transducer from overranging. It is
responsible for the non-linear behavior during positive perturbations.
The electronic limitation is explained by the speed at which the
electronic system can discharge. It is responsible for the non-linear
behavior during negative perturbations.

The experimental work performed with a standard transducer
(by standard it is meant that the transducer had the same adjustment
as when received from the Foxboro Company) showed that it can follow
positive ramp inputs with ramp rates of up 30% of the adjusted span
per second. We call this the critical ramp rate. As will be
explained in chapter 6, for ramp inputs with ramp rate lower than the
critical the transducer showed a time delay of about .28 sec.
Therefore, it is a reasonable assumption to consider the transducer
as a linear system for situations when the pressure perturbation
integrated in a time interval of .28 sec results in a value lower
than $30\% * .28/2 = 4.2\%$ of the adjusted span. The corresponding value
for the magnitude of a step perturbation is 15% of the adjusted span.

For negative perturbations the result of the negative step
response showed that for negative inputs the minimum gradient on the
output of the transducer is -27% of the adjusted span per second
(this value corresponds to the minimum value of the derivative of
equation 5-1). Assuming the time delay of .28 sec we conclude that
the transducer can be assumed a linear system if the negative
perturbation integrated in a time interval of .28 sec results in a
value (in absolute value) lower than $27\% * .28/2 = 3.7\%$ of the adjusted

span. The corresponding value for the magnitude of a step

perturbation is 13.5% of the adjusted span.

CHAPTER 6

PROPOSED 'IN-SITU' TESTS FOR FOXBORO
PRESSURE TRANSDUCERS

6.1 Introduction

The existing method for response time measurements of
pressure transducers that is accepted by the Nuclear Regulatory
Commission (NRC) (34) is described in references 35 and 20. It is a
direct method of determining response time and consists of applying
an unterminated ramp to the transducer. The time lag between the
instant at which the variable reaches a given value and the instant at
which the output of the transducer is equivalent to that value is
measured. This time lag is defined as 'time delay' (20).

In order to bound the response time of the transducer, two
unterminated ramps are recommended. The first one (slow) is selected
based on the slowest transient for which automatic protective action
is required by design. The second one (fast) is selected based on
the fastest transient for which automatic protective action is
required.

The reason for using two ramps is that previous studies
(14,20) have shown that the time delay for some pressure transducers
is a function of the ramp rate. The use of the two ramps is an
attempt to obtain the most conservative value for the time delay.

The time interval between tests is not specified by the NRC.
It only specifies that the program of tests must be such that
"significant changes in failure rates can be detected before multiple

failures occur". One problem with periodic testing of transducers that make part of the protective system is that some of the transducers are inside of the containment and can be accessed only during the shutdown periods of the reactor. Therefore the measurement of response time for these transducers using the current method can be performed only during the shutdown of the reactor. The development of a remote testing procedure would be very helpful in testing pressure transducers.

In this chapter a method is presented for remote in-situ' testing the Foxboro force balance pressure transducer. The result of the test can be easily associated with the response of the transducer to a step input perturbation and gives a conservative result for the time delay of the transducer when it is submitted to an increasing ramp input. A second test, which requires access to the transducer is also presented for 'in-situ' testing. This second test provides the time delay of the transducer for positive and negative step perturbations.

Neither one of the proposed tests require access to the pressure sensing lines.

In order to help understand the principle of the tests being proposed for Foxboro pressure transducers, a brief review of their operation follows:

  1- The pressure being applied to the transducer is converted into a force signal that propagates through the mechanical system to move the lever system (see Figure 2-1 on page 10) and the ferrite disk.

2- The motion of the ferrite disk triggers an electrical
signal that causes a DC current flowing through the
electronic system to change. The displacement of the
ferrite disk from its equilibrium position is an error
signal.

3. The DC current, the output of the transducer, flows
through the feedback coil generating a feedback force that
causes the ferrite disk and the mechanical system to
return to the original position.

Since the DC current is the origin of the force that balances
the system, then any perturbation in the DC current will unbalance the
system, creating a transient condition for the transducer. The
feedback coil is also responsible for the balancing of the system.
The 'in-situ' tests are based on using the DC current and the feedback
coil to disturb the system.

6.2 Remote 'In-situ' Test

The remote 'in-situ' test is possible because of the
non-linearity in the mechanical part of the transducer. This
non-linearity is due to the presence of an overranging stopping point
on one side and the structure of the transducer on the other. These
physical parts restrict the motion of the lever system, and
consequently the motion of the ferrite disk in both directions,
clockwise and counterclockwise. Since the displacement of the
ferrite disk is an error signal, a limitation in the motion of the
disk implies a limitation on the magnitude of the error signal, which
makes the system non-linear.

Experimental work has shown that a step change in pressure of about 15% of the adjusted span causes the lever system to rest at the stopping point until the feedback moment is strong enough to return the system to the original position. While the lever system stays at the stopping point the magnitude of the error signal is the maximum. For any step perturbation in pressure with magnitude higher than 15% of the adjusted span the lever sytem goes to the stop position, and the response of the transducer can be divided in three parts. The first one corresponding to the time interval during which the lever system moves toward the stopping position; the second part corresponding to the time interval during which the lever system remains at the stopping position, and the third part of the response corresponding to the time interval during which the lever system moves to the original position, away from the stopping point.

To illustrate the presence of the three regions, a test was made in which the transducer was submitted to a sudden change in pressure. The initial and final pressure were set equal to 0 and 69% of the adjusted span, respectively. The value 69% was chosen to obtain the data in a scale suitable for comparisons with the results of the 'in-situ' tests. The result of the experiment is shown in Figure 6-1. It also shows the response of the transducer when the pressure (corresponding to 69% of the span) was suddenly removed.

To monitor the sudden perturbation a fast sensor (a Validyne pressure transducer model DP15TL) was utilized. As can be seen in Figure 6-1, the dynamics of the Foxboro transducer is such that, for practical applications the sudden perturbation can be assumed as a step perturbation.
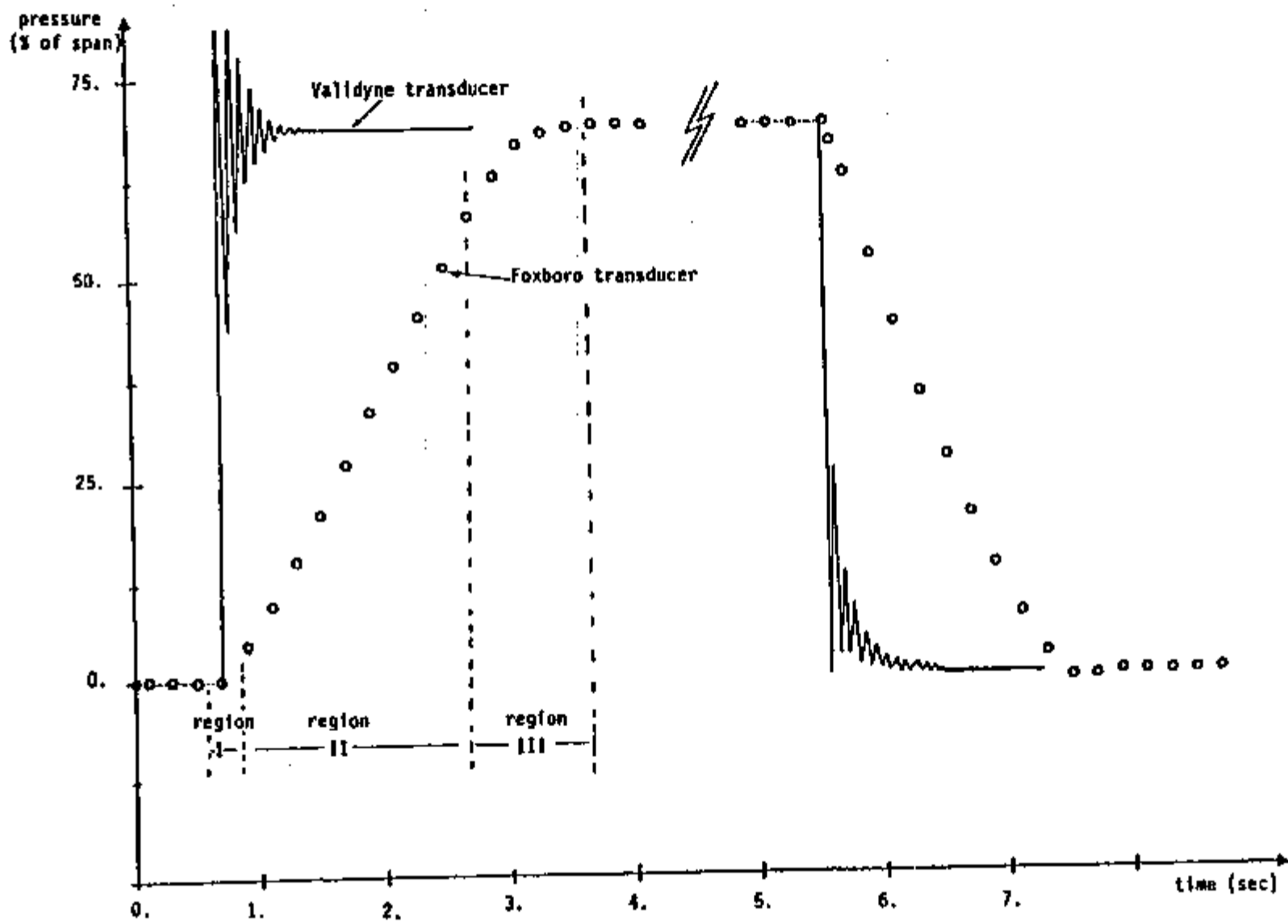
Figure 6-1. Response of the transducer to a 'step' perturbation

An analysis of the result showed that the second part of the step response gives the biggest gradient that can be present in the output of the transducer. We define this gradient as the critical ramp rate. The corresponding ramp is defined as the critical ramp.

If the transducer is submitted to a ramp input with a ramp rate lower than the critical, then the stopping point is not reached, and the transducer behaves as a linear system. However, if the applied ramp rate is larger than the critical ramp rate, then the stopping point is reached, the transducer becomes non-linear and it will show the critical ramp as its output.

If, for ramp inputs with ramp rate lower than the critical, the transducer can be assumed as a first order system then for these inputs the time delay is constant. However for ramp inputs with ramp rate higher than the critical the time delay is expected to increase, because the output of the transducer is the critical ramp (see Figures 5-1 and 5-2 on pages 164 and 165, respectively). The maximum time delay is obtained when the transducer is submitted to a step perturbation (a ramp with ramp rate equal to infinity). The time delay for the step is the time lag between the application of the step and the time necessary for the critical ramp (output of the transducer) to reach the desired value.

In order to show that this conclusion is correct, a set of experiments was performed in which the transducer was submitted to a series of positive ramp inputs, starting at 0% of the adjusted span. The time delay measured was determined as the time lag between the instant in which the pressure reached 37.5% of the span, and the

instant in which the output of the transducer reached the value
corresponding to 37.5% of the span. The value 37.5% corresponds to
an output current signal of 25mA and was chosen for two reasons: to
allow easy reading on the strip chart recorder used and to allow the
application of ramps with high gradient without damaging the Validyne
transducer used as a reference. The results of the experiment are
shown in Figures 6-2 and 6-3, where it is clear that the step
response gives a conservative value for the time delay.

Since the principal characteristic of the step perturbation
is that it causes the lever system to reach the stopping point, there
is a remote way of achieving the same condition: removing the DC
current that flows through the transducer. When we remove the DC
current we also remove the moment that balances the system, and the
lever system moves to the stopping point.

When the power is turned back on, the lever system will be at
the stopping position, and the magnitude of the error signal is the
maximum possible. Since the error signal is the maximum, the DC
current increases in the same way as in response to the step
perturbation.

We note that the feedback motor and the power supply are
connected in series (see Figure 2-6 on page 19). Therefore, the
simplest way to remove the current is to remove the power that is
being supplied to the circuit.

The remote 'in-situ' test is as follows:

1- With the transducer subject to a pressure equal to or
    higher than 15% of its span, remove the power being
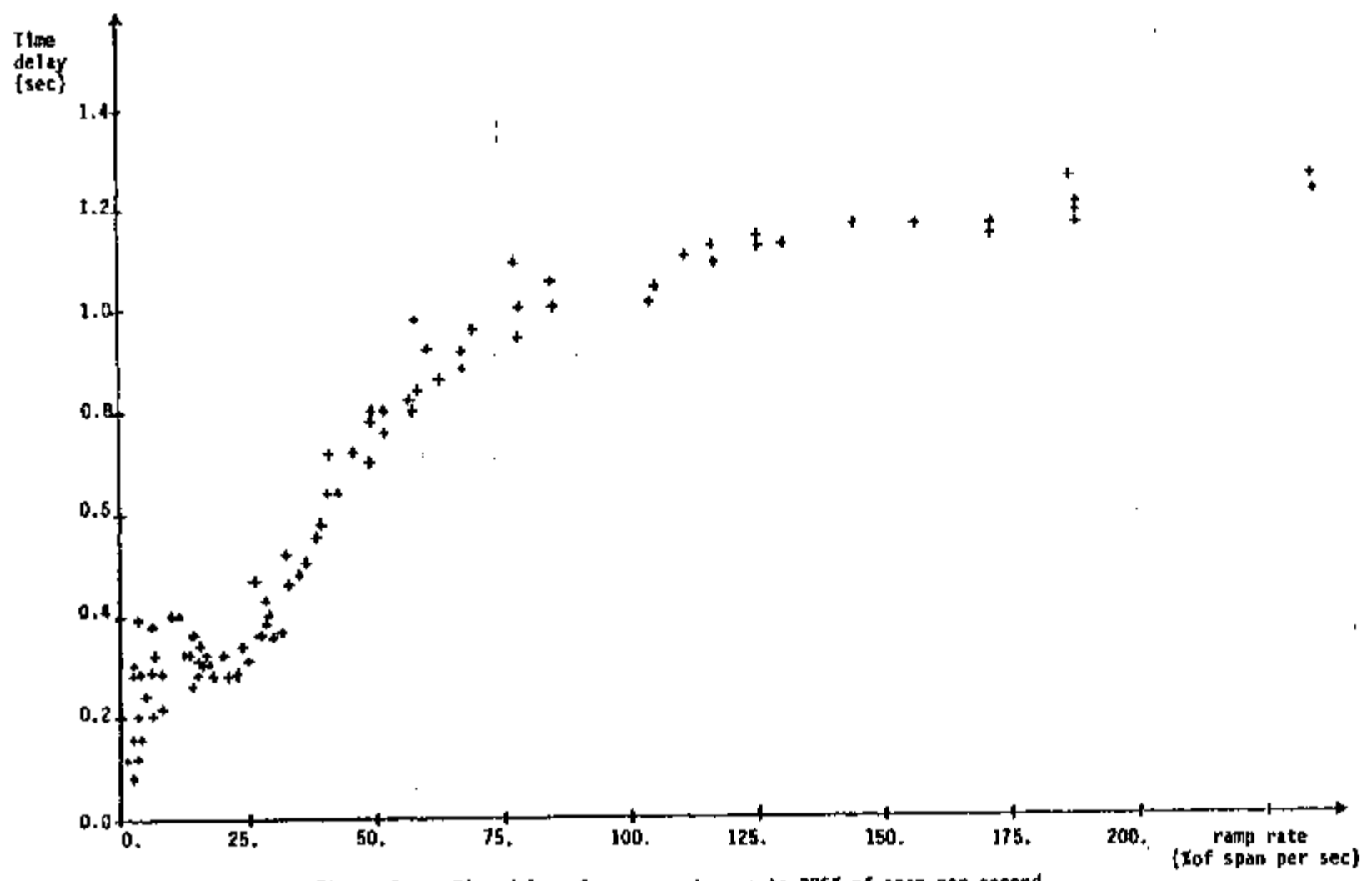
Figure 6-2. Time delay for ramp rates up to 225% of span per second (see text for conditions of measurement)
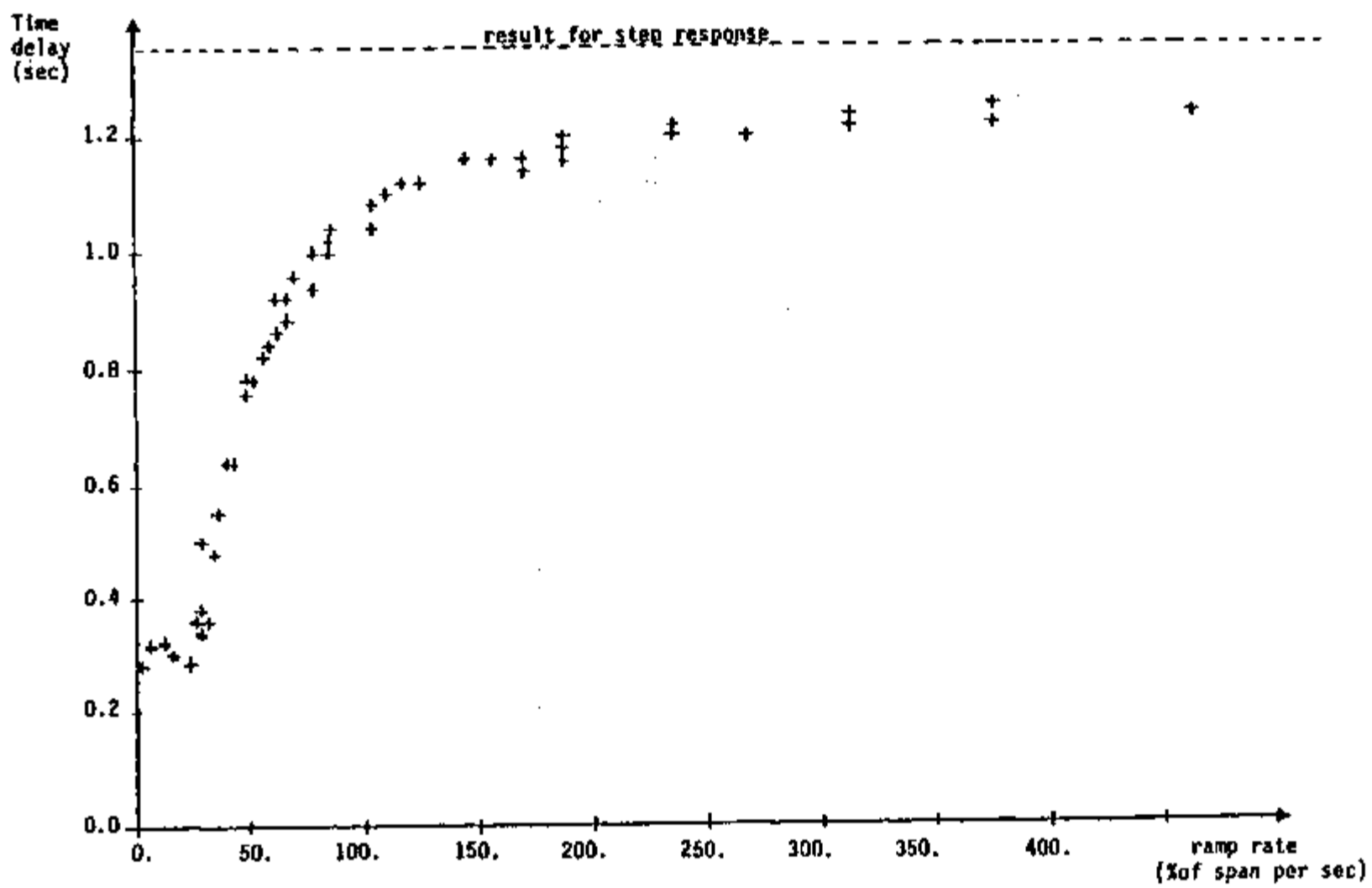
Figure 6-3. Time delay for ramp rates up to 450% of span per second
(see text for conditions of measurement)

supplied to it (open the circuit)

2- Wait about 10 seconds for the complete discharge of the
electronic components.

3- Turn on the power being supplied to the transducer and make
a record of the output signal.

To show the similarities of the step and remote test
responses, an experiment was performed in which the transducer was
submitted to a sudden perturbation. After reaching the new steady
state situation the remote test was performed. The result of the
test is shown in Figure 6-4, where the step response is superimposed
for comparison.

The initial part of the remote test transient is influenced
by the electronics of the transducer. When the power is first
applied to the electronic circuit the amplitude of oscillation in the
oscillator is null (see Figure 2-6 on page 19). Then a current of
about 3 mA starts to flow through the circuit. When the oscillator
is activated the current starts to build up, and after it reaches the
maximum gradient the transducer responds exactly as it does when
submitted to a step perturbation.

6.3 Local 'In-situ' Test

As explained in section 3.3.2, the force motor produces a
negative moment that is given by $K_{fm}I_{dc}$, where I_{dc} is the value of
the DC current. K_{fm} is a constant that depends on the number of
turns in the feedback coil and the magnitude of the magnetic field in
the region occupied by the coil. Considering that the resistance of
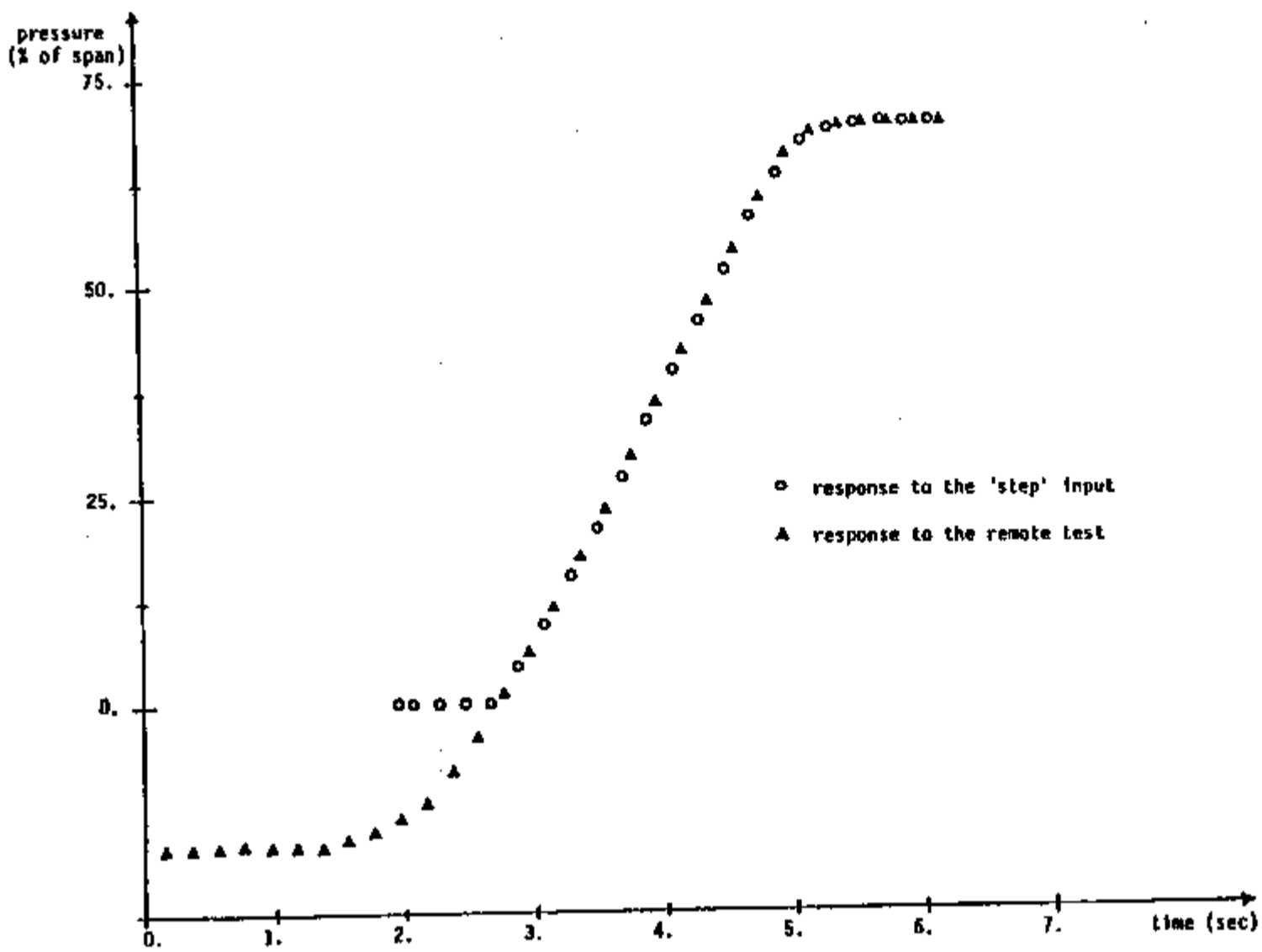
Figure 6-4. Response of the Foxboro transducer to the remote 'in-situ' test

pressure (% of span)

- response to the 'step' input
- response to the remote test

time (sec)

the coil is R, the constant K_{fm} can be written as $K_b R$, where K_b is another constant. Therefore, the magnitude of the moment that balances the system can be rewritten as $K_b RI_{dc}$. The local 'in-situ' test is based in changing the current that flows through the transducer while maintaining the moment required to balance the system. If we change R from R to R', to have the same moment the current will change from I_{dc} to I'_{dc}, with $RI_{dc} = R'I'_{dc}$.

Assuming that the electronic circuit of the transducer is adjusted for operation at the condition identified by 'high' in Figure 2-6 on page 19, the total resistance of the coil is equal to 173 ohms. If during an equilibrium situation we short circuit points 2 and 4, the DC current will flow only through the coil with resistance 42 ohms. This means that a new equilibrium state will be established with the value of I'_{dc} equal to 173/42 times the original value. Since we removed part of the feedback moment, the lever system will move toward the stopping point, and the perturbation can be associated with the response of a positive step input. When the connection between points 2 and 4 is open, the current flows again through an effective restance of 173 ohms. Since the decrease of the current is not instantaneous, the situation is such that the feedback moment is higher than the one required to balance the system. Then the lever system moves toward the structure of the transducer, a situation that can be associated with a negative step in pressure.

The local 'in-situ' test was performed with the transducer available for measurements under the following conditions:

1- the transducer was set to operate at condition 'high'

(resistance equal to 173 ohms).

2- no pressure was applied to the transducer (which

represents an output current equal to 10 mA).

3- at time T0 points 2 and 4 where short-circuited.

4- At time T1 the connection between points 2 and 4 was

removed.

The results obtained with the local 'in-situ' test are shown in
Figure 6-5. In order to compare the results with the step response,
the later is superimposed in the same figure.

6.4 Interpretation of the Remote Test

The work developed in this section is based in experimental
results obtained with two Foxboro transducers. Both are model E13DM
and were calibrated to the same span of pressure. The calibration
curves are given in Figure 6-6. The first transducer (serial number
3010955) will be referred to as sensor #1 and the second (serial
number 3032882) as sensor #2. Sensor #2 was the one used in the
comparison of the results described in section 4.2.

In the first stage of the work it was noticed that the
response of sensor #2 was much slower than the response of sensor #1.
The response of both sensors to the remote 'in-situ' test is shown in
Figure 6-7. A physical inspection of sensor #2 revealed that the
ferrite disk had broken, and the disk had been replaced. It was
concluded that during the replacement the disk was not properly
positioned. The position of the disk was readjusted and a new
calibration was performed. The calibration curve for the transducer
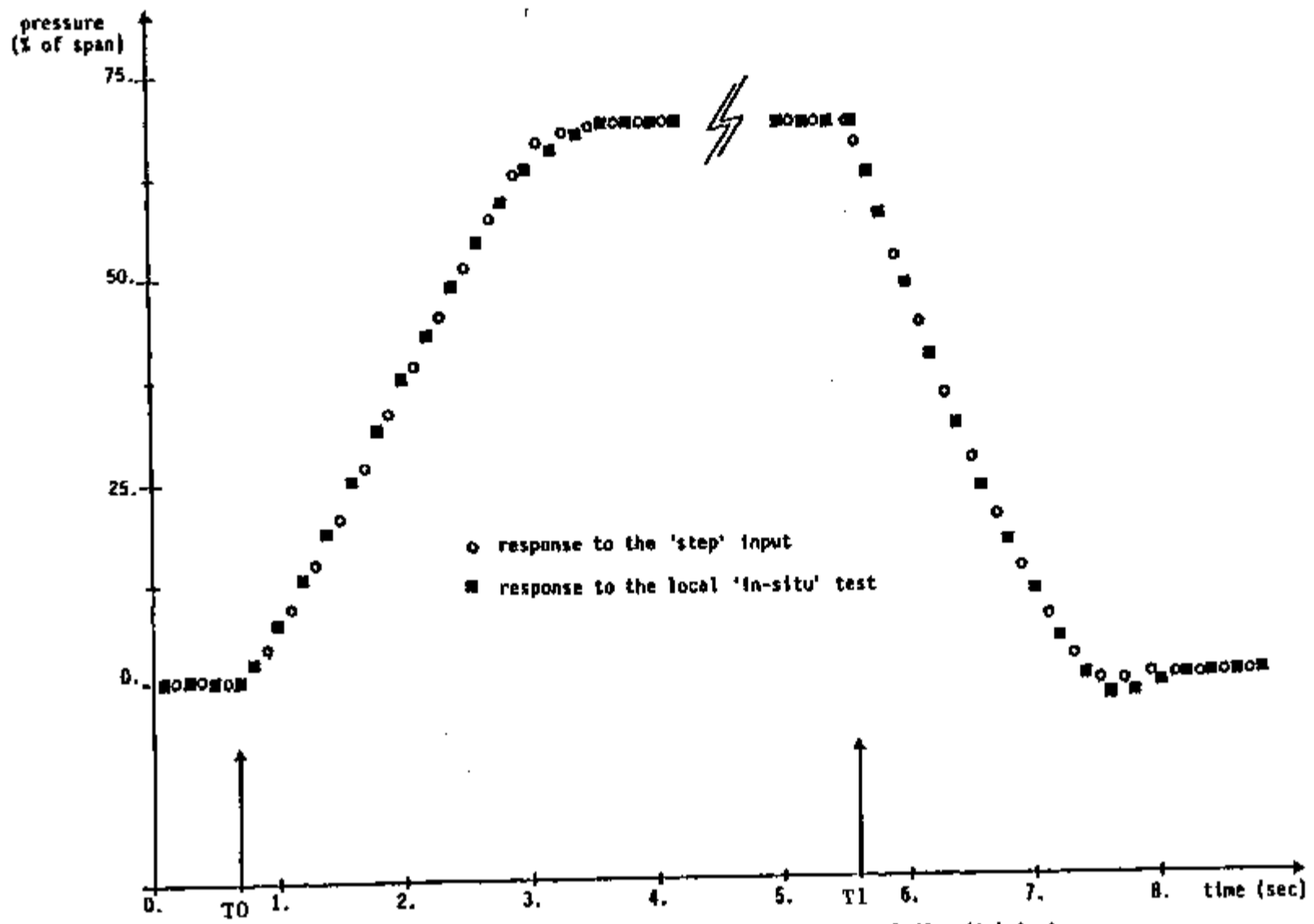
Figure 6-5. Response of the Foxboro transducer to the local 'in-situ' test
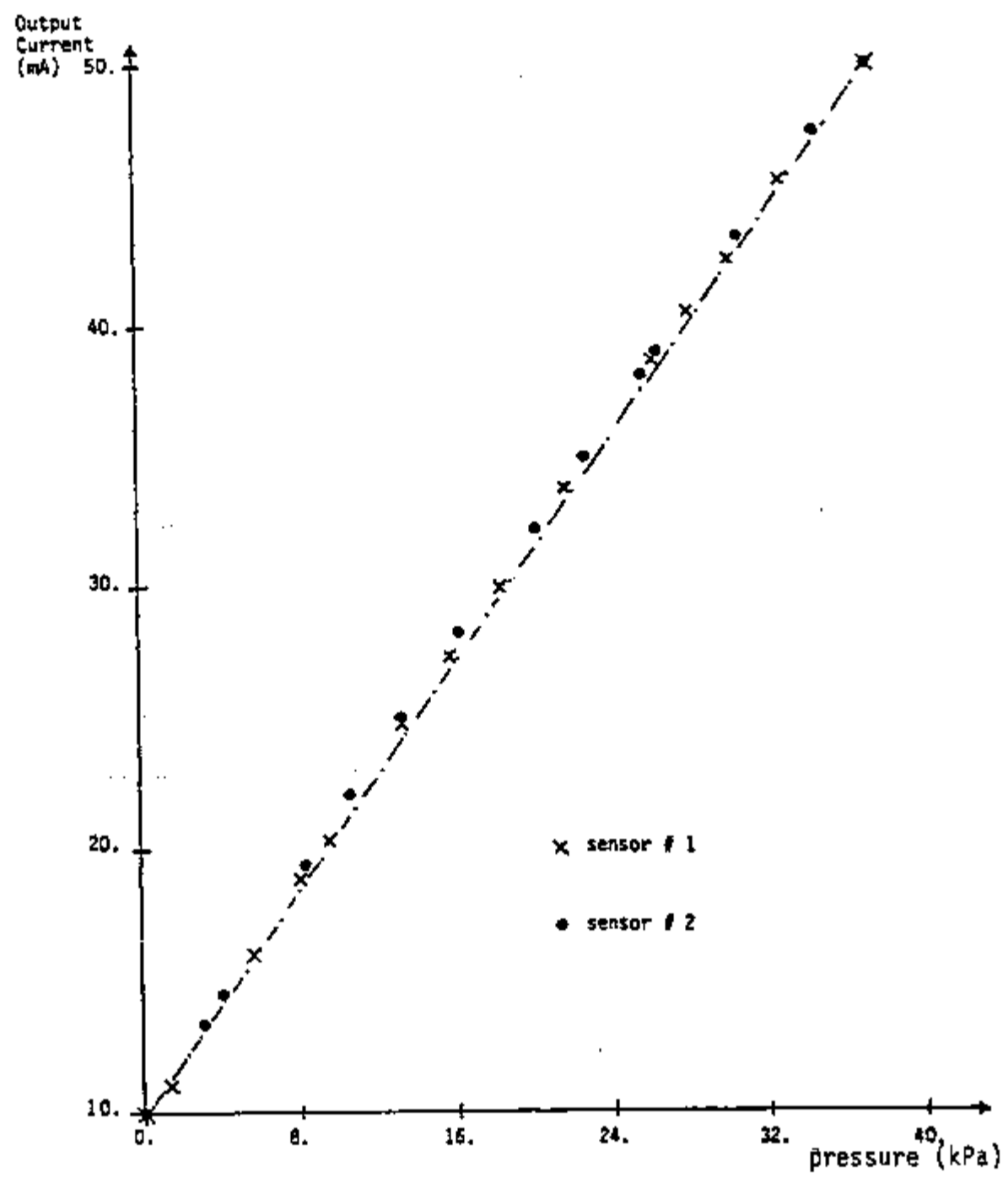
Figure 6-6. Calibration curves
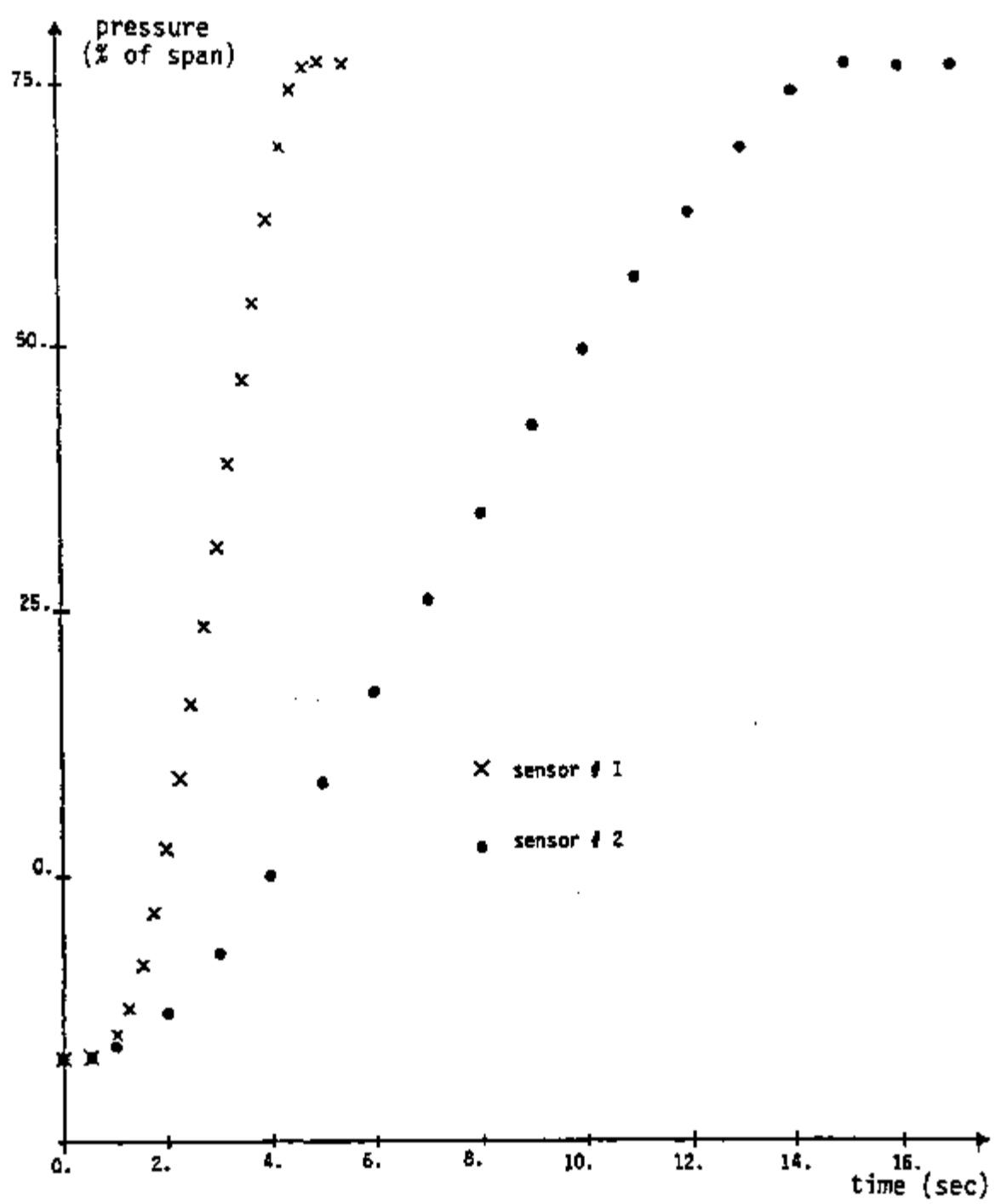
Figure 6-7. Response of sensor # 2 after replacement
(without proper adjustment)

remained the same, but its response changed. The new response is
shown in Figure 6-8.

A further adjustment was made on the position of the disk.
This time it was adjusted in such was that it could reach the plastic
coating on top of the detector before the lever system reached the
stopping point. The response to the remote test for the new
situation is shown in Figure 6-9. Figure 6-9 shows that the critical
ramp rate is higher than before. It also shows that the behavior
of the response curve after it starts to depart from the critical
ramp is different from the previous cases. The difference is
is atributed to two causes:

    1- The plastic coating was being compressed and acted as
       a spring.

    2- there is an adhesive effect that tries to hold the
       ferrite disk and the coating surface together.

In order to associate the response of the remote test with
the time delay curve shown in Figures 6-2 and 6-3, the following
procedure is suggested.

    1- perform the remote test as explained in section 6-2.

    2- verify that the critical ramp is present in the response.
       As concluded in this section the presence of the
       critical ramp in the response of the remote test is
       mainly a function of the existing pressure at the time
       of the test.

    3- make a least squares fit of an exponential $a + b\exp(-ct)$
       to the part of the curve that departs from the critical
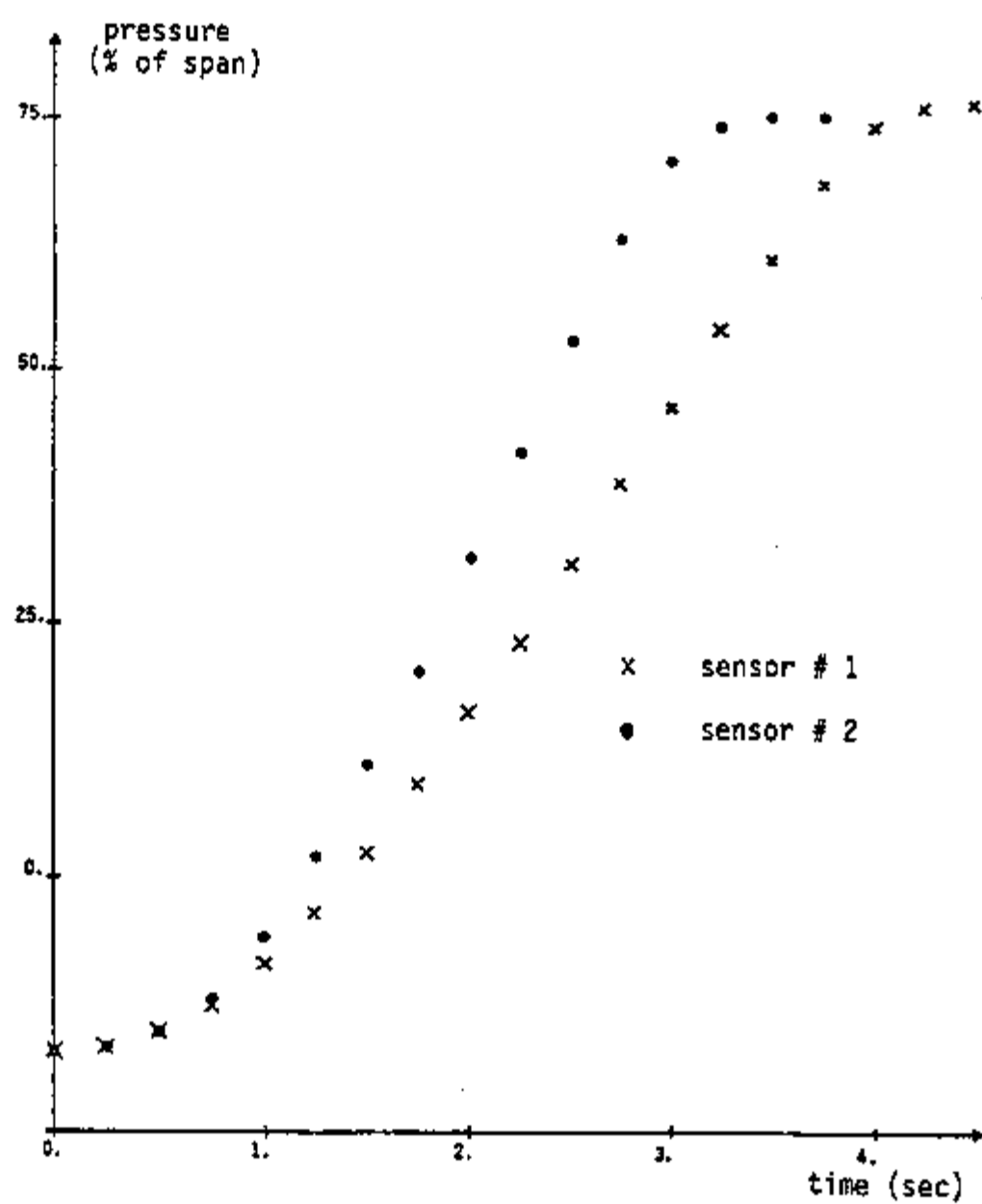
Figure 6-8.   Response of sensor # 2 after
adjustment
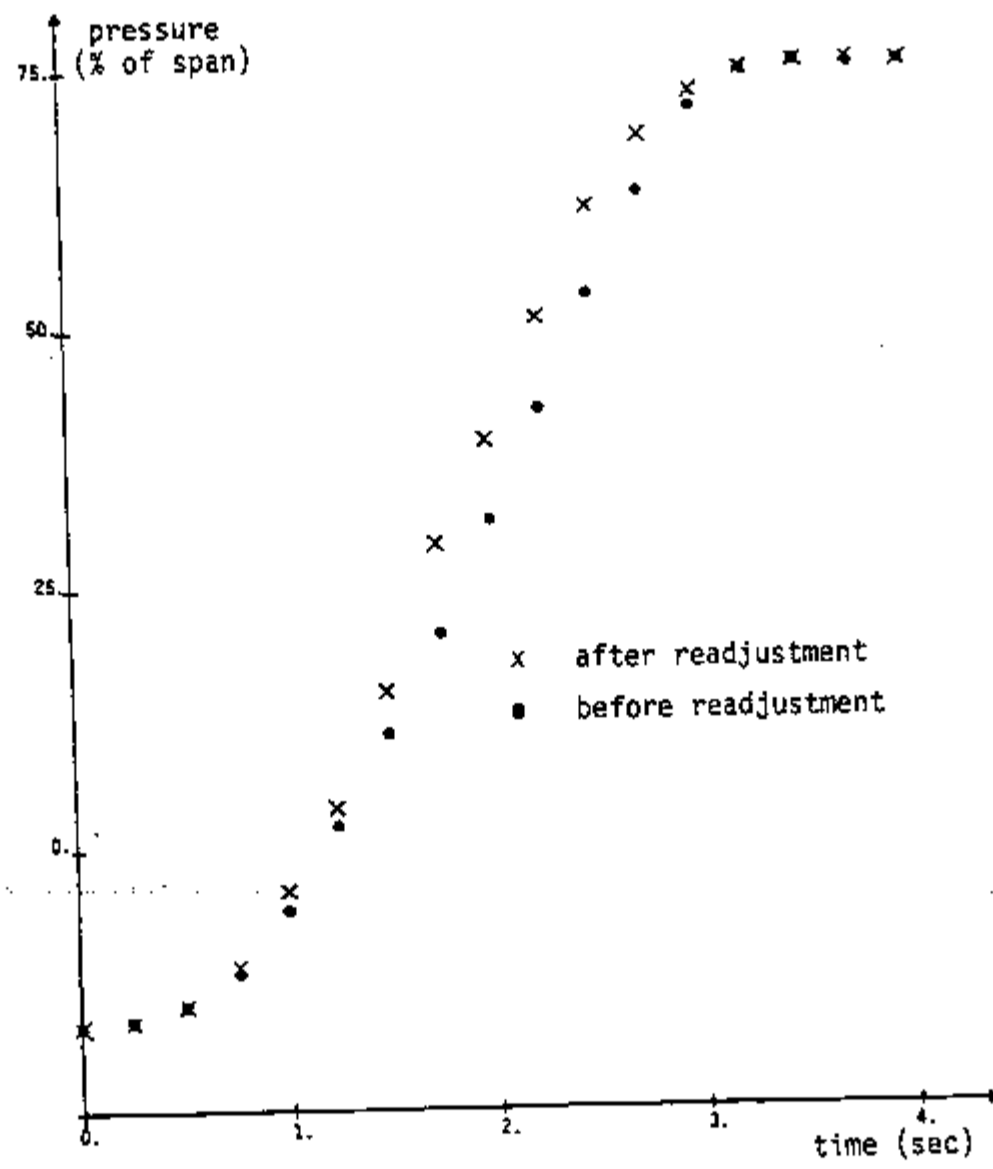
Figure 6-9. Response of sensor # 2 after readjustment

ramp. The inverse of c is the time constant for a first order linear system, and is an estimate of the time delay for ramps with ramp rate lower than the critical.

4- For ramp rates higher than the critical draw a graph with the two ramps and determine the time lag between the two curves for the desired pressure. This time is defined as t_d. If the critical ramp is given by $P_c(t) = P_o + r_c t$, and the input ramp is assumed as $P_i(t) = P_o + r_i t$, the value of t_d for a desired pressure P is (see Figure 6-10):

$$t_d(P) = (P - P_o) \left(\frac{1}{r_c} - \frac{1}{r_i} \right)$$

5- $t_d + 1/c$ is an estimate of the time delay for the desired ramp input.

It is important to note that for Foxboro transducers the time delay is a function of the ramp rate and the initial and final pressures.

The procedure suggested to correlate the remote test and the time delay curve was applied to sensor #1. The result is shown in Figure 6-11.
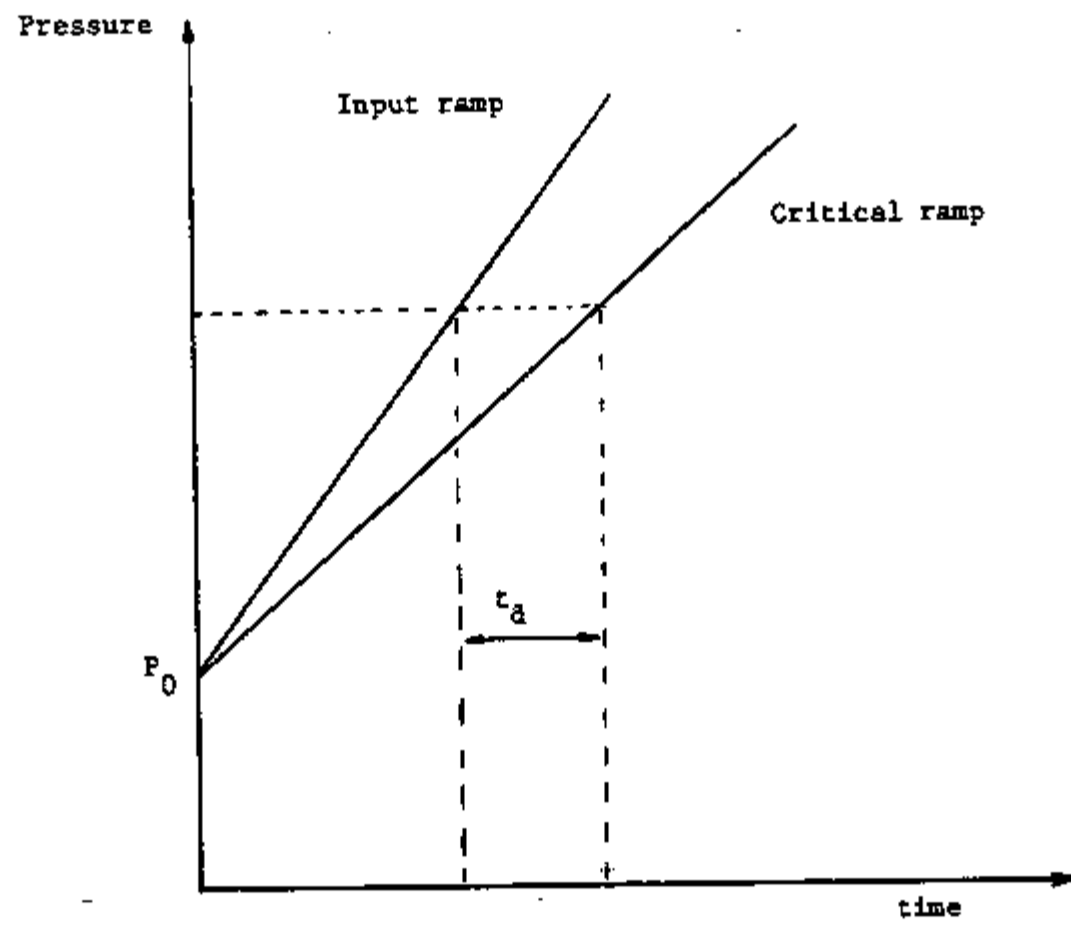
Figure 6-10.   Determination of t_d
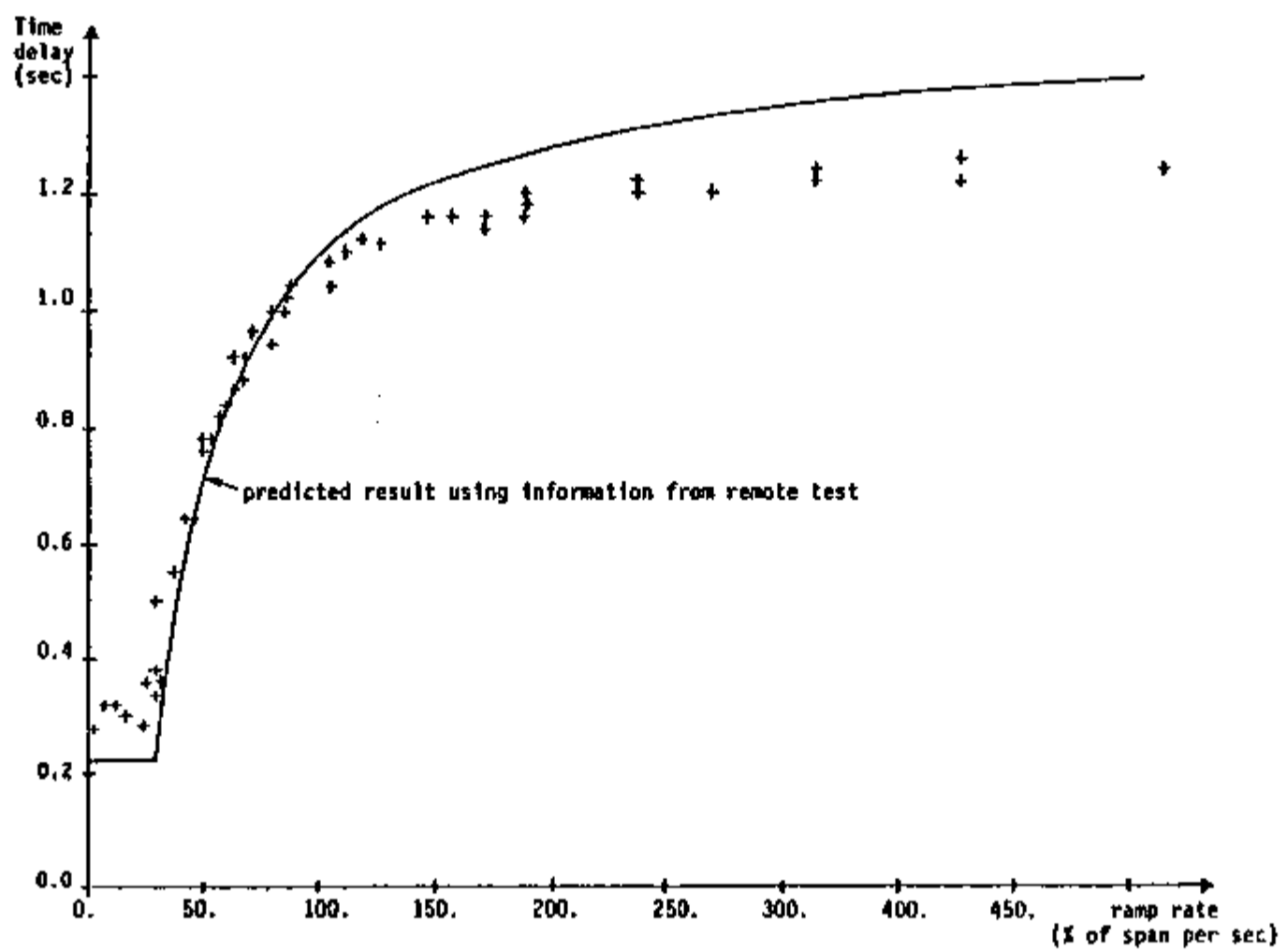
Figure 6-11. Predicted time delay as a function of ramp rate
(see text for conditions of measurement)

predicted result using information from remote test

CHAPTER 7

CONCLUSIONS AND RECOMMENDATIONS

The conclusions reported herein are based on the work
performed with the transducer used as reference (see Chapter 2). For
a qualitative analysis these conclusions can be extended to the other
models of Foxboro transducers, but for a quantitative analysis
additional work is necessary.

Three are the major conclusions of this work: 1) The
transducer is a linear system for normal conditions of operation.
2) Theoretical model and experimental test results compare very well.
3) Its principle of operation allows the transducer to be remotelly
tested.

It was concluded in chapter 5 that unless the transducer is
submitted to perturbations that integrated in a time interval of .28
sec result in a value greater than 4.2% of the adjusted span, the
transducer is a linear system. The ramp input necessary to obtain an
integrated value equal to 4.2% of the adjusted span is 30% of the
adjusted span per second. The step input necessary to obtain the
same integrated value is 15% of the adjusted span.

For larger perturbations the transducer becomes a non-linear
system. The non-linear behavior of the transducer is understood, and
it is characterized by how fast the electronic system can be charged
or discharged (the terms charge and discharge are used to indicate
increase and decrease, respectively, in the current that flows
through the electronic system of the transducer). For negative

perturbations the limit in the discharging speed is imposed by the characteristics of the electronic system. For positive perturbations it is imposed by a limitation in the displacement of a ferrite disk. The ferrite disk is the interface between the mechanical and the electronic systems of the transducer.

The linear model developed in chapter 3 showed good agreement with experimental data. It also showed that the dynamics of the transducer are strongly dependent of three subsystems: the electronics, the lever system, and the sensing element (diaphragm). As described in chapter 3 the transfer functions for the electronic system and sensing element can be obtained empirically. Once these transfer functions have been obtained they can be easily implemented in the computational program shown in Appendix D. This allows one to obtain quantitative results for the frequency response of other models of Foxboro transducers.

Finally, the origin of the balancing force in the transducer is the DC current that flows through the electronic system. This DC current is also the output signal from the transducer. Since the current is a signal to which we have access from a remote location (for example we can use a switch to open or close a circuit), we concluded that it is possible to remote test the transducer. As shown in section 6.4 the test is simple, and the results are meaningful.

LIST OF REFERENCES

LIST OF REFERENCES

1- U.S.Nuclear Regulatory Commission, Periodic Testing of Electric Power and Protection Systems, Regulatory Guide 1.118 (Nov. 1977)

2- J.B.Reid, Process Instrumentation for Westinghouse Nuclear Steam Supply Systems (4 Loops Plants Using WCID 7300 Series Process Instrumentation) WCAP 7913 (Jan.1973)

3- J.A.Thie, Instrumentation Integrity and Response Time Testing Utilizing System Noise, Proceedings of the Second Power Plant Dynamics Control and Testing Symposium, (Sep. 1975) paper n. 10.

4- D.N.Fry, Experience in Reactor Malfunction Diagnosis Using On-line Noise Analysis, Nuclear Technology vol.10 (Mar. 1971) pp. 273-282.

5- B.R.Upadhyaya, notes of class.

6- R.Espefalt et al., Noise Measurements for Plant Surveillance and Anomaly Detection in Nuclear Power Stations, IAEA Symposium on Nuclear Power Plant Control and Instrumentation, Cannes (Apr. 1978).

7- V.Bauernfeind, Vibration and Pressure Signals as Source of Information for an On-line Vibration Monitoring System in PWR Power Plants, Nuclear Engineering and Design 40(1977) pp. 403-420.

8- V.Bauernfeind et al., Importance and Use of In-core Vibration and Pressure Measurements for Determination of Correct Behavior of Pressure Vessel Internals, IAEA Symposium on Nuclear Power Plants Control and Instrumentation, Prague (Jan.1973)pp. 111-121.

9- W.H.Dio et al., On-Line Surveillance of LWR Primary Systems, Progress in Nuclear Energy (London: Pergamon Press, 1977) Vol.1, pp. 747-758.

10- W.Bastl and D.Wach, On-load Vibration and Noise Monitoring in Sodium Cooled and Light Water Reactors, Proceedings of the Second Power Plant Dynamics Control and Testing Symposium, (Sep. 1975) paper n. 11

11- B.R.Upadhyaya and T.W.Kerlin, Estimation of Response Time Characteristics of Platinum Resistance Thermometers by the Noise Analysis Technique, ISA Transactions vol. 17 n. 4 (1978) pp. 21-37.

12- The American Society of Mechanical Engineers, A Guide for the Dynamic Calibration of Pressure Transducers, ANSI B88.1-1972.

13- H.B.Jones,Jr. et al., Transient pressure Measurements in Liquid Propellant Rocket Thrust Chambers, ISA Transactions, Vol.4, n.2 (Apr. 1965) pp. 116-132

14- D.G.Cain and C.G.Foster, A Practical Means for Pressure Transducer Response Verification, Nuclear Technology (Dec. 1977), vol.36 pp. 275-284.

15- T.W.Hunt, Experimental and Analytic Studies of Electromechanical Transducer Systems for Transient Pressure Measurements, WAPD-TM-343 (Aug. 1964)

16- F.Abdullah and L.Finkelstein, A Review of Mathematical Modelling of Instrument Transducers, International Measurement Confederation, Ninth World Congress, Berlin (May 1982) pp. 279-286.

17- R.Gopal and W.Ciaramitaro, Experiences with Diagnostic in Nuclear Power Plants, Progress in Nuclear Energy, (Oxford: Pergamon Press, 1977) vol.1 pp. 759-779.

18- S.M.Wu et al.,The Determination of Time Constants of Reactor Pressure and Temperature Sensors: The Dynamic Data System Method. Nuclear Science and Engineering 72 (1979), pp. 84-96.

19- S.M.Wu and M.S.Ouyang, A Note on Estimation of Pressure Sensor Time Constant From the Normal Operating Data, Nuclear Science and Engineering 81 (1982) pp. 298-299.

20- C.G.Foster et al., Sensor Response Time Verification, PB-260554 (Oct. 1976).

21- J.F.Pierce and T.J.Paulus, Applied Eletronics, (Ohio: Charles E. Merrill Publishing Company, 1972) pp. 137-204 and 624-647.

22- J.L.Lyons, The Designer's Handbook of Pressure Sensing Devices, (New York: Van Nostrand Reinhold Co., 1980) pp. 101-144.

23- R.H.Perry, Engineering Manual, (New York: McGraw Hill Book Company Inc., 1962) pp. 3-78:3-100.

24- W.F.Stokey, Shock and Vibration Handbook, Vol.1, Chapter 7 (Ed. C.M.Harris and C.E.Gede) (New York: McGraw Hill Book Co., 1961)

25- W.T.Thomson, Theory of Vibration With Applications, (New Jersey: Prentice-Hall Inc., 1981)

26- S.Timoshenko et al., Vibration Problems in Engineering,(New York: John Wiley & Sons, 1974)

27- W.T.King and E.L.Machado, Standard Fortran Plotting Library for PDP-11/44 RSX-11M, Oak Ridge National Laboratory, Instrumentation and Control Division (AUG.1982).

28- E.C.Snelling, Soft Ferrites, (London: London Iliffe Books Ltd., 1969) p. 171.

29- T.W.Kerlin, Frequency Response Testing in Nuclear Reactors, (New York: Academic Press, 1974)

30- T.W.Kerlin et al., Identification of Nuclear Systems, Nuclear Technology vol. 36 (Nov. 1977) pp. 7-38.

31- E.L.Machado and J.March-Leuba, Personal communication.

32- S.Timoshenko and J.M.Lessells, Applied Elasticity, (York: The Mapple Press Co., 1925) pp50-97,260-295.

33- J.A.Mullens, Personal communication.

34- U.S. Nuclear Regulatory Commission, Response Time Testing of Protection System Instrument Channels, Draft Regulatory Guide and Value/Impact Statement, (Jan. 1982)

35- Instrument Society of America, Response Time Testing of Nuclear Safety Related Instrument Channels, Draft 0, ISA-DS 67.06 (Oct. 1980)

36- J.F.Boland, Nuclear Reactor Instrumentation (In-Core), (New York: Gordon and Breach Science Publishers, 1970) pp. 23, 45-122.

37- F.J.Oliver, Practical Instrumentation Transducers, (New York: Hayden Book Company Inc., 1971) pp. 146-172.

38- J.Hall, A Guide to Pressure Monitoring Devices, Instruments and Control Systems (APR.1978) pp. 19-26.

39- S.P.Timoshenko, Vibration-Beams, Plates and Shells - Benchmark Papers in Acoustics, Chapter 1, (Ed. A.Kalnine and C.Dyn) (Pensylvannia: Dowden, Hutchinsen and Ross Inc., 1976)

40- F.S.Tse et al., Mechanical Vibrations, Theory and Applications, (Boston: Allyn and Bacon, Inc., 1978) pp. 253-270.

41- D.Young, Handbook of Engineering Mechanics, Chapter 61, (Ed. W.Flugge) (New York: McGraw Hill Book Co., 1962)

APPENDIXES

APPENDIX A

PRESSURE TRANSDUCERS FOR NUCLEAR APPLICATIONS

A.1 Introduction

Only four manufacturs produce pressure transducers for protective systems of nuclear power plants: Rosemount Inc., ITT/Barton, Westinghouse Electric Corporation, and The Foxboro Company. The Foxboro transducer was described in Chapter 2. Rosemount, ITT/Barton and Westinghouse transducers are described in this section.

The transducers described in this appendix have one point in common with Foxboro transducers: They all use a two-step approach to develop the output signal. The first step is conversion of pressure into displacement. The second step is conversion of the displacement into the current signal. The transducers manufactured by Rosemount and ITT/Barton have another point in common with Foxboro transducers: They are available with two different electronic circuits. One designed to give an output DC current signal between 4 and 20 mA, and the other to give an output DC current between 10 and 50 mA. The Westinghouse Veritrak transducer is available only with an electronic circuit to give an output DC current between 4 and 20 mA.

Other types or transducers exist and information about them can be found in the literature (36,37,38).

A.2 Rosemount Pressure Transducers.

Rosemount pressure transducers are devices that associate an applied differential pressure with the capacitance of the transducer. The low pressure side of the transducer can be open to the atmosphere for gauge measurements, closed with vacuum for absolute pressure

measurements, or connected to a low pressure line, for differential pressure measurements. The main component of the transducer is called a δ-cell*, shown in Figure A-1. It consists of three diaphragms and an oil fluid that fills the internal space of the cell.

The two external diaphragms are under the action of the two different pressures, isolating the cell from the fluid in the pressure sensing lines. The internal diaphragm is a sensing element, and has a metallic circular plate at its center. This plate is combined with two other capacitor plates mounted at the inner part of the transducer to form a capacitor system (a system of two parallel plates capacitors connected in series).

A change in pressure at either side of the cell is transmitted from the process line to the sensing diaphragm through the isolating diaphragms and the oil that fills the cell. This causes the internal diaphragm to bend and displaces the inner capacitor plate from its equilibrium position. The inner plate moves toward one of the fixed capacitor plates and away from the other.

Since the capacitance of each capacitor is proportional to the distance between its plates, the final result is that one of the capacitors has its capacitance increased, while the other has it decreased. The differential capacitance, which is assumed to be proportional to the differential pressure that is being applied to the transducer, is converted into a DC current signal.

---

* δ-cell is a trademark of Rosemount Inc.

A.3 ITT/Barton Pressure Transducers

There are two models of ITT/Barton pressure transducers that are used on nuclear power plants. The first one, model 764, is designed for differential pressure applications. The other, model 763, is used for absolute pressure applications.

The main component of the model 764 is called the Differential Pressure Unit (DPU). It is a mechanical device consisting of a dual bellows assembly, enclosed by a set of two pressure housings, and a motion cantilever beam. As seen in Figure A-2, the dual bellows assembly consists of two internally connected bellows, a center plate, overrange valves, a temperature compensator, and a range spring assembly. The internal volume of the bellows assembly is filled with a non-corrosive fluid. The motion sensing cantilever beam is also sealed within this environment.

The two bellows are connected by a valve shaft. Attached to the shaft is the tip of the motion sensing cantilever beam. It is restrained at the other end by the body of the transducer. Bonded to the beam there are two strain gages, one on each side, which are connected to form active arms of a bridge circuit.

During operation of the transducer the two bellows have a displacement which is proportional to the difference in pressure across the transducer. This displacement causes the cantilever beam to bend, compressing one strain gage and stretching the other. The gage that is under tension has its resistance increased, and the other has it decreased. As result, the bridge circuit changes, resulting in a signal that is further converted into a DC current signal.
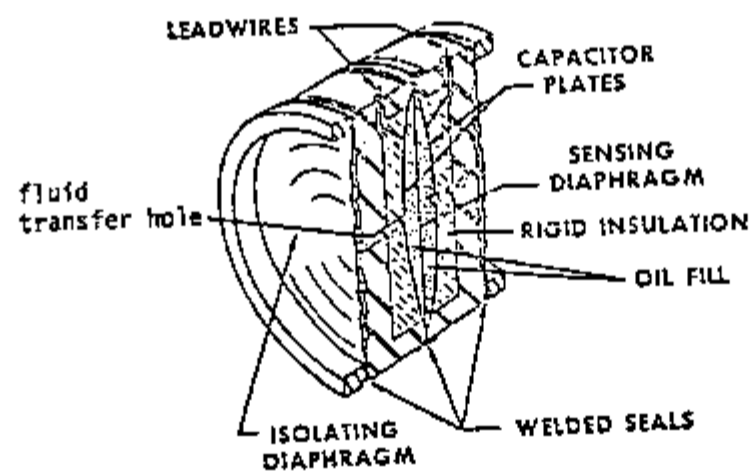
Figure A-1.   δ-cell^{TM}   used in Rosemount pressure transducers
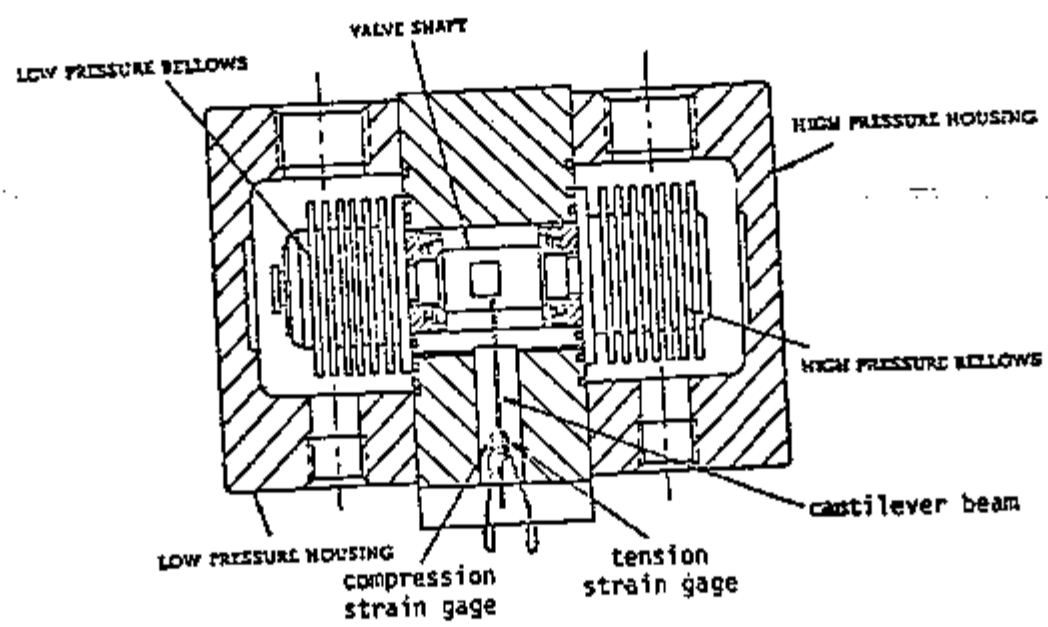
Figure A-2.   Differential pressure unit used on
ITT/Barton pressure transducer model 764

The ITT/Barton pressure transducer model 763 has the same principle of operation as the model 764. The difference is the way in which the pressure change is converted into bending of the cantilever beam. For model 763, this conversion is accomplished by use of a C-type Bourdon tube and a flexible wire. The C-type Bourdon tube is an arc-shaped metal tube with elliptical cross-section. It is sealed at one end, and with the opposite end attached to the pressure line. The pressure applied to the internal wall of the tube stretches it, causing a motion of the sealed end. A flexible wire connected between the closed end of the tube and the tip of the motion cantilever beam transmits the motion to the tip. This causes the beam to bend and generates the compressing-stretching effect of the strain gauges. This effect changes the resistance of the bridge circuit, and generates a signal that is further converted into the DC current signal.

A.4 - Veritrak Pressure Transducers.

The operation of Veritrak pressure transducers, as the ITT/Barton, is based in changing the resistance of a strain gage. There are two basic concepts of Veritrak transducers, one for differential pressure applications, and the other for absolute pressure applications. The design of the transducer used for measurement of gauge pressure is the same as the one used for absolute pressure. The main component of the transducer is a capsule assembly within which there is a flexure on which has been deposited a "bridge network of strain sensitive resistive elements".

In absolute pressure transducers, as shown in Figure A-3, a diaphragm isolates the sensitive element from the process lines, transmiting the force generated by the pressure to the flexure where the sensitive elements have been deposited. In differential pressure transducers there are two diaphragms, connected by a pushrod. The pushrod is also connected with the flexure which has the sensitive elements. A differential pressure causes the diaphragm-pushrod system to move toward the chamber of lower pressure, causing the flexure to bend.
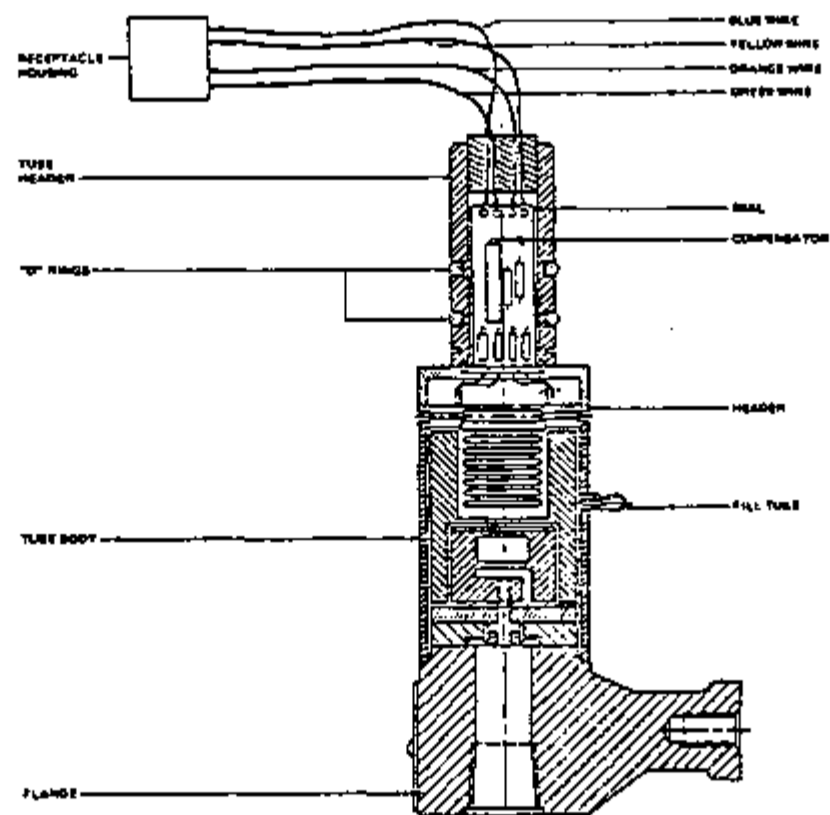
Figure A-3. Veritrak absolute pressure transducer

APPENDIX B

THEORY OF VIBRATION IN CONTINUOUS BEAMS

B.1 Introduction

In this work three equations were used for analysis of vibration of continuous beams. The first equation is necessary to study longitudinal vibrations along the beams; the second to study the transversal vibration of the beam using Euler Bernoulli's formulation, and the third also used to study transversal vibrations, but now assuming Timoshenko's formulation.

The equations are linear, and are based on the assumption of small oscillations about an equilibrium position. The references used in this appendix are 24,26,39,40 and 41.

B.2 Longitudinal Vibrations of Elastic Beams.

To start the analysis of longitudinal vibrations, we consider an elastic beam of constant cross sectional area A. We consider also that the beam is made of homogeneous and isotropic material, and make the further assumption that when the beam is under vibration each cross sectional plane remains perpendicular to the axial direction of the beam.

Referring to Diagram B-1, which shows a beam of length L with a differential element of length dx located at distance x from the origin, we note that the beam is under the action of two forces: $F(x_1,t)$ acting on the left end, and $F(x_2,t)$ acting on the right end. These forces are assumed to be uniformly distributed over the cross section at which they are acting.

We denote by $u(x,t)$ the longitudinal displacement, at time t, of the cross sectional plane that was originally at position x. To
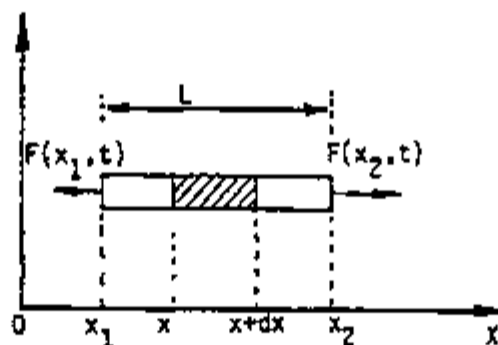
Diagram B-1

study the vibration of the differential element located at position x
we make use of Newton's second law (see Diagram B-2):

$$F(x,t) + \frac{\partial F}{\partial x}(x,t)dx - F(x,t) = \rho A dx \frac{\partial^2 u(x,t)}{\partial t^2} \qquad (B-1)$$

in which ρ is the density of the beam, A is the cross sectional
area, and $F(x,t)$ is the resultant force, at time t, of the internal
axial stress on the cross section at x.
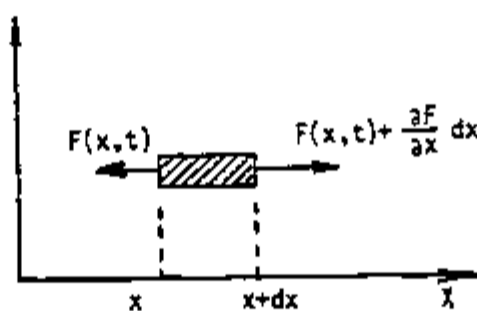
Diagram B-2

Expressing F(x,t) is terms of the axial stress S(x,t), and using Hooke's law to express S(x,t) in terms of the axial strain ε(x,t) we obtain:

$$F(x,t) = S(x,t)A = \varepsilon(x,t)AE \tag{B-2}$$

where E is the elasticity modulus for the material of the beam.

According to the definition of the axial strain ε, it is given by the variation of the length dx divided by dx:

$$\varepsilon(x,t) = \frac{[u(x,t) + \frac{\partial u(x,t)}{\partial x} dx] - u(x,t)}{dx} = \frac{\partial u(x,t)}{\partial x} \tag{B-3}$$

Using relations B-1 through B-3 we obtain

$$\frac{\partial^2 u(x,t)}{\partial x^2} = \frac{1}{c^2} \frac{\partial^2 u(x,t)}{\partial t^2} \tag{B-4}$$

where $c = \sqrt{E/\rho}$.

Equation B-4 is the one dimensional wave equation, and indicates that the vibration takes place in the axial direction with velocity c, which is the speed of the sound in the material of the beam.

Since u(x,t) is the displacement from the equilibrium position, we can use the notation $\delta u(x,t)$, and Equation B-4 becomes:

$$\frac{\partial^2 \delta u(x,t)}{\partial x^2} = \frac{1}{c^2} \frac{\partial^2 \delta u(x,t)}{\partial t^2} \tag{B-5}$$

One of the techniques used to solve partial differential equations, like Equation B-5, is Laplace transformation. We start by transforming Equation B-5 with respect to time:

$$\int_0^\infty e^{-st} \frac{\partial^2 \delta u(x,t)}{\partial x^2} \, dt = \int_0^\infty \frac{e^{-st}}{c^2} \frac{\partial^2 \delta u(x,t)}{\partial t^2} \, dt \tag{B-6}$$

On the left side of Equation B-6 we can remove the operator $\partial^2/\partial x^2$ from inside of the integral, and integrating the right side by parts, we obtain:

$$\frac{\partial^2}{\partial x^2} \left\{ \int_0^\infty e^{-st} \delta u(x,t) dt \right\} = \frac{1}{c^2} \left\{ s^2 \int_0^\infty e^{-st} \delta u(x,t) dt - s\delta u(x,o) \right.$$

$$\left. - \frac{\partial \delta u(x,t)}{\partial t} \Big|_{t=0} \right\} \tag{B-7}$$

By definition $\int_0^\infty e^{-st} \delta u(x,t) dt$ is the Laplace transform of $\delta u(x,t)$ (with respect to time), and since we have steady state initial condition, we may rewrite Equation B-7 as:

$$\frac{\partial^2 \delta u(x,s)}{\partial x^2} = \frac{s^2}{c^2} \delta u(x,s) \tag{B-8}$$

The general solution for Equation B-8 is:

$$\delta u(x,s) = A_1(s)e^{sx/c} + A_2(s)e^{-sx/c} \tag{B-9}$$

where $A_1(s)$ and $A_2(s)$ are two functions, of s, that must be determined by applying the proper boundary conditions. The two typical boundary conditions are:

1-Fixed end at coordinate x = p : u(p,t) = 0.

2-End subject to a force F(p,t) : $AE \frac{\partial u(x,t)}{\partial x}\Big|_{x=p} = F(p,t)$.

We note here that the boundary conditions can be Laplace transformed in order to be applied as boundary conditions for solving Equation B-9. We also note that in the second type of boundary condition we have a generic force that can be caused by a spring, a mass under acceleration, a damper, or no force at all, which give the condition of a free end.

In this work we have special interest in the case when the ends of the beam are subject to axial forces. Referring to Diagram B-1, the boundary conditions are:

$$AE \frac{\partial \delta u(x,t)}{\partial x}\Big|_{x=x_p} = \delta F(x_p,t) \text{ where } x_p = x_1, x_2 \qquad \text{(B-10)}$$

Equation B-10 may be Laplace tranformed to result:

$$AE \frac{\partial \delta u(x,s)}{\partial x}\Big|_{x=x_p} = \delta F(x_p,s) \qquad \text{at } x_p = x_1, x_2 \qquad \text{(B-11)}$$

Applying the boundary conditions above to Equation B-9, we obtain the final equation for $\delta u(x,s)$ as follows:

$$\delta u(x,s) = \frac{c}{sAE} \left[\frac{\delta F(x_2,s)\cosh[(x-x_1)s/c] - \delta F(x_1,s)\cosh[(x-x_2)s/c]}{\sinh(sL/C)} \right]$$

$$\text{(B-12)}$$

One remark about this solution is that it does not impose any requirement about the length L of the beam, and if L is small then $\sinh(sL/c)$ may be approximated by sL/c, $\cosh[(p-x)s/c]$ can be approximated by 1, and the result for $\delta u(x,s)$ becomes:

$$\delta u(x,s) = \frac{c^2}{s^2 AEL} \{\delta F(x_2,s) - \delta F(x_1,s)\} \qquad \text{(B-13)}$$

Since $c^2 = E/\rho$ and $M = AL\rho$ is the total mass of the beam,

then $\delta u(x,s)$ may now be rewritten as:

$$\delta u(x,s) = \frac{1}{Ms^2} \{\delta F(x_2,s) - \delta F(x_1,s)\} \qquad \text{(B-14)}$$

which represents the equation of motion for a rigid system.

B.2 Transversal Vibrations of Elastic Beams Using Euler-Bernoulli
    Formulation

We start the analysis by considering the static case when the

beam is under the action of an external couple M at the ends. In this

situation we have pure bending. In addition to the assumptions made

in the study of longitudinal vibrations (constant cross sectional area

and beam made of homogeneous and isotropic material), we assume that:

1- after the bending of the beam, cross sectional planes

remain planes, and normal to the longitudinal fibers of the

beam.

2- the beam has a longitudinal plane of symmetry, and the

couples are acting on this plane.

With these assumptions we note that cross sections mm' and rr'

(see Diagram B-3) became, after bending, inclined to each other. We

also note that the longitudinal fibers on the convex side suffer

extension, and the ones on the concave side suffer compression, with a

layer, represented by nn', remaining unchanged with respect to its

length (this layer is called the neutral surface).
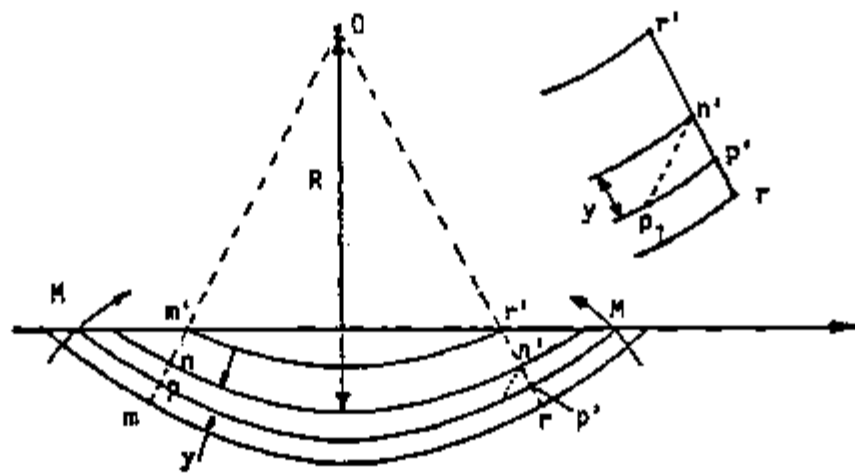
Diagram B-3

Drawing n'p$_1$ parallel to np, where pp' is a fiber at a
distance y from the neutral surface, and using similarity of sectors
(between sectors Opp' and n'p$_1$p') we obtain the following relation for
the elongation of fiber pp' :

$$\epsilon(pp') = \frac{p'p_1}{nn_1} = \frac{y}{R} = \epsilon(y) \tag{B-15}$$

where R=On represents the radius of curvature of the bent beam (for the
neutral surface).

Since the elongation for the layers in the convex side
(contraction for the layers in the concave side), remains in the
prolongation of the line containing the original fiber, we can say
that $\epsilon(y)$ is an axial strain (axial in the sense that it is parallel
to the neutral surface). Therefore, it may be expressed in terms of
the axial stress S. Using Hooke's law to relate the strain $\epsilon(y)$ with
the axial stress S, as done on section B.1, we obtain:

$$\epsilon(y) = \frac{y}{R} = \frac{S}{E} \tag{B-16}$$

To determine the radius of curvature R, we use the condition that the distribution of stress over any surface must result in a couple that balances the external couple M. This condition is mathematically expressed as:

$$\int_A SydA = \int_A \frac{Ey^2}{R} dA = M \tag{B-17}$$

where dA is an element of area. Using the definition for inertia moment of area ($I = \int_A y^2 dA$), and since we assumed that the beam is made of homogeneous and isotropic material, then:

$$R = \frac{EI}{M} \tag{R-18}$$

From a geometrical analysis, of the bent beam, we obtain the following relations for the displacement of the section located at x:

$$-u(x) = R - w(x) \tag{B-19}$$

$$w^2(x) = d^2 + x^2 \tag{B-20}$$

The negative sign in $u(x)$ is to indicate that $u(x)$ is negative if the bending is assumed as shown in Diagram B-4.

Differentiating Equations B-19 and B-20 twice, and using the fact that $R \gg x$ and that $w(x)$ is approximatelly the same as R, we obtain:

$$\frac{\partial^2 u(x)}{\partial x^2} = \frac{\partial^2 w(x)}{\partial x^2} \qquad \text{(B-21)}$$

and

$$\frac{\partial^2 w(x)}{\partial x^2} = 1/R \qquad \text{(B-22)}$$

Combining Equations B-18, B-21 and B-22 we obtain the equation for the curvature of the beam (flexure equation):

$$\frac{\partial^2 u(x)}{\partial x^2} = \frac{1}{R} = \frac{M}{EI} \qquad \text{(B-23)}$$

Once we obtained the differential equation for the curvature of the beam, relating $u(x)$ and $M(x)$, we can now analyze the situation when the beam is undergoing transversal vibration.

Diagram B-5 shows a free body diagram of an element of length dx and cross sectional area A which is under the action of shearing forces V, a distributed force $F(x,t)$ and a bending moment M.
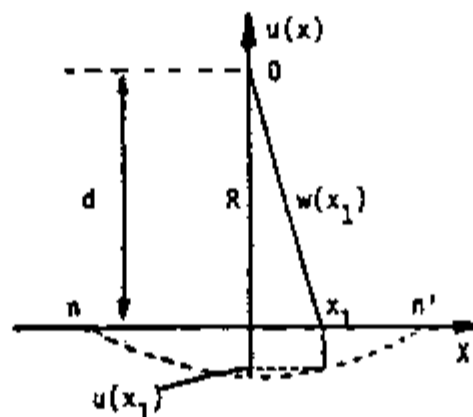
Diagram B-4
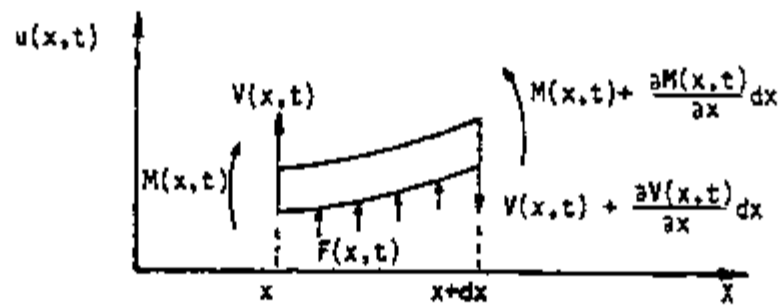
Diagram B-5

Assuming that the disturbance is very small, we neglect the rotation of the element. The balance of forces and momentum about point x+dx gives:

$$V(x,t) - [V(x,t) + \frac{\partial V(x,t)}{\partial x} \, dx] + F(x,t) = \rho A dx \, \frac{\partial^2 u(x,t)}{\partial t^2} \quad \text{(B-24a)}$$

$$-M(x,t) + [M(x,t) + \frac{\partial M(x,t)}{\partial x} \, dx] - V(x,t)dx - \int F(x,t)x dx = 0 \quad \text{(B-24b)}$$

From Equations B-24a and B-24b we obtain:

$$-\frac{\partial V(x,t)}{\partial x} + F(x,t) = \rho A \frac{\partial^2 u(x,t)}{\partial t^2} \quad \text{(B-25a)}$$

$$\frac{\partial M(x,t)}{\partial x} = V(x,t) \quad \text{(B-25b)}$$

Differentiating Equation B-25b with respect to x and combining the result with Equations B-25a and B-23, the last one differentiated twice with respect to x, we obtain:

$$\frac{\partial^2}{\partial x^2}\left[EI \frac{\partial^2 u(x,t)}{\partial x^2}\right] + \rho A \frac{\partial^2 u(x,t)}{\partial t^2} = F(x,t) \qquad (B-26)$$

where $F(x,t)$ is a force acting in the direction of u.

Assuming that EI is constant Equation B-26 can be rewritten as:

$$EI \frac{\partial^4 u(x,t)}{\partial x^4} + \rho A \frac{\partial^2 u(x,t)}{\partial t^2} = F(x,t) \qquad (B-27)$$

Equation B-27 is linear and can be written in terms of disturbances from the equilibrium position as:

$$EI \frac{\partial^4 \delta u(x,t)}{\partial x^4} + \rho A \frac{\partial^2 \delta u(x,t)}{\partial t^2} = \delta F(x,t) \qquad (B-28)$$

Following the same procedure as the one used with longitudinal vibrations, to solve Equation B-28 we start by Laplace transforming it with respect to time:

$$\int_0^\infty e^{-st} EI \frac{\partial^4 \delta u(x,t)}{\partial x^4} dt + \int_0^\infty e^{-st} \rho A \frac{\partial^2 \delta u(x,t)}{\partial t^2} dt = \int_0^\infty e^{-st} \delta F(x,t) dt$$

$$(B-29)$$

We can remove the operator $\partial^4/\partial x^4$ from inside of the first integral, and since we are dealing with the transient part, the initial conditions are zero. Equation B-29 becomes (after using the definition of the Laplace transform):

$$EI \frac{\partial^4 u(x,s)}{\partial x^4} + s^2 \rho A \delta u(x,s) = F(x,s) \qquad (B-30)$$

In this work Equation B-30 will be required in situations
where there is no force being applied at position x of the beam:
$\delta F(x,t)=0$, or when there is a force being applied at one point $x=p$:
$\delta F(x,t) = F(t)\delta_D(x-p)$, where $\delta_D(x-p)$ is the function delta of Dirac.

In terms of Laplace transforms these conditions are written as
$\delta F(x,s)=0$ and $\delta F(x,s)=\delta F(s)\delta_D(x-p)$ respectively.

The general solution for Equation B-30 when $\delta F(x,s)=0$
(homogeneous equation) is:

$$\delta u_3(x,s) = A_1(s)e^{\sqrt{jsc}\,x} + A_2(s)e^{-\sqrt{jsc}\,x} + A_3(s)e^{j\sqrt{jsc}\,x} + A_4(s)e^{-j\sqrt{jsc}\,x} \qquad (B-31)$$

where $c3 = \sqrt{\dfrac{\rho A}{EI}}$

$j = \sqrt{-1}$, and $A(s)$ are functions of s that will be determined using
the proper boundary conditions.

To solve Equation B-30 for points where $\delta F(x,s)=\delta F(s)\delta_D(x-p)$
we integrate the equation within $2\Delta x$ about point p and take the limit
as Δx goes to zero:

$$\lim_{\Delta x \to 0} EI \left. \frac{\partial^3 \delta u(y,s)}{\partial x^3}\right|_{p-\Delta x}^{p+\Delta x} = \delta F(p,s) \qquad (B-32)$$

Equations B-31 and B-32 form the essence of this part, and are
the basic equations required for the analysis of transversal
vibrations that is needed in the development of the dynamic model of
the transducer.

B.3 Transversal Vibrations of Elastic Beams Using Timoshenko
Formulation

During transversal vibration of a beam, besides being
translated in the direction perpendicular to the axis of the beam,
each element also suffers rotation, and the angle of rotation (ψ) is
equal to the slope of the deflected beam (see Diagram B-6):

$$\psi = \frac{\partial u(x,t)}{\partial x} \tag{B-33}$$

Thus there is a distributed inertia couple, called the rota-
tory inertia effect, which is given by:

$$J \frac{\partial^2 \psi(x,t)}{\partial t^2} = - I\rho \frac{\partial^2}{\partial t^2} [\frac{\partial u(x,t)}{\partial x}] \tag{B-34}$$

per unit length. (The negative sign is used because the rotation is
being assumed in the counterclockwise sense, negative momentum, and
$\partial u/\partial x$ is positive)
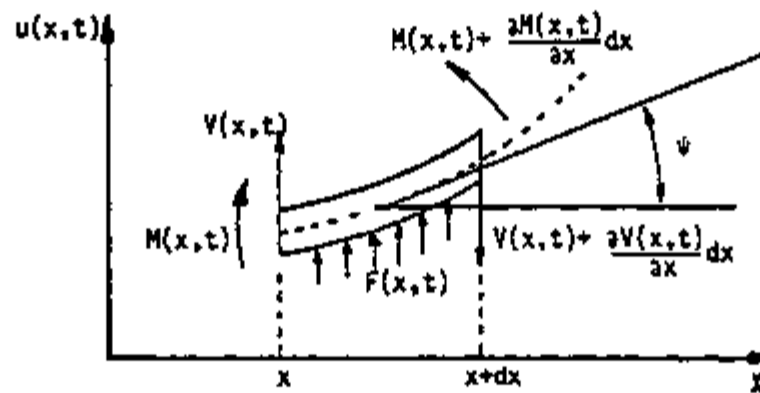
Diagram B-6

When the cross sectional dimensions of the beam are small in comparison with its length, the correction for the rotatory inertia is very small and can be neglected. However, when the cross sectional dimensions are comparable to the length of the beam, then the corrections may be of considerable importance in studying the vibration of the beam.

In addition to the rotatory inertia, there is another term that needs to be included in the dynamic equations for the beam. It is a correction due to the shear deformation. Due to the shear, the rectangular element shown in Diagram B-6 tends to acquire a diamond shape without rotating. This phenomenon causes a decrease in the slope of the center line. Referring to Figure B-6, the total deflection is given by u, and the slope due the bending process is given by ψ. Due to the shear force, the beam axis is diplaced in a way that tends to decrease the deflection of the beam, and the actual result is:

$$\frac{\partial u}{\partial x} = \psi - \gamma \qquad (B-35)$$

where ψ is the correction due to the shear effect.

The balance of forces and momentum for the differential element shown in Diagram B-6 gives:

$$-\frac{\partial V(x,t)}{\partial x} + F(x,t) = \rho A \frac{\partial^2 u(x,t)}{\partial t^2} \qquad (B-36a)$$

and

$$\frac{\partial M(x,t)}{\partial x} - V(x,t) = J \frac{\partial^2 \psi(x,t)}{\partial t^2} \qquad (B-36b)$$

From theory of elasticity we have that:

$$V(x,t) = -KGA \left[\frac{\partial u(x,t)}{\partial x} - \psi(x,t) \right] \qquad (B-37)$$

and

$$M(x,t) = EI \frac{\partial \psi(x,t)}{\partial x} \qquad (B-37b)$$

where G is the shear modulus : $G = \frac{E}{2(1+\mu)}$

μ is Poisson's ratio and K is a constant that depends of the geometry of the beam.

Equations above can be substituted in Equations B-36a and B-36b to give:

$$KGA \frac{\partial}{\partial x} \left[\frac{\partial u(x,t)}{\partial x} - \psi(x,t) \right] + F(x,t) = \rho A \frac{\partial^2 u(x,t)}{\partial t^2} \qquad (B-38a)$$

$$\frac{\partial}{\partial x} \left[EI \frac{\partial \psi(x,t)}{\partial x} \right] + KGA \left[\frac{\partial u(x,t)}{\partial x} - \psi(x,t) \right] = J \frac{\partial^2 \psi(x,t)}{\partial t^2} \qquad (B-38b)$$

As in the previous cases these Equations can be written in terms of disturbances form the equilibrium position:

$$KGA \frac{\partial}{\partial x} \left[\frac{\partial \delta u(x,t)}{\partial x} - \delta\psi(x,t) \right] + \delta F(x,t) = \rho A \frac{\partial^2 \delta u(x,t)}{\partial t^2} \qquad (B-39a)$$

$$\frac{\partial}{\partial x} \left[EI \frac{\partial \delta\psi(x,t)}{\partial x} \right] + KGA \left[\frac{\partial \delta u(x,t)}{\partial x} - \delta\psi(x,t) \right] = J \frac{\partial^2 \delta\psi(x,t)}{\partial t^2} \qquad (B-39b)$$

Assuming EI constant, and Laplace transforming Equations B-39a and B-39b with respect to the variable t we obtain:

$$KGA \frac{\partial}{\partial x} [\frac{\partial \delta u(x,s)}{\partial x} - \delta \psi(x,s)] + \delta F(x,s) = \rho As^2 \delta u(x,s) \quad (B-40a)$$

$$EI \frac{\partial^2 \delta \psi(x,s)}{\partial x^2} + KGA [\frac{\partial \delta u(x,s)}{\partial x} - \delta \psi(x,s)] = Js^2 \delta \psi(x,s) \quad (B-40b)$$

Equations B-40a and b-40b were used to find the dynamic response for only one element of the system, one component of the flexural system. The solution of the equations is discussed in the section regarding the modeling for that element.

APPENDIX C

INFORMATION PROVIDED BY THE FOXBORO COMPANY

The Foxboro Company

Foxboro, MA 02035 U.S.A.
(617) 543-8750

July 2, 1982

Mr. Lawrence F. Miller
The University of Tennessee
6507 Hunters Glen Drive
Knoxville, Tennessee   37921

Dear Mr. Miller:

Enclosed is some of the material and information you requested. Some information is confidential and cannot be provided. We hope our submittals will help you.

Please contact me with any further questions.

Very truly yours,

THE FOXBORO COMPANY

John A. Sears
Sr. Test and Evaluation Engineer
Corporate Quality Assurance Laboratory

Sea
Enclosures

FOXBORO

Department 383 Test Report No. ~~██████~~   Page 2

IV Summary of Test Results

Note: Due to the narrow span being used and the high pressure, the
       setability of the gauge is ±0.3% of span.

A. Calibration Characteristics

    See Graph No. 1.

B. Overrange Pressure Effects (2000 psi for 10 sec)

Number of Overrange Pressurizations	Output Shift after each Overrange Pressurization, (%)
1	+7.5
2	+0.9
3	+0.4
4*	<0.1
5	+0.40
6	+0.40

    *Unit Rezeroed

    FEI spec: Overrange effect is less than 0.5% for maximum
               position overrange.

C. Transient Temperature Effects

    (50°F change in one hour from 80°F to 130°F)

    See Graph No. 2.

    FEI spec: For a 100°F change in Ambient Temperature above 80°F
               zero shall shift less than ±2.5% and span shall change
               less than ±0.75%.

                                          Model E116-M Cal Range
                                          500 to 800 psi

D. Step Response (0 to 50% Input Step)

    | | 500 to 650 psi Step ||
	Up	Down
Dead Time, Seconds	0.04	0.04
50% Response, Seconds	0.58	0.64
90% Response, Seconds	1.02	1.22
100% Response, Seconds	1.32	1.46

    FEI spec: None

233

Department 383 Test Report No. ▓▓▓▓▓   Page 3

V Summary of Test Results (continued)

   D. Transient Temperature Effects

       See Graph No. 2.   *Model E13DM*
                                                Cal. Range 0 - 10" H₂O

   E. Step Response

       I. 50% Step, "H₂O   0 to 50   50 to 0   FEI Spec.

           a. Dead Time, sec.   0.034   0.012
           b. 50% Response Time, sec. 0.609   0.568
           c. 90% Response Time, sec. 1.042   1.167   None
           d. Transient Overshoot, % 2.0   3.5
           e. Settling Time, sec.   1.404   1.654

Graph No. 5
Frequency Response Characteristics
Input Frequency vs Magnitude Ratio
Input = 50% ±2   Range: 0-150" H₂O
P/13DN-SAM 1 Style A d/p cell   S/N 200201
R. J. Cardio   Feb. 1969

Input Frequency in cps

Graph No. 16
Frequency Response Characteristics
Input Frequency vs. Output Phase Shift
Range 0-150 Kc
Input 5.02 +57
B/19PN-5741   Style A O/P Cell S/N 2032612
R J Cardia   Feb. 1969

Output Phase Shift in Degrees

Input Frequency in cps

GRAPH NO. 6

FREQUENCY RESPONSE CHARACTERISTICS.
AMPLITUDE RATIO + PHASE ANGLE vs FREQUENCY
RANGE 0-140 P.S.I. INPUT 157.0 P.S.I. ± 40 P.S.I.

DEC '69
TEST PROCEDURE NO. 8-3-A-13
ROY P. LINDQUIST

2 - E116M-SA02-0
ELEC. GAUGE PNEU. TRANS.
SN 21E2303, OV

PHASE - DEG - O-

AMPLITUDE - DB

S/N 2/22309

S/N 2/22304

164

Freq. Response Setup

1. Osc - Oscillator freq. range .001 — 1KHz
   adjustable amplitude, sine wave.

2. Current supply — a current source range (minimum)
   0-100 mA capable of being modulated by an
   oscillator

3. I/P Converter - Current to Air Converter
   Input Current Range 4-20 mA or 10-50 mA
   Optimal Output Pressure Range 3-15 psi

Most I/p converters can be adjusted
below 3psi output so that lower inH₂O
ranges can be tested.

J. Saers
7/2/82

Figure 3 — Vector Mechanism
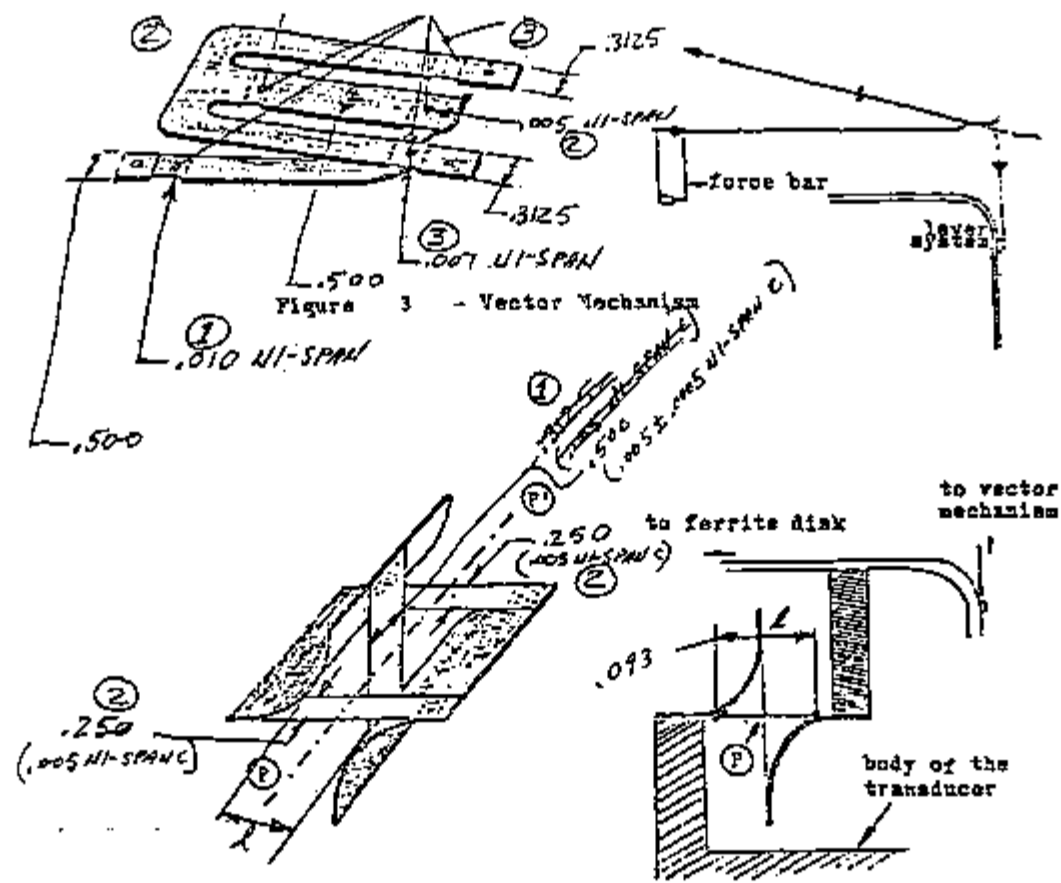
Figure 4 — Pivoting point formation
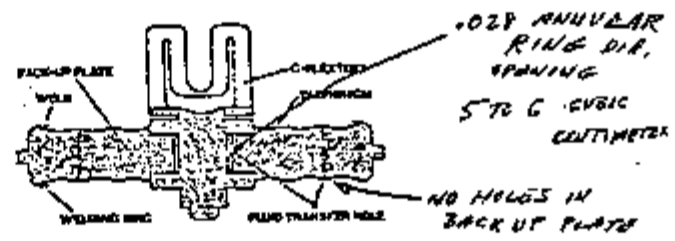
Figure 5 — SENSING ELEMENT (CAPSULE)

(a)

FIG 3.

ITEM 1   .010 NI-SPAN-C 0.500 WIDE

ITEM 2   .005 NI-SPAN-C 0.500 WIDE

ITEM 3   .007 NI-SPAN-C 0.3125 WIDE

(b)

MEASURED ONE UNIT .0054

FIG 4

ITEM 1   .005 $^{\pm.0005}$ NI-SPAN-C   ~~0.3125 WIDE~~ ~~.500 WIDE~~

ITEM 2   .0054 NI-SPAN-C 0.250 WIDE

(c)

l_3

l_4

l_5

l_1 l_2 LEVER LENGTHS
                IN INCHES

DETECTOR

l_6 FORCE $l_1 = 1.500''$
                   MOTOR $l_2 = .812$

                               $l_3 = 3.047$
           0.7 #/in $l_4 = 1.857$

           .005 INCH THICK $l_5 = 2.672$

l_7 $l_6 = 4.718$

           4 SQ" AREA. $l_7 = 2.843$

                               $l_8 = 1.880$

LOW { HIGH   (VECTOR ANGLE) $\theta = 6° MIN$

                               $15° MAX,$

           MED CAPSULE
           300 lbs/in
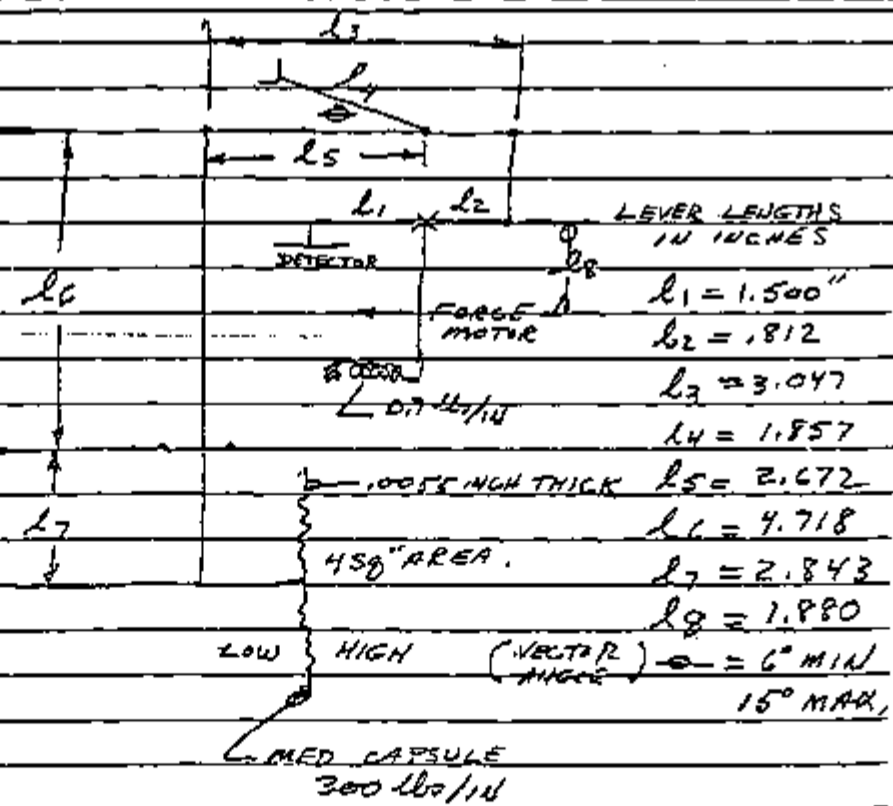
D.   NOT AVAILABLE

e.   NO

F.   (a) SPACE FILLED WITH FLUID
IS 5 TO 6 CUBIC CENTIMETERS

(b) TRANSFER HOLES

DIA. .5375

.028 ANNULAR
RING DIA. OPENING

DIA. .5935
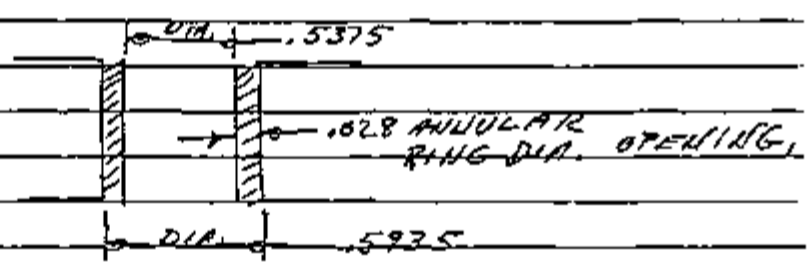
APPENDIX D

COMPUTATIONAL PROGRAM

```
C*********************************************************************
C
C
C            PROGRAM TO CALCULATE THE TRANSFER FUNCTION
C            FOR A FOXBORO PRESSURE TRANSDUCER MODEL E13DM
C
C            DEVELOPED BY ADALBERTO JOSE SOARES
C                      SEPT. 1982
C
C*********************************************************************
      IMPLICIT REAL*8 (A-H,O-Z)
      DIMENSION SV(100),G(15,2),SVR(100),
     NA(15,15,2),B(15,15,2),D(15,2)
      LOGICAL*1 LABX(30),LABY(30),LABT(30),TIT(10,30),LABR(30)
      OPEN(UNIT=4,NAME='DATAFIT',CARRIAGECONTROL='LIST')
```

```
      WRITE(5,33)
   33 FORMAT(2X,'INPUT PARAMETER ICON AS FOLLOWS :'/
     &10X,'ICON = 1 FOR LINEAR TRANSFER FUNCTION'/
     &10X,'ICON = 2 FOR LOG TRANSFER FUNCTION'/
     &10X,'ICON = 3 FOR FREQUENCY RESPONSE AND FIT')
      READ(5,34)ICON
   34 FORMAT(I4)
      WRITE(5,35)
   35 FORMAT(2X,'OBS. THE FINAL PLOT IS AS FOLLOWS :'/
     &10X,'FOR ICON = 1 AND 2 :'/
     &10X,'     LOG(MAG) OR PHASE VS [IMAG(S),REAL(S)]'/
     &10X,'FOR ICON = 3 : LOG(MAG) OR PHASE VS FREQUENCY')
      WRITE(5,61)
   61 FORMAT(2X,'INPUT IPLO AS FOLLOWS:'/
     &10X,'IPLO = 1 FOR OUTPUT OF MAGNITUDE'/
     &10X,'IPLO = 2 FOR OUTPUT OF PHASE')
      READ(5,34)IPLO
      WRITE(1,7)ICON
      WRITE(1,7)IPLO
    7 FORMAT(I2)
C********************************************************
C
C          GENERAL PARAMETER DEFINITION
C                   EM = ELASTICITY MODULUS   : LBF/PSI
C                   RO = DENSITY              : LBM/IN**3
C          OBS: THE CALCULATION IS PERFORMED
C               USING ENGLISH UNITS AND AT THE
C               END OF THE PROGRAM A CONVERSION IS
C               MADE TO INTERNATIONAL UNITS BY USING
C               CONVERSION FACTORS.
C********************************************************
      EM = 28.D+6
      EMNI = 30.D+6
      RO = .29
      RONI = .32
C********************************************************
C
C          DIVIDE RO BY GC
C********************************************************
      RO = RO/(32.2*12)
      RONI = RONI/(32.2*12.)
      PI = 2.*DASIN(1.0D0)
C********************************************************
C
C          PARAMETERS FOR DIAPHRAGM
C********************************************************
      DIND = 3.243
      DKDI = 332.
      ADI = 3.86
      CDI = 216.
C********************************************************
C          PARAMETERS FOR LEVER SYSTEM
C********************************************************
      STIFLV = 10.08
      DINRLV = 2.39D-4*(STIFLV + 7.96)
      CDAMP = 17.4*2.*DINRLV
      RAMRAT = 2642.
      ABREAK = .225
      XL = .812
      XD = 1.50
```

```
C******************************************************************
C   PARAMETERS FOR CONNECTION   (ELEMENT # 9)
C******************************************************************
      DL9=.745
      EM9=EMNI
      RO9=RONI
      CC9=DSQRT(EM9/RO9)
      AR9=1.14D-3
      CONS9=CC9/(AR9*EM9)
C******************************************************************
C     PARAMETERS FOR VECTOR MECHANISM   (ELEMENT # 8)
C******************************************************************
      DKB=3.499
      DKA=22.91
      C1=-1.073
      C2=1.366
      C3=-.436
      C4=.514
      C5=-1.73
      DM8=7.9D-5
      P8PG=1.73
      P9PG=1.38
      TETAGO=.045
      GAMA9O=PI/2.-.035
      GAMADO=.140
      GAMA8O=.025
      WD=2.06
      DMID=3.11
      PARU1=P8PG*DCOS(TETAGO) + P9PG*DSIN(GAMA9O)
      PARU2=PARU1*DCOS(GAMADO)
      PARU1=-PARU1*DSIN(GAMADO)
      PARU3=DM8*(C4*DSIN(GAMADO) + C5*DCOS(GAMADO))
      PARU4=DKB*C1*C2/WD - DKA*DCOS(GAMA8O - GAMADO)/DMID
C******************************************************************
C       PARAMETERS FOR FORCE-BAR   (ELEMENT # 7)
C******************************************************************
      EM7 = EM
      RO7 = RO
      AR7 = .255
      DIN7 = 5.18D-3
      CC7 = DSQRT((RO7*AR7)/(EM7*DIN7))
      Y7 = -2.843
      Y8 = 4.718
      CONS7 = (2.*EM7*DIN7*(CC7/2.)**1.5)
C******************************************************************
C       PARAMETERS FOR FIFTH ELEMENT OF C-FLEXURE (ELEMENT#6)
C******************************************************************
      EM6 = EM
      RO6 = RO
      DL6 = .249
      AR6 = 2.8D-3
      CC6 = DSQRT(EM6/RO6)
      CONS6 = CC6/(AR6*EM6)
C******************************************************************
C         PARAMETERS FOR FOURTH ELEMENT OF C-FLEXURE (ELEMENT #5)
C******************************************************************
      EM5 = EM
      RO5 = RO
      DL5 = .450
      AR5 = 2.73D-3
```

```
      DIN5 = 8.65D-6
      DKF=5./6.
      DJP=DIN5*RO5
      DMIPO=.3
      DGP=2.*(1.+DMIPO)
      DGP=EM5/DGP
      PARD1=RO5/(DKF*DGP) + DJP/(EM5*DIN5)
      PARD2=RO5/(DKF*DGP)- DJP/(EM5*DIN5)
      PARD3=4.*RO5*AR5/(EM5*DIN5)
C***********************************************
C       PARAMETERS FOR THIRD ELEMENT OF C-FLEXURE (ELEMENT #4)
C***********************************************
      EM4=EM
      RO4=RO
      DL4=.69
      AR4=2.66D-3
      CC4=DSQRT(EM4/RO4)
      CONS4=CC4/(AR4*EM4)
C***********************************************
C       PARAMETERS FOR SECOND ELEMENT OF C-FLEXURE (ELEMENT #3)
C***********************************************
      EM3 = EM
      RO3 = RO
      DL3 = 1.187
      AR3 = 1.145D-2
      DIN3=6.58E-6
      CC3 = DSQRT(RO3*AR3/(EM3*DIN3))
      CONS3 = DIN3*EM3*DSQRT(2.*CC3**2)
C***********************************************
C       PARAMETERS FOR FIRST ELEMENT OF C-FLEXURE (ELEMENT #2)
C***********************************************
      EM2=EM
      RO2 = RO
      DL2 = .09
      AR2 = .0353
      CC2 = DSQRT(EM2/RO2)
      CONS2 = CC2/(AR2*EM2)
C***********************************************
C
C       SELECTION OF VALUES FOR S
C       S = DREA + J*DIMA
C            WHERE J = IMAG. SYMBOL
C                 DREA IS THE REAL PART OF S AND
C                 DIMA IS THE IMAGINARY PART
C
C
C***********************************************
      AHG = PI/2.
      SV(1) = PI/500.
      SV(2)=1.5*SV(1)
      SV(3)=2.0*SV(1)
      SV(4)=3.0*SV(1)
      SV(5)=4.0*SV(1)
      SV(6)=6.0*SV(1)
      SV(7)=7.5*SV(1)
      DO 1 I = 8,26
      SV(I) = SV(I-7)*10.
    1 CONTINUE
      SV(27) = SV(26) + PI
      SV(28) = SV(27) + PI
```

```
      DO 3 I=29,43
    3 SU(I) = SU(I-1) + 2.*PI
      DO 4 I=44,70
    4 SU(I) = SU(I-1) + 5.*PI
      IF(ICON -2)72,76,72
   76 DO 77 I=1,40
   77 SU(I) = SU(I+7)
   72 CONTINUE
      DO 114 I=1,14
      SUR(I)=SU(I)
  114 CONTINUE
      DO 115 I=15,31
      SUR(I)=SUR(I-1) + .2*PI
  115 CONTINUE
      DO 116 I=32,40
      SUR(I)=SUR(I-21)*10.
  116 CONTINUE
      ANGDG=ANG*180./PI
      READ(3,10)JZ,(LABX(I),I=1,30)
      READ(3,10)JZ,(LABY(I),I=1,30)
      READ(3,10)JZ,(LABR(I),I=1,30)
      IF(IPLO-1)74,74,73
   73 DO 75 I=1,30
      LABY(I)=LABR(I)
   75 CONTINUE
   74 CONTINUE
      DO 9 J=1,10
      READ(3,10)JZ,(TIT(J,I),I=1,30)
      IF(JZ)11,11,9
   11 JZ=J-1
      GO TO 12
    9 CONTINUE
      JZ=J
   12 CONTINUE
   10 FORMAT(I3,30A1)
      WRITE(1,18)(LABX(I),I=1,30)
      WRITE(1,18)(LABY(I),I=1,30)
   18 FORMAT(4X,30A1)
      DO 13 J=1,JZ
      WRITE(1,14)J,(TIT(J,I),I=1,30)
   13 CONTINUE
      WRITE(1,14)
   14 FORMAT(1X,I3,30A1)
      IF(ICON-1)37,38,37
   38 WRITE(5,39)
   39 FORMAT(2X,'INPUT STEP VALUE')
      READ(5,40)STEP
      WRITE(5,71)STEP
   71 FORMAT(2X,F5.2)
   40 FORMAT(F5.2)
   37 CONTINUE
      IF(ICON-3)41,42,41
   41 NPTX=40
      NPTY=40
      GO TO 43
   42 NPTX=1
      NPTY=70
      WRITE(4,81)NPTY
   81 FORMAT(1X,I4,',')
   43 CONTINUE
```

```fortran
      WRITE(1,6)
    6 FORMAT(1X,6X,'FREQ',6X,'GL',7X,'GOVLS',7X,'GCH',
     *9X,'GVM',6X,' GFB',8X,'GFLE',5X,'GDIA',9X,'GOVER',5X,'GOVDI')
      DO 2 I=1,NPTX
      IF(ICON-2)44,45,46
   46 DREA=0.
      DROA=DREA
      GO TO 47
   45 DREA=-SVR(I)
      DROA=-DREA
      GO TO 47
   44 DREA=(I-21)*STEP
      DROA=DREA
   47 WRITE(1,55)DROA
   55 FORMAT(1X,E10.4)
      DO 2 J=1,NPTY
      IF(ICON-2)48,49,49
   48 DIMA=(J-21)*STEP
      GO TO 50
   49 DIMA=SU(J)
   50 IF(DREA)51,52,51
   52 IF(DIMA)51,53,51
   53 DIMA=.005
   51 CONTINUE
C************************************************************
C      G(1) =TF FOR FORCE MOTOR =CONSTANT
C************************************************************
      G(1,1) = -.0312
      G(1,2) = 0.
C************************************************************
C      G(2) = TF FOR SPRING = CONSTANT
C************************************************************
      G(2,1)= -5.31
      G(2,2) =0.
C************************************************************
C      G(3) = TF FOR LEVER SYSTEM , DISPL. X TORQUE
C************************************************************
      P1=DINRLV*(DREA**2-DIMA**2)+CDAMP*DREA+STIFLV
      P2=2.*DINRLV*DREA*DIMA+CDAMP*DIMA
      G(3,1)=1.50*P1/(P1**2+P2**2)
      G(3,2)=-1.50*P2/(P1**2+P2**2)
C************************************************************
C      G(4) = TF FOR ELECTRONICS : ASSUMED KNOWN
C************************************************************
      P1=ABREAK+DREA
      G(4,1)=RAMRAT*P1/(P1**2+DIMA**2)
      G(4,2)=-RAMRAT*DIMA/(P1**2+DIMA**2)
  444 FORMAT(2X,2(2X,D10.4))
C************************************************************
C      G(5) = TF FOR LEVER SYSTEM : OVERALL
C************************************************************
      CALL TIMES(G(3,1),G(3,2),G(4,1),G(4,2),R1,R2)
      CALL TIMES(R1,R2,G(1,1),G(1,2),RA1,RA2)
      CALL TIMES(G(2,1),G(2,2),G(3,1),G(3,2),RB1,RB2)
      P1=1.-RA1-RB1
      P2=-RA2-RB2
      CALL DIVIDE(R1,R2,P1,P2,G(5,1),G(5,2))
C************************************************************
C      CONNECTION
C************************************************************
```

```
        R1=DL9*DREA/CC9
        R2=DL9*DIMA/CC9
        CALL SINHE(R1,R2,RA1,RA2)
        CALL TIMES(DREA,DIMA,RA1,RA2,RB1,RB2)
        CALL DIVIDE(CONS9,0.,RB1,RB2,B(9,9,1),B(9,9,2))
        A(9,10,1)=-B(9,9,1)
        A(9,10,2)=-B(9,9,2)
        CALL COSHE(R1,R2,RA1,RA2)
        CALL TIMES(B(9,9,1),B(9,9,2),RA1,RA2,A(9,9,1),A(9,9,2))
        B(9,10,1)=-A(9,9,1)
        B(9,10,2)=-A(9,9,2)
        R1=XL**2*G(5,1)
        R2=XL**2*G(5,2)
        P1=XD*G(4,1)
        P2=XD*G(4,2)
        CALL DIVIDE(R1,R2,P1,P2,RA1,RA2)
        RA1=RA1-B(9,10,1)
        RA2=RA2-B(9,10,2)
        CALL DIVIDE(B(9,9,1),B(9,9,2),RA1,RA2,D(1,1),D(1,2))
        G(6,1)=D(1,1)*XL
        G(6,2)=D(1,2)*XL
        D(11,1)=G(6,1)
        D(11,2)=G(6,2)
C******************************************************************
C        VECTOR MECHANISM
C******************************************************************
        P1 = PARV3*(DREA**2 + DIMA**2) + PARV4
        P2=PARV3*2.*DREA*DIMA
        CALL DIVIDE(PARV1,0.,P1,P2,B(8,8,1),B(8,8,2))
        CALL DIVIDE(PARV2,0.,P1,P2,B(8,9,1),B(8,9,2))
        P3=C3=DSIN(GAMADO)
        CALL DIVIDE(P3,0.,P1,P2,A(8,8,1),A(8,8,2))
        P3=-C3*DCOS(GAMADO)
        CALL DIVIDE(P3,0.,P1,P2,A(8,9,1),A(8,9,2))
        CALL PARCAL(A(9,9,1),A(9,9,2),D(1,1),D(1,2),A(9,10,1),
       *A(9,10,2),B(8,9,1),B(8,9,2),R1,R2)
        CALL DIVIDE(B(8,8,1),B(8,8,2),R1,R2,G(7,1),G(7,2))
        D(12,1)=G(7,1)
        D(12,2)=G(7,2)
C******************************************************************
C        OVERALL AFTER VECTOR MECHANISM
C******************************************************************
        CALL TIMES(G(7,1),G(7,2),G(6,1),G(6,2),R1,R2)
        CALL TIMES(R1,R2,G(5,1),G(5,2),G(8,1),G(8,2))
C******************************************************************
C        FORCE-BAR
C******************************************************************
        PP = DSQRT(CC7/2.)=Y8
        QQ = DSQRT(CC7/2.)=Y7
        CALL DBRDOT(DREA,DIMA,RUT1,RUT2)
        CALL TIMES(PP,0.,RUT1,RUT2,PP1,PP2)
        CALL TIMES(QQ,0.,RUT1,RUT2,QQ1,QQ2)
        CALL SINE(PP1,PP2,PP1S,PP2S)
        CALL COSINE(PP1,PP2,PP1C,PP2C)
        CALL COSHE(PP1,PP2,PP1CH,PP2CH)
        CALL SINHE(PP1,PP2,PP1SH,PP2SH)
        CALL SINE(QQ1,QQ2,QQ1S,QQ2S)
        CALL COSINE(QQ1,QQ2,QQ1C,QQ2C)
        CALL COSHE(QQ1,QQ2,QQ1CH,QQ2CH)
        CALL SINHE(QQ1,QQ2,QQ1SH,QQ2SH)
```

```
      CALL TIMES(PP1S,PP2S,PP1C,PP2C,RA1,RA2)
      CALL TIMES(PP1SH,PP2SH,PP1CH,PP2CH,RB1,RB2)
      CONSA1=RA1-RB1
      CONSA2=RA2-RB2
      CALL TIMES(QQ1SH,QQ2SH,QQ1CH,QQ2CH,RA1,RA2)
      CALL TIMES(QQ1C,QQ2C,QQ1S,QQ2S,RB1,RB2)
      CONSB1=RA1-RB1
      CONSB2=RA2-RB2
      CALL TIMES(QQ1CH,QQ2CH,QQ1CH,QQ2CH,RA1,RA2)
      CALL TIMES(QQ1C,QQ2C,QQ1C,QQ2C,RB1,RB2)
      CONSC1=RA1+RB1
      CONSC2=RA2+RB2
      CALL TIMES(PP1CH,PP2CH,PP1CH,PP2CH,RA1,RA2)
      CALL TIMES(PP1C,PP2C,PP1C,PP2C,RB1,RB2)
      CONSD1=RA1+RB1
      CONSD2=RA2+RB2
      CALL TIMES(CONSA1,CONSA2,CONSC1,CONSC2,RA1,RA2)
      CALL TIMES(CONSB1,CONSB2,CONSD1,CONSD2,RB1,RB2)
      CALL TIMES(RUT1,RUT2,RUT1,RUT2,R1,R2)
      CALL TIMES(RUT1,RUT2,R1,R2,RC1,RC2)
      CALL TIMES(CONS7,0.,RC1,RC2,R1,R2)
      P1=RA1+RB1
      P2=RA2+RB2
      CALL TIMES(P1,P2,R1,R2,RA1,RA2)
      CALL DIVIDE(1.,0.,RA1,RA2,PAR1,PAR2)
     —CALL TIMES(QQ1SH,QQ2SH,QQ1SH,QQ2SH,RA1,RA2)
      CALL TIMES(QQ1S,QQ2S,QQ1S,QQ2S,RB1,RB2)
      CONSE1=RA1+RB1
      CONSE2=RA2+RB2
      CALL TIMES(QQ1CH,QQ2CH,QQ1S,QQ2S,RA1,RA2)
      CALL TIMES(QQ1C,QQ2C,QQ1SH,QQ2SH,RB1,RB2)
      CONSF1=RA1+RB1
      CONSF2=RA2+RB2
      CALL TIMES(PP1SH,PP2SH,PP1C,PP2C,RA1,RA2)
      CALL TIMES(PP1S,PP2S,PP1CH,PP2CH,RB1,RB2)
      CONSG1=RA1+RB1
      CONSG2=RA2+RB2
      CALL TIMES(PP1SH,PP2SH,PP1SH,PP2SH,RA1,RA2)
      CALL TIMES(PP1S,PP2S,PP1S,PP2S,RB1,RB2)
      CONSH1=RA1+RB1
      CONSH2=RA2+RB2
      CALL TIMES(CONSF1,CONSF2,CONSG1,CONSG2,RA1,RA2)
      CALL TIMES(RA1,RA2,PAR1,PAR2,A(7,8,1),A(7,8,2))
      CALL TIMES(CONSC1,CONSC2,CONSH1,CONSH2,RA1,RA2)
      CALL TIMES(CONSA1,CONSA2,CONSB1,CONSB2,RB1,RB2)
      R1=RA1+RB1
      R2=RA2+RB2
      CALL TIMES(PAR1,PAR2,R1,R2,B(7,8,1),B(7,8,2))
      B(7,7,1)=A(7,8,1)
      B(7,7,2)=A(7,8,2)
      CALL TIMES(CONSD1,CONSD2,CONSE1,CONSE2,RA1,RA2)
      R1=RA1+RB1
      R2=RA2+RB2
      CALL TIMES(PAR1,PAR2,R1,R2,A(7,7,1),A(7,7,2))
      CALL PARCAL(A(8,8,1),A(8,8,2),G(7,1),G(7,2),A(8,9,1),
     MA(8,9,2),B(7,8,1),B(7,8,2),R1,R2)
      CALL DIVIDE(B(7,7,1),B(7,7,2),R1,R2,G(9,1),G(9,2))
      D(13,1)=G(9,1)
      D(13,2)=G(9,2)
      CALL TIMES(G(9,1),G(9,2),G(8,1),G(8,2),G(10,1),G(10,2))
```

```
C*****************************************************
C       FIRST ELEM. OF C-FLEXURE
C*****************************************************
      P1=DL6/CC6
      CALL TIMES(DREA,DIMA,P1,0.,R1,R2)
      CALL SINHE(R1,R2,RA1,RA2)
      CALL TIMES(DREA,DIMA,RA1,RA2,RB1,RB2)
      CALL DIVIDE(CONS6,0.,RB1,RB2,A(6,7,1),A(6,7,2))
      CALL COSHE(R1,R2,RA1,RA2)
      CALL TIMES(A(6,7,1),A(6,7,2),RA1,RA2,B(6,7,1),B(6,7,2))
      B(6,6,1)=-A(6,7,1)
      B(6,6,2)=-A(6,7,2)
      A(6,6,1)=-B(6,7,1)
      A(6,6,2)=-B(6,7,2)
      P1=B(6,7,1)/2.
      P2=B(6,7,2)/2.
      CALL PARCAL(A(7,7,1),A(7,7,2),G(9,1),G(9,2),A(7,8,1),A(7,8,2),
     #P1,P2,R1,R2)
      CALL DIVIDE(B(6,6,1),B(6,6-2),R1,R2,D(4,1),D(4,2))
C*****************************************************
C       SECOND ELEMENT OF C-FLEXURE
C*****************************************************
      CALL TIMES(DREA,DIMA,DREA,DIMA,SS1,SS2)
      CALL TIMES(SS1,SS2,SS1,SS2,S41,S42)
      RA1=PARD2**2*S41-PARD3*SS1
      RA2=PARD2**2*S42-PARD3*SS2
      CALL DBROOT(RA1,RA2,PP1,PP2)
      QQ1=(PARD1*SS1 - PP1)/2.
      QQ2=(PARD1*SS2 - PP2)/2.
      PP1=(PARD1*SS1 + PP1)/2.
      PP2=(PARD1*SS2 + PP2)/2.
      PAR1=(PP1 - QQ1)*ROS*AR5
      PAR2=(PP2 - QQ2)*ROS*AR5
      CALL TIMES(PAR1,PAR2,SS1,SS2,RA1,RA2)
      CALL DBROOT(QQ1,QQ2,Q1,Q2)
      CALL DBROOT(PP1,PP2,P1,P2)
      CALL TIMES(Q1,Q2,P1,P2,RB1,RB2)
      CALL DIVIDE(RB1,RB2,RA1,RA2,PAR1,PAR2)
      CALL TIMES(P1,P2,DL5,0.,RA1,RA2)
      CALL SINHE(RA1,RA2,RB1,RB2)
      CALL COSHE(RA1,RA2,RS1,RS2)
      CALL DIVIDE(Q1,Q2,RB1,RB2,CONSA1,CONSA2)
      CALL TIMES(Q1,Q2,DL5,0.,RA1,RA2)
      CALL SINHE(RA1,RA2,RB1,RB2)
      CALL DIVIDE(P1,P2,RB1,RB2,CONSB1,CONSB2)
      CALL COSHE(RA1,RA2,RB1,RB2)
      CALL TIMES(RS1,RS2,CONSA1,CONSA2,CONSC1,CONSC2)
      CALL TIMES(RB1,RB2,CONSB1,CONSB2,CONSD1,CONSD2)
      CONSE1=CONSC1-CONSD1
      CONSE2=CONSC2-CONSD2
      CALL TIMES(CONSE1,CONSE2,PAR1,PAR2,A(5,5,1),A(5,5,2))
      CONSF1=CONSB1-CONSA1
      CONSF2=CONSB2-CONSA2
      CALL TIMES(CONSF1,CONSF2,PAR1,PAR2,A(5,6,1),A(5,6,2))
      B(5,5,1)=-A(5,6,1)
      B(5,5,2)=-A(5,6,2)
      B(5,6,1)=-A(5,5,1)
      B(5,6,2)=-A(5,5,2)
      RA1=A(6,7,1)/2.
      RA2=A(6,7,2)/2.
```

```fortran
      CALL PARCAL(A(6,6,1),A(6,6,2),D(4,1),D(4,2),RA1,RA2,
     *B(5,6,1),B(5,6,2),R1,R2)
      CALL DIVIDE(B(5,5,1),B(5,5,2),R1,R2,D(5,1),D(5,2))
C*******************************************************************
C        THIRD ELEMENT OF C-FLEXURE
C*******************************************************************
      R1=DL4*DREA/CC4
      R2=DL4*DIMA/CC4
      CALL SINHE(R1,R2,RA1,RA2)
      CALL TIMES(DREA,DIMA,RA1,RA2,RB1,RB2)
      CALL DIVIDE(CONS4,0.,RB1,RB2,A(4,5,1),A(4,5,2))
      CALL COSHE(R1,R2,RA1,RA2)
      CALL TIMES(RA1,RA2,A(4,5,1),A(4,5,2),B(4,5,1),B(4,5,2))
      B(4,4,1)=-A(4,5,1)
      B(4,4,2)=-A(4,5,2)
      A(4,4,1)=-B(4,5,1)
      A(4,4,2)=-B(4,5,2)
      CALL PARCAL(A(5,5,1),A(5,5,2),D(5,1),D(5,2),A(5,6,1),A(5,6,2),
     *B(4,5,1),B(4,5,2),R1,R2)
      CALL DIVIDE(B(4,4,1),B(4,4,2),R1,R2,D(6,1),D(6,2))
C*******************************************************************
C        FOURTH ELEMENT OF C-FLEXURE
C*******************************************************************
      R1 = DSQRT(CC3/2.)*DL3/2.
      CALL TIMES(RUT1,RUT2,R1,0.,P1,P2)
      CALL SINE(P1,P2,PP1,PP2)
      CALL SINHE(P1,P2,QQ1,QQ2)
      CALL TIMES(PP1,PP2,PP1,PP2,RA1,RA2)
      CALL TIMES(QQ1,QQ2,QQ1,QQ2,RB1,RB2)
      CONSA1=RA1+RB1
      CONSA2=RA2+RB2
      CALL COSINE(P1,P2,PAR1,PAR2)
      CALL COSHE(P1,P2,R1,R2)
      CALL TIMES(QQ1,QQ2,R1,R2,RA1,RA2)
      CALL TIMES(PP1,PP2,PAR1,PAR2,RB1,RB2)
      CONSB1=RA1+RB1
      CONSB2=RA2+RB2
      CALL TIMES(QQ1,QQ2,PAR1,PAR2,RA1,RA2)
      CALL TIMES(PP1,PP2,R1,R2,RB1,RB2)
      CONSC1=RA1+RB1
      CONSC2=RA2+RB2
      CALL TIMES(RUT1,RUT2,RUT1,RUT2,RA1,RA2)
      CALL TIMES(RUT1,RUT2,RA1,RA2,P1,P2)
      CALL TIMES(P1,P2,CONSA1,CONSA2,PAR1,PAR2)
      PAR1=PAR1*CONS3
      PAR2=PAR2*CONS3
      P1=-2.*PAR1
      P2=-2.*PAR2
      CALL DIVIDE(CONSB1,CONSB2,P1,P2,A(3,3,1),A(3,3,2))
      CALL DIVIDE(CONSC1,CONSC2,PAR1,PAR2,A(3,4,1),A(3,4,2))
      B(3,3,1)=-A(3,4,1)/2.
      B(3,3,2)=-A(3,4,2)/2.
      B(3,4,1)=-2.*A(3,3,1)
      B(3,4,2)=-2.*A(3,3,2)
      CALL PARCAL(A(4,4,1),A(4,4,2),D(6,1),D(6,2),A(4,5,1),A(4,5,2),
     *B(3,4,1),B(3,4,2),P1,P2)
      CALL DIVIDE(B(3,3,1),B(3,3,2),P1,P2,D(7,1),D(7,2))
C*******************************************************************
C        FIFTH ELEMENT OF C-FLEXURE
C*******************************************************************
```

```fortran
      P1=DLE/CC2
      CALL TIMES(DREA,DIMA,P1,0.,R1,R2)
      CALL SINHE(R1,R2,RA1,RA2)
      CALL TIMES(RA1,RA2,DREA,DIMA,RB1,RB2)
      CALL DIVIDE(CONS2,0.,RB1,RB2,A(2,3,1),A(2,3,2))
      CALL COSHE(R1,R2,RA1,RA2)
      CALL TIMES(RA1,RA2,A(2,3,1),A(2,3,2),B(2,3,1),B(2,3,2))
      B(2,2,1)=-A(2,3,1)
      B(2,2,2)=-A(2,3,2)
      A(2,2,1)=-B(2,3,1)
      A(2,2,2)=-B(2,3,2)
      CALL PARCAL(A(3,3,1),A(3,3,2),D(7,1),D(7,2),A(3,4,1),A(3,4,2),
     *B(2,3,1),B(2,3,2),P1,P2)
      CALL DIVIDE(B(2,2,1),B(2,2,2),P1,P2,D(8,1),D(8,2))
C*****************************************************
C       G(11) = T.F. FOR FLEXURAL SYSTEM
C*****************************************************
      CALL TIMES(D(4,1),D(4,2),D(5,1),D(5,2),P1,P2)
      CALL TIMES(D(7,1),D(7,2),D(8,1),D(8,2),R1,R2)
      CALL TIMES(D(6,1),D(6,2),P1,P2,RA1,RA2)
      CALL TIMES(RA1,RA2,R1,R2,G(11,1),G(11,2))
      CALL TIMES(G(10,1),G(10,2),G(11,1),G(11,2),G(12,1),G(12,2))
C*****************************************************
C
C       G(13) = T.F. FOR DIAPHRAGM
C
C*****************************************************
      CALL TIMES(DREA,DIMA,DREA,DIMA,P1,P2)
      PAR1=DIND*P1 + CDI*DREA + DKDI
      PAR2=DIND*P2 + CDI*DIMA
      CALL DIVIDE(1.,0.,PAR1,PAR2,B(1,2,1),B(1,2,2))
      B(1,1,1)=-ADI*B(1,2,1)
      B(1,1,2)=-ADI*B(1,2,2)
      CALL PARCAL(A(2,2,1),A(2,2,2),D(9,1),D(8,2),A(2,3,1),A(2,3,2),
     *B(1,2,1),B(1,2,2),P1,P2)
      CALL DIVIDE(B(1,1,1),B(1,1,2),P1,P2,G(13,1),G(13,2))
      CALL TIMES(G(12,1),G(12,2),G(13,1),G(13,2),G(15,1),G(15,2))
      IF (J-1)101,108,101
101   IF(J-10)102,108,102
102   IF(J-20)103,108,103
103   IF(J-40)107,108,107
108   A(1,1,1)=B(1,1,1)
      A(1,1,2)=B(1,1,2)
      A(1,2,1)=B(1,2,1)
      A(1,2,2)=B(1,2,2)
      DO 109 K=1,9
110   FORMAT(2X,8(2X,D10.4))
109   CONTINUE
107   CONTINUE
      IF(IPLO-1)63,63,64
63    CONTINUE
      CALL DIVIDE(G(15,1),G(15,2),G(4,1),G(4,2),G(14,1),G(14,2))
      G3=DSQRT(G(3,1)**2+G(3,2)**2)/4.45
      G5=DSQRT(G(5,1)**2+G(5,2)**2)*8.85
      G6=DSQRT(G(6,1)**2+G(6,2)**2)*.0254
      G7=DSQRT(G(7,1)**2+G(7,2)**2)
      G9=DSQRT(G(9,1)**2+G(9,2)**2)
      G11=DSQRT(G(11,1)**2+G(11,2)**2)
      G13=DSQRT(G(13,1)**2+G(13,2)**2)*6.45D-4
      G15=DSQRT(G(15,1)**2+G(15,2)**2)*1.45D-4
```

```
      G12=DSQRT(G(12,1)**2+G(12,2)**2)/4.45
      G3=DABS(G3)
      G5=DABS(G5)
      G6=DABS(G6)
      G7=DABS(G7)
      G9=DABS(G9)
      G11=DABS(G11)
      G13=DABS(G13)
      G15=DABS(G15)
      G12=DABS(G12)
      GO TO 65
   64 CONTINUE
      CALL ANGULO(G(3,1),G(3,2),G3)
      CALL ANGULO(G(5,1),G(5,2),G5)
      CALL ANGULO(G(6,1),G(6,2),G6)
      CALL ANGULO(G(7,1),G(7,2),G7)
      CALL ANGULO(G(9,1),G(9,2),G9)
      CALL ANGULO(G(11,1),G(11,2),G11)
      CALL ANGULO(G(13,1),G(13,2),G13)
      CALL ANGULO(G(15,1),G(15,2),G15)
      CALL ANGULO(G(12,1),G(12,2),G12)
   65 CONTINUE
      IF(ICON-3)56,57,57
   56 FREQ=DIMA
      GO TO 58
   57 FREQ=DIMA/(2.*PI)
      D(8,1)=D(8,1)-1
      WRITE(4,82)FREQ,G(14,1),G(14,2)
   82 FORMAT(1X,D10.4,',',D10.4,',',D10.4,',')
   58 CONTINUE
      WRITE(1,5)FREQ,G3,G5,G6,G7,G9,G11,G13,G15,G12
    5 FORMAT(1X,10(1X,E10.4))
    2 CONTINUE
      STOP
      END
```

```fortran
      SUBROUTINE DIVIDE(PRE,PIM,SRE,SIM,RRE,RIM)
      REAL*8 PRE,PIM,SRE,SIM,RRE,RIM,TT1,TT2,TT3
      IF(DABS(SIM).GT.1.0D-17) GO TO 9951
      IF(DABS(SRE).GT.1.0D-17) GO TO 9951
      IF(DABS(SRE).GT.DABS(SIM)) GO TO 9952
      TT1=(SRE/SIM)*SRE + SIM
      TT2=(SRE/SIM)*PRE + PIM
      TT3=(SRE*SIM)/PIM - PRE
      GO TO 9953
 9952 TT1=SRE + (SIM/SRE)*SIM
      TT2=PRE + (SIM/SRE)*PIM
      TT3=PIM - (SIM/SRE)*PRE
      GO TO 9953
 9951 TT1=SRE**2 + SIM**2
      TT2=SRE*PRE + SIM*PIM
      TT3=SRE*PIM - SIM*PRE
 9953 RRE=TT2/TT1
      RIM=TT3/TT1
      RETURN
      END




      SUBROUTINE TIMES(PRE,PIM,SRE,SIM,RRE,RIM)
      REAL*8 PRE,PIM,SRE,SIM,RRE,RIM
      RRE=PRE*SRE - PIM*SIM
      RIM=PIM*SRE + PRE*SIM
      RETURN
      END




      SUBROUTINE COSINE(PRE,PIM,RRE,RIM)
      REAL*8 PRE,PIM,RRE,RIM,TT1,TT2
      TT1=(DEXP(PIM) + DEXP(-PIM))/2.
      TT2=(DEXP(PIM) - DEXP(-PIM))/2.
      RRE=DCOS(PRE)*TT1
      RIM=-DSIN(PRE)*TT2
      RETURN
      END




      SUBROUTINE SINE(PRE,PIM,RRE,RIM)
      REAL*8 PRE,PIM,RRE,RIM,TT1,TT2
      TT1=(DEXP(PIM) + DEXP(-PIM))/2.
      TT2=(DEXP(PIM) - DEXP(-PIM))/2.
      RRE=DSIN(PRE)*TT1
      RIM=DCOS(PRE)*TT2
      RETURN
      END
```

```
      SUBROUTINE PARCAL(A1,A2,B1,B2,C1,C2,D1,D2,E1,E2)
      REAL*8 A1,A2,B1,B2,C1,C2,D1,D2,E1,E2
      REAL*8 TT1,TT2,TT3,TT4
      TT1=A1-D1
      TT2=A2-D2
      CALL TIMES(B1,B2,C1,C2,TT3,TT4)
      E1=TT1+TT3
      E2=TT2+TT4
      RETURN
      END


      SUBROUTINE COSHE(PRE,PIM,RRE,RIM)
      REAL*8 PRE,PIM,RRE,RIM,TT1,TT2
      TT1=(DEXP(PRE) + DEXP(-PRE))/2.
      TT2=(DEXP(PRE) - DEXP(-PRE))/2.
      RRE=TT1*DCOS(PIM)
      RIM=TT2*DSIN(PIM)
      RETURN
      END


      SUBROUTINE SINHE(PRE,PIM,RRE,RIM)
      REAL*8 PRE,PIM,RRE,RIM,TT1,TT2
      TT1=(DEXP(PRE) - DEXP(-PRE))/2.
      TT2=(DEXP(PRE) + DEXP(-PRE))/2.
      RRE=TT1*DCOS(PIM)
      RIM=TT2*DSIN(PIM)
      RETURN
      END


      SUBROUTINE D2ROOT(PRE,PIM,RRE,RIM)
      REAL*8 PRE,PIM,RRE,RIM,TT1,TT2,PI
      TT1=PRE**2+PIM**2
      TT1=DSQRT(TT1)
      TT1=DSQRT(TT1)
      CALL ANGULO(PRE,PIM,TT2)
      RRE=TT1*DCOS(TT2)
      RIM=TT1*DSIN(TT2)
      RETURN
      END


      SUBROUTINE ANGULO(P1,P2,P3)
      REAL*8 P1,P2,P3,PI
      PI=2.*DASIN(1.0D0)
      IF(P1-0.D0)880,881,880
  881 IF(P2-0.D0)882,883,883
  882 P3=3.*PI/2.
      GO TO 888
  883 P3=PI/2.
      GO TO 888
  880 P3=DATAN(P2/P1)
      IF(P1-0.D0)884,888,888
  884 P3=P3-PI
  888 RETURN
      END
```

```
2
1
    FREQUENCY IN HZ
    MAGNITUDE
  1 T.F.FOR LEV.SYSTEM :N/(MM)
  2 OVERALL AF.LEV.SYST:MA/(MM)
  3 T.F.CONNECTION :N/N
  4 T.F. FOR VECTOR MECH.:N/N
  5 T.F.FOR FORCE BAR     :N/N
  6 T.F. FOR E-FLEXURE  :N/N
  7 T.F. DIAPHRAGM :N/(N/MM**2)
  8 OVER.FOR SENSOR :MA/(N/MM**2)
  9 OVERALL AF.DIAPHRAGM :MA/N

      FREQ        GL         GOVLS        GCN         GVM         GFB         GFLE        GDIA         GOVER       GOVDI
0.0000E+00
  0.1000E-02 0.3344E-01 0.2746E+03 0.2062E-01 0.1404E+00 0.6026E+00 0.1000E+01 0.2332E-02 0.1117E-02 0.4790E+00
  0.1500E-02 0.3344E-01 0.2746E+03 0.2062E-01 0.1404E+00 0.6026E+00 0.1000E+01 0.2332E-02 0.1118E-02 0.4790E+00
  0.2000E-02 0.3344E-01 0.2746E+03 0.2062E-01 0.1404E+00 0.6026E+00 0.1000E+01 0.2333E-02 0.1118E-02 0.4790E+00
  0.3000E-02 0.3344E-01 0.2746E+03 0.2062E-01 0.1404E+00 0.6026E+00 0.1000E+01 0.2333E-02 0.1118E-02 0.4790E+00
  0.4000E-02 0.3344E-01 0.2746E+03 0.2062E-01 0.1404E+00 0.6026E+00 0.1000E+01 0.2333E-02 0.1118E-02 0.4790E+00
  0.6000E-02 0.3344E-01 0.2746E+03 0.2062E-01 0.1404E+00 0.6026E+00 0.1000E+01 0.2333E-02 0.1118E-02 0.4790E+00
  0.7500E-02 0.3344E-01 0.2746E+03 0.2062E-01 0.1404E+00 0.6026E+00 0.1000E+01 0.2333E-02 0.1118E-02 0.4790E+00
  0.1000E-01 0.3344E-01 0.2746E+03 0.2062E-01 0.1404E+00 0.6026E+00 0.1000E+01 0.2333E-02 0.1118E-02 0.4790E+00
  0.1500E-01 0.3344E-01 0.2746E+03 0.2062E-01 0.1404E+00 0.6026E+00 0.1000E+01 0.2333E-02 0.1118E-02 0.4790E+00
  0.2000E-01 0.3344E-01 0.2746E+03 0.2062E-01 0.1404E+00 0.6026E+00 0.9999E+00 0.2333E-02 0.1118E-02 0.4789E+00
  0.3000E-01 0.3344E-01 0.2745E+03 0.2062E-01 0.1404E+00 0.6026E+00 0.9999E+00 0.2333E-02 0.1118E-02 0.4788E+00
  0.4000E-01 0.3344E-01 0.2745E+03 0.2062E-01 0.1404E+00 0.6026E+00 0.9998E+00 0.2334E-02 0.1117E-02 0.4786E+00
  0.6000E-01 0.3344E-01 0.2743E+03 0.2062E-01 0.1403E+00 0.6026E+00 0.9998E+00 0.2334E-02 0.1117E-02 0.4783E+00
  0.7500E-01 0.3344E-01 0.2741E+03 0.2062E-01 0.1403E+00 0.6026E+00 0.9996E+00 0.2335E-02 0.1116E-02 0.4777E+00
  0.1000E+00 0.3344E-01 0.2737E+03 0.2062E-01 0.1403E+00 0.6026E+00 0.9997E+00 0.2337E-02 0.1115E-02 0.4768E+00
  0.1500E+00 0.3348E-01 0.2725E+03 0.2062E-01 0.1401E+00 0.6026E+00 0.9996E+00 0.2342E-02 0.1111E-02 0.4741E+00
  0.2000E+00 0.3346E-01 0.2709E+03 0.2062E-01 0.1399E+00 0.6026E+00 0.9994E+00 0.2349E-02 0.1106E-02 0.4705E+00
  0.3000E+00 0.3348E-01 0.2664E+03 0.2062E-01 0.1393E+00 0.6026E+00 0.9990E+00 0.2366E-02 0.1091E-02 0.4606E+00
  0.4000E+00 0.3351E-01 0.2603E+03 0.2062E-01 0.1385E+00 0.6026E+00 0.9984E+00 0.2390E-02 0.1071E-02 0.4478E+00
  0.6000E+00 0.3359E-01 0.2457E+03 0.2062E-01 0.1368E+00 0.6026E+00 0.9976E+00 0.2434E-02 0.1014E-02 0.4164E+00
  0.7500E+00 0.3366E-01 0.2331E+03 0.2062E-01 0.1354E+00 0.6026E+00 0.9964E+00 0.2453E-02 0.9588E-03 0.3906E+00
  0.1000E+01 0.3386E-01 0.2116E+03 0.2062E-01 0.1332E+00 0.6026E+00 0.9949E+00 0.2448E-02 0.8650E-03 0.3484E+00
  0.1500E+01 0.3440E-01 0.1735E+03 0.2062E-01 0.1300E+00 0.6026E+00 0.9909E+00 0.2258E-02 0.6850E-03 0.2777E+00
  0.2000E+01 0.3514E-01 0.1449E+03 0.2062E-01 0.1280E+00 0.6026E+00 0.9867E+00 0.1951E-02 0.4430E-03 0.2274E+00
  0.3000E+01 0.3744E-01 0.1094E+03 0.2062E-01 0.1254E+00 0.6025E+00 0.9762E+00 0.1406E-02 0.2950E-03 0.1674E+00
  0.4000E+01 0.4078E-01 0.9056E+02 0.2063E-01 0.1239E+00 0.6025E+00 0.9650E+00 0.1027E-02 0.1388E-03 0.1351E+00
  0.4500E+01 0.4281E-01 0.8476E+02 0.2063E-01 0.1230E+00 0.6024E+00 0.9600E+00 0.8847E-03 0.1106E-03 0.1249E+00
  0.5000E+01 0.4498E-01 0.8066E+02 0.2063E-01 0.1221E+00 0.6024E+00 0.9540E+00 0.7630E-03 0.9064E-04 0.1174E+00
  0.6000E+01 0.4885E-01 0.7644E+02 0.2063E-01 0.1201E+00 0.6023E+00 0.9485E+00 0.5763E-03 0.6294E-04 0.1081E+00
  0.7000E+01 0.4939E-01 0.7649E+02 0.2063E-01 0.1179E+00 0.6021E+00 0.9362E+00 0.4348E-03 0.4872E-04 0.1040E+00
  0.8000E+01 0.4444E-01 0.7943E+02 0.2063E-01 0.1164E+00 0.6019E+00 0.9236E+00 0.3312E-03 0.3512E-04 0.1060E+00
  0.9000E+01 0.3640E-01 0.8153E+02 0.2063E-01 0.1186E+00 0.6018E+00 0.9159E+00 0.2553E-03 0.2810E-04 0.1101E+00
  0.1000E+02 0.2879E-01 0.7412E+02 0.2063E-01 0.1304E+00 0.6019E+00 0.9282E+00 0.2095E-03 0.2333E-04 0.1114E+00
  0.1100E+02 0.2282E-01 0.5649E+02 0.2062E-01 0.1469E+00 0.6025E+00 0.9660E+00 0.2004E-03 0.2008E-04 0.1001E+00
  0.1200E+02 0.1836E-01 0.3999E+02 0.2062E-01 0.1555E+00 0.6031E+00 0.1004E+01 0.2303E-03 0.1708E-04 0.7760E-01
  0.1300E+02 0.1508E-01 0.2830E+02 0.2062E-01 0.1587E+00 0.6033E+00 0.1026E+01 0.2934E-03 0.1644E-04 0.5602E-01
  0.1400E+02 0.1240E-01 0.2063E+02 0.2062E-01 0.1553E+00 0.6034E+00 0.1015E+01 0.3638E-03 0.1531E-04 0.4042E-01
  0.1500E+02 0.1088E-01 0.1582E+02 0.2062E-01 0.1536E+00 0.6033E+00 0.1009E+01 0.4588E-03 0.1472E-04 0.2990E-01
  0.1600E+02 0.9176E-02 0.1201E+02 0.2062E-01 0.1518E+00 0.6033E+00 0.1002E+01 0.5907E-03 0.1343E-04 0.2273E-01
  0.1700E+02 0.7775E-02 0.9514E+01 0.2062E-01 0.1509E+00 0.6032E+00 0.9958E+00 0.4273E-03 0.1112E-04 0.1773E-01
  0.1800E+02 0.6599E-02 0.7684E+01 0.2062E-01 0.1493E+00 0.6032E+00 0.9898E+00 0.5864E-03 0.8853E-05 0.1412E-01
  0.1900E+02 0.6196E-02 0.6809E+01 0.2062E-01 0.1484E+00 0.6031E+00 0.9843E+00 0.5110E-03 0.3858E-05 0.1146E-01
  0.2000E+02 0.5527E-02 0.5213E+01 0.2062E-01 0.1476E+00 0.6031E+00 0.9792E+00 0.4357E-03 0.4119E-05 0.9441E-02
  0.2250E+02 0.4267E-02 0.3490E+01 0.2062E-01 0.1462E+00 0.6029E+00 0.9679E+00 0.3008E-03 0.1867E-05 0.6139E-02
  0.2500E+02 0.3400E-02 0.2447E+01 0.2062E-01 0.1453E+00 0.6028E+00 0.9581E+00 0.2234E-03 0.9419E-06 0.4234E-02
  0.2750E+02 0.2776E-02 0.1780E+01 0.2062E-01 0.1446E+00 0.6027E+00 0.9494E+00 0.1732E-03 0.7884E-06 0.3051E-02
  0.3000E+02 0.2311E-02 0.1349E+01 0.2062E-01 0.1442E+00 0.6025E+00 0.9412E+00 0.1379E-03 0.3181E-06 0.2274E-02
  0.3250E+02 0.1958E-02 0.1044E+01 0.2062E-01 0.1438E+00 0.6024E+00 0.9336E+00 0.1160E-03 0.2020E-06 0.1741E-02
  0.3500E+02 0.1676E-02 0.8259E+00 0.2062E-01 0.1435E+00 0.6022E+00 0.9264E+00 0.9814E-04 0.1330E-06 0.1360E-02
  0.3750E+02 0.1453E-02 0.6644E+00 0.2062E-01 0.1433E+00 0.6021E+00 0.9195E+00 0.8434E-04 0.9144E-07 0.1087E-02
  0.4000E+02 0.1272E-02 0.5430E+00 0.2062E-01 0.1431E+00 0.6019E+00 0.9129E+00 0.7342E-04 0.6465E-07 0.8808E-03
  0.4250E+02 0.1123E-02 0.4496E+00 0.2062E-01 0.1430E+00 0.6017E+00 0.9066E+00 0.6460E-04 0.4671E-07 0.7228E-03
  0.4500E+02 0.9994E-03 0.3767E+00 0.2062E-01 0.1428E+00 0.6015E+00 0.9002E+00 0.5735E-04 0.3444E-07 0.6007E-03
  0.4750E+02 0.8950E-03 0.3187E+00 0.2062E-01 0.1427E+00 0.6013E+00 0.8945E+00 0.5132E-04 0.2589E-07 0.5043E-03
  0.5000E+02 0.8068E-03 0.2722E+00 0.2062E-01 0.1427E+00 0.6011E+00 0.8882E+00 0.4623E-04 0.1977E-07 0.4274E-03
  0.5250E+02 0.7300E-03 0.2343E+00 0.2062E-01 0.1426E+00 0.6008E+00 0.8824E+00 0.4189E-04 0.1530E-07 0.3652E-03
  0.5500E+02 0.6648E-03 0.2032E+00 0.2062E-01 0.1425E+00 0.6006E+00 0.8768E+00 0.3817E-04 0.1200E-07 0.3148E-03
  0.5750E+02 0.6070E-03 0.1773E+00 0.2062E-01 0.1425E+00 0.6004E+00 0.8713E+00 0.3494E-04 0.9522E-08 0.2725E-03
  0.6000E+02 0.5560E-03 0.1557E+00 0.2062E-01 0.1424E+00 0.6001E+00 0.8658E+00 0.3212E-04 0.7633E-08 0.2376E-03
  0.6250E+02 0.5117E-03 0.1375E+00 0.2062E-01 0.1424E+00 0.5998E+00 0.8604E+00 0.2964E-04 0.6177E-08 0.2083E-03
  0.6500E+02 0.4736E-03 0.1220E+00 0.2062E-01 0.1423E+00 0.5996E+00 0.8552E+00 0.2745E-04 0.5043E-08 0.1836E-03
  0.6750E+02 0.4380E-03 0.1088E+00 0.2062E-01 0.1423E+00 0.5993E+00 0.8500E+00 0.2551E-04 0.4148E-08 0.1626E-03
  0.7000E+02 0.4078E-03 0.9741E-01 0.2062E-01 0.1423E+00 0.5990E+00 0.8449E+00 0.2377E-04 0.3438E-08 0.1446E-03
  0.7250E+02 0.3799E-03 0.8756E-01 0.2062E-01 0.1422E+00 0.5987E+00 0.8399E+00 0.2221E-04 0.2868E-08 0.1291E-03
  0.7500E+02 0.3548E-03 0.7901E-01 0.2062E-01 0.1422E+00 0.5984E+00 0.8350E+00 0.2081E-04 0.2408E-08 0.1157E-03
  0.7750E+02 0.3321E-03 0.7153E-01 0.2062E-01 0.1422E+00 0.5981E+00 0.8301E+00 0.1954E-04 0.2035E-08 0.1041E-03
  0.8000E+02 0.3116E-03 0.6497E-01 0.2062E-01 0.1422E+00 0.5977E+00 0.8253E+00 0.1838E-04 0.1728E-08 0.9393E-04
  0.8250E+02 0.2928E-03 0.5919E-01 0.2062E-01 0.1421E+00 0.5974E+00 0.8206E+00 0.1730E-04 0.1479E-08 0.8503E-04
  0.8500E+02 0.2758E-03 0.5408E-01 0.2062E-01 0.1421E+00 0.5970E+00 0.8160E+00 0.1638E-04 0.1264E-08 0.7719E-04
  0.8750E+02 0.2601E-03 0.4954E-01 0.2062E-01 0.1421E+00 0.5966E+00 0.8114E+00 0.1551E-04 0.1090E-08 0.7026E-04
```

APPENDIX E

ADDITIONAL SENSITIVITY RESULTS

Parameter	identification	Figure
ρ	density.	E-1
K_{sp}	stifness of spring used for zero adjustment.	E-2
K_{se}	'spring constant' for sensing element.	E-3
L_2	length of element number 2	E-4
A_2	cross sectional area of element number 2	E-5
A_3	cross sectional area of element number 3	E-6
ν_3	a parameter defined in Equation 3-14 (see page 45) .	E-7
L_4	length of element number 4	E-8
A_4	cross sectional area of element number 4	E-9
L_5	length of element number 5	E-10
A_5	cross sectional area of element number 5	E-11
K	geometric factor for Timoshenko's formulation. . . .	E-12
μ	Poisson's ratio.	E-13
L_6	length of element number 6	E-14
A_6	cross sectional area of element number 6	E-15
A_7	cross sectional area of force bar.	E-16
K_a	stifness for transferring element (vector mechanism)	E-17
K_b	stifness for supporting element (vector mechanism)	E-18
C_1	parameter defined in Equation 3-87 (see page 70) . .	E-19
C_2	parameter defined in Equation 3-88 (see page 71) . .	E-20
C_4	parameter defined in Equation 3-90 (see page 72) . .	E-21
C_5	parameter defined in Equation 3-91 (see page 72) . .	E-22
$\theta_g(0)$	angle shown in Figure 3-10 (see page 58)	E-23
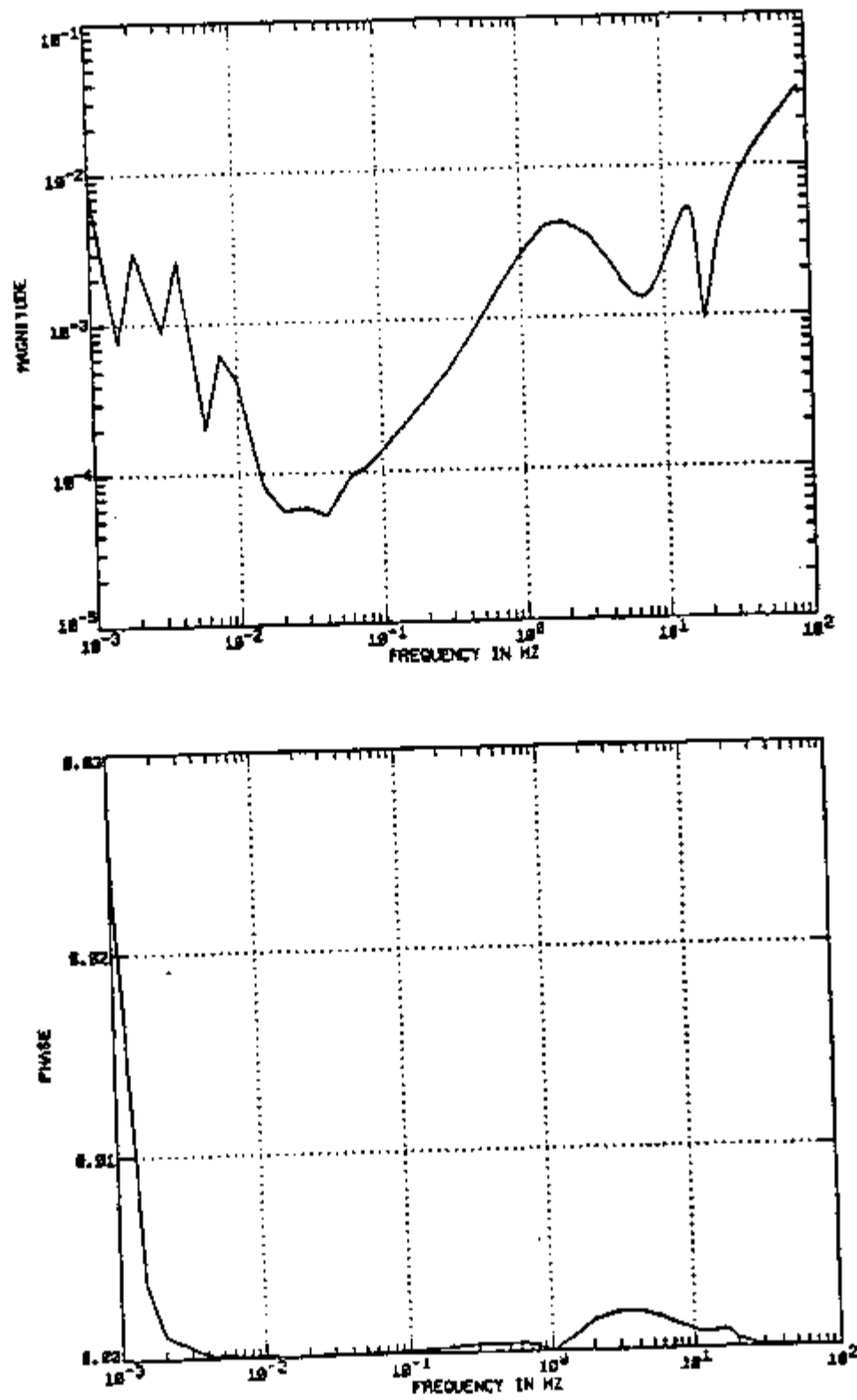
Figure E-1. Sensitivity with respect to parameter ρ
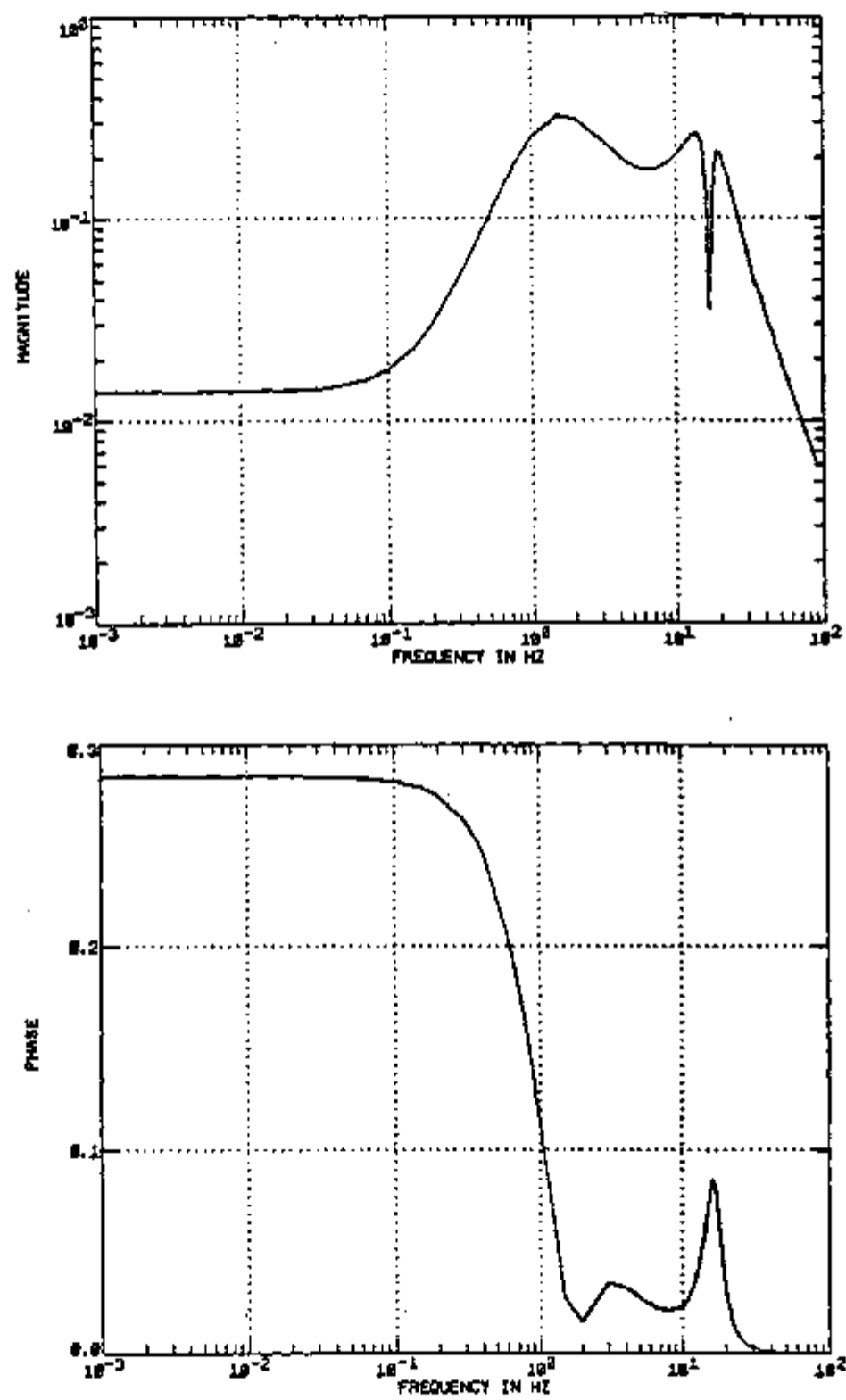
Figure E-2. Sensitivity with respect to parameter K_{sp}
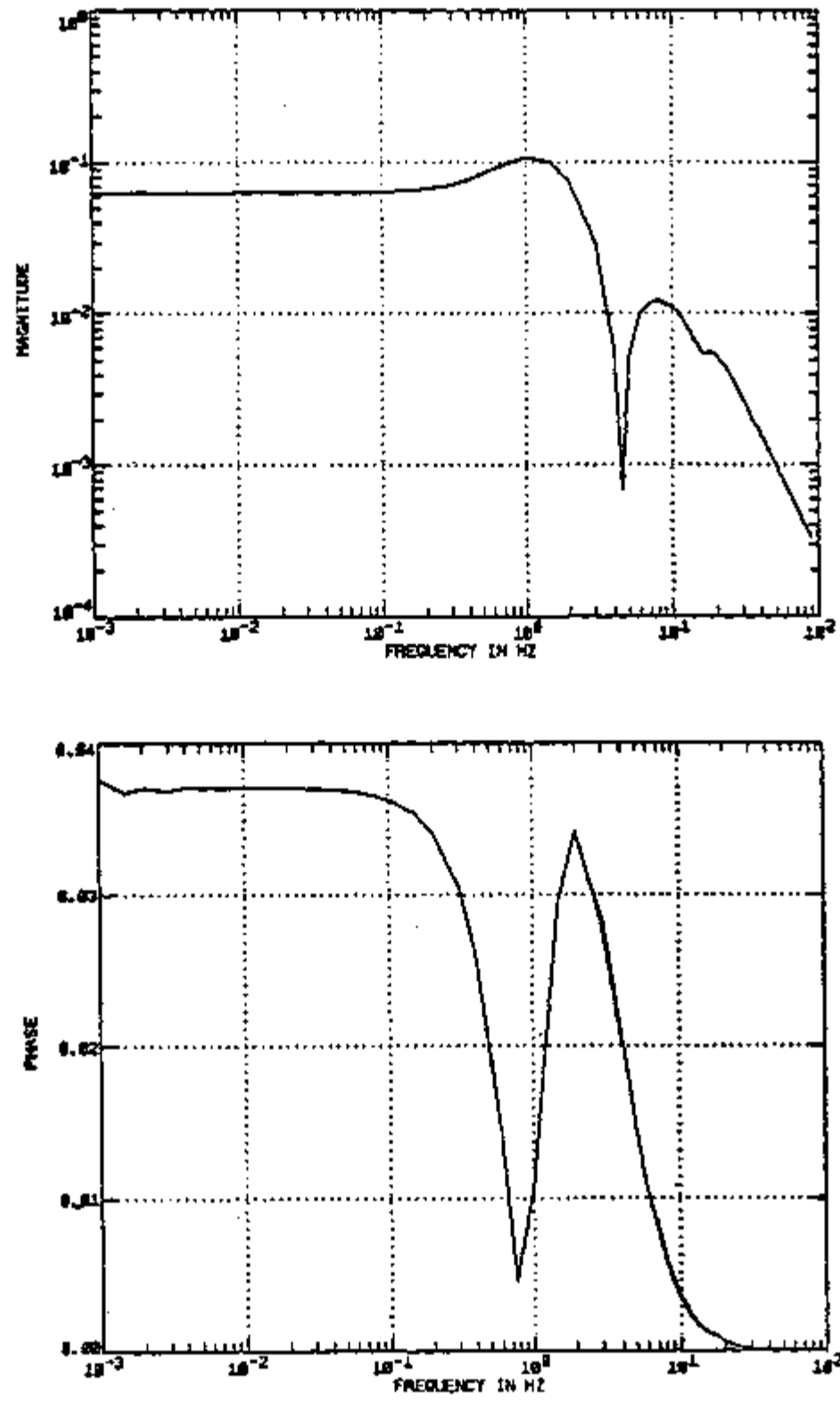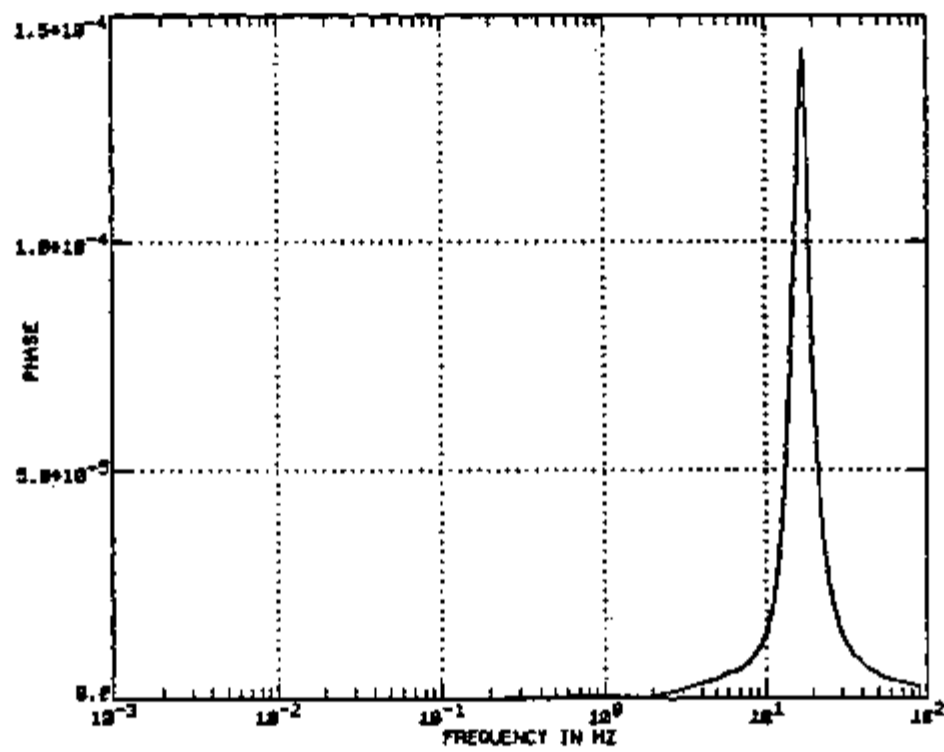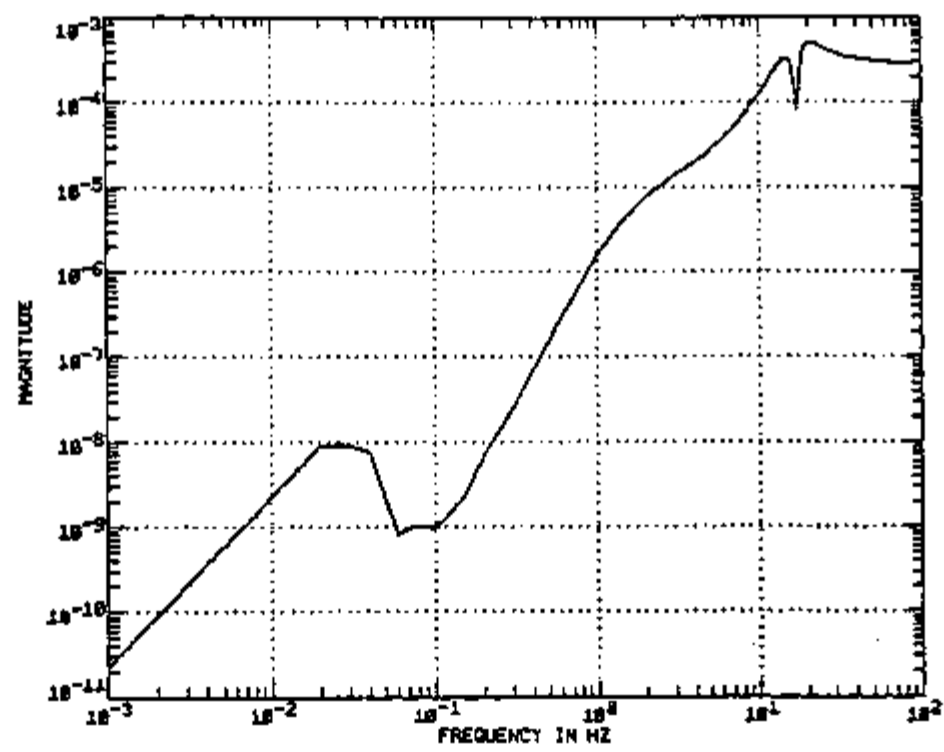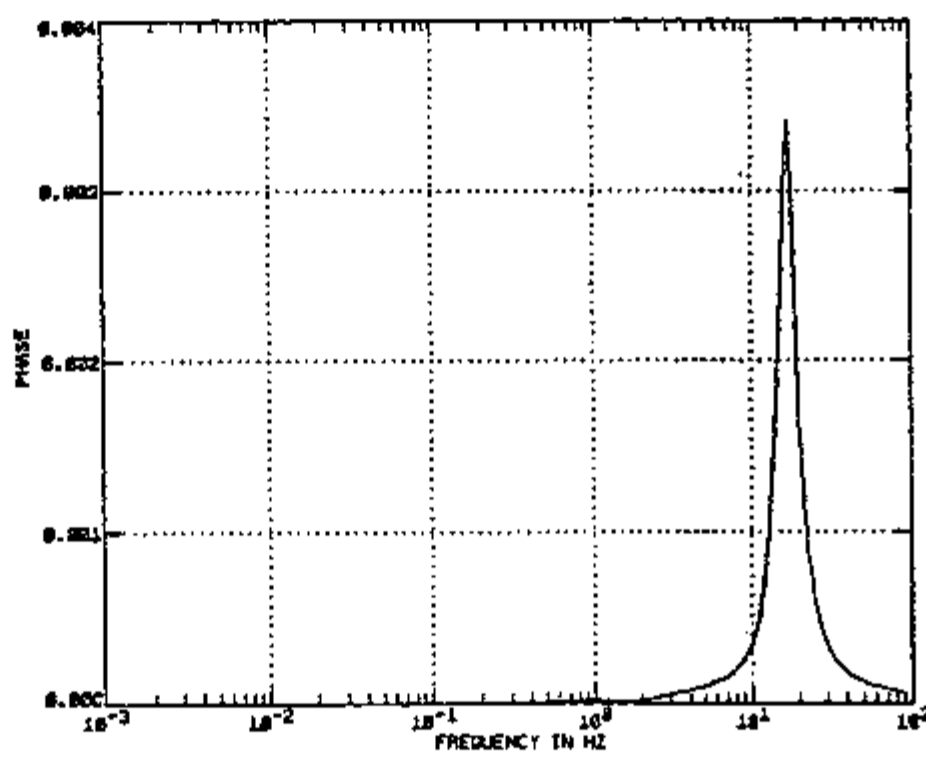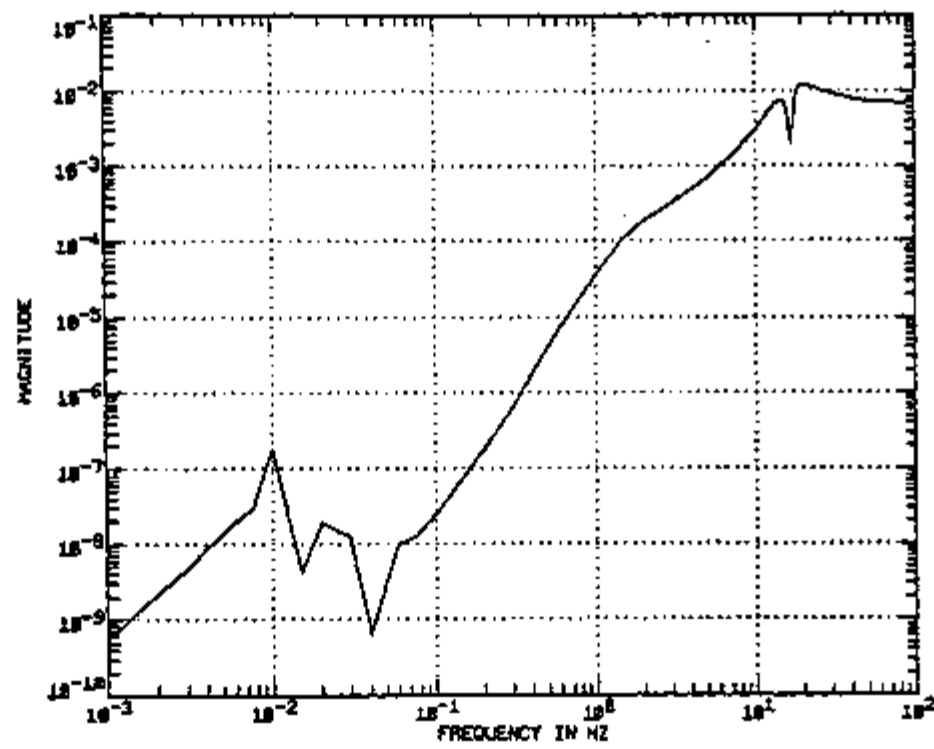
Figure E-3. Sensitivity with respect to parameter K_{se}
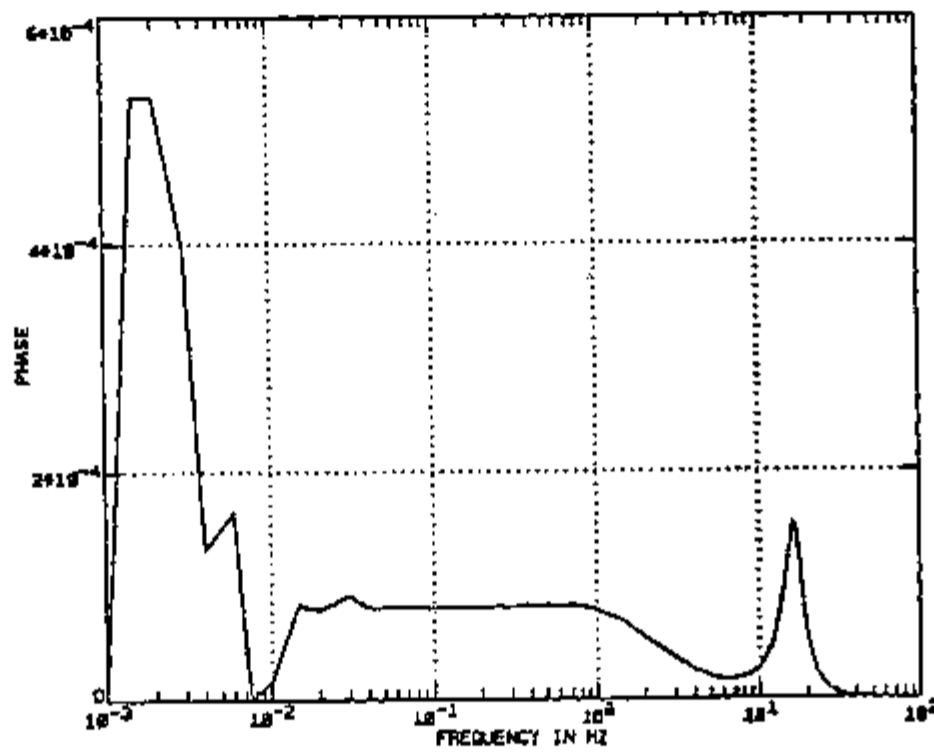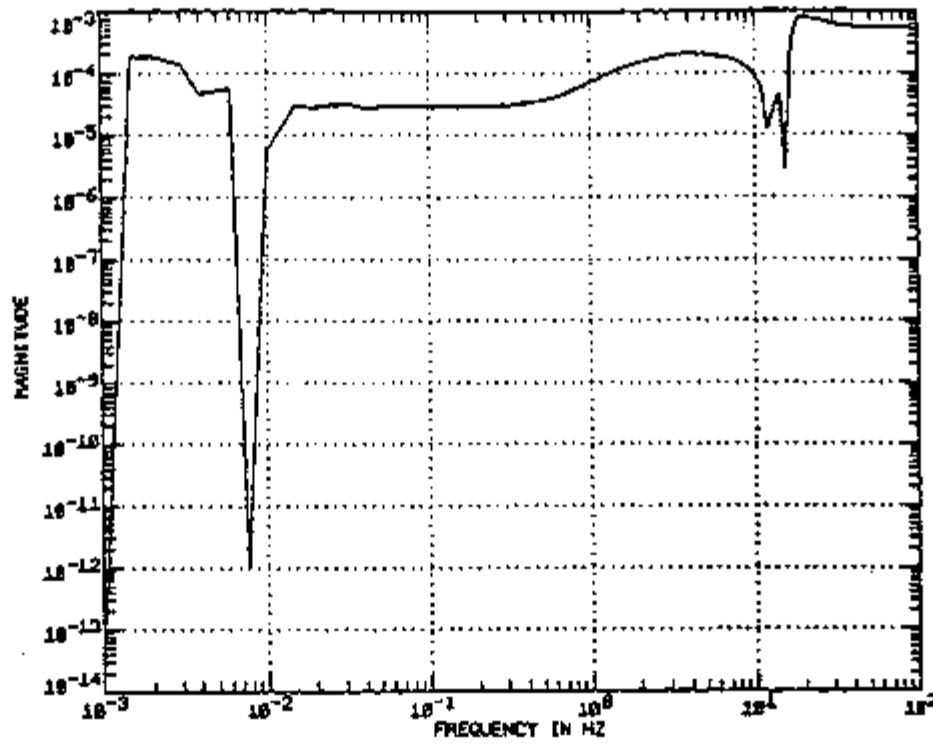
Figure E-4. Sensitivity with respect to parameter L_2
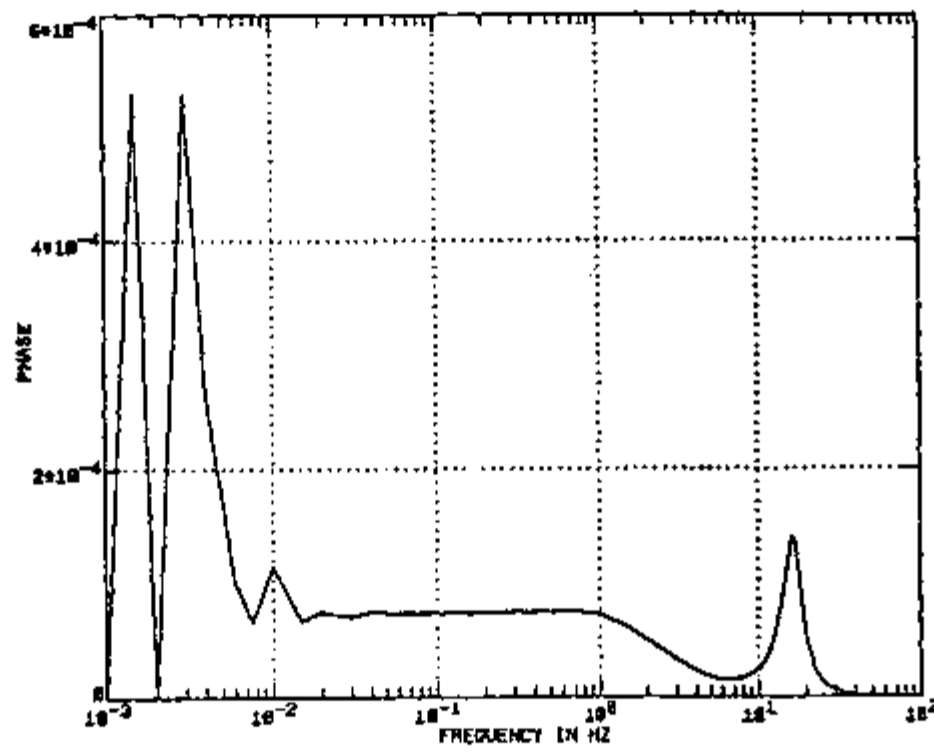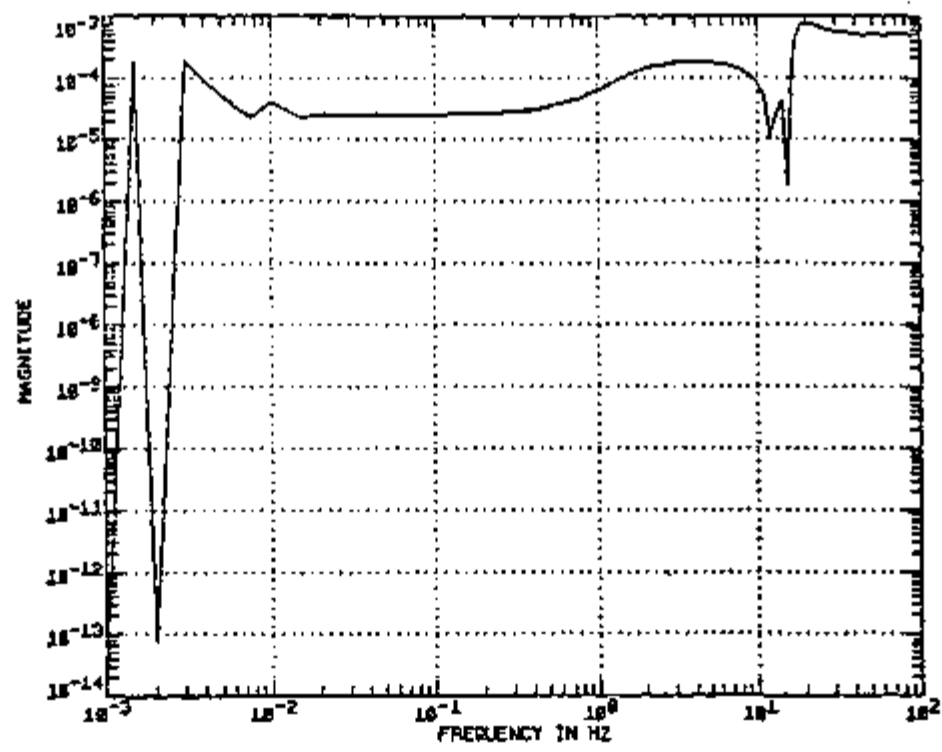
Figure E-5. Sensitivity with respect to parameter A_2
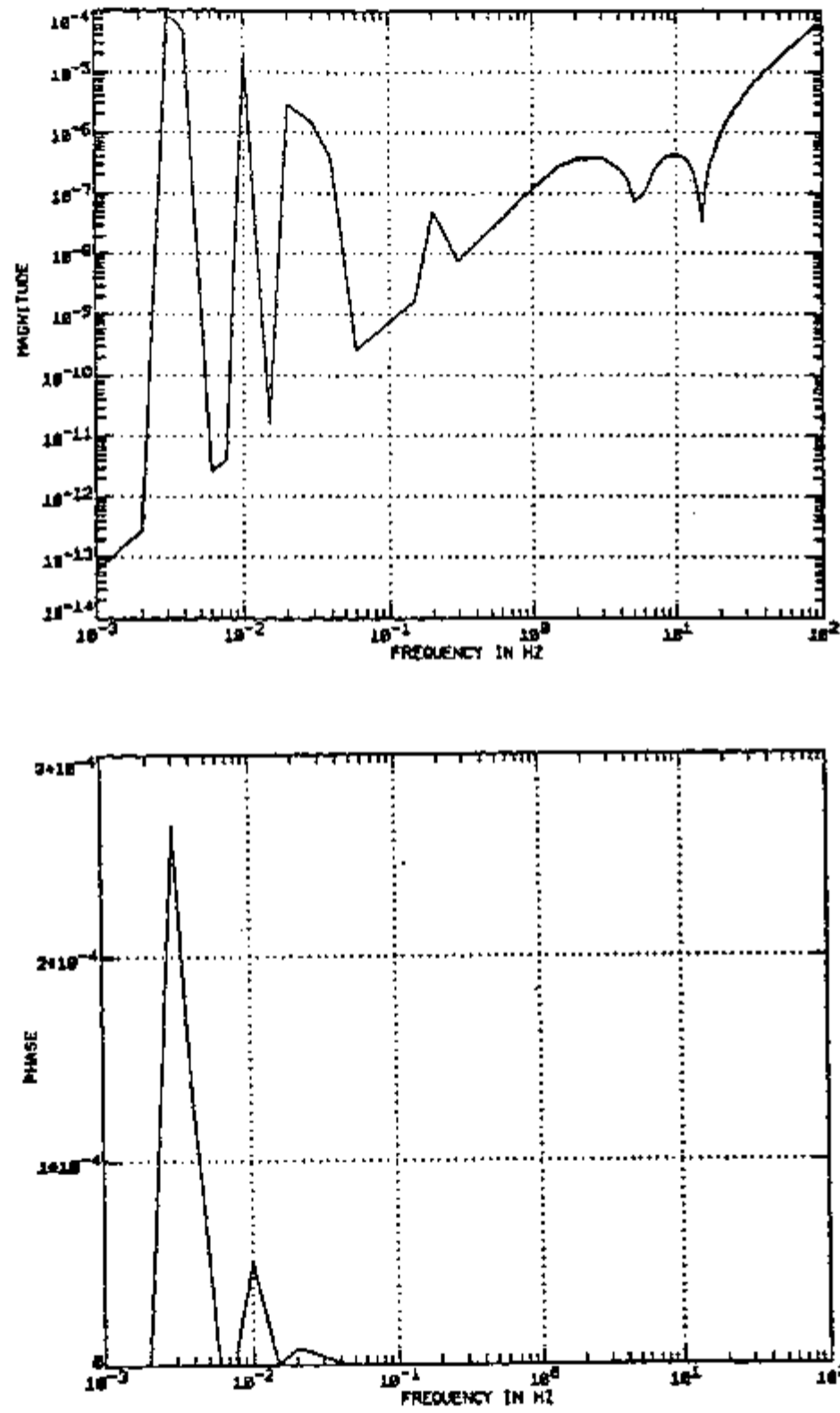
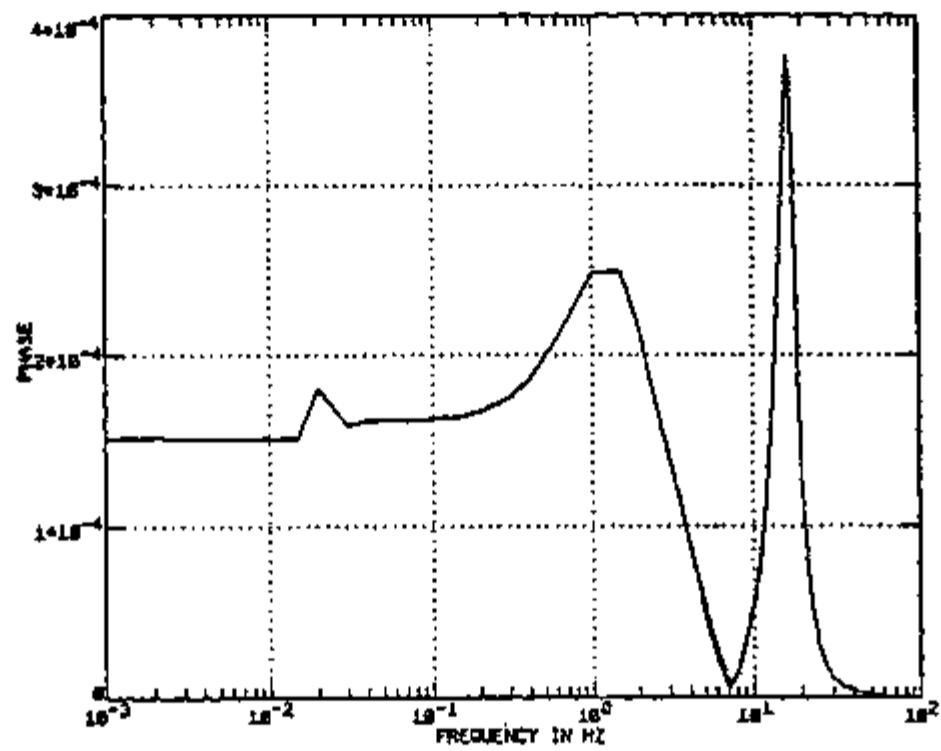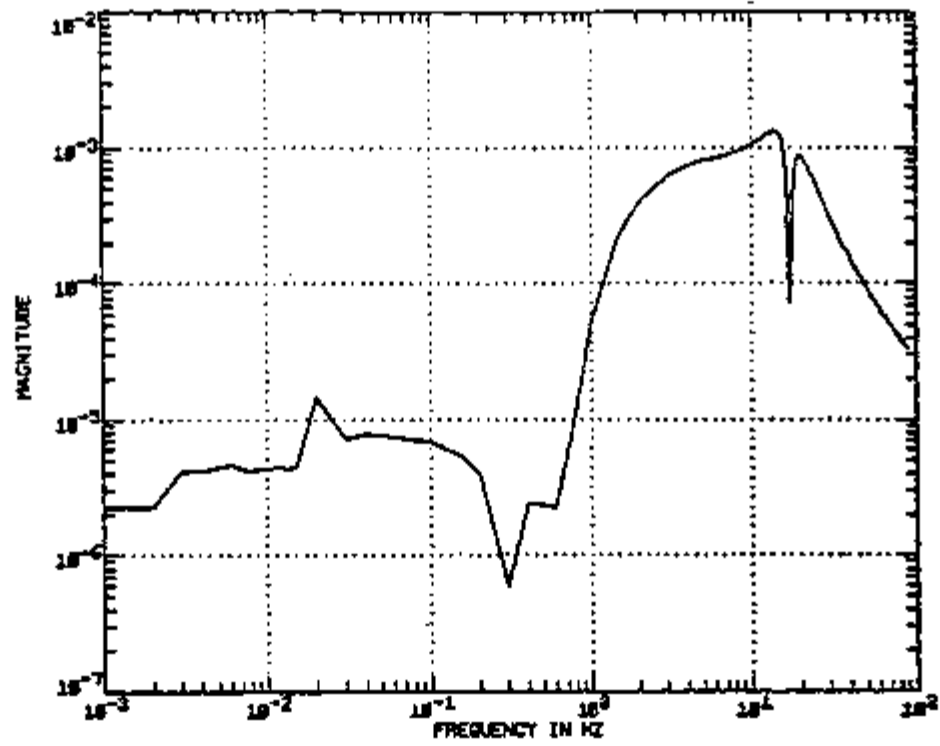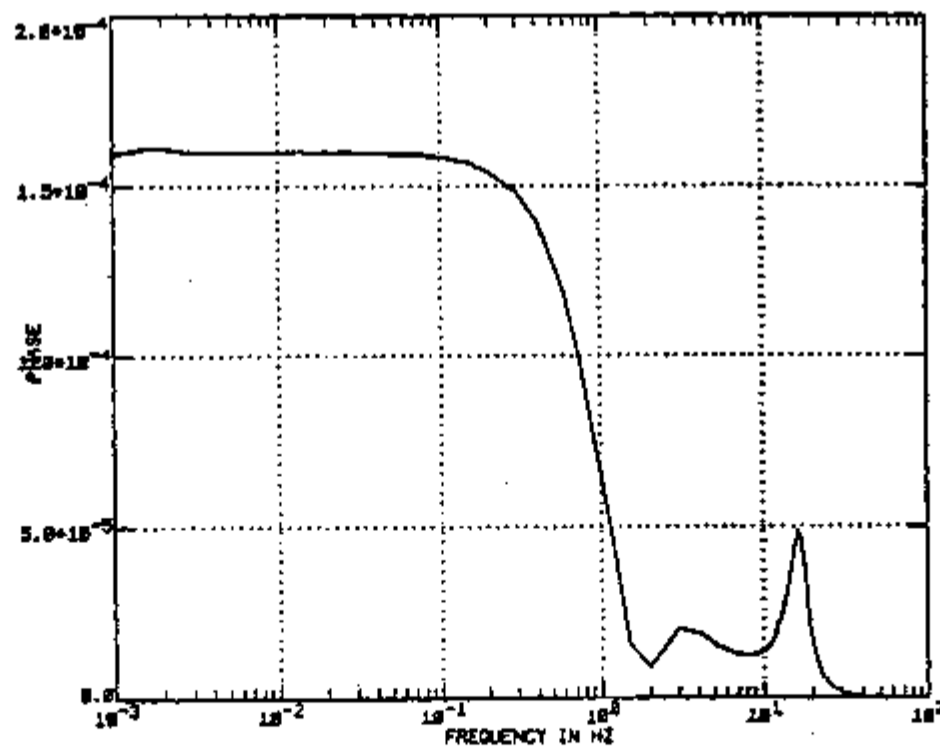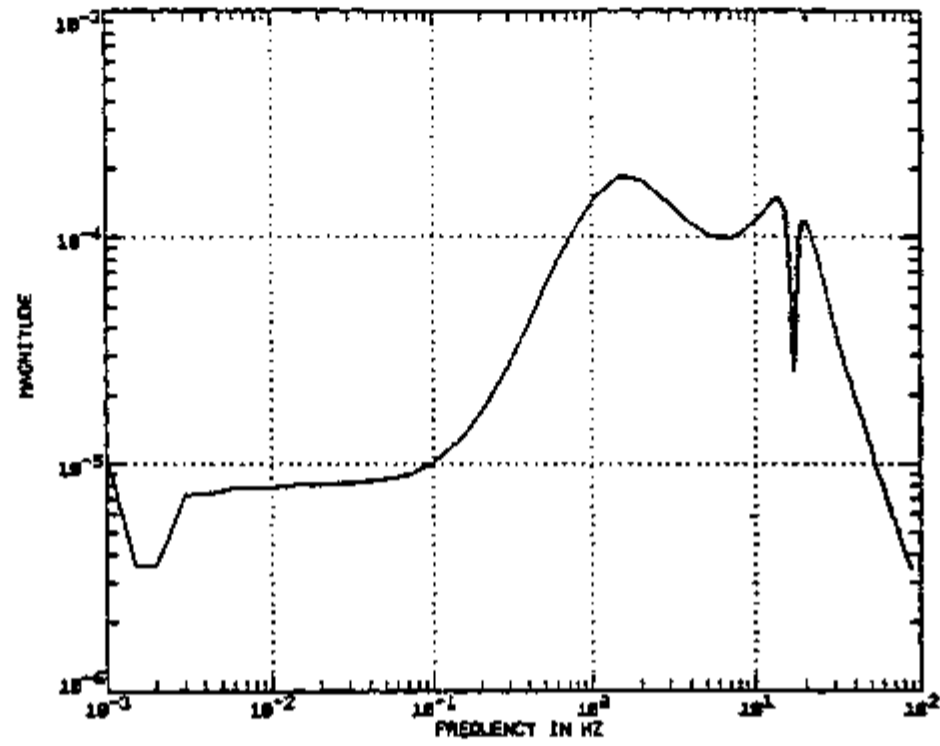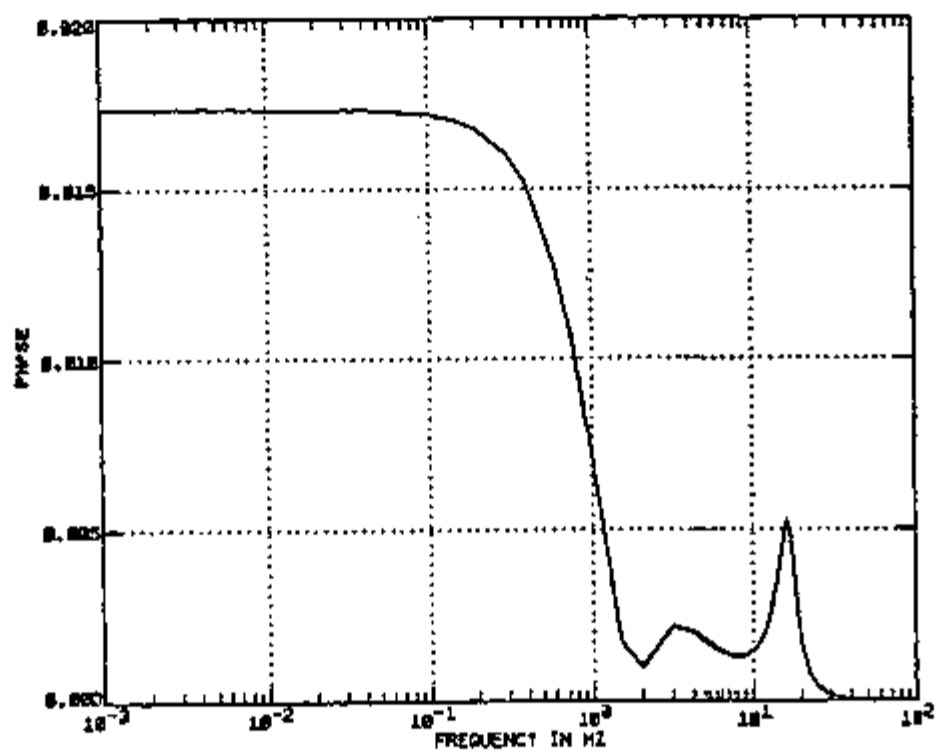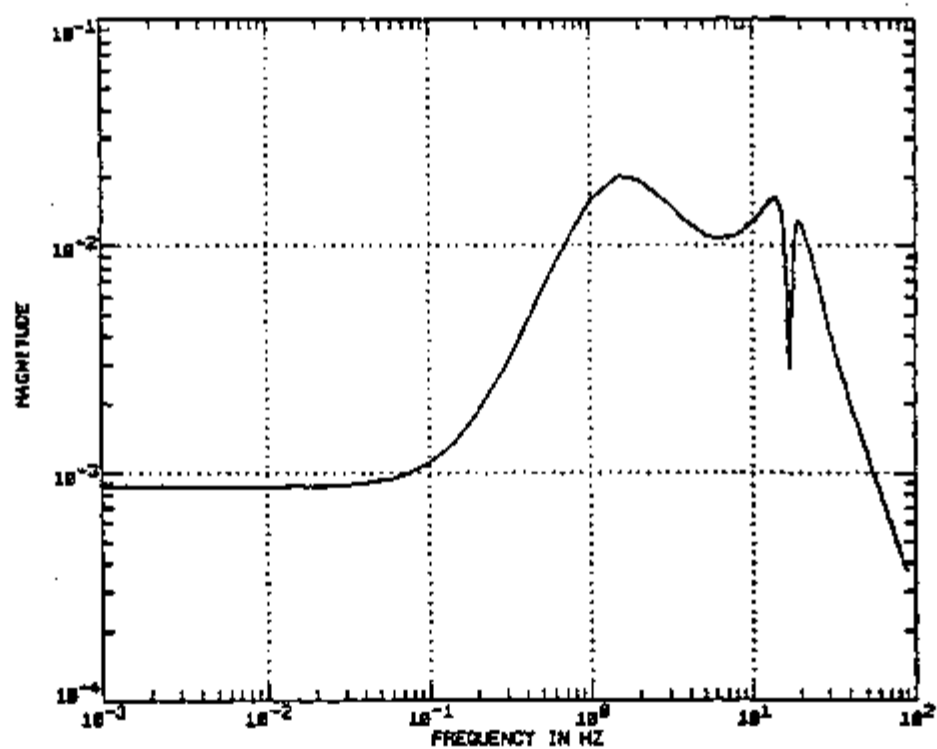Figure E-6. Sensitivity with respect to parameter A_3
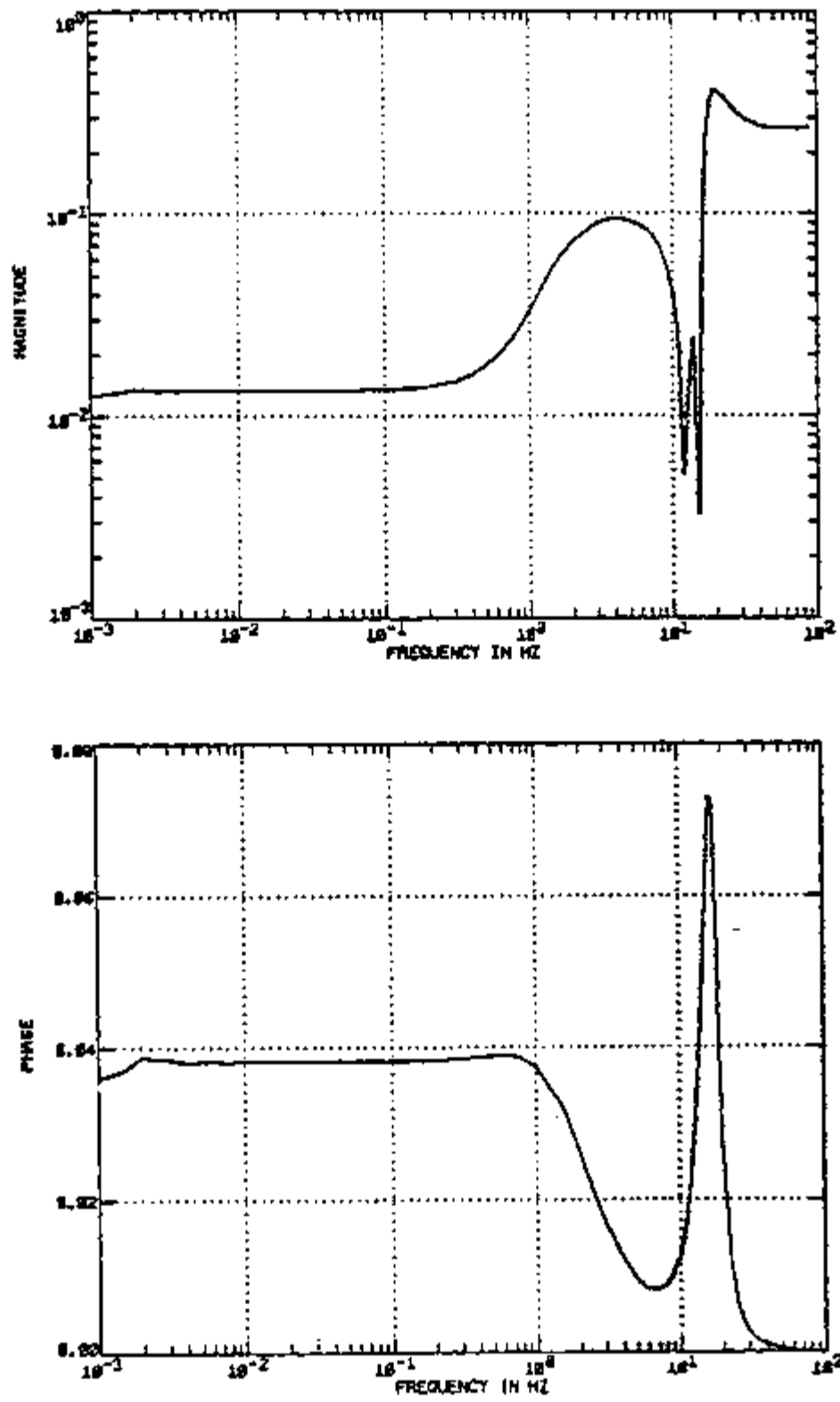
Figure E-7. Sensitivity with respect to parameter ν_3
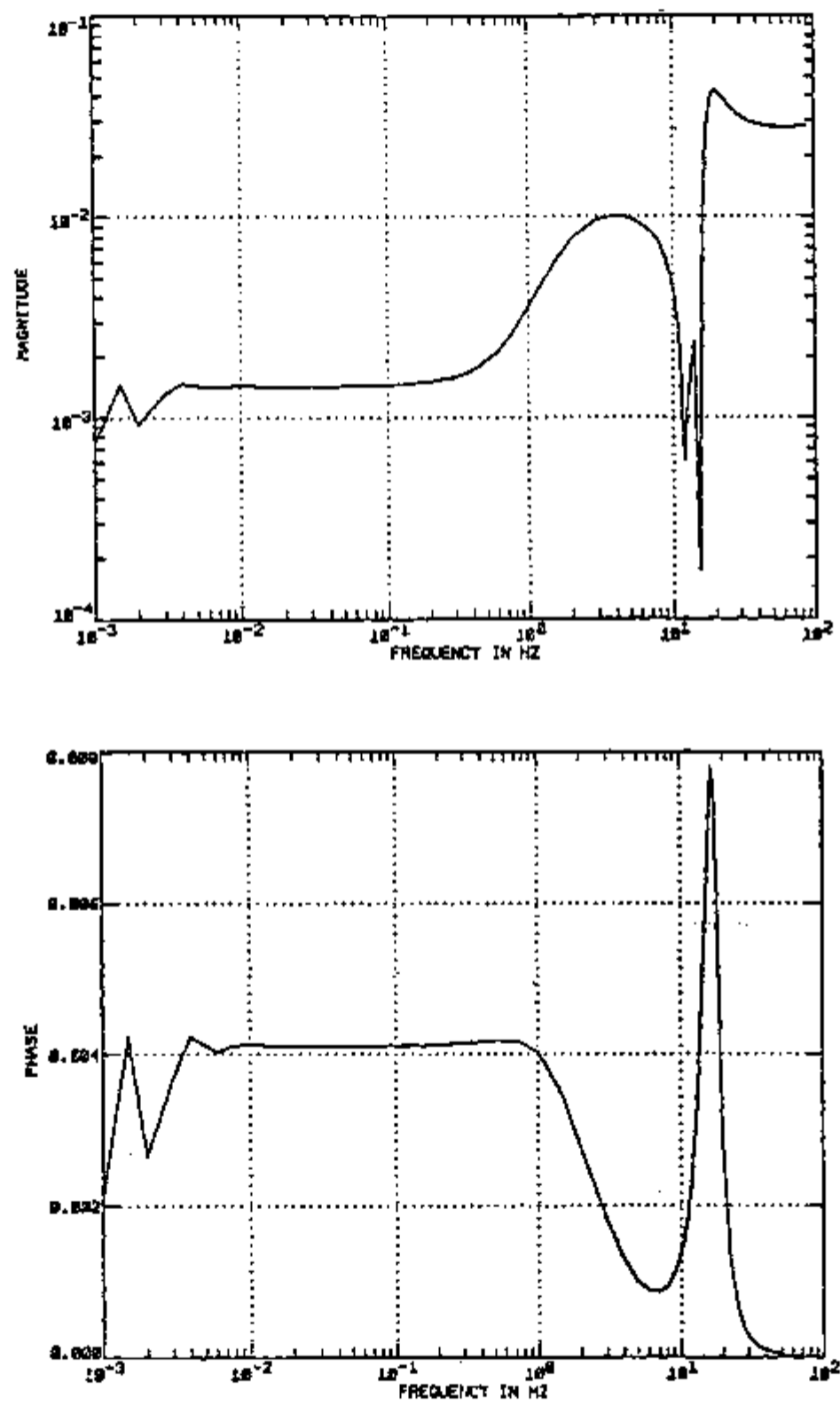
Figure E-8. Sensitivity with respect to parameter L_4
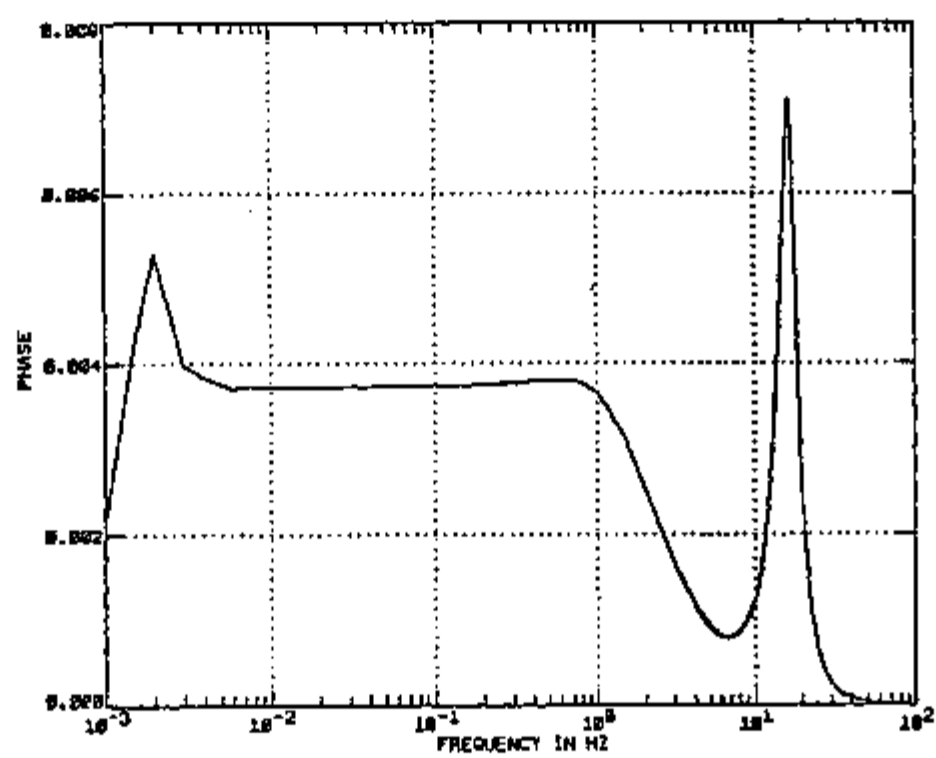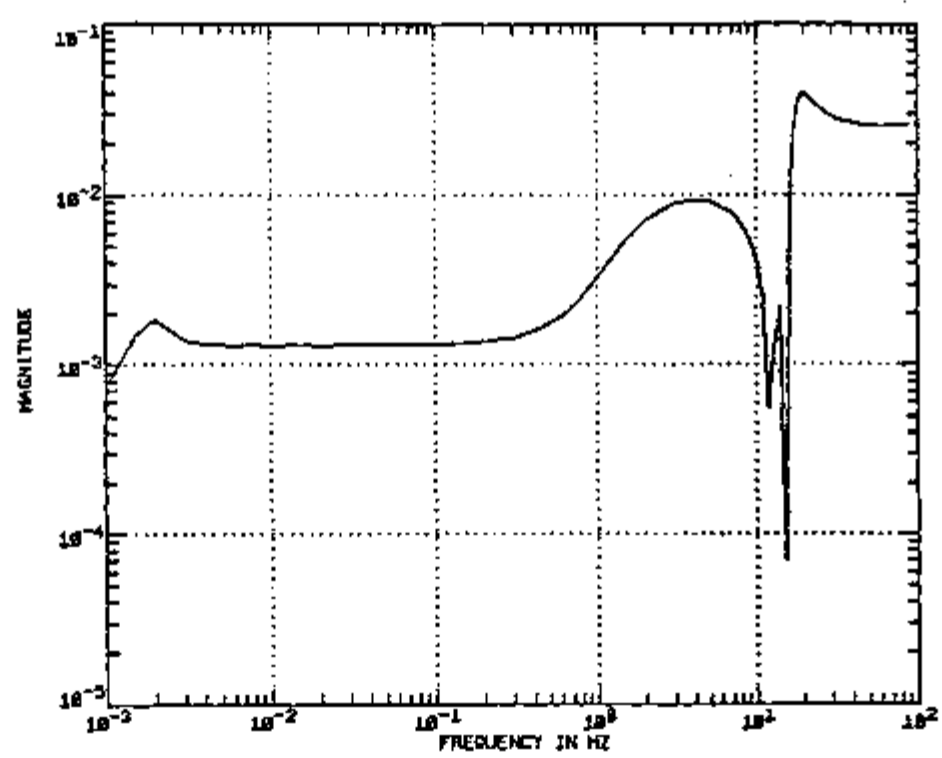
Figure E-9.   Sensitivity with respect to parameter A_4
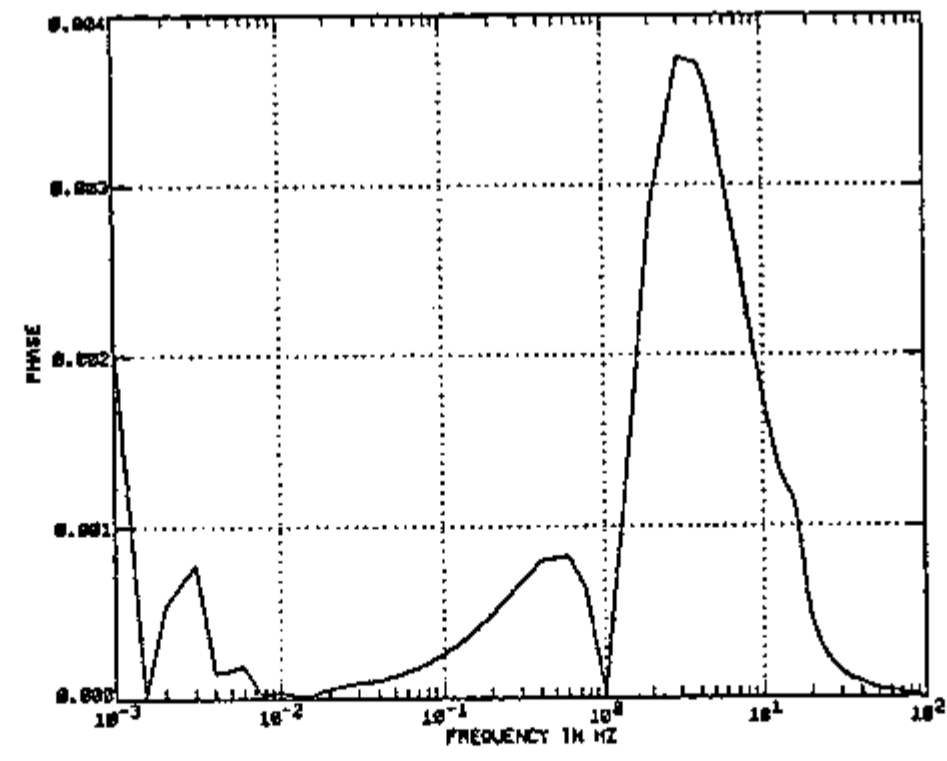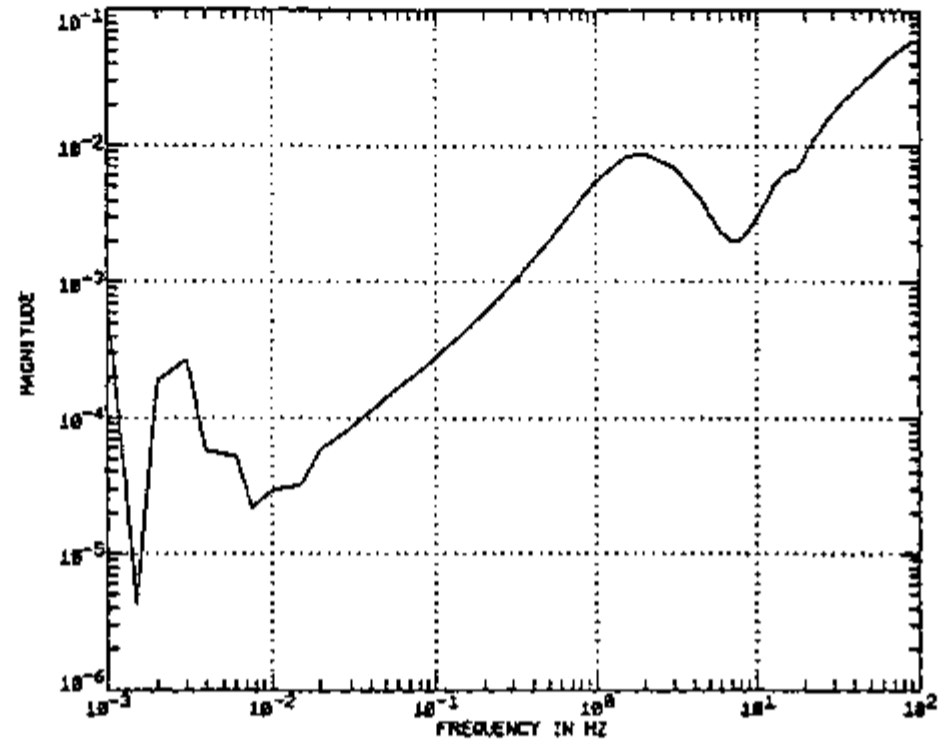
Figure E-10. Sensitivity with respect to parameter L_S
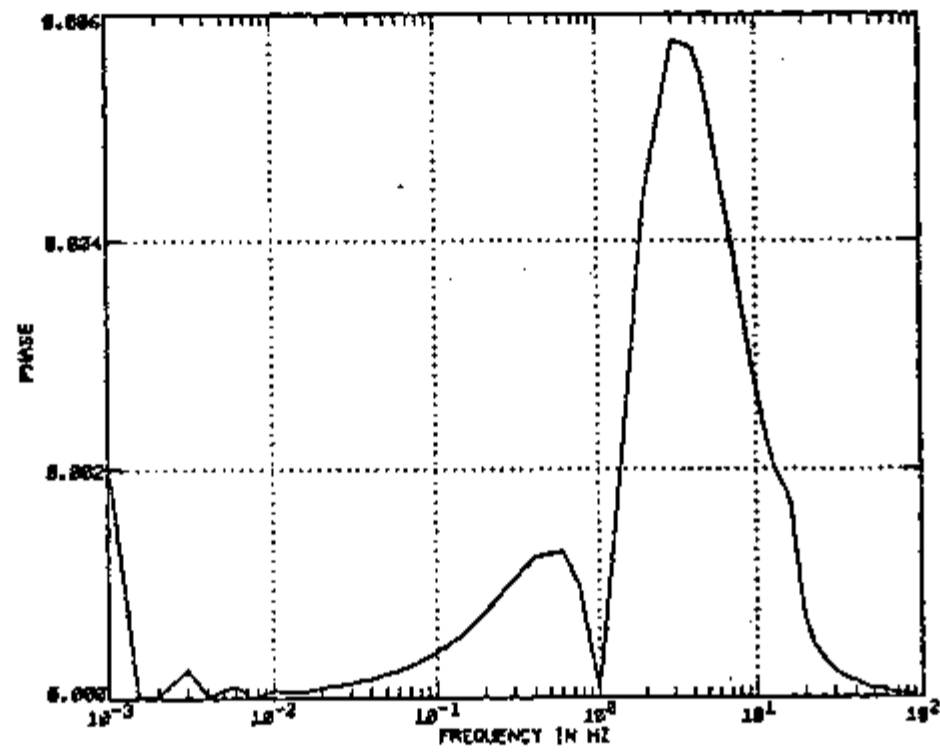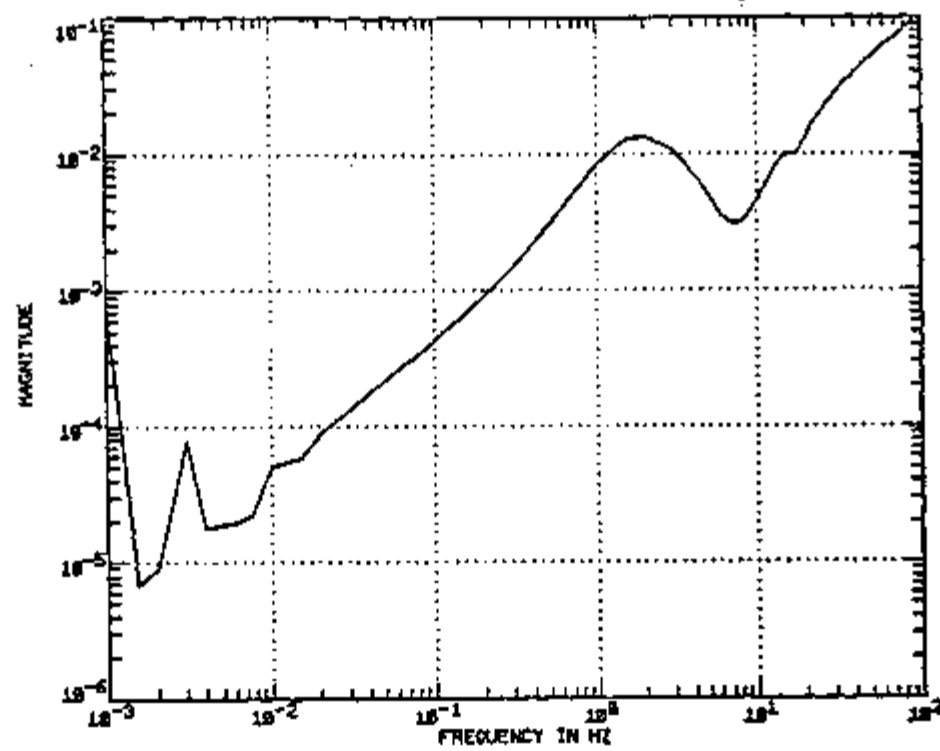
Figure E-11. Sensitivity with respect to parameter A_5
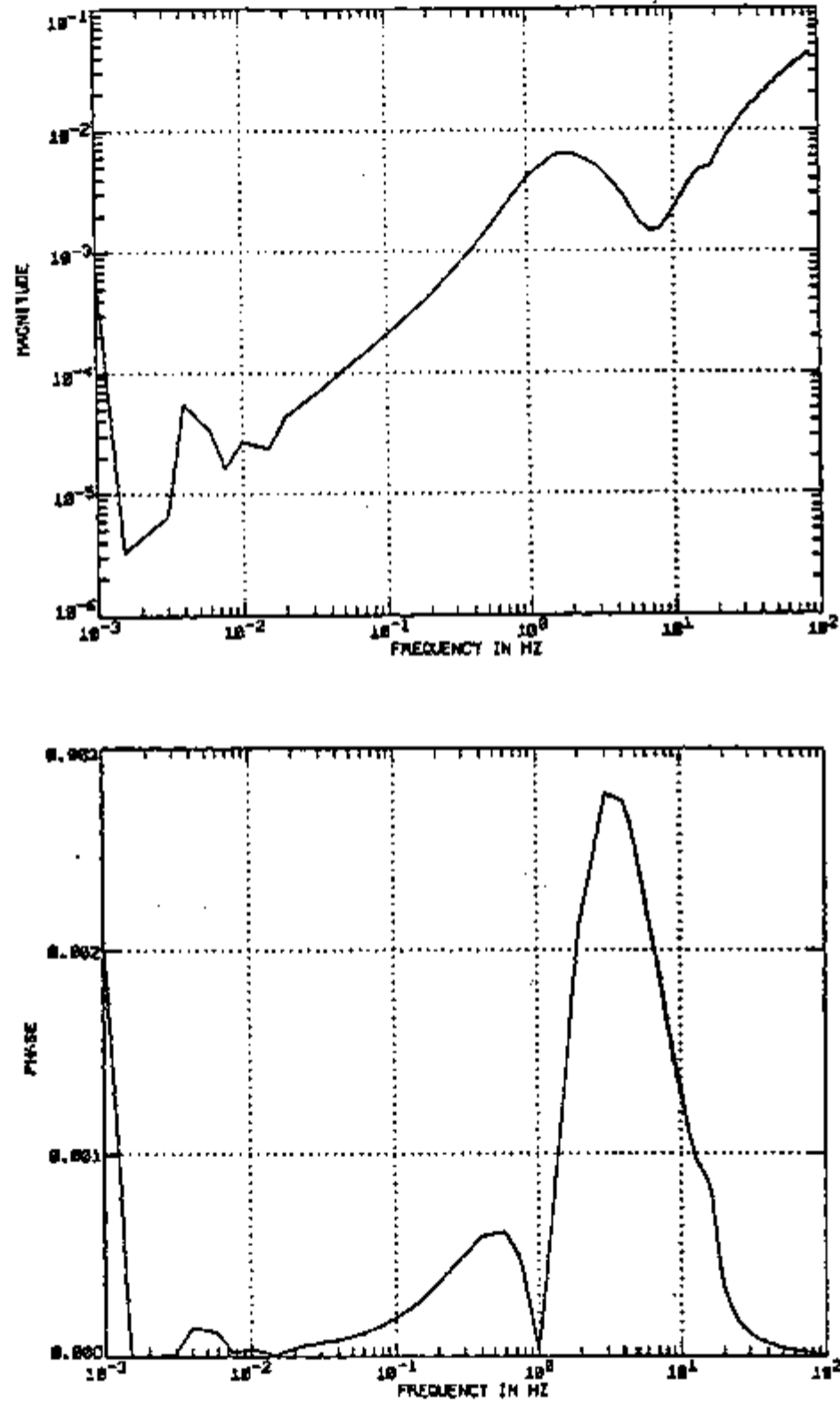
Figure E-12. Sensitivity with respect to parameter K
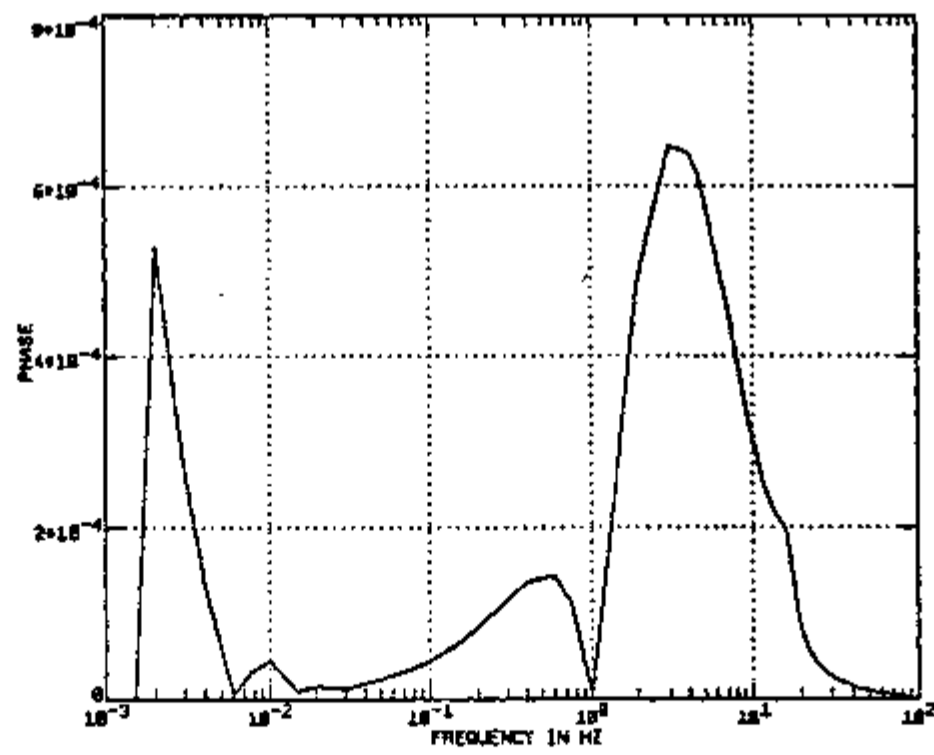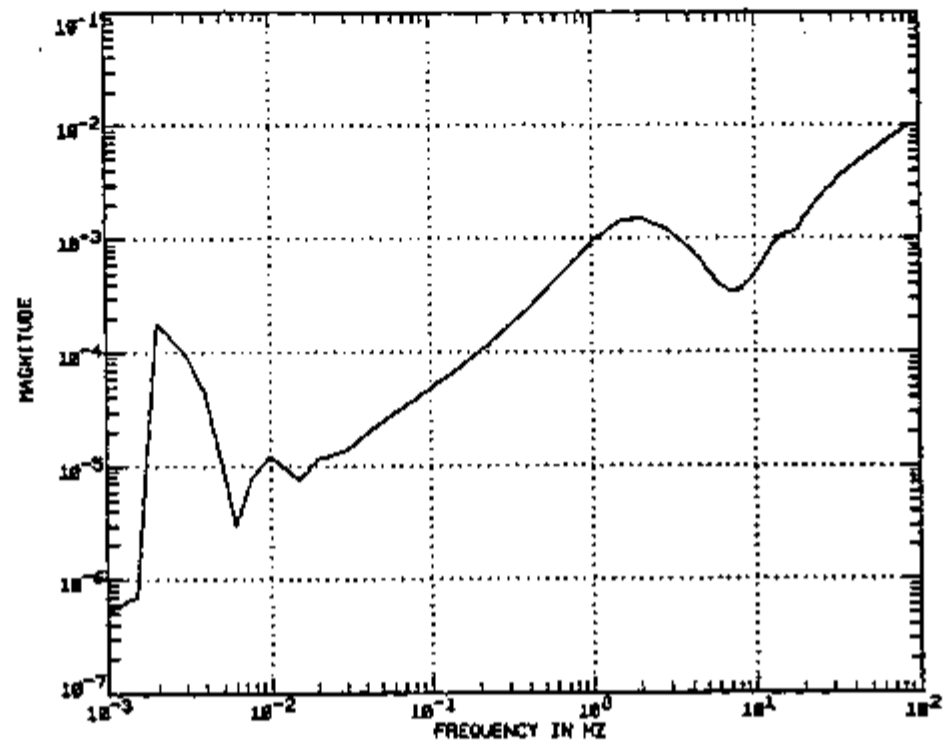
Figure E-13. Sensitivity with respect to parameter μ
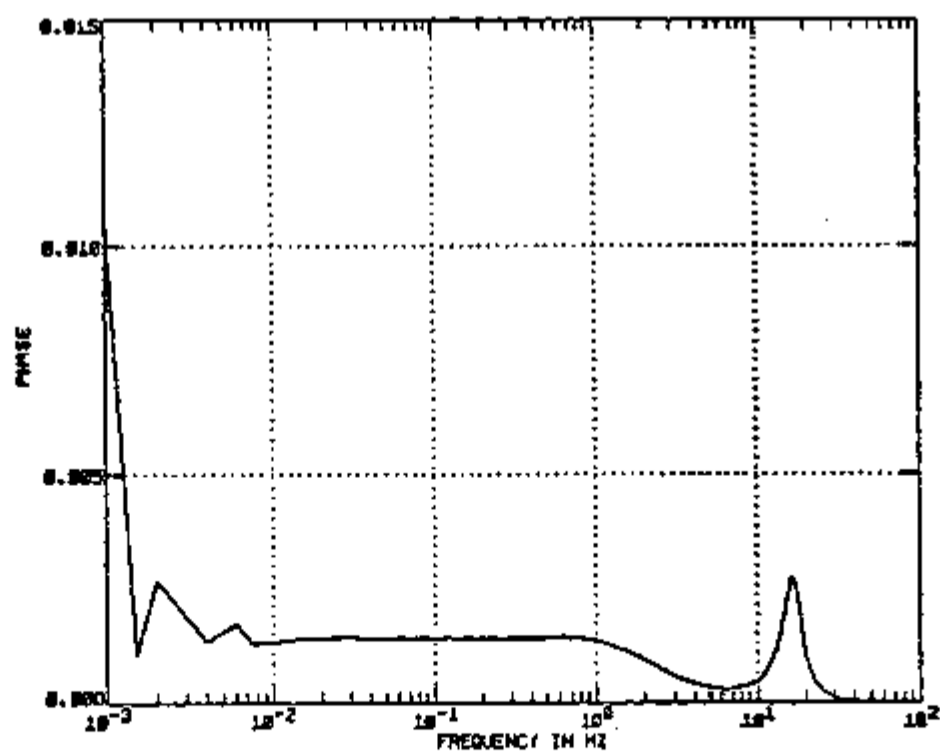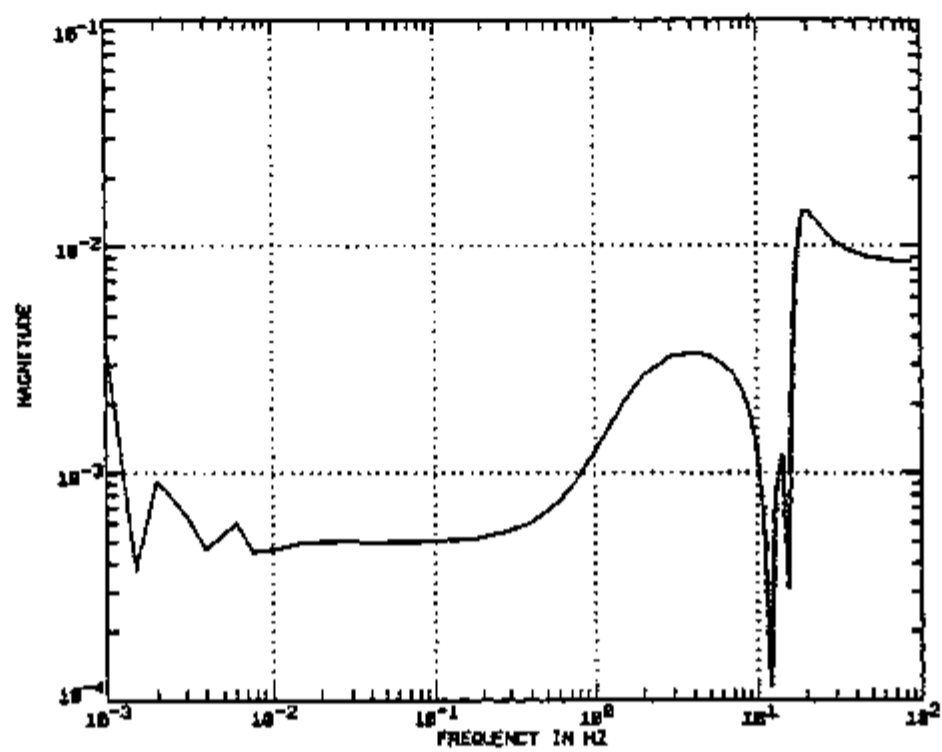
Figure E-14. Sensitivity with respect to parameter L_6
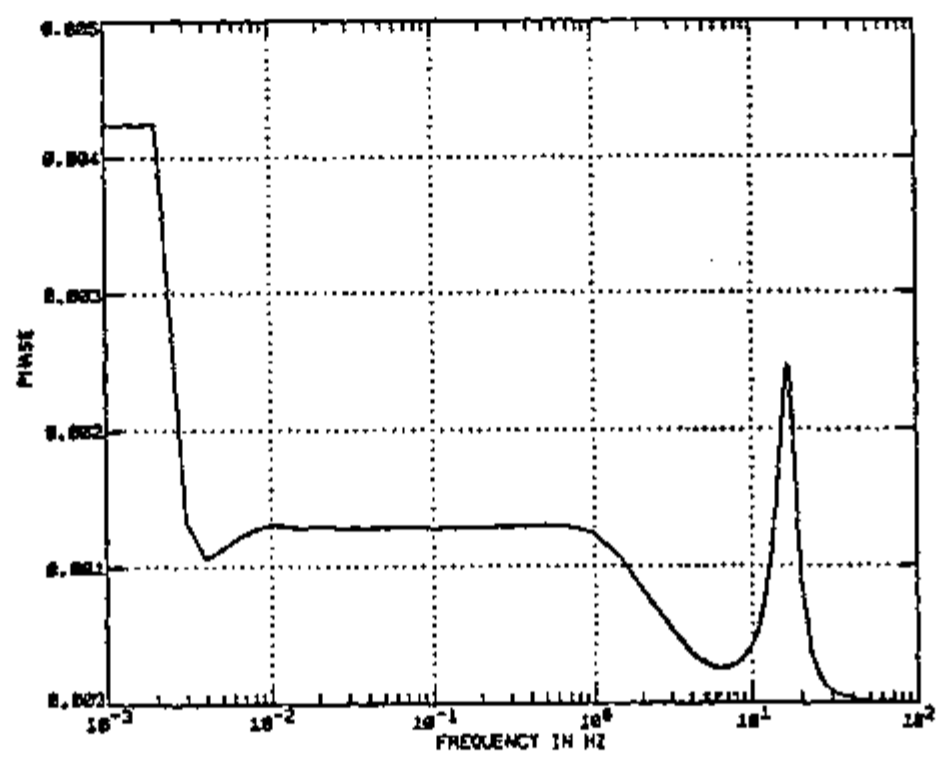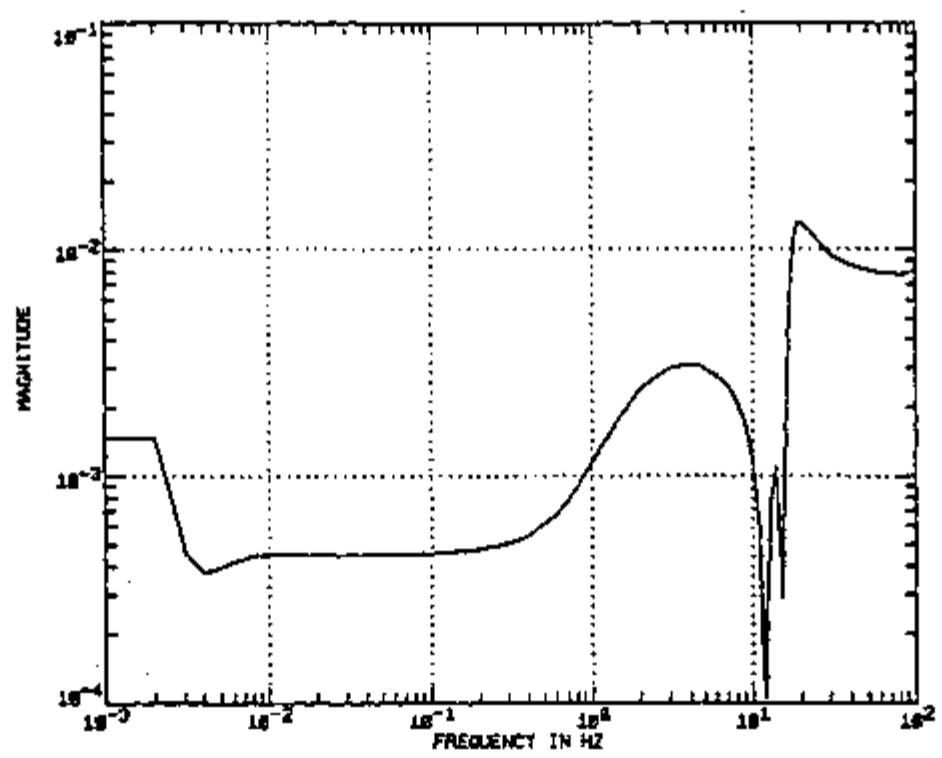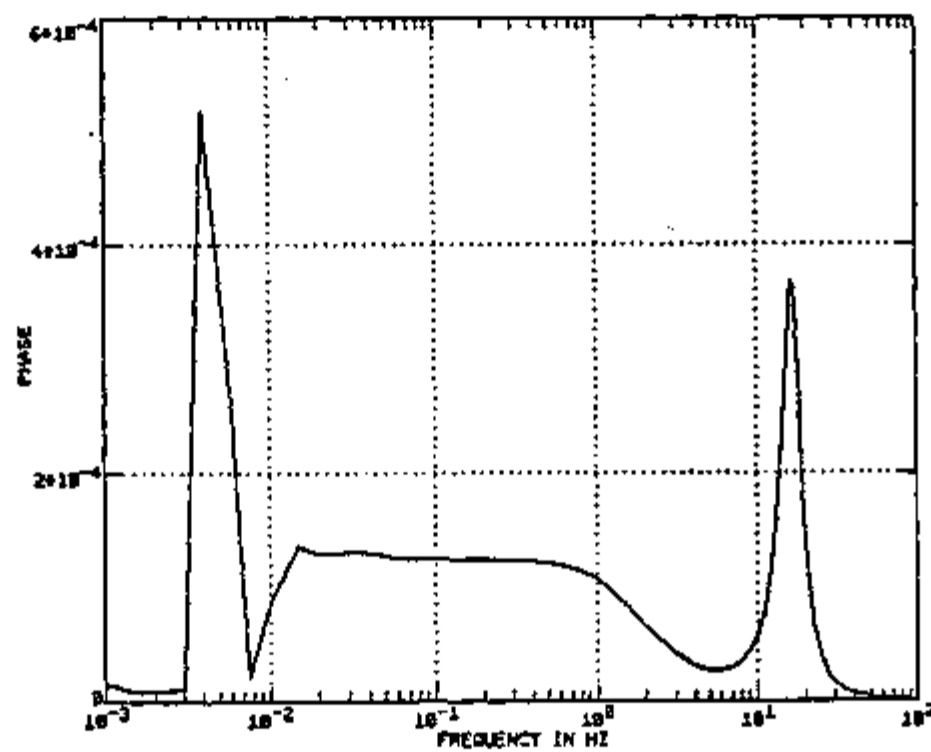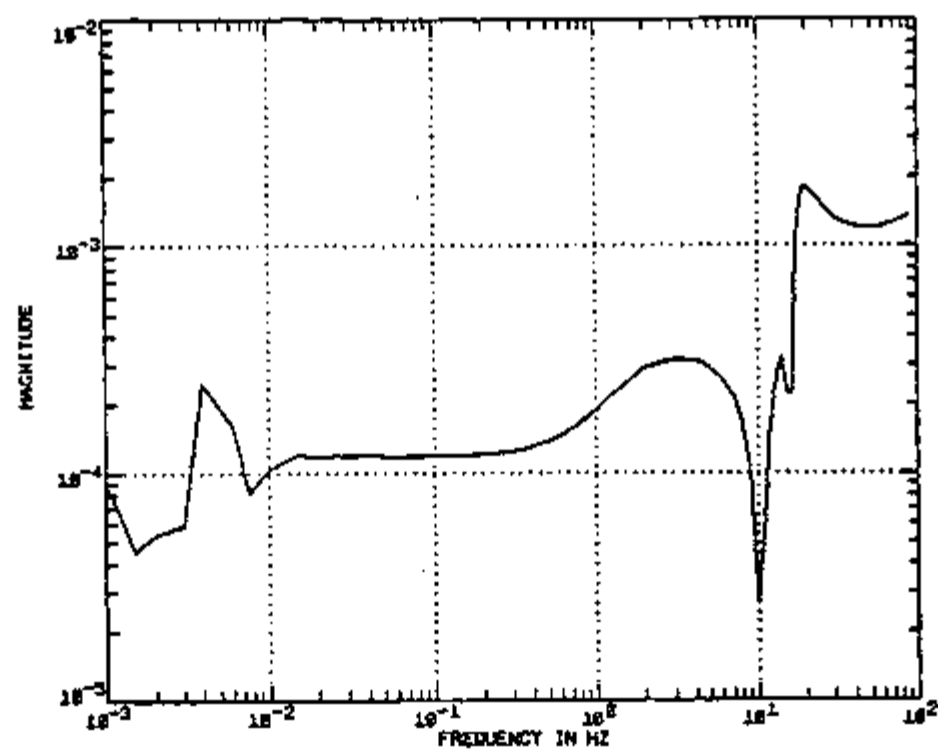
Figure E-15. Sensitivity with respect to parameter R_6
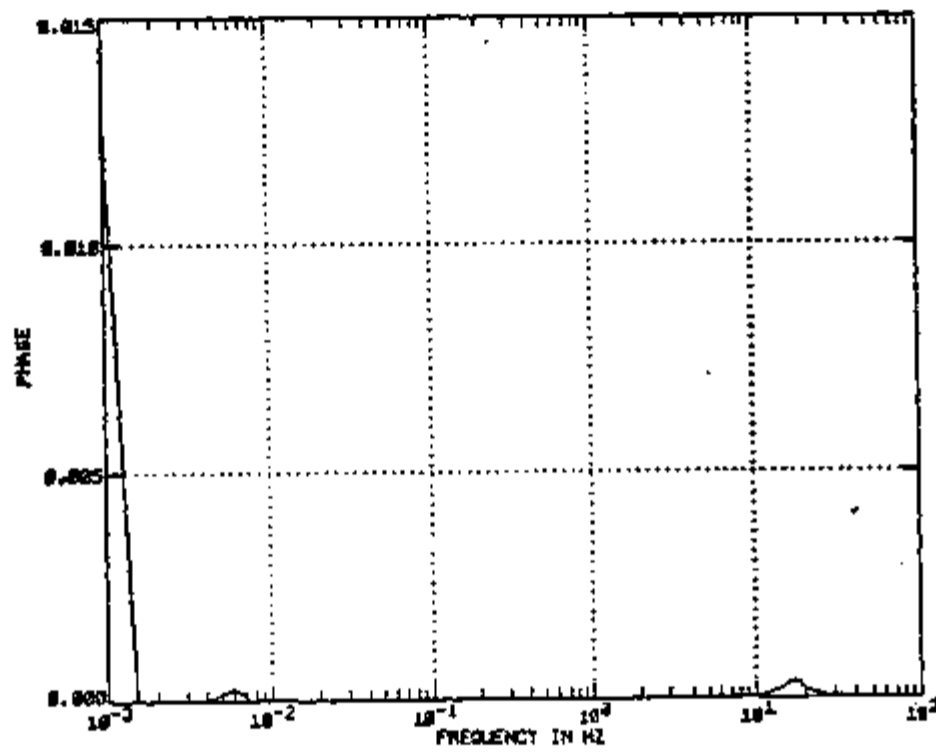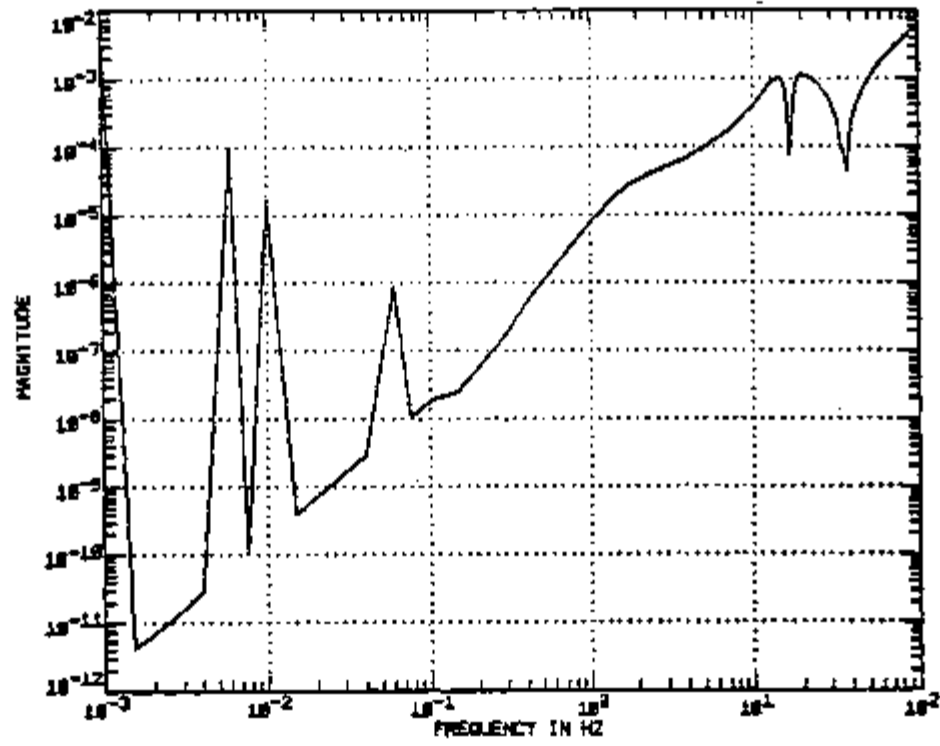
Figure E-16. Sensitivity with respect to parameter A_7
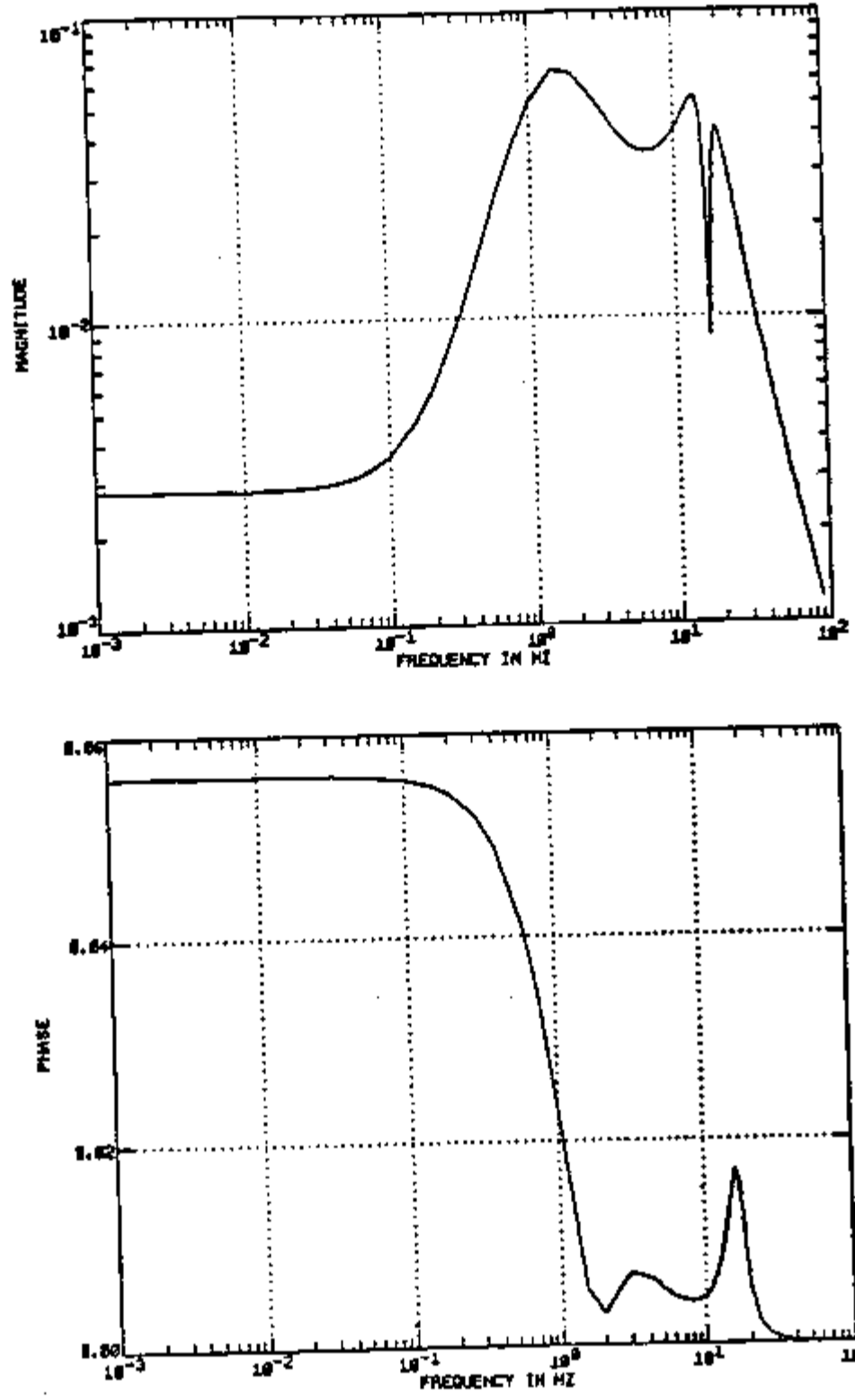
Figure E-17. Sensitivity with respect to parameter K_a
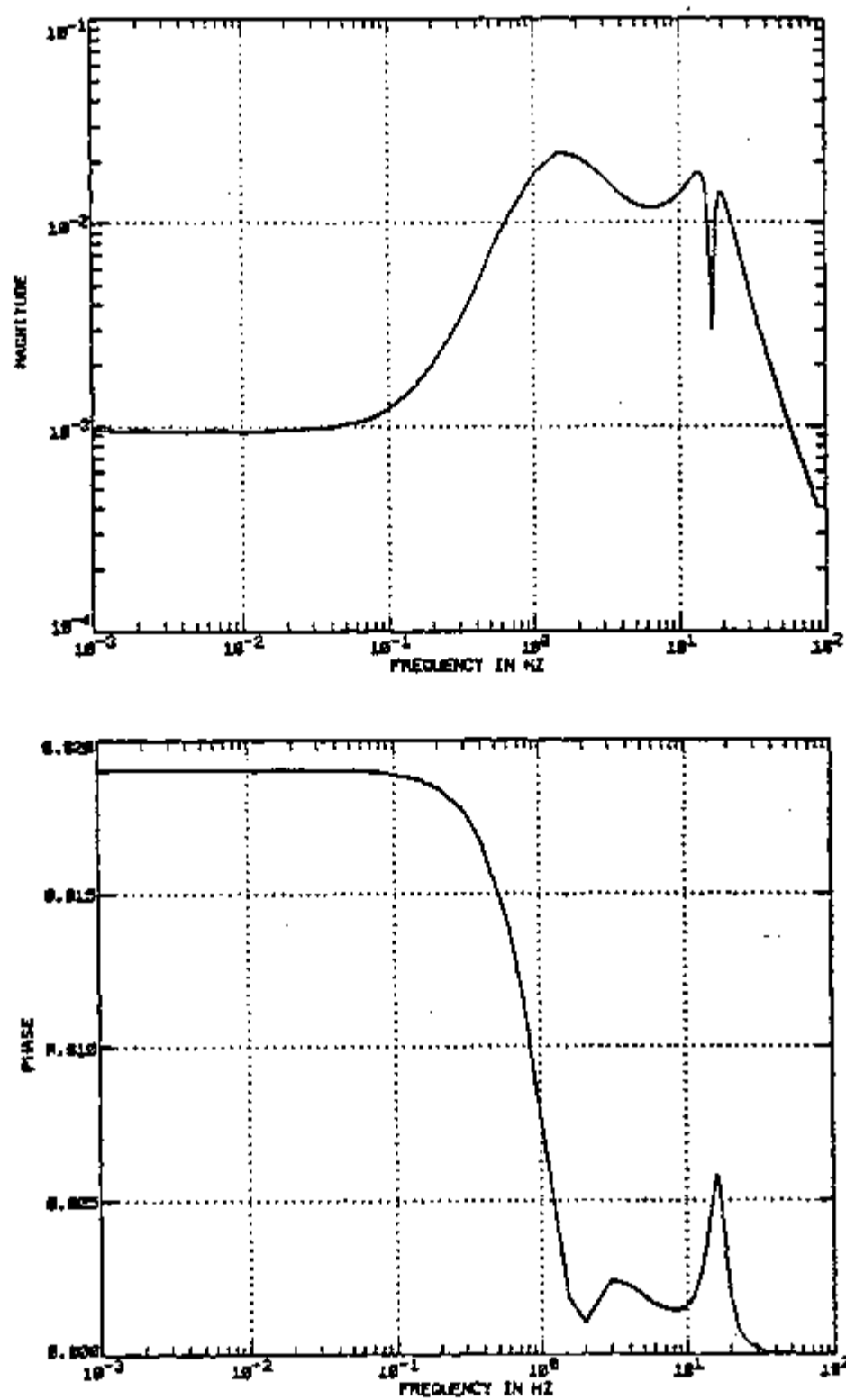
Figure E-18. Sensitivity with respect to parameter K_b
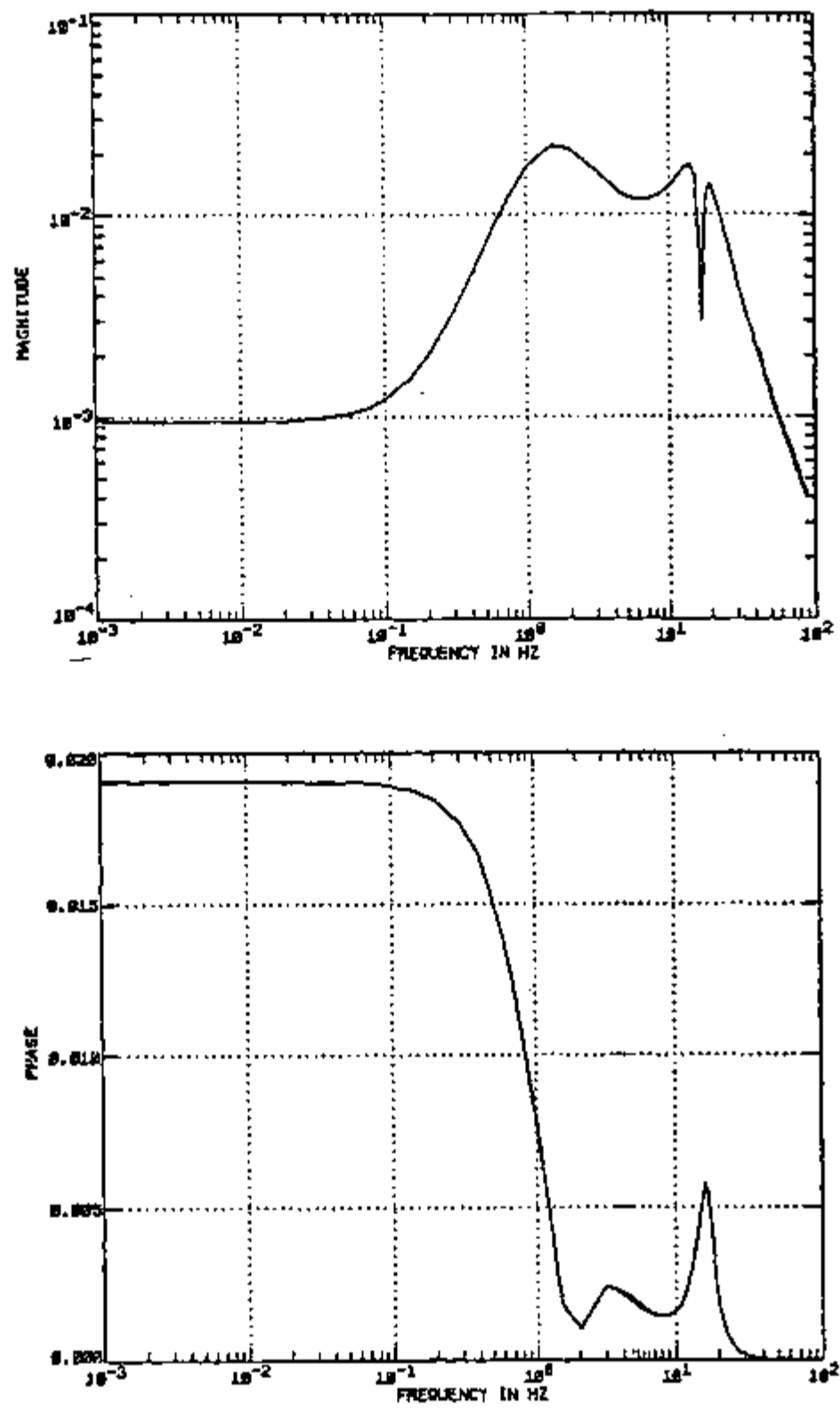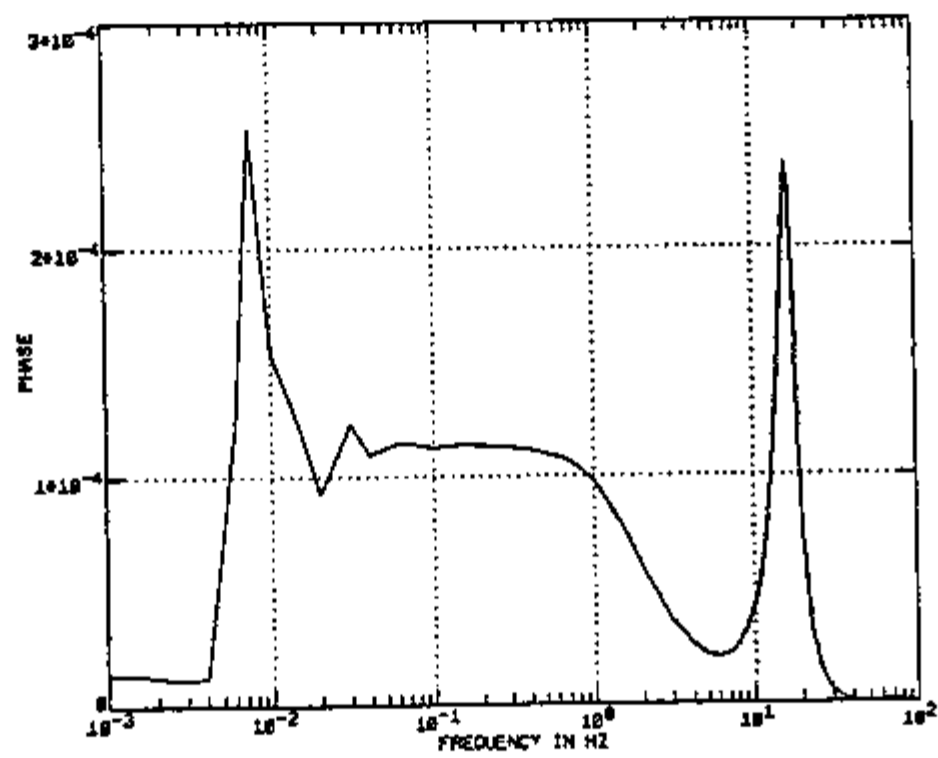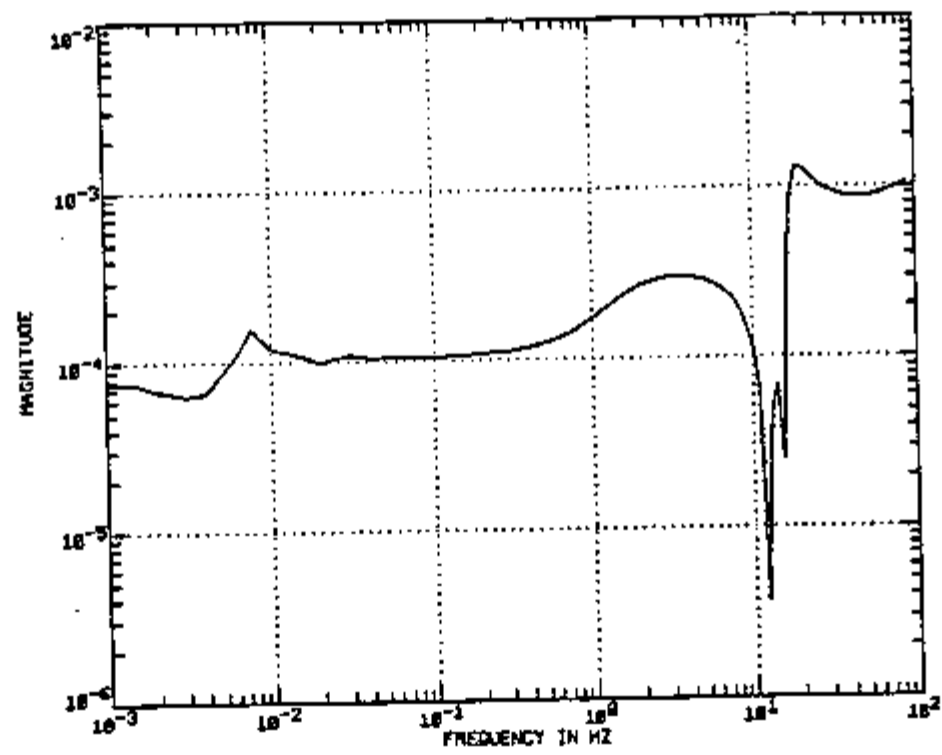
Figure E-19. Sensitivity with respect to parameter C_1
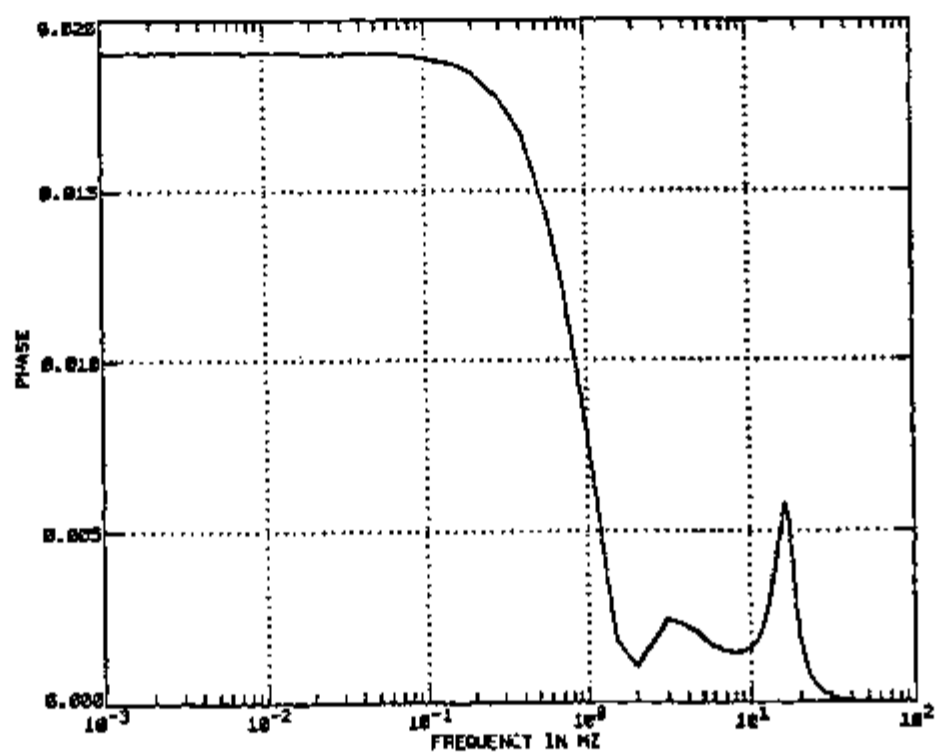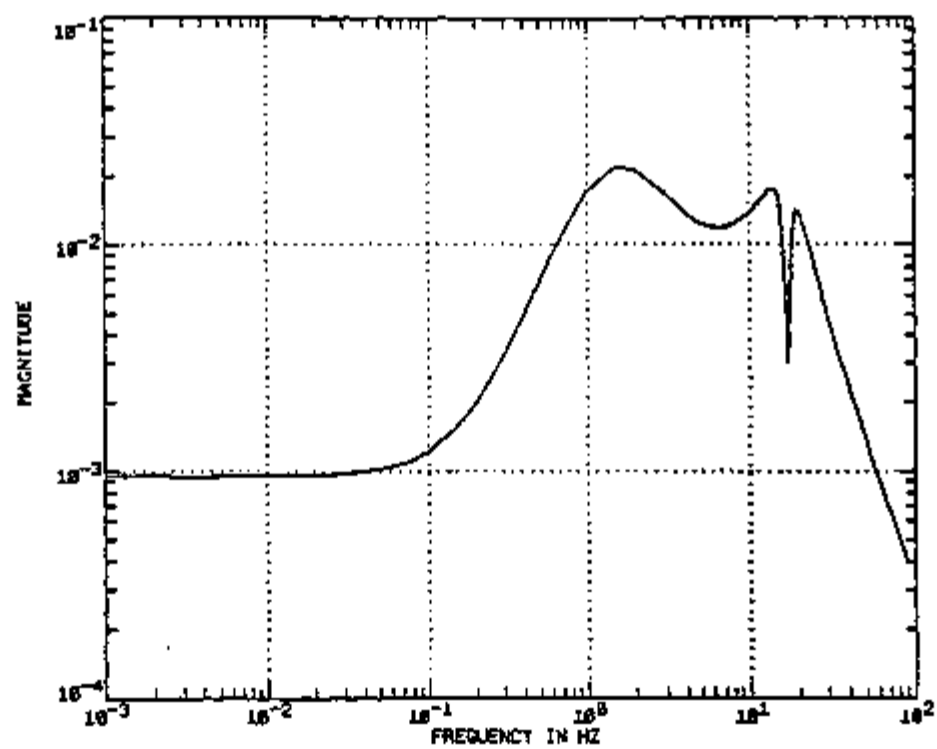
Figure E-20. Sensitivity with respect to parameter C_2

Figure E-21. Sensitivity with respect to parameter C_4

Figure E-22. Sensitivity with respect to parameter C_5

Figure E-23. Sensitivity with respect to parameter $\theta_g(0)$

Figure E-24. Sensitivity with respect to parameter $Y_\beta(0)$

Figure E-25. Sensitivity with respect to parameter $P_h P_d$
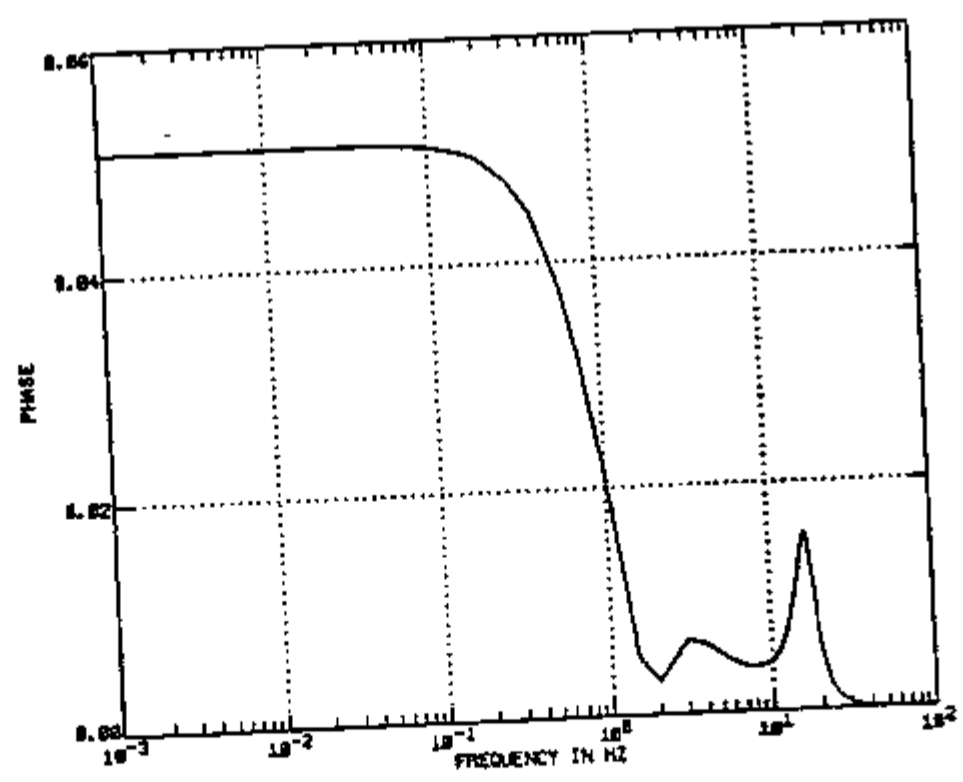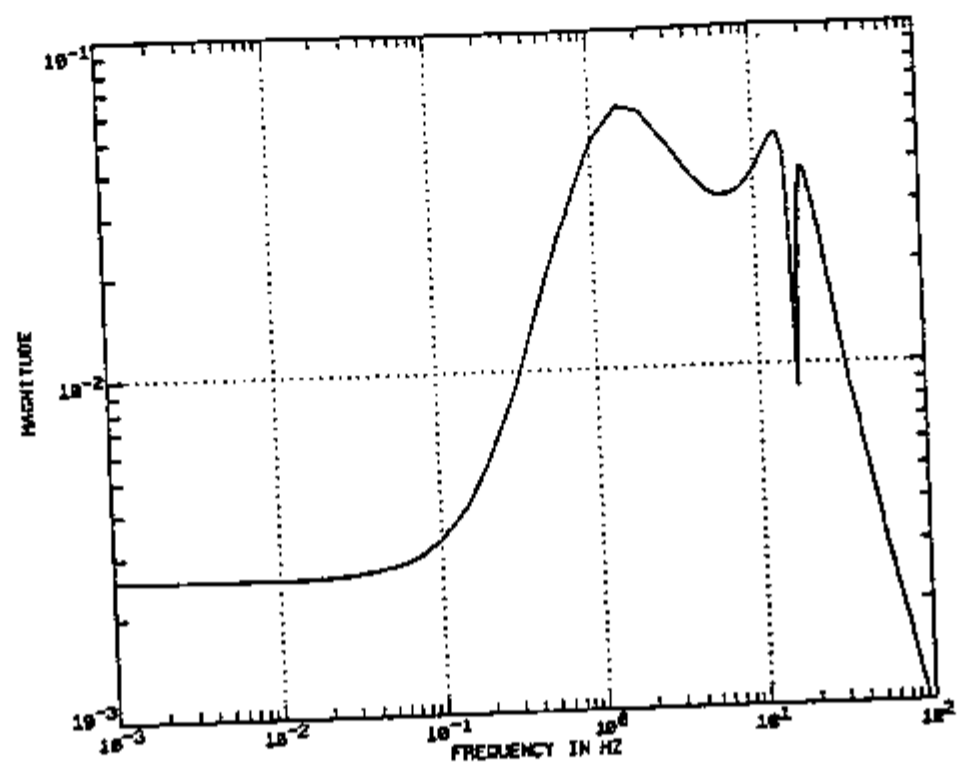
Figure E-26. Sensitivity with respect to parameter $P_8 P_d$

Figure E-27. Sensitivity with respect to parameter L_g

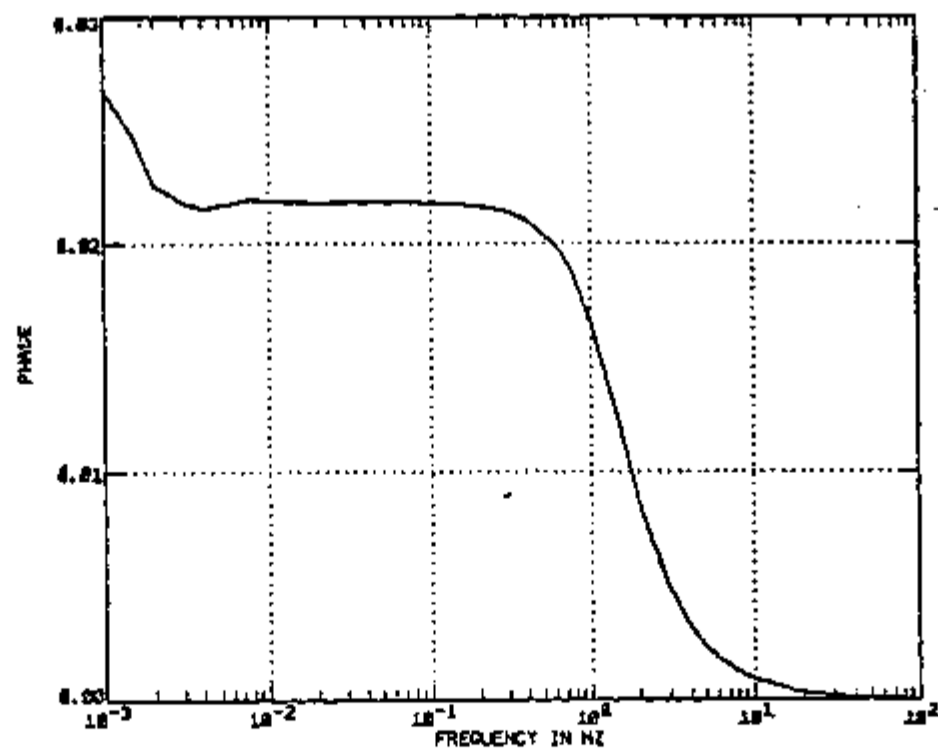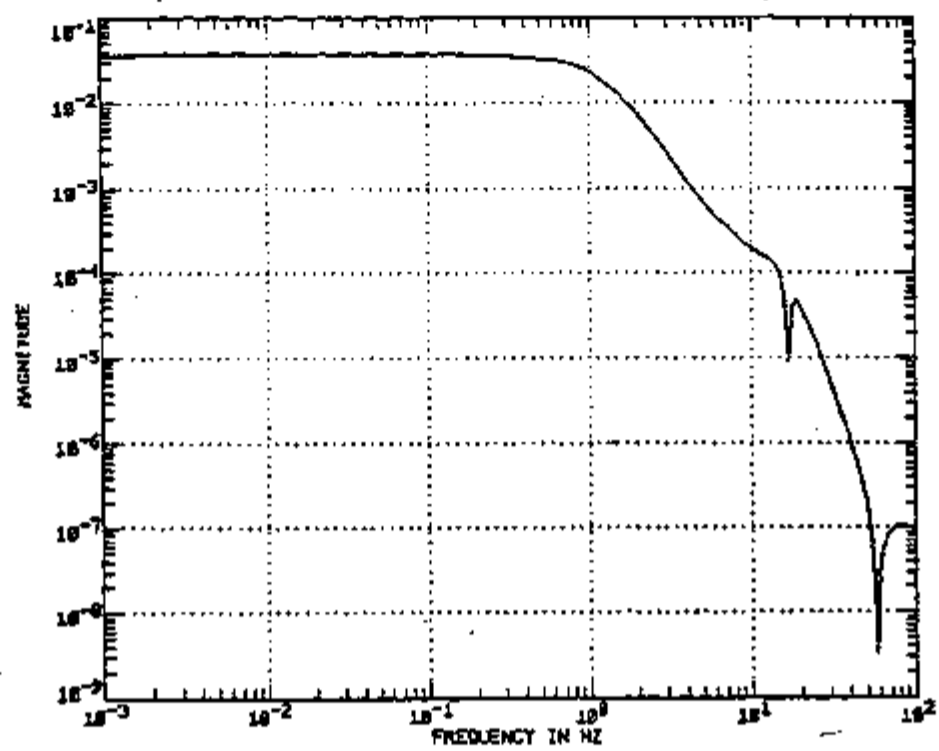Figure E-28. Sensitivity with respect to parameter A_g

Figure E-29. Sensitivity with respect to parameter p

VITA

Adalberto José Soares was born in Vizeu, Portugal on December 13, 1950. In 1953 he moved with his parents to Sao Paulo, Brazil. He attended elementary schools in that city. In 1967 he started working in a bank organization while attending evening school at 'Colegio Fernao Dias Paes' (equivalent to high school). He graduated in 1968. In 1970 he was admitted at the 'Instituto de Fisica da Universaidade Sao Paulo' (Institute of Physics), where he attended evening school and from which he graduated in 1973. On January of 1974 he received a scholarship from 'Instituto de Pesquisas Energeticas e Nucleares' (IPEN), former 'Instituto de Energia Atomica', and left the bank organization. On March of that year he became a employe of the Institute, and began the study toward the Master's degree at the 'Escola Politecnica da Universidade Sao Paulo' (College of Engineering). The degree was awarded in 1977.

In 1978 he was awarded a scholarship from 'Comissao Nacional de Energia Nuclear', from Brazil, to study for the Ph. D. degree at The University of Tennessee, Knoxville. He obtained the degree on December 1982.

Adalberto is married to the former Miss Angela Berti, of Sao Paulo, Brazil, and has a daughter named Carla Alessandra and a son named Marco Antonio.